



**NTNU – Trondheim**  
Norwegian University of  
Science and Technology

# Steep Fracture Patterns And Their Characteristics Within The Triassic De Geerdalen Formation On Svalbard

An emphasis on regional trends, local  
variations and lithological controls

**Gareth Steven Lord**

Petroleum Geosciences

Submission date: June 2013

Supervisor: Atle Mørk, IGB

Co-supervisor: Alvar Braathen, The University Centre in Svalbard (UNIS)

Norwegian University of Science and Technology  
Department of Geology and Mineral Resources Engineering



## Abstract

This study documents and discusses the nature of steep fracture orientations, their densities and their relationships to lithological types, which has been observed within the Triassic De Geerdalen Formation on Svalbard. The study is based entirely on field data collected over a period of two field seasons in Central Spitsbergen, Western Edgeøya and Central and Northern Hopen, with the intent of understanding the regional variations in these fractures.

Fracture orientations have been analysed on a regional scale and their mode of formation is related to significant regional tectonic trends and also local structural styles. Density data and fracture characteristics within differing lithologies are based on scan-line data recorded in the field at numerous locations. The average fracture spacing and average fractures per metre has been the primary components of this discussion; and these are related to regional stratigraphic trends seen within the De Geerdalen Formation and the nature of sedimentological variations within the unit.

It has been observed that throughout Svalbard there is a prominent affinity of steep fracturing to a NNW-SSE and ENE-WSW trend, with a further fracture set of NNE-SSW being observed on the island of Hopen. NNW-SSE trending fractures have been related to periods of extension along major N-S trending structural lineaments during the late-Mesozoic, with subsequent augmentation by Cenozoic compressional tectonics, uplift and unloading. ENE-WSW trending fractures seen throughout Svalbard are related to Late-Cretaceous and Palaeogene compressional tectonics along the West-Spitsbergen margin. Where they are deduced to have formed normal to the maximum stress of this compression, again these are suggested to have been augmented by later periods of uplift and unloading. Extensional fracturing seen on the Island of Hopen which is in contrast to the regional styles of Central Spitsbergen and Western Edgeøya, has been seen to be in close orientation to offshore faulting to the east of Svalbard in the Northern Barents Sea.

Fracture densities are observed to show clear increases in spacing and decreases in average fractures per metre as bed thickness observed with sandstone beds. Results from sandstone and shale beds suggest a similar trend but with discrepancies at Hopen, whilst shale dominated beds show a good trend of density decreasing with bed thickness, but this lithological type is under-represented within the dataset.



## Aknowledgements

My thanks are first and foremost extended to Atle Mørk of SINTEF Petroleum Research and Professor II at NTNU, for offering the fantastic opportunity to study the Triassic of Svalbard. His kindness, patience, valuable discussions and humour, has helped considerably to take the edge of the workload. Furthermore my thanks are expressed to my co-supervisor Professor Alvar Braathen.

A gratuitous thank you is extended to the Svalbard Science forum and the Research Council of Norway, for their generous funding, which has aided fieldwork in the region greatly. The University Centre in Svalbard has offered excellent logistical support throughout all periods of fieldwork and I also wish to tender my thanks to the UNIS CO<sub>2</sub> Lab.

I further extend my thanks to SINTEF Petroleum Research for their fantastic support throughout the entirety of this project with note to; fieldwork, logistics, office space and coffee!

Finally, I wish to send my thanks to all the great friends who have accompanied myself on fieldwork; assisting in tedious, prolonged and often uncomfortable days of data collection. Notably field assistants; Even Nikolaisen and Turid Haugen, and also PhD candidate Tore Klausen.

*Thank you!*



## Contents

Preface .....	4
1. Introduction.....	6
2. Regional Geological Setting .....	8
2.1 Regional Tectonic Setting and Linear Trends .....	8
2.2 Triassic Stratigraphy of Svalbard.....	14
2.3 Triassic Infill Patterns of the Barents Sea .....	21
3. Fractures.....	26
3.1 Previous Fracture Studies in the Triassic of Svalbard .....	26
3.2 Fracture Classification .....	28
4. Fieldwork .....	31
4.1 Current Triassic Stratigraphy and Tectonics of Field Areas in Central Spitsbergen .....	34
4.1.1 Deltanaset - Sassenfjorden.....	39
4.1.2 Trehøgdene - Sassendalen.....	42
4.1.3 Northern Agardhbukta – Storfjorden.....	44
4.2 Current Triassic Stratigraphy and Tectonics of Field Areas in Western Edgeøya.....	45
4.2.1 Blanknuten .....	48
4.2.2 Klinkhamaren, Muen, Slåen & Kvalpyntfjellet.....	49
4.3 Current Triassic Stratigraphy and Tectonics of Field Areas on Central and Northern Hopen .....	51
4.3.1 Nørdstefjellet Channel Complex.....	55
4.3.2 Binnedalen .....	56
4.3.3 Blåfjellet Channel.....	57
4.3.4 Russevika Beach Section.....	58
4.3.5 Johan Hjortfjellet – Styggdalen and Lykkedalén.....	59
5. Methodology.....	61
5.1 Sedimentological Logs .....	61
5.2 Fracture Orientation Data .....	61
5.3 Fracture Scan-Lines .....	62
5.4 Field Fracture Classification .....	62
5.4.1 Steep Fractures: .....	63
6. Results .....	65
6.1 Sedimentological Logs & Scan-line Data.....	65
6.2 Fracture Orientations.....	66

6.2.1 Regional Fracture Orientations.....	66
6.2.2 Local Fracture Trends.....	71
6.3 Fracture Densities and Lithological Relationships.....	80
6.3.1 Regional Trends – Fracture density and bed thickness by area.....	82
6.3.2 Regional Trends – Fracture density and bed thickness by lithological association. .....	86
7. Discussion.....	100
7.1 Regional Fracture Orientations.....	100
7.2 Fracture Density – Regional Variations and Lithological Controls.....	106
8. Conclusions.....	112
9. References.....	115
10. Appendix 1 –Stratigraphical Logs and Composite Fracture Orientation Data.....	129
Appendix 1.1 – Central Spitsbergen.....	130
Appendix 1.1.1 – Deltaneset.....	132
Appendix 1.1.2 – Konusdalen.....	133
Appendix 1.1.3a – Trehøgdene (Tre-1).....	134
Appendix 1.1.3b – Trehøgdene (Tre-2).....	135
Appendix 1.1.4 – Agardhbukta.....	136
Appendix 1.2 – Western Edgeøya.....	137
Appendix 1.2 .1 – Klinkhamaren.....	137
Appendix 1.2 .2 – Blanknuten.....	138
Appendix 1.2 .3 – Slåen.....	139
Appendix 1.3 – Central & Northern Hopen.....	140
Appendix 1.3.1 – Nørdstefjellet.....	140
Appendix 1.3.2 – Binnedalen.....	141
Appendix 1.3.3 – Blåfjellet.....	142
Appendix 1.3.4 – Styggdalen.....	143
Appendix 1.3.5 – Russevika.....	144
Appendix 1.3.6 – Lykkedalen.....	145
11. Appendix 2 – Fracture Data.....	146
Appendix 2.1 – Central Spitsbergen Fracture Data.....	147
Appendix 2.1.1 – Deltaneset.....	147
Appendix 2.1.2 – Konusdalen.....	156
Appendix 2.1.3 – Trehøgdene 1.....	158



---

Appendix 2.1.4 – Trehøgdene 2.....	163
Appendix 2.1.5 – Agardhbukta .....	166
Appendix 2.2 – Western Edgeøya Fracture Data.....	167
Appendix 2.2.1 – Klinkhamaren.....	167
Appendix 2.2.2 – Blanknuten .....	169
Appendix 2.2.3 – Slåen.....	174
Appendix 2.2.4 – Muen .....	179
Appendix 2.2.5 – Kvalpyntfjellet .....	181
Appendix 2.3 – Central & Northern Hopen Fracture Data.....	183
Appendix 2.3.1 – Nørdstefjellet .....	183
Appendix 2.3.2 – Binnedalen .....	184
Appendix 2.3.3 – Blåfjellet.....	189
Appendix 2.3.4 – Styggdalen .....	190
Appendix 2.3.5 - Russevika .....	193
Appendix 2.3.6 - Lykkedalen.....	194
12. Appendix 3 – Composite Scan-Line Data Tables .....	197
Appendix 3.1 – Regional Scan-Line Data.....	197
Appendix 3.2 – Regional Scan-Line Data: Sandstone Beds .....	198
Appendix 3.3 – Regional Scan-Line Data: Sandstone & Shale Beds .....	199
Appendix 3.4 – Regional Scan-line-Data: Shale Beds .....	200

## Preface

First and foremost, this thesis is being undertaken at the Norwegian University of Science and Technology (NTNU) in Trondheim, The University Centre in Svalbard (UNIS) and has also been heavily supported by SINTEF Petroleum Research. The thesis is supervised by both Professor Atle Mørk of NTNU and Professor Alvar Braathen of UNIS. This thesis is a compulsory consignment of the MSG2 Petroleum Geology course, at NTNU and holds a value of 30 credits. Furthermore this thesis supersedes an earlier project report, Lord (2012), which focussed on a similar scheme of fracture classification in relation to lithology in Svalbard focussing on areas in Central Spitsbergen.

The data presented within this thesis represents two field seasons worth of detailed observation and data collection, throughout the Triassic exposures of the De Geerdalen Formation on Svalbard. During each of these seasons, fieldwork has been conducted in co-operation with the UNIS CO<sub>2</sub> Lab and alongside various other research institutions and industry representatives.

Specifically for work conducted and data collected on the island of Hopen, much of this has only been possible with the joint operation and collaboration with many individuals, alongside company and institutional support (e.g. SINTEF, NPD, Lundin Norway, Idemitsu, RWE, Wintershall, Det Norske, NGU, Total, ENI Norge). Throughout this thesis, any instances where data and observations collected by other members of the project team have been used; references are made to the individual.

On the island of Hopen, primary sedimentological analysis of the De Geerdalen Formation conducted in recent years, has been provided by PhD candidate Tore Klausen of the University of Bergen along with various co-authors. In addition to this, a detailed 3D geo-model of various parts of the island has been produced by master student Kristoffer Hoppland Solvi, of the NTNU. The geo-model has integrates data from Klausen and Mørk (Submitted) see Solvi (2013). Recent palynological dating studies for the island has also been conducted by Vigran et al. (submitted) as has further work throughout Hopen and Central Spitsbergen by master student Marianne Ask of the University of Bergen (Ask 2013).

Fieldwork and data collection on Edgeøya and Eastern Spitsbergen has been somewhat sporadic, despite a dedicated expedition to Edgeøya with Wintershall,

during the summer of 2012. The dataset from the island is comparatively sparse on comparison with other locations, as the expedition maintained its own mandate; with data collection for this work exploiting only the short amount of time available at each location.

Fieldwork throughout Central Spitsbergen however, has been conducted more thoroughly and successfully; by the undertaking of specific expeditions to localities purely for this and earlier projects. This has been supported logistically by the University Centre in Svalbard (UNIS) and funded by the Research council of Norway, through the Svalbard Science Forum Arctic Field Grant (No. 1772).

In this entire project, the objective is to incorporate a widespread series of data from the field areas visited, in order to produce a more regional understanding of fracture development throughout the Late-Triassic rocks of Svalbard. This is designed to further an understanding of how regional tectonics impact fracture orientations throughout a large area and how variations in lithological types and facies can affect the nature of fracture development; both on a large and small scale.

## 1. Introduction

Svalbard, as it can be seen today, is home to some of the most thrilling and undeniably scenic landscapes in the world. In addition to its dramatic topography, delicate flora and wildlife, Svalbard has experienced a very long-lived and diverse geological history that has made it an appealing destination for the discerning geoscientist for centuries. Ever since the first Norwegian geological expeditions of Keilhau in 1827 (Syssemmannen 2008), geoscientists have frequented the archipelago in a bid to unlock the regions complex past.

The map displayed in Figure 1, demonstrates the high arctic latitude of this remote archipelago and it should be remembered that fieldwork in this region is often difficult and to an extent somewhat dangerous.

The objective of this thesis is to analyse and interpret the nature of steep fracturing within of the Triassic De Geerdalen Formation of Svalbard, by discussing regional tectonic controls on fracture orientation and lithological controls on fracture characteristics. This will be achieved in a twofold manner. Firstly, by the implementation of fracture orientation data onto geological maps, in order to discuss tectonic controls on both a regional and local scale. Secondly, by the application of fracture density data into sedimentological sections and by graphical analysis, this will allow for a constraint of lithological controls on fracture densities to be discussed.

The intent of this method is to enable an understanding of the effects of lithology and invariably facies, upon the nature of fracture patterning and distributions throughout the Triassic De Geerdalen Formation on Svalbard and gain an insight and understanding into their mode of formation.



**Figure 1:** A, Overview map displaying the high arctic location of the Svalbard archipelago. B, Overview map of Svalbard, its main islands and prominent settlements. Base map adapted from Norwegian Polar Institute.

## 2. Regional Geological Setting

The objective of this chapter is to focus upon building a firm and scientifically driven insight into the regional and Triassic Geology of the Svalbard Archipelago. Large scale tectonic controls within the region will be discussed, in order to form a solid grounding in Svalbard's tectonic past, whilst an overview of basin infill and a detailed description of the regions stratigraphy will focus specifically upon the Triassic.

### 2.1 Regional Tectonic Setting and Linear Trends

The archipelago of Svalbard and the north western Barents Sea has experienced a long and complex series of tectonic events. This has resulted in the spectacular landscape that is visible in the region today and an exciting offshore geology, hosting an exciting future for hydrocarbon exploration (Johansen et al. 1992; Doré 1995; Grogan et al. 1999). The modern day region around Svalbard can be described, most simply, as the uplifted corner of the Barents Sea shelf (Steel and Worsley 1984; Harland 1997; Worsley 2008).

This platform area is bound to the north and west by large-scale fault systems at passive continental margins formed during the Cenozoic (Myhre and Eldholm 1988, Leever et al. 2011), see Figure 2. Therefore the tectonic framework of Svalbard is dominated, in general, by prominent north-south and north west-south east trending linear structures, as shown in Figure 2, (Eiken 1985; Myrhe and Eldholm 1988; Gabrielsen et al. 1990; Dallmann 1999). To the east of Svalbard in the regions around Kong Karls Land a prominent north east – south west structural trend has been observed offshore (Gabrielsen et al. 1990; Johansen et al 1992; Grogan et al. 1999; Høy and Lundschieen 2011). The faulting and basin formation to the east of Svalbard is suggested by Faleide et al. (2008) to be Late-Palaeozoic in age and related to a period of failed rifting. Some of these structural lineaments have seen repeated activity throughout time, since the Devonian period (Lamar et al. 1986) and some have been observed to be undergoing present tectonic activity (Dallmann in prep.).

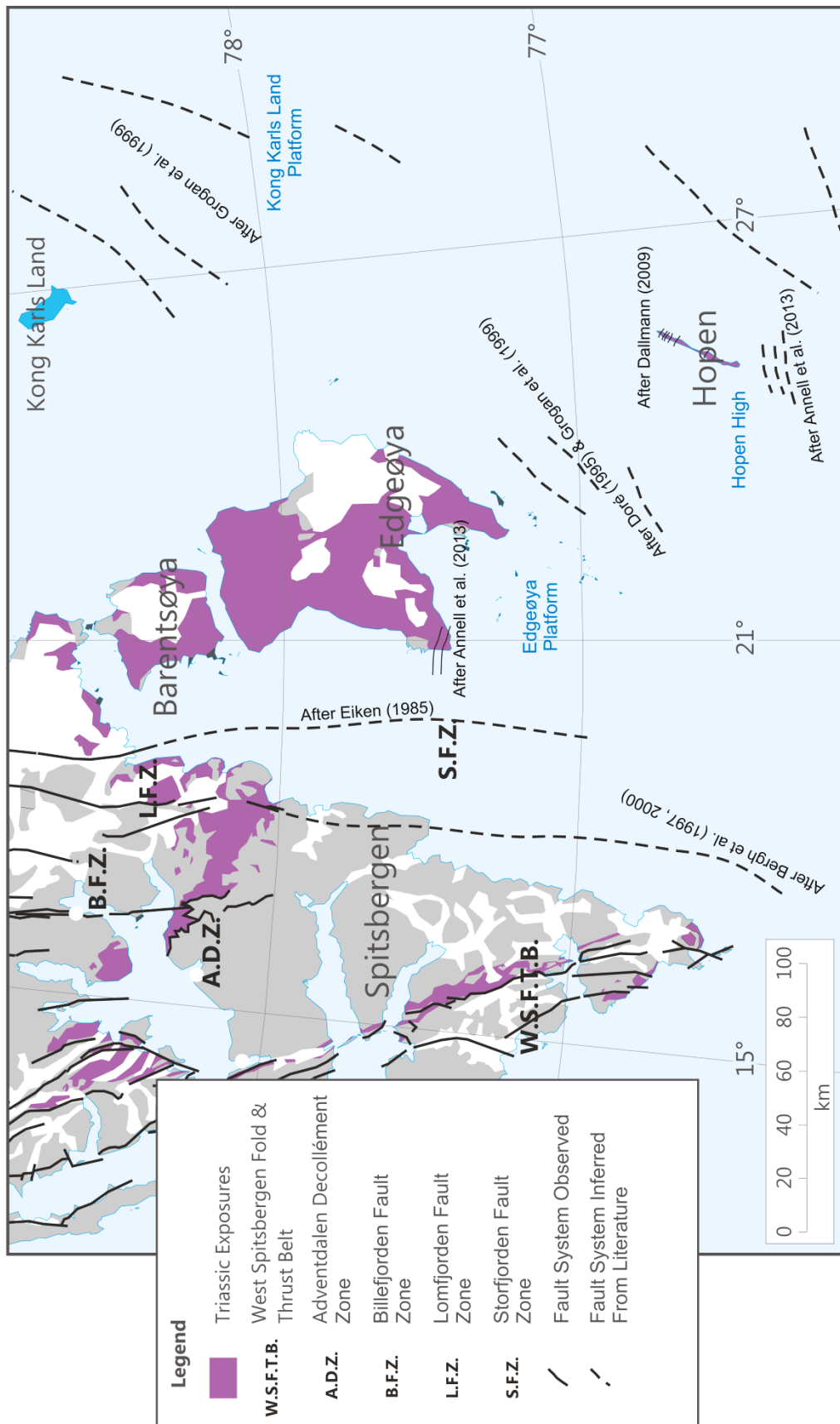
Throughout time the continental segment that forms Svalbard as it is seen today, has slowly migrated northwards from lower, temperate latitudes into its high arctic position, (Elvevold et al. 2007). Tectonic activity despite being long lived was mostly concentrated during the late-Devonian, Carboniferous times and again later, during

the early-Cenozoic (Worsley 2008). Most of these tectonic developments are reflected in the variable thickness of the regions stratigraphy, generally highlighted by alterations in facies and transport direction, alongside prominent tectonically derived structures.

Svalbard itself can be segmented in to a number of tectonic zones, bound and demarcated by prominent structural lineaments (e.g. Haremo and Andresen 1992; Bælum and Braathen 2012). These faults can be generally named from west to east as; the Hornsund Fault Zone, to the south (only to c.N75°) is the Knølegga Fault Zone (Sundvor and Eldholm 1976), the Forelandsundet Graben, West Spitsbergen Fold and thrust Belt, the Billefjord Fault Zone (Harland et al. 1974; Harland 1974; Bælum and Braathen 2012) and the Lomfjord Fault Zone (Harland 1979; Bergh et al. 1997).

At the onset of a phase of sea floor spreading during the early Oligocene (Myhre and Thiede 1995), Greenland was adhered to the American plate and a new seaway emerged between the new American/Greenland plate and the Eurasian plates (Bergh et al. 1997; Bruhn and Steel 2003). This phase occurred at the Palaeocene-Eocene boundary (Våagnes 1997) and resulted in a complex augmentation of the regions eastern margin. This evolution was comprised of two large scale shear-segment margins, the first; the Senja Fracture zone (Myhre and Eldholm 1988) propagating throughout the mainland of northern Norway and into the Barents Sea shelf (Berndt et al. 2001). With the second major shear segment being the Hornsund Fault Zone, comprised of the palaeo-Hornsund Fault and the Inner-Hornsund Fault (Bergh et al. 2011).

The Hornsund Fault Zone originally acted as a shear zone during the Eocene, however this altered abruptly to an extensional regime, during the early Oligocene (e.g. Myhre et al. 1982; Myhre and Eldholm 1988). It is an almost continuous lineament, trending north-south between the latitudes of N74-79°; however its character (with regards to fault throws) varies considerably along strike. The offshore paleo-Hornsund Fault (Bergh et al. 2011), has the largest of structural expressions within this zone continuous almost to the sea floor (Myhre and Eldholm 1988).



**Figure 2:** An overview structural map of the Northern Barents Sea and South Eastern Svalbard, showing notable fault systems and structural features. Inferred fault systems are shown alongside literature in which they are also noted.



Onshore in Svalbard, the next major structural complex is the 'West Spitsbergen Fold and Thrust Belt', shown in Figure 2, (Lowell 1972; Müller and Spielhagen 1990; Lyberis and Manby 1993; Leever et al. 2011), also termed the 'West Spitsbergen Orogenic Front' by Harland (1979). This massive complex of structures formed at a transform boundary between Greenland and the western Barents Sea, during the Atlantic separation in the Late Cretaceous (Lyberis and Manby 1993; Braathen et al. 1999). Within this compressional regime approximately 20-40 km of crustal shortening occurred, perpendicular to the margins axis (Bergh et al. 1997; Leever et al. 2011).

The province of Cenozoic deformation can be split into prominent zones where obverse structural styles can be seen (Braathen et al. 1999). A hinterland zone to the west, a basement involved fold-thrust complex, a central zone of thin skinned folding and thrusting (Bergh et al. 1997), along with an eastern zone representing a foreland province (Braathen et al. 1999).

This feature dominates the Central Spitsbergen tectonic geology and resulted in the formation of the Central Spitsbergen Basin, an asymmetric synclinal structure of Palaeocene-Eocene age (Braathen et al. 1997; Leever et al. 2011); which forms a near north south trending foredeep basin, termed the Central Tertiary Basin (Müller and Spielhagen 1990; Braathen et al. 1997; Leever et al. 2011). This synclinal structure features a shallow dipping eastern limb and a near vertical western limb that has experienced more intense deformation due to compressional tectonics.

The basin was in-filled with sediments of Cenozoic age, derived from the erosion of a mountain belt formed during orogenesis (Bruhn and Steel 2003), by the migrating thrust sheets and by intense folding (Bælum and Braathen 2012; Helland-Hansen 2010). Structures formed within this compressional regime were emplaced atop strata with an existing regional dip to the south/south east, which had resulted from moderate uplift during the Cretaceous. This uplift allowed for the regional erosion, which has resulted in the general bedrock pattern seen throughout Svalbard today; which is characterised by the presence of older strata and basement being exposed to a greater extent in the north and north-west of Svalbard (Worsley 2008).

The eastern structural boundary to the central basin is the Billefjord Fault Zone (Harland et al. 1974; Harland 1979; Manby et al. 1994; Dallmann et al. 2002;

Braathen 2012). This is a long lived and well known (see Harland et al. 1974 and references therein) structural lineament which has had a significant impact upon structural styles in Svalbard (Bælum and Braathen 2012). The Billefjord Fault Zone was activated during a transcurrent and contractional regime in the Caledonian-Devonian (Haremo and Andresen 1992) and then again during the Carboniferous; where its style changed to an extensional regime resulting in the formation of a half-graben structure (Harland et al. 1974; Haremo and Andresen 1992; Bergh et al. 2012). Jurassic and Cretaceous aged stratigraphical sequences, seen within close proximity to the Billefjorden Fault Zone, are observed to display a notable thickness reduction (Haremo et al. 1990) with Cretaceous sequences to the south of Isfjord (in Nordenskiöld Land) displaying an extensional trend. With a westwards throw of faulting, which is believed have occurred during the Early-Cretaceous, (Parker 1966; Harland et al. 1974)

Further activity occurred during the Cenozoic, where contractional reactivation along existing faults took place (Bælum and Braathen 2012). The Billefjord Fault Zones present day style reflects a zone some 10 kilometres (20-30 at its widest) in width and 150 kilometres in length. A point of note from Bælum and Braathen (2012), relevant to this thesis; is that there is strong evidence for the control of extensional styles by older structural lineaments.

In addition to the folding and thrusting to the west and the Billefjord faulting to the east, the Mesozoic succession in the Central Tertiary Basin is also host to a prominent décollement zone (Parker 1966; Major and Nagy 1972; Haremo et al. 1990; Haremo and Andresen 1992; Andresen et al. 1994). The floor thrust is situated in soft shales of the Middle-Triassic, Bravaisberget and Botneheia Formations, and the roof thrust is situated in the upper Janusfjellet Subgroup, shales of the Agardhfjellet Formation (Haremo et al. 1990; Braathen et al. 1999). This is also of important note, as the Triassic stratigraphy in Central Spitsbergen that are intended for fracture analysis by this thesis, lie sandwiched within this décollement zone.

Some 15 km to the east of the Billefjord Fault Zone lays the Lomfjord Fault Zone (Harland 1979; Andresen et al. 1988; Maher and Craddock 1988; Nøttvedt and Rasmussen 1988); again this feature is an elongate, prominently defined, north-south trending, structural complex, which can be seen to split the Ny-Friesland high from

the east Svalbard depression (Dallmann et al. 2002). The Lomfjorden Fault Zone, like that within Billefjord, shows evidence of a thin skinned contractional style, dominant during the Cenozoic which is seen to be consistent with the general east-west crustal shortening throughout Spitsbergen (Maher and Craddock 1988).

Throughout Storfjorden, a wide seaway between eastern Spitsbergen and the islands of Edgeøya and Barentsøya, a prominently defined fault system has been observed by Eiken (1985), within seismic sections shot along an east west transect. This structure termed the 'Storfjorden Fault Zone' (Eiken 1985), is reported to be host to numerous extensional normal faults featuring westward fault plane dips and offsets of over one kilometre (Eiken 1985). These faults are interpreted as being in a, north north west-south south east, orientation and hold a strong affinity to major structures seen onshore to the west, in Spitsbergen. These structures are suggested to be of Permian age or older and are most probably relatable to Devonian - Early Carboniferous extensional movements related to a phase of graben development at that time (Steel and Worsley 1984; Eiken 1985).

The structural geology of onshore Eastern Svalbard, notably the areas of Edgeøya, Barentsøya and Hopen is relatively unascertained. The Eastern Svalbard region is essentially defined by its near flat lying strata of post-Caledonian age, overlying basement complex (Lock et al. 1978). As the regional tectonics of Svalbard are essentially characterised by north-south trending lineaments discussed previously it would seem a sensible suggestion that so too are any recent tectonic structures on Edgeøya and this is reported by Lock et al. (1978). However, Edgeøya can be seen to rest on platform structure (Bergsager 1986; Gabrielsen et al. 1990) and this is also shown by Lock et al. (1978) who, by way of structure contour mapping noted that the structural style is dominated by a series of gentle domes. This overall tectonic style is relatively consistent with the foreland province defined by Braathen et al. (1999). However aside one large fault seen in southern Edgeøya, at Negerpynten (Klubov 1965; Lock et al. 1978) no large-scale tectonic lineaments are reported, this holds true for the present Norwegian Polar Institute geological map for Edgeøya (Dallmann et al. 2002; Dallmann in prep.).

To the east of the Svalbard the southern margins of the Edgeøya platform are defined by a series of ENE trending fault systems (Grogan et al. 1999; Glørstad-Clark

et al. 2010) displaying a downwards stepping style of terraces towards the Sørkapp Basin. To the north in the region of Kong Karls Land, the structural style is dominated by NE trending flexures defined at the Mesozoic level, that have later been reactivated as reverse faults during the Mesozoic and Cenozoic (Grogan et al. 1999).

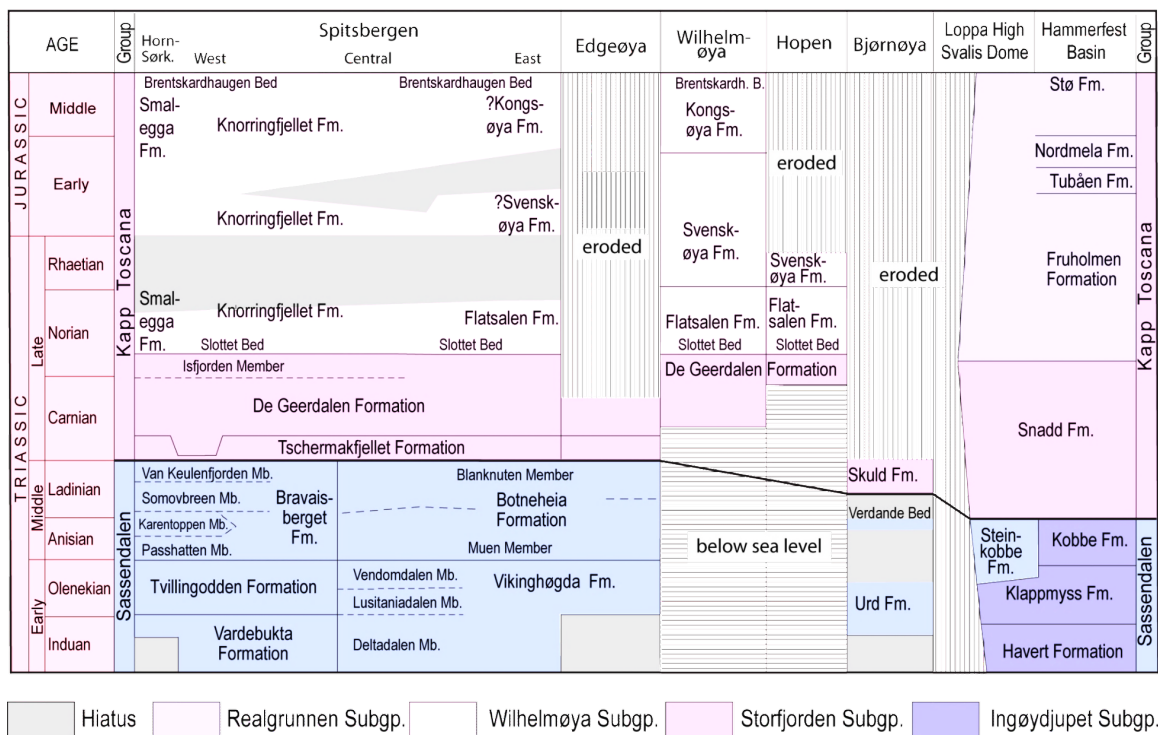
In terms of the Hopen region of Svalbard, very little can be stated about large scale regional tectonics, given the platform structure of the Edgeøya and Barentsøya region and its distance from larger structural lineaments, it is most likely a component of this domal/ foreland province structure. However, based on the current Norwegian Polar Institute geological map (Dallman 2009) and a previous version by Smith et al. (1975), Hopen can be seen to hold an array of structures not yet reported in Eastern Svalbard. These will be discussed in greater detail in a forthcoming chapter on the specific geology of the island.

## **2.2 Triassic Stratigraphy of Svalbard**

The primary unit of interest to this thesis is the Late Triassic sandstones and shales of the Carnian to early-Norian (Buchan et al. 1965; Tozer and Parker 1968; Korčinskaja 1982) aged De Geerdalen Formation. However in order to correctly position the stratigraphic component into context, the Triassic stratigraphy, subdivision and nomenclature of Svalbard must be understood. The regional stratigraphic subdivision of formations presented throughout this thesis, is at present defined by the work of Mørk et al. (1999), in the current Svalbard lithostratigraphic lexicon. However, this chapter will also include a detailed historical overview of recent stratigraphic nomenclature (post 1960), for the benefit of clarity and understanding. Figure 3 shows a complete overview of the Mesozoic succession of Svalbard and the Barents Sea, produced by Vigran et al. (Submitted).

The rocks of the Early Triassic, Induan and Olenekian (Tozer and Parker, 1968; Korčinskaja 1982; Weitschat and Dagys, 1989; Mørk et al. 1999) stages, in central Spitsbergen and islands of eastern Svalbard, is host to the grey shales of the Vikinghøgda Formation (Mørk et al. 1999). These lie unconformably atop the Permian carbonaceous lithologies and mark a significant hiatus in deposition (Worsley, 2008). However, in southern and western Spitsbergen the silty shales of the Induan aged (Buchan et al. 1965; Tozer and Parker, 1968; Korčinskaja 1982; Weitschat and Dagys, 1989) Vardebukta Formation, overlain by the darker shales

and silts of the Olenekian (Tozer and Parker, 1968; Korčinskaja 1982; Weitschat and Dagens, 1989) Tvillingodden Formation (Mørk et al. 1999), are in place of the Vikinghøgda Formation (Mørk et al. 1999). This is due to lithostratigraphic correlation, as they are however time equivalent units. All three units represent sediments deposited in a marine environment, with the Vikinghøgda Formation showing evidence for stacked transgressive, regressive cycles (Mørk et al. 1989; Mørk and Smelror 2001).



**Figure 3:** An overview table of the Early to Middle Mesozoic successions of Svalbard and the Barents Sea. From Vigran et al. (Submitted).

The Vardebukta Formation was originally defined by Buchan et al. (1965) then again with its current definition by Mørk et al. (1982). The Tvillingodden Formation was first described by Buchan et al. (1965) as the 'Sticky Keep Formation', then again as the 'Pitnerodden Formation' by Pčelina (1983). The exposures forming the currently formalised Vikinghøgda Formation (Mørk et al. (1999), have undergone a series of stratigraphic definitions by numerous workers. The first definition was by Buchan et al. (1965) who defined two units; the 'Vardebukta' and 'Sticky Keep' Formations. Lock et al. (1978) defined the rocks within the lower 'Barentsøya Formation'. Mørk et al. (1982) defined the Deltadalen and Sticky Keep Member, retaining Lock et al. (1978)'s

Barentsøya Formation, whilst Pčelina (1983)'s scheme defined the rocks as the Vardebukta and Wichebukta Formations in central and eastern Svalbard.

Overlying the Vikinghøgda Formation in all but south and western Spitsbergen are the prominent, black, cliff forming paper shales of the Anisian-Ladinian (Tozer and Parker, 1968; Korčinskaja 1982; Weitschat and Lehmann, 1983) aged Botneheia Formation (Pčelina 1983). The equivalent Bravaisberget Formation (Mørk et al. 1982; Mørk et al. 1999; Krajewski et al. 2007) takes its place in southern and western Spitsbergen, overlying the Tvillingodden Formation. These 'paper' shales as they are commonly referred to, due to their highly friable nature, have tendency to cleft into thin sheets and are associated with a high organic content (Mørk et al. 1982; Mørk et al. 1999). These units are all classified within the Sassendalen Group of Svalbard (Buchan et al. 1965; Mørk et al. 1982, 1999).

Atop the black marine shales of the Botneheia/ Bravaisberget Formation are the units of the Late Triassic to Mid Jurassic aged Kapp Toscana Group, defined first by Buchan et al. (1965). The group's current definition is defined by Harland et al. (1974). Within this group are two presently defined sub-groups; the lower Storfjorden Subgroup and the upper Wilhelmøya Subgroup (Worsley 1973; Mørk et al. 1999).

The lowest stratigraphical unit of the Storfjorden Subgroup of Spitsbergen is the sediments of the Early Carnian (Korčinskaja 1982; Dagys et al. 1993) Tschermakfjellet Formation (Mørk et al. 1999), the unit represent an upward coarsening, shale dominated sediment package deposited in a pro-delta environment and is found to be stratigraphically extensive throughout Svalbard. The unit was first defined by Buchan et al. (1965) as a member unit within the Kapp Toscana Formation (Buchan et al. 1965). The current definition of the unit and formal description of the formation was provided by Mørk et al. (1982, 1999).

Atop the Tschermakfjellet Formation lie the Carnian – early Norian aged (Tozer and Parker 1968; Korčinskaja 1982) sediments of the De Geerdalen Formation that was originally defined as a member unit by Buchan et al. (1965), within the Kapp Toscana Formation. The De Geerdalen Formation was formalised by Mørk et al. (1982). In the upper part of the De Geerdalen Formation, shales typically become an increasingly dominant lithology, with prominent green and red beds representing the Norian aged Isfjorden Member, first described by Pčelina (1983).

The De Geerdalen Formation in central Spitsbergen is overlain by the Knorringfjellet Formation of the Wilhelmøya Subgroup, which is reportedly deposited throughout the Norian to Bathonian (Pčelina 1965; Bjærke and Dypvik 1977; Korčinskaja 1980; Bäckström and Nagy 1985; Mørk et al. 1999).

The Wilhelmøya Subgroup is extensive in both throughout time and area, as it can be found throughout much of Svalbard. The lowermost is entitled the Flatsalen Formation on Hopen (Mørk et al. 1999) in the south east and the Smalegga Formation in the area of Sørkapp Land (Mørk et al. 1999). Throughout central Spitsbergen the Knorringfjellet Formation is defined within the Wilhelmøya Subgroup, consisting of an upwards coarsening succession which is observed to become more condensed in western Spitsbergen.

The Wilhelmøya Subgroup is by on large, a stratigraphically extensive unit and extends discontinuously through time, to near the end of the middle-Jurassic Bathonian period (Pčelina 1965; Bjærke and Dypvik 1977; Korčinskaja 1980; Bäckström and Nagy 1985), at a time only slightly preceding the Callovian, the Wilhelmøya Subgroup terminates at the Brentskardhaugen Bed (Mørk et al. 1982; Bäckström and Nagy 1985; Mørk et al. 1999). It is then superseded by the dark, marine shales of the Adventdalen Group and Janusfjellet Subgroup (Mørk et al. 1999).

Early stratigraphic descriptions from Edgeøya can also be found within the publications of Falcon (1928), Buchan et al. (1965), Flood et al. (1971), Lock et al. (1978), Mørk et al. (1982) and Krajewski (2008); however these authors all featured varying stratigraphic subdivisions of the units seen on Edgeøya. The subdivision used for this thesis for the stratigraphy of Edgeøya will follow the work of Mørk et al. (1999).

The Triassic exposures of Edgeøya can alike Central Spitsbergen be subdivided into one of the two early-middle Triassic stratigraphic groups found in Svalbard, either the Sassendalen Group (Buchan et al. 1965), or the Kapp Toscana Group (Harland et al. 1974). The lowermost exposures of Edgeøya, defined within the Sassendalen Group, were originally named as the Sticky Keep and Botneheia formations by Buchan et al. (1965). These were then downgraded into member units by Flood et al. (1971), where on Edgeøya and Barentsøya they were classified within the Kongresfjellet

Formation (Flood et al. 1971). The units were then grouped and re-defined as the Barentsøya Formation by Lock et al. (1978) in a scheme that was later used by Mørk et al. (1982). However, following the work of Mørk et al. (1999) the units were again, separated, ranked as individual formations and defined as the Vikinghøgda and Botneheia Formations.

The lower, Vikinghøgda Formation, is often scree covered, with the boundary between the overlying Botneheia Formation being very difficult to constrain and is rarely seen. This is with the exception of small creeks, where weathered surfaces are uncovered, or along coastal sections where wave action has allowed for the formation to be exposed.

The Botneheia Formation can be seen as a scree slope culminating in a prominent black cliff of dark, bituminous, marine shales, often termed the 'paper shales' (Mørk et al. 1982; Mørk et al. 1999; Krajewski 2008) throughout Edgeøya.

The primary cause for the redefinition of the Barentsøya Formation by Mørk et al. (1999), following the work of Lock et al. (1978), was at the time for historical reasons, but as the Botneheia Formation is a prominent unit and laterally extensive throughout Svalbard it is also a significant unit for geological mapping. Significant advances in the understanding of the Botneheia Formation has been made in recent years, most notably in the work of Krajewski (2008), whom defined two members within the formation; shales of the Muen Member at its base and the calcareous siltstones of the Blanknuten Member at the top (the Blanknuten Member is previously defined in Mørk et al. 1982, 1999).

Atop the Botneheia Formation of Edgeøya, as with Central Spitsbergen, lie the early Carnian aged (Korčinskja 1982; Dagys et al. 1993) grey shales of the Tschermakfjellet Formation (Buchan et al. 1965; Mørk et al. 1982, 1999).

The uppermost stratigraphical unit of Edgeøya is that of the Carnian (Tozer and Parker, 1968; Korčinskja 1982) De Geerdalen Formation, again originally defined as a member unit of the Edgeøya Formation by Buchan et al. (1965) but formalised as a separate formation by Flood et al. (1978) and Mørk et al. (1982). Both the Tschermakfjellet and De Geerdalen Formations are within the Storfjorden Subgroup of the Kapp Toscana Group on Edgeøya.



The stratigraphical units of Hopen present somewhat of an oddity in the overall stratigraphy. This is due to their age being relative to that of central Spitsbergen whilst representing the most proximal deltaic exposures of the De Geerdalen Formation (offshore equivalents can be seen in the Snadd Formation of the Barents Sea). The exposures of Hopen also are stratigraphically younger than those of Edgeøya and this discrepancy is due to the nature of clinoform distribution (see following chapter) throughout the east and south eastern region of Svalbard.

The exposures on the island of Hopen are exclusively Triassic in age with three formations being present on the island, currently formalised by Mørk et al. (1999). However the published record of Hopen's stratigraphy is also, like much of Svalbard, highly varied. The earliest geology specific works, such as those of Flood et al. (1971), Pčelina (1972) and Worsley (1973) devised suitable stratigraphic nomenclature, with the work of Pčelina (1972) being the first to provide a detailed stratigraphic dating of the island.

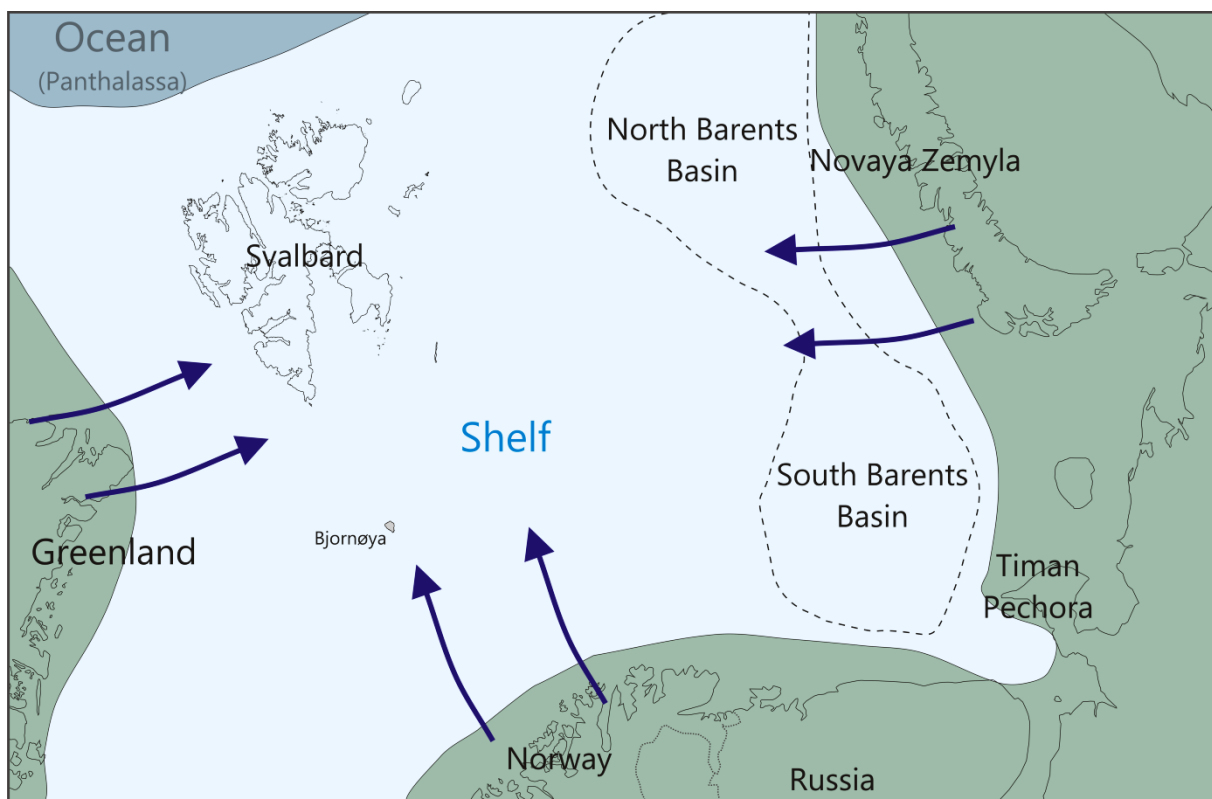
Flood et al. (1971) defined the entire stratigraphical sequence of the island to the De Geerdalen Formation based on lithological similarities; this was also accepted by Cox and Smith (1973). Worsley (1973) defined the upper units of the island within the Wilhelmøya Formation, whilst Smith (1974) placed these within the Kapp Toscana Formation. Smith et al. (1975) provided a new nomenclature, defining the units on Hopen within the Kapp Toscana Group but due to their distance from Spitsbergen defined them as equivalent, but not same units. The lowermost was defined by Smith et al. (1975) as the Iversenfjellet Formation correlatable with the De Geerdalen Formation of Flood et al. (1971) with the overlying units being defined as the Flatsalen Shale Formation and the Lyngfjellet Sandstone Formation. Both equivalent to Worsley (1973)'s Wilhelmøya Formation.

The latest stratigraphical scheme of Mørk et al. (1999) incorporates much of this historical nomenclature for Hopen, but with more emphasis on regional correlation of units. The lowermost units are interpreted as the most proximal deltaic sediments of the De Geerdalen Formation in the Storfjorden Subgroup, of the Kapp Toscana Group. Pčelina (1983) also highlighted the presence of the Isfjorden Member at Hopen, however whilst the upper exposures of the De Geerdalen Formation are prominently different from underlying lithologies, these have been determined to be

far more distal in nature. Therefore, an informal unit, the Hopen member has recently been proposed and discussed in the works of Solvi (2013) and Ask (2013), in order to counter this problem. The overlying Flatsalen Shale Formation has been re-named simply as the Flatsalen Formation, ranked within the Wilhemøya Subgroup (Mørk et al. 1999) with the pronounced carbonaceous Slottet Bed as the basal marker bed. Atop this unit lies the prominent white sandstones of the Svenskøya Formation, re defined from Smith et al. (1975)'s Lyngefjellet Sandstone Formation by Mørk et al. (1999) to be stratigraphically relatable to exposures of Smith et al. (1976)'s formation of the same name present on Kong Karls Land.

### 2.3 Triassic Infill Patterns of the Barents Sea

The Permian orogenic processes that resulted in the formation of the Uralide Mountains ceased throughout the Late-Devonian to Late-Permian (Puchkov 2009). This tectonic episode resulted in the formation of a mountain belt along the continental margin of the Siberian Terrane and topographic high was accompanied by a shallow basin featuring a submerged shelf stretching outwards and deepening northwards towards the Palaeo-Panthalassa Sea as shown in Figure 4. This is believed to have been situated between the Siberian Terrane and the Greenland-American plate (Riis et al. 2008; Torsvik and Cocks 2004; Torsvik et al. 2012).



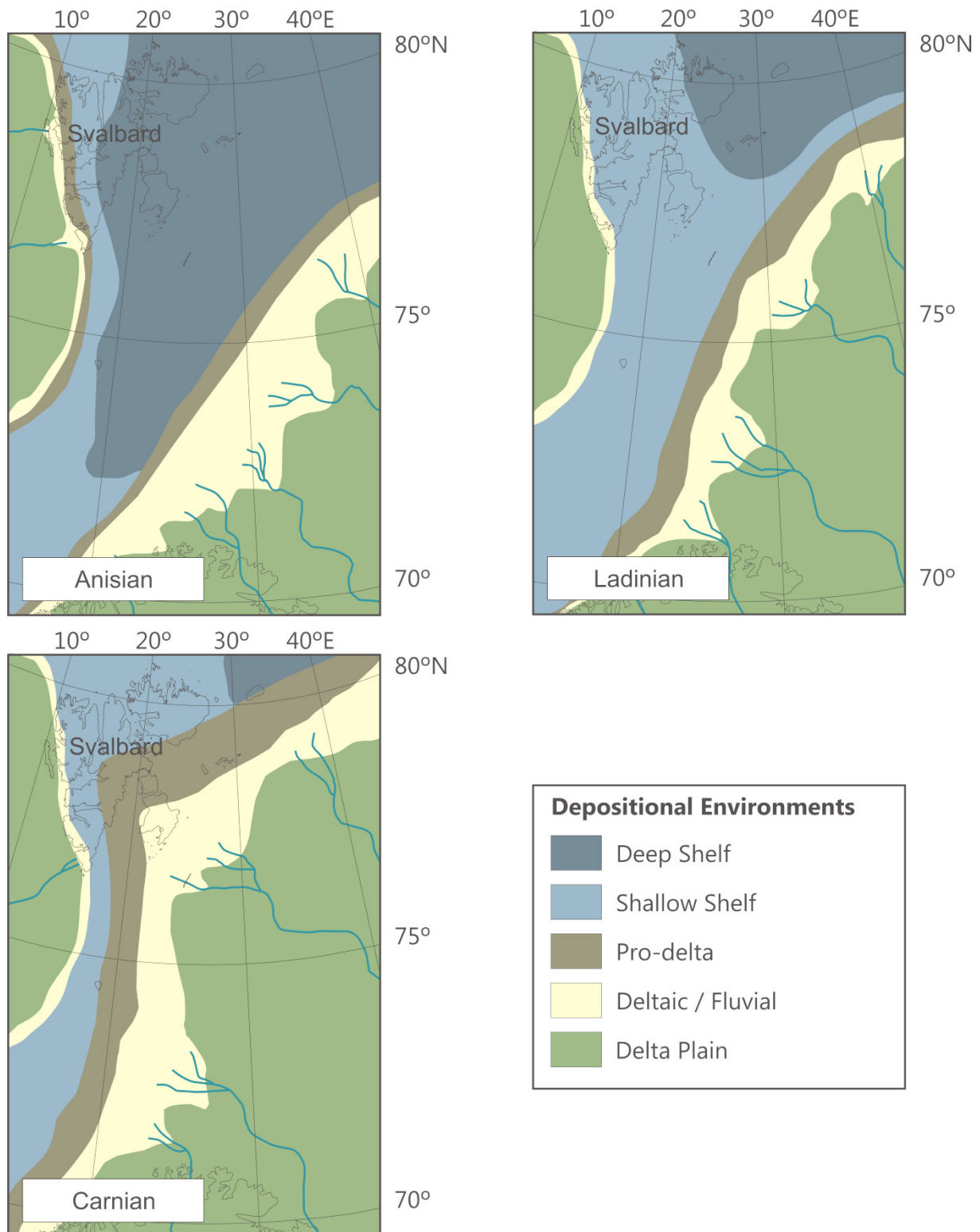
**Figure 4:** A Palaeogeographical reconstruction map of the Barents Shelf environment during the Early Triassic. Directional arrows show the migration of sediments from onshore areas into the shallow shelf environment. The figure is an adaptation of those by Cocks and Torsvik (2007) and Riis et al. (2008).

The landmass that now forms Svalbard, existed in the north western margins of this shelf juxtaposed against the Greenland-American plate (Torsvik and Cocks 2004, Torsvik et al. 2012), in the realms of a relatively deep marine setting. Within this marine realm, abrupt transgressive-regressive cycles are preserved in the rock record as a series of alternating, upwards coarsening packages of sand and mud (Mørk et al. 1989; Mørk and Smelror 2001).

Throughout the Middle Triassic, highly organic rich mudstones and shales hosting high phosphate content were deposited within the marine settings of this region (Mørk et al. 1982). These shales of the Botneheia Formation were deposited in relatively anoxic conditions (Mørk and Bjorøy 1984). These fluctuations in sea level led to deposition of marine muds, in the deepest areas of these boreal basins, with siltstones and sandstones being deposited in a pro-delta environment in the more shore-face environments, at the basin margins (Mørk et al. 1982).

Throughout the Late Triassic the deepest marine settings underwent continual deposition of pro-delta shale sediments (Mørk et al. 1982), atop the deep marine shales of the Botneheia Formation. These grey shales, with relatively low organic content are often described as the 'Purple Shale' (Falcon 1928) due to their prominent red/purple coloured weathering surface. These shales are defined stratigraphically as the Tschermakfjellet Formation (Mørk et al. 1999).

The uplifted landmasses of the Uralian Mountains to the east of this sea shelf, allowed for significant sediment yield, see Figure 5 (Riis et al. 2008; Glørstad-Clark et al. 2010; Miller et al. 2012), thus in the Late-Triassic (Carnian) large rivers and deltaic depositional environments became prominent in the margins of this seaway (Nystuen et al. 2008; Riis et al. 2008). Provenance studies of the southern Barents Sea; by numerous workers e.g. Glørstad-Clark et al. (2010), Mørk (1999) and Riis et al. (2008) support the theory for a strong eastern and south eastern input of clastic sediments, with a provenance area most likely in the regions around the Uralian Mountains (Glørstad-Clark et al. 2010; Riis et al. 2008). The original provenance hypotheses, as mentioned in Riis et al. 2008 page 331, note that Birkenmajer (1977) and Lock et al. (1978) considered the sediment provenance location for Triassic strata to be located somewhat around the areas of Nordaustlandet and northern Spitsbergen, where pre-Caledonian rocks are prominently exposed. However, recent seismic and core studies (Glørstad-Clark et al. 2010; Riis et al. 2008) noted the presence of west and north westerly dipping Carnian aged clinofolds in the Barents Sea Shelf. Coupled with comparisons of rock mineral compositions, contest these earlier theories (Riis et al. 2008).



**Figure 5:** An overview diagram of the nature of depositional environment throughout the Middle to Late Triassic in the region of the Barents Sea Shelf. Note the nature of deltaic progradation through eastern and central Svalbard during the Carnian. Figure is an adaptation and simplification from that by Riis et al. (2008).

This sediment yield from the east and south east was significant enough to infill the basin considerably, with large volumes of sand. The resultant effect being the aerially

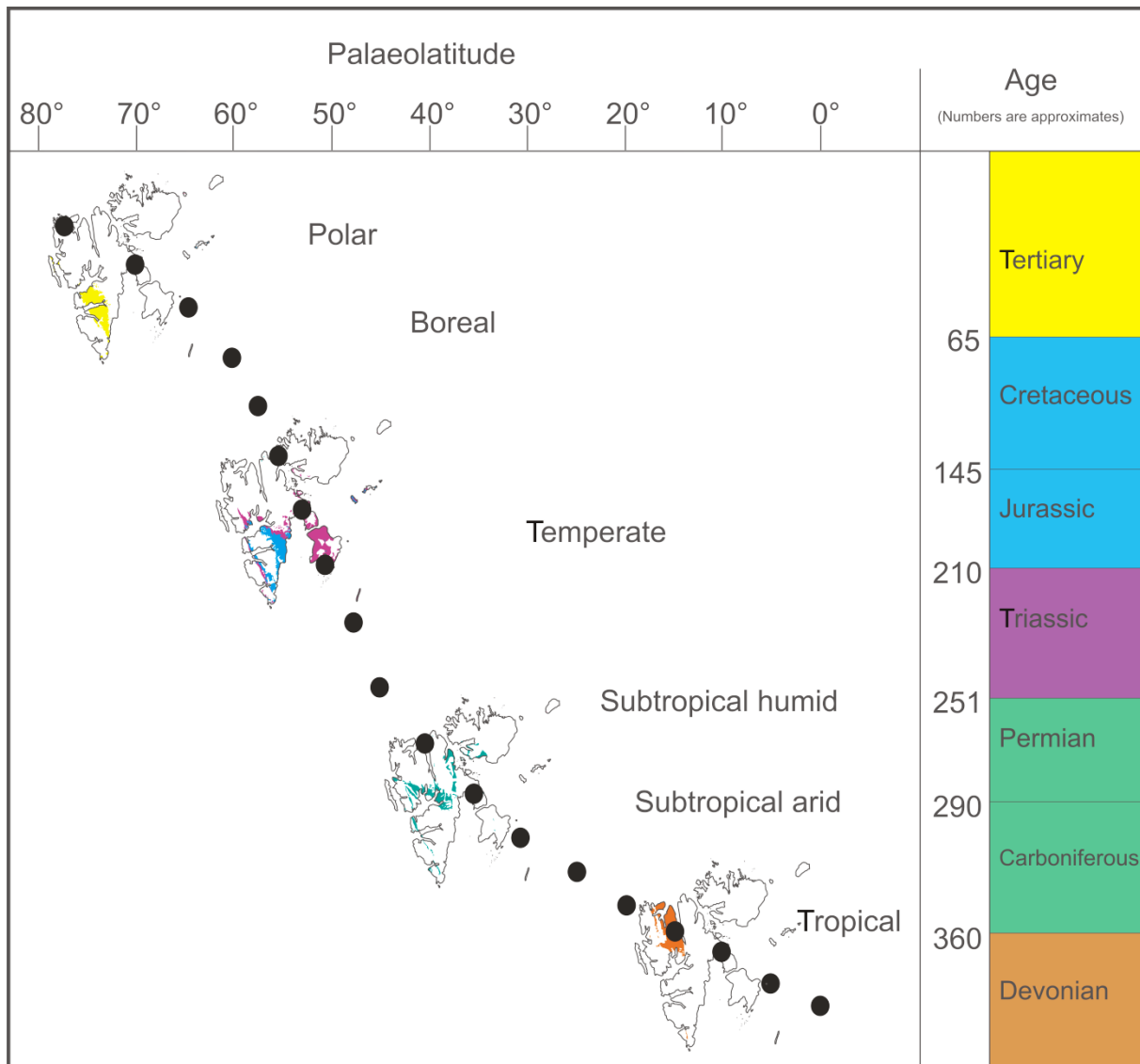
extensive presence of tidal, deltaic and fluvial deposits of the De Geerdalen Formation (Buchan et al. 1965; Lock et al. 1978; Mørk et al. 1982). The sandstone and shale dominant De Geerdalen Formation represent the progradation of a large scale transgressive deltaic system, into this shallow marine setting (Mørk et al. 1982, 1989; Riis et al. 2008). These sandstone rich units are eventually overlain by the uppermost Triassic sandstones of the Wilhelmøya Subgroup, which represent a condensed interval unit from a shallow marine environment host to an erosional base (Mørk et al. 1989) and numerous unconformities in deposition throughout (Mørk et al. 1999).

This system of sediment progradation throughout the Barents Sea can be viewed in seismic lines shot to the east and south east of Svalbard (Glørstad-Clark et al. 2010; Høy and Lundschieen 2011). These studies have interpreted and mapped a succession of clinoform belts that can be seen to be gently dipping to the north-west and within this series; Anisian, Ladinian and Carnian age (with the potential for a Norian) clinoforms, have been observed. This offshore interpretation of Triassic sequences has been extrapolated by this thesis to onshore Svalbard, where it is designed to form the basis of the first order pseudo-mechanical stratigraphy for the De Geerdalen Formation.

Palaeo-latitude reconstructions, as shown in Figure 6, through this time show that the location of Svalbard was situated in a relatively temperate zone at approximately 55-60°N, with only a gentle northwards shift from sub-tropical to temperate climates during the Mesozoic (Worsley 2008).

Regardless, the greatest northwards migration of Svalbard is suggested to have begun with a moderate migration in the Devonian (Torsvik et al. 2012). This was then followed by a period of relative stability during the Mesozoic culminating in a more intense northwards shift throughout the Cenozoic, at the onset of sea floor spreading along the north-Atlantic margin. This opening occurred initially in the Labrador Sea some 67Ma and concluded approximately 33 Ma (Torsvik et al. 2012); whilst the opening of the Norwegian-Greenland Sea and the formation of the Arctic Basin commenced approximately 55 Ma (Chalmers and Laursen 1995; Torsvik et al. 2012). The continental breakup of Laurasia and formation of these new seaways (Atlantic and Norwegian-Greenland Seas) resulted in the European plate shifting northwards

thus positioning the Barents Sea Shelf and Svalbard into its present high-Arctic position.



**Figure 6:** A palaeolatitude reconstruction, after Elvevold (2007), showing the generally perceived rate of continental migration of the Svalbard landmass throughout time. Note the greatest rate of drift being throughout the Permian to Triassic.

### 3. Fractures

#### 3.1 Previous Fracture Studies in the Triassic of Svalbard

The region of Central Spitsbergen has seen several recent fracture studies related to the UNIS CO<sub>2</sub> Lab both at student and research institution level. This is due to the nature of fracturing within the proposed Triassic reservoir, chosen by the UNIS CO<sub>2</sub> Lab.

The earliest study into fracture characteristics within the De Geerdalen Formation in Central Spitsbergen was conducted by Master Student, Gard Ole Waerum throughout the summer field season of 2010 (See Waerum 2011). This study focussed primarily on the nature of fracturing within both the sedimentary strata of the De Geerdalen Formation and the dolerite intrusions of the Diabasodden Suite, on the mountain of Botneheia in Sassenfjorden.

This thesis concluded that the region of Botneheia was heavily dominated by NNE – SSW and E – W fracture orientations, in both the De Geerdalen Formation and Diabasodden Suite dyke. With a stronger affinity for ENE – WSW and NNW – SSE being seen within the intrusive rocks. It was noted that within the De Geerdalen Formation fractures of all three modal types were observed (see following section for discussion of fracture modes and classification). Furthermore the thesis concluded that fractures within the De Geerdalen Formation; the NNE – SSW trending set were the oldest in age, with E – W trending sets being younger. Furthermore Waerum (2011) concluded that due to this presence of all three fracture modes and the dominance of fracture orientations aligning both perpendicularly and normal to regional structural lineaments and styles suggested a strong regional tectonic influence on fracture orientations. The presence of Type I mode fractures with an orientation to the NNW-SSE has been observed by Waerum (2011) and the formation of these is related to Cenozoic compression, the nature of Cretaceous dolerite intrusive rocks and extension along the Billefjorden Fault Zone.

A further study conducted during the summer field season of 2011 by Master Student Laura Farrell of the University of Edinburgh (See Farrell 2011), also focussed on the nature of fracturing within the De Geerdalen Formation in relation to the UNIS CO<sub>2</sub> Lab. This study however was primarily focussed on the appraisal of the UNIS CO<sub>2</sub> Lab and therefore discussion with regards to fractures is only a minor component.



Regardless, the study area focussed on the Triassic succession of Deltaneset, Konusdalen and a further valley and therefore conclusions made are of direct importance to this thesis.

Farrell (2011) concluded that the majority of fractures in the area are orientated along a NE – SW strike, parallel to the regional stress, resulting from Cenozoic compression in the west. The work also concluded that there is no evidence for bed thickness controlling the nature of fracture sets. Fractures were determined to be primarily mode I in style, showing no prominent displacement, with Mode II fractures also being seen in some locations. Furthermore Farrell (2011) concluded that most layer internal fractures are confined to sandstone beds within the De Geerdalen Formation at Deltaneset, with fracture planes terminating against beds above and below the host bed. This suggests that lithology has significant control on the nature and characteristics of fractures in this area.

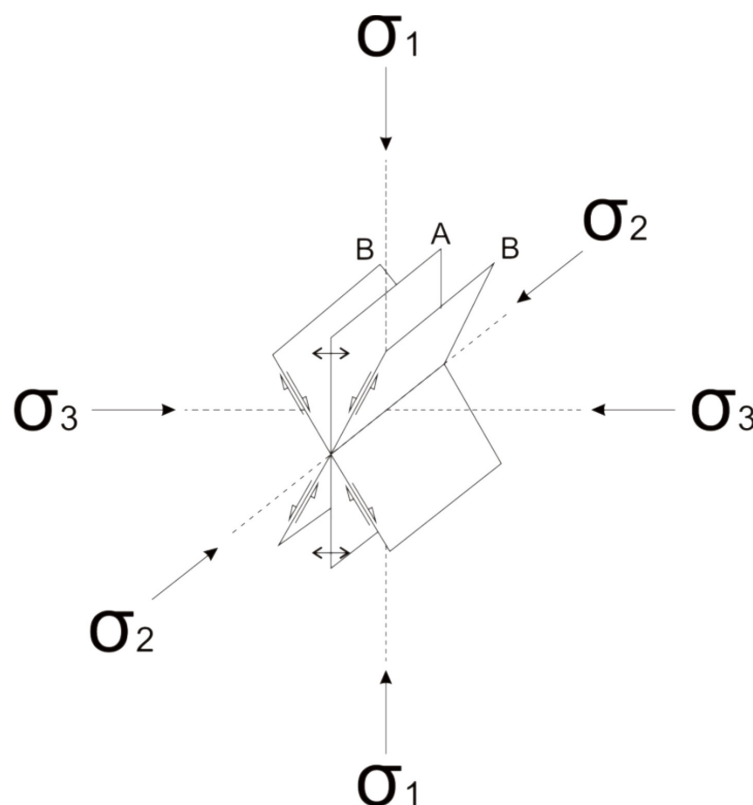
Studies by workers of the UNIS CO<sub>2</sub> Lab have also been conducted within the field area of Deltaneset and also further afield within Sassenfjorden. Ogata et al. (2012) studied fractures within the De Geerdalen Formation both in core from the Adventdalen CO<sub>2</sub> wells and also outcrops in the region around Deltaneset.

This study by Ogata (2012) also contained a detailed observation of fractures and concluded that within the De Geerdalen Formation, fractures can be subdivided into a notable mechanical stratigraphy consisting of; massive to laminated intervals of shale, which host abundant low-angle shear fractures; Beds of massive to thinly-bedded, heterogeneous, intervals of shale and silt, which predominantly contain non-systematic, pervasive bed-confined fractures and massive to laminated, moderately bedded, fine-coarse-grained sandstones containing a lower frequency of mostly steep fractures. The study also concludes the presence of both high and low angle, NE - SW trending shear fractures, within the overlying Knorringsfjellet Formation and also relates their development to compression during the Cenozoic.

### 3.2 Fracture Classification

Within the field areas most of the rock strata that has been observed for fracture characteristics can be defined as relatively un-deformed. Therefore, this lends well to gaining understanding the nature of fracture distributions within layered sedimentary rocks, which do not feature heavy fold or fault deformation.

Fractures form in layered sedimentary rocks as they undergo brittle deformation, which will occur when the tensile strength of the bed, or beds in question, is exceeded in response to stress; see Figure 7. There are deemed to be three primary modes of fractures, all shown in Figure 8; Mode I, II and III (Kulander et al. 1979; Freund 1990; Twiss and Moores 2007). The method of opening of each fracture mode is a result of either; tensile stress in Mode I fractures, shear stress in Mode II fracture formation or shear stress resulting in tearing and the creation of Mode III fractures (Freund 1990; Twiss and Moores 2007).



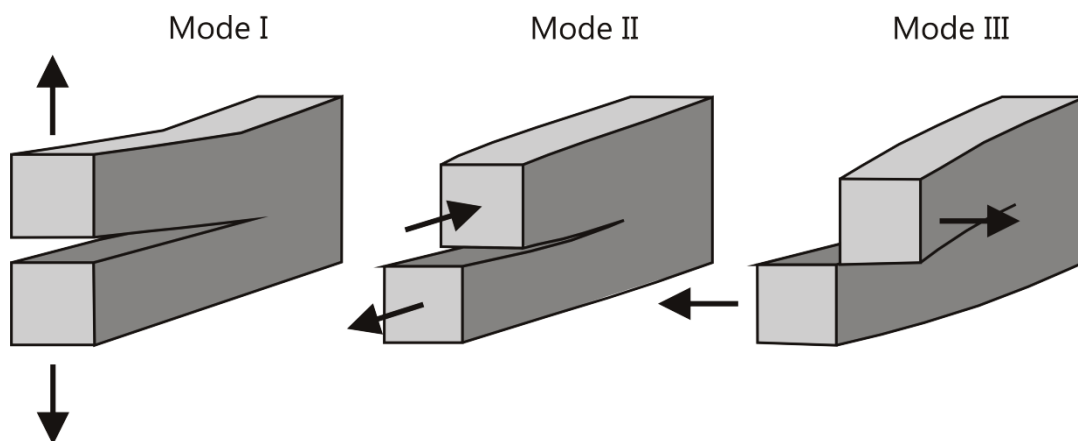
**Figure 7:** Redrawn after Nelson (1985) this schematic Figure highlights the mode of fracture formation with regards to stress. **A**, represents an extensional fracture plane, whilst **B** represents those formed as shear fractures, note the displacement arrows. Stress is denoted by Sigma ( $\sigma$ ).

Mode I fractures, also termed Opening-mode fractures (Bai and Pollard 2000), form within an extensional stress regime and fracture propagation occurs along a plane

normal to that with the least tectonic stress value (Freund 1990; Twiss and Moores 2007). Furthermore these generally feature a vertical or sub-vertical fracture plane (Nelson 1985) and often form orthogonal to layer boundaries, whereby they may be confined to individual beds (Helgeson and Aydin 1991; Gross and Engelder 1995).

Mode II fracture formation features an associated component shear movements along the fracture plane and are recognised by the presence of lineation's along the fracture surface or offset across the fracture plane (Twiss and Moores 2007). Irregular failure and kink failure, where a non-linear fracture plane occurs, is formed as a combination of both Mode I and II (Olson & Pollard, 1989) fracture styles.

Mode III fractures also form as a result of failure in response to shearing, however these differs to those of Mode II, in that they combine a cutting motion alongside an element of rotation during propagation (Twiss and Moores, 2007) and these may also be termed Hybrid fractures (Ramsey and Chester 2004). A combination of both Mode I and Mode III fractures may also create a distorted and twisted fracture plane with an associated component of echelon structures (Pollard et al. 1982). The two most common fracture types described by Nelson (1985) refer to those that propagate as a result of either shearing, appropriately termed shear fractures and those that propagate as a response to all tensile stresses being compressive.



**Figure 8:** A schematic diagram showing the nature of fracture opening modes, in response to tensile stresses. Adapted after Twiss and Moores (2007).

Field fracture morphology, as described in Nelson (1985), can be subdivided into four key types; open fractures, deformed fractures (both gouge filled and slickensided fracture planes), mineral-filled fractures and vuggy fractures. Open fractures possess no notable evidence for deformation or evidence for mineral cementation along the

fracture plane (Nelson 1985). Deformed fractures often display evidence for offset along the fracture plane, with gouge fractures being somewhat in-filled with material derived from the fracture plane itself as a result of abrasion on the fracture walls. Slickensided fractures display a striated surface of mineral growth or a polished surface that has occurred syn-deformation, as a result of pulverisation and cataclasis of the host rock (Nelson 1985). Mineral filled fractures refer to those which have previously been open and in-filled with secondary or diagenetic crystalline growth, whilst vuggy fractures refer to those where dissolution of an earlier mineral cement has occurred essentially re-opening the fracture.

The notion of fracture stratigraphy (Laubach et al. 2009) focusses primarily on the extent and intensity of fractures, as opposed to that of mechanical stratigraphy, which focuses on subdividing units into distinct mechanical zones, such as that of in the works of Ogata (2012) and Braathen et al. (2012). Fracture stratigraphy is based more on the lithological properties and the responses to deformation. Fracture is a method that has long been appreciated (e.g. Willis 1984; Currie et al. 1962). Understanding this relationship can aid in significantly improving insight into paleo-stress calculations, as well as constraining the nature of subsurface fluid flow, such as water or hydrocarbons (Underwood et al. 2002).

In mildly deformed rocks where little or no faulting or folding is present, it is often the case that the individual bed lithology, thickness and its mechanical properties will affect the nature of deformation with regards to fracturing (Hanks et al. 1997; Underwood et al. 2002). However, it is important to note that stratigraphical controls on fracture patterns and zonation will also be discretely influenced by the larger scale mechanical stratigraphy, which can vary greatly from that of the sediment stratigraphy, as noted by Gross et al. (1995) and Hanks et al. (1997).

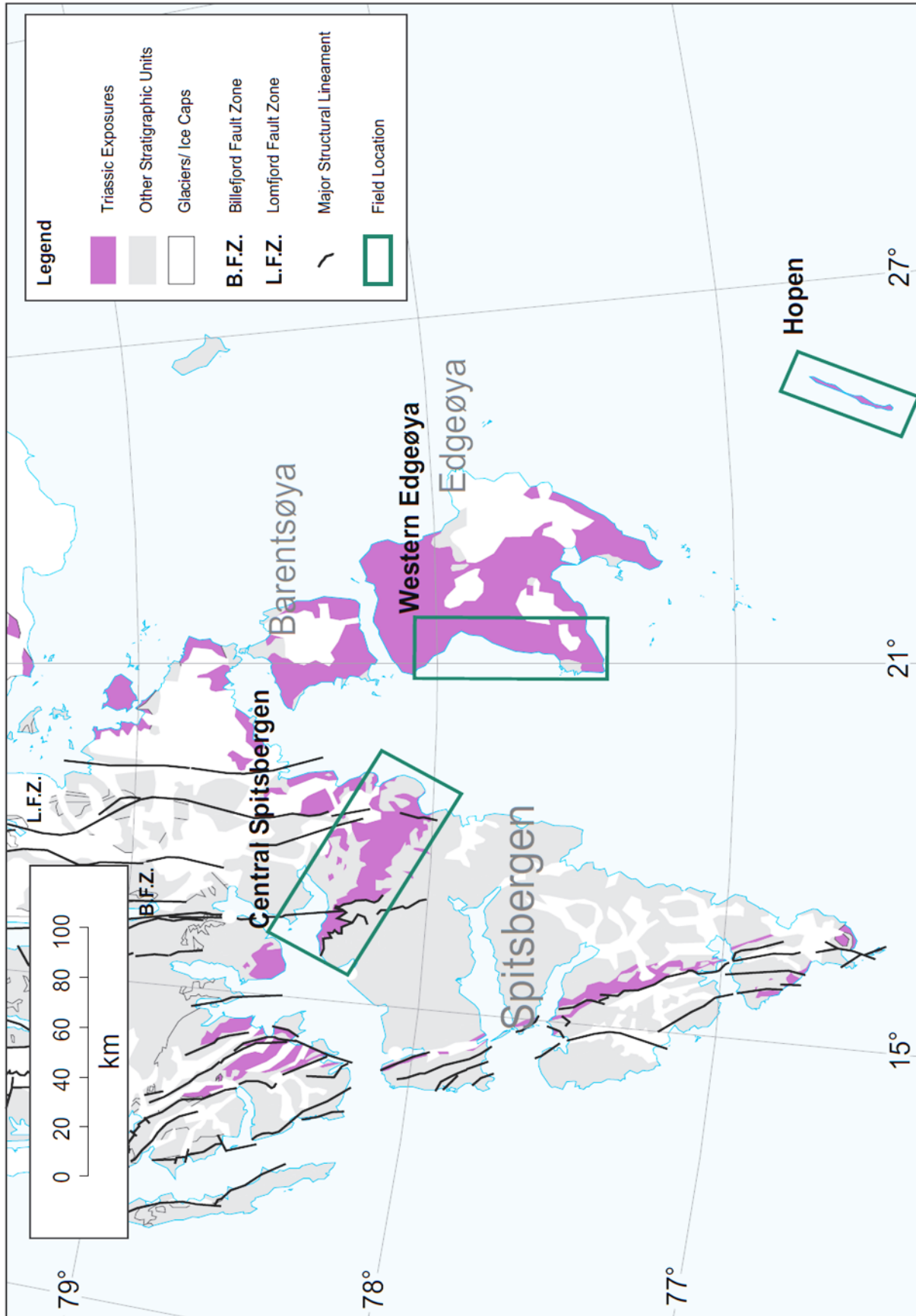
## 4. Fieldwork

The field campaign associated with this project allowed for extensive dataset throughout the region of Svalbard to have been collected, which has occurred over two field seasons, through the summers of 2011 and 2012. An overview map of field areas visited, within their regional context, is displayed in Figure 9.

Fracture specific studies for this project commenced in July 2011, within the area of Sassenfjorden at the locality of Deltanaset. Here numerous outcrops along the beach section and also those within a narrow valley known as Konusdalen, were observed. At these locations sedimentological logs have been drawn and the nature of fracturing recorded. Fieldwork during this period was conducted in co-operation with master student Laura Farrell formerly of the University of Edinburgh and the UNIS CO<sub>2</sub> Lab. Two detailed reports from this location have been produced (Farrell 2011; Lord 2012). In addition a larger scale field campaign by the UNIS CO<sub>2</sub> Lab superseded this work, with data and observations being published by Ogata (2012).

Later in the field season of 2011 the island of Hopen situated in the south east of Svalbard was visited by an expedition consisting primarily of representatives of; The Norwegian Petroleum Directorate, SINTEF Petroleum Research, Lundin Petroleum, Idemitsu Petroleum Norge, accompanied by a contingent of students and researchers from various higher education and research institutions. The aim of the expedition was to focus on revising the lithostratigraphical knowledge of Hopen and update the existing Norwegian Polar Institute geological map, with benefit being to help constrain offshore-onshore correlations in the Northern Barents Sea.

Hopen was later revisited for a limited period during July 2012 with a short return expedition to Deltanaset following shortly after. In order to constrain data, between Central Spitsbergen and Hopen, a 9 day expedition to Edgeøya organised by SINTEF Petroleum Research and Wintershall was exploited, in order to gather as extensive fracture dataset as possible for this project. In addition to the work undertaken at the locality of Deltanaset a further location was visited in August 2012 and focussed on the mountain of Trehøgden, flanking the valley of Sassendalen.



**Figure 9:** Overview map of Svalbard, displaying the regions in which field areas belong and the presence of Triassic Exposures within Svalbard. Base map edited from Norwegian Polar Institute.

During the field season, numerous excursions with various oil companies were conducted and any available opportunity to collect fracture and sedimentological data was exploited. These extra excursions allowed for a further locality in Agardhbukta, on the east coast of Spitsbergen to be visited, where the uppermost (Isfjorden Member) of the De Geerdalen Formation is exposed along a coastal section. This spread of localities essentially compiles a dataset of fractures and sedimentological logs throughout the 'Triassic belt' of central and eastern Svalbard.

This chapter will discuss the regional and local geology of field locations visited throughout the various field campaigns and will compliment this with detailed maps and figures. In addition to this these maps will provide a reference for data locations and will display log names, traces and fracture scan-line locations where applicable.

## 4.1 Current Triassic Stratigraphy and Tectonics of Field Areas in Central Spitsbergen

The regional tectonic geology of Central Spitsbergen field area is essentially dominated by; the large scale Cenozoic transpressional tectonic structures to the west, a central foreland basin zone and a foreland provincial zone to the east (Braathen et al. 1999).

The Early-Cenozoic orogeny, which has resulted in the formation of the West Spitsbergen Fold and Thrust Belt, is the contractional fold and thrust belt tectonic expression (Dallman et al. 1993; Bergh et al. 1997); brought on by a major, intra-cratonic, transpressive, dextral transform (Orvin 1940; Harland 1969; Birkenmajer 1972; Bergh and Andresen 1990; Braathen et al. 1999; Leever et al. 2011) along the continental margins between Greenland and Svalbard. This formed essentially as a result of sea floor spreading, during the opening of the North-Atlantic and Arctic Ocean (Myhre et al. 1982; Eldholm et al. 1987). The region is dominated by structural deformation, primarily; en-echelon folding, prominent strike-slip faults with associated smaller, local extensional features (Bergh and Andresen 1990).

This orogenic event induced basin formation in the hinterland of this migrated fold and thrust belt, resulting in a gentle synformal basin formed as a gravitational depression in front of a migrating thrust wedge, with an associated component of local transtension (Braathen et al. 1999; Bruhn and Steel 2003). This has later been filled with sediments derived from the mountains formed in the west, now forming the stratigraphy of the Van Mijenfjorden Group with the Firkanten Formation as the lowest stratigraphical unit. These Cenozoic sediments lay atop a regional unconformity of Cretaceous age at the base of the basin (Steel and Worsley 1984; Maher et al. 1995; Braathen et al. 1999; Bruhn and Steel 2003).

The Locations to the east within the foreland province (Braathen et al. 1999) can be seen to be dissected by the Billefjorden and Lomfjorden Fault Zones, both long lived faults formed by earlier tectonic episodes during the Caledonian (Johannessen and Steel 1992; Leever et al. 2011) which have seen reactivation and inversion throughout the Cenozoic (Ringset and Andresen 1988; Andresen et al. 1992).

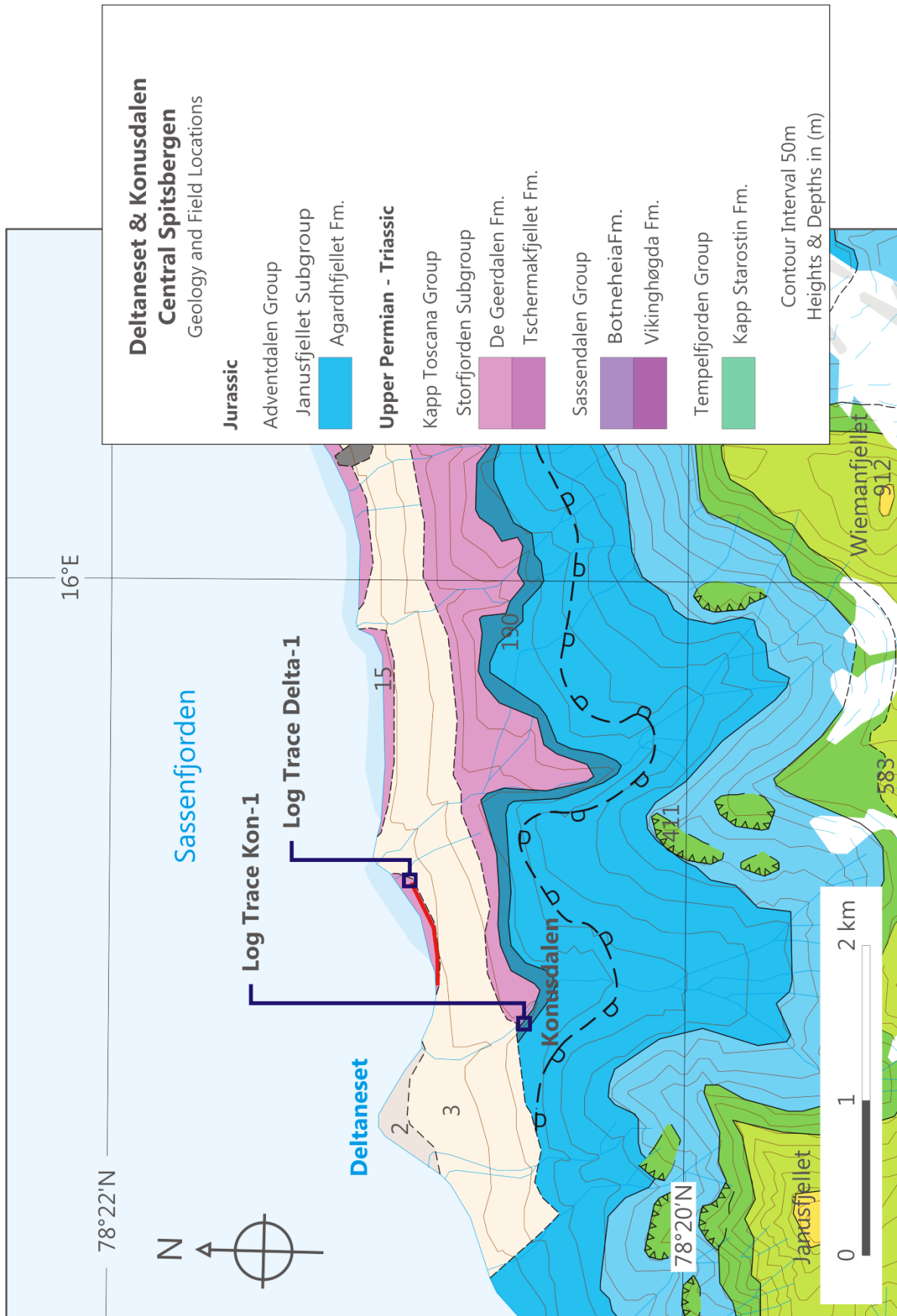
Throughout the Adventdalen area lays a prominent thrust zone formed as a result of Cenozoic compressional tectonics, where floor and roof thrusts have detached within



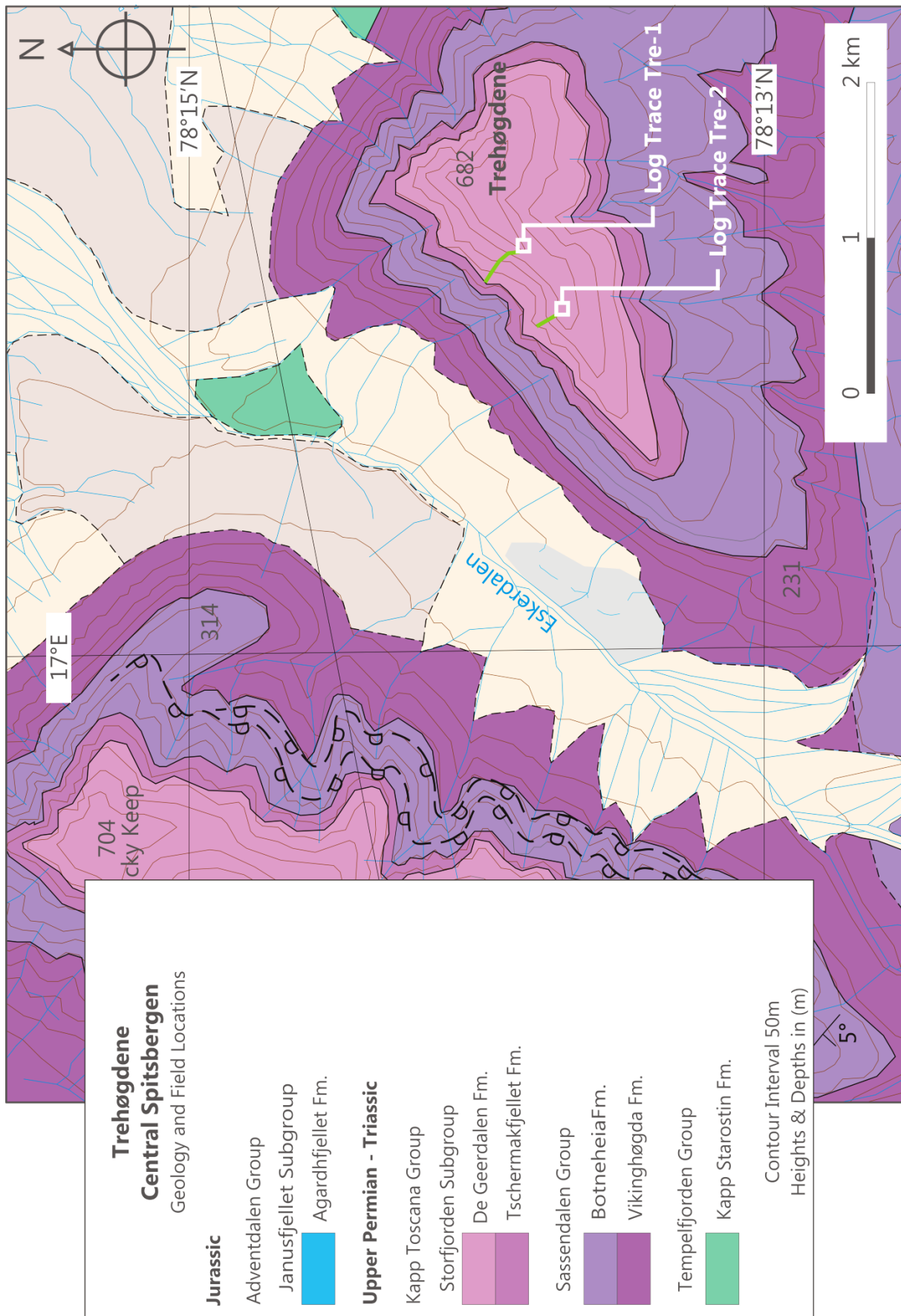
soft shales of Triassic and Jurassic age (Haremo et al. 1990; Major et al. 1992). The upper roof thrust of this fault duplex has been inferred to emerge from within Jurassic shales of the Agardhfjellet Formation at Deltaneset (Haremo et al. 1990; Major et al. 1992), whilst the floor thrust can be seen to emerge from within Triassic shales on the mountain of Dalsnuten, in close proximity to the field area of Trehøgdene.

In terms of fracture patterning throughout Central Spitsbergen, it must be maintained that these lineaments can have a significant controlling impact on the orientation of fracturing seen within exposures.

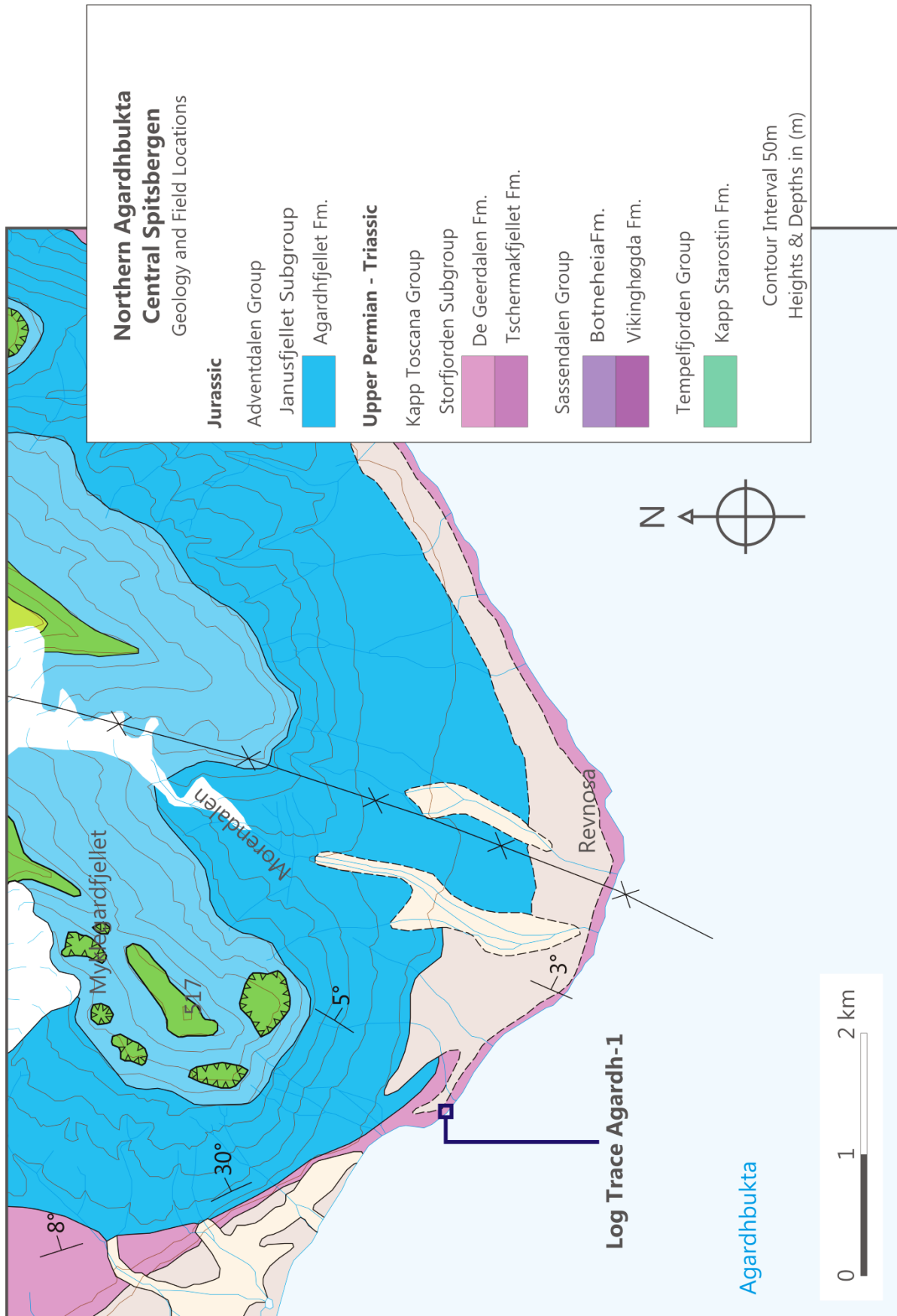
The stratigraphy of Central Spitsbergen is highly diverse and outcrops in and around the visited field areas (Shown in figures 8, 9 and 10) show a range of stratigraphy from the upper Permian through to the Cenozoic. The lowest stratigraphical unit seen in field areas of Central Spitsbergen is that of the Permian, Kapp Starostin Formation (Major et al. 1992; Mørk et al. 1999). This is subsequently overlain with the entire Triassic succession at Trehøgdene, with only the uppermost of the De Geerdalen Formation being exposed at Deltaneset and Agardhbukta (Major et al. 1992). The succession overlying the Triassic, consists of the Late Jurassic to Early Cretaceous strata of the Adventdalen Group and Janusfjellet Subgroup (Parker 1967; Dypvik et al. 1991; Mørk et al. 1999). This is then unconformably overlain unconformably by the Cenozoic (Paleocene – Eocene) Van Mijenfjorden Group (Harland 1969; Manum and Thronsen 1986; Major et al. 1992).



**Figure 10:** Geological map of the Deltaneset and Konusdalen Field Locations. The log trace of Delta-1 is shown in red. Map edited after Major et al. (1992).



**Figure 11:** Geological map of the mountain of Trehøgdene and field locations on the NW flank. Log traces of Tre-1 and Tre-2 are shown in green. Map edited after Major et al. (1992).



**Figure 12:** Geological map of field location in northern Agardhbukta. Note the presence of a synclinal feature to the east of the field location. Map edited after Major et al. (1992).

#### 4.1.1 Deltaneset – Sassenfjorden

N78° 20' E15° 50'

Deltaneset, (map shown in Figure 8) as the name suggests is a small melt-water fed delta protruding in to the east west trending glacially formed Sassenfjord. Here excellent exposures of the middle-upper Triassic succession has been observed in two key outcrops; the cliff exposures along the eastern Deltaneset beach and the small outcrops within the valley of Konusdalen. Despite the relative inconsistency of exposure and in general poor quality of outcrops present here, it is possible to obtain sedimentological logs through the upper De Geerdalen and lower Knorringfjellet Formations. Furthermore the area also lends itself well to fracture data collection given the good quality of exposure along the coastal section. Recent studies relating to the understanding of fractures in the region around Longyearbyen have been undertaken. The work of Ogata et al. (2012) especially compliments this thesis as does that of Senger et al. (2011), with regards to field areas in Central Spitsbergen.

With note to the regional geology of this specific location Deltaneset lies on the north western limb of Cenozoic formed, central Spitsbergen basin's syncline (Major et al. 1992), with regionally dipping beds to the south west of approximately 2-3°. The locality of Festningen represents the opposing limb of this syncline, where more intensely deformed and near vertically dipping beds are present. Deltaneset also represents some of the closest exposures of the De Geerdalen Formation to the UNIS CO<sub>2</sub> Lab well sites, an area of extreme interest given the chosen reservoir target for CO<sub>2</sub> injectivity being the Triassic succession (UNIS CO<sub>2</sub> Lab 2012; Olausen et al. 2011; Braathen et al. 2012).

#### 4.1.1.1 Deltaneset Beach - Sassenfjorden

N78° 20' E15° 53'

The cliff section present along the eastern beach at Deltaneset (figures 10 and 13) offers excellent exposures and allows for a vertical stratigraphy, through the upper De Geerdalen Formation including the Isfjorden Member (type section by Pčelina, 1983 and Mørk et al., 1999 is at Storfjellet in Sabine Land) of approximately 50-55 m to be observed. Beds here dip gently towards the west-south west and a wide variation in lithologies and facies is present. The exposures here represent the lowest stratigraphical units measured in this area.



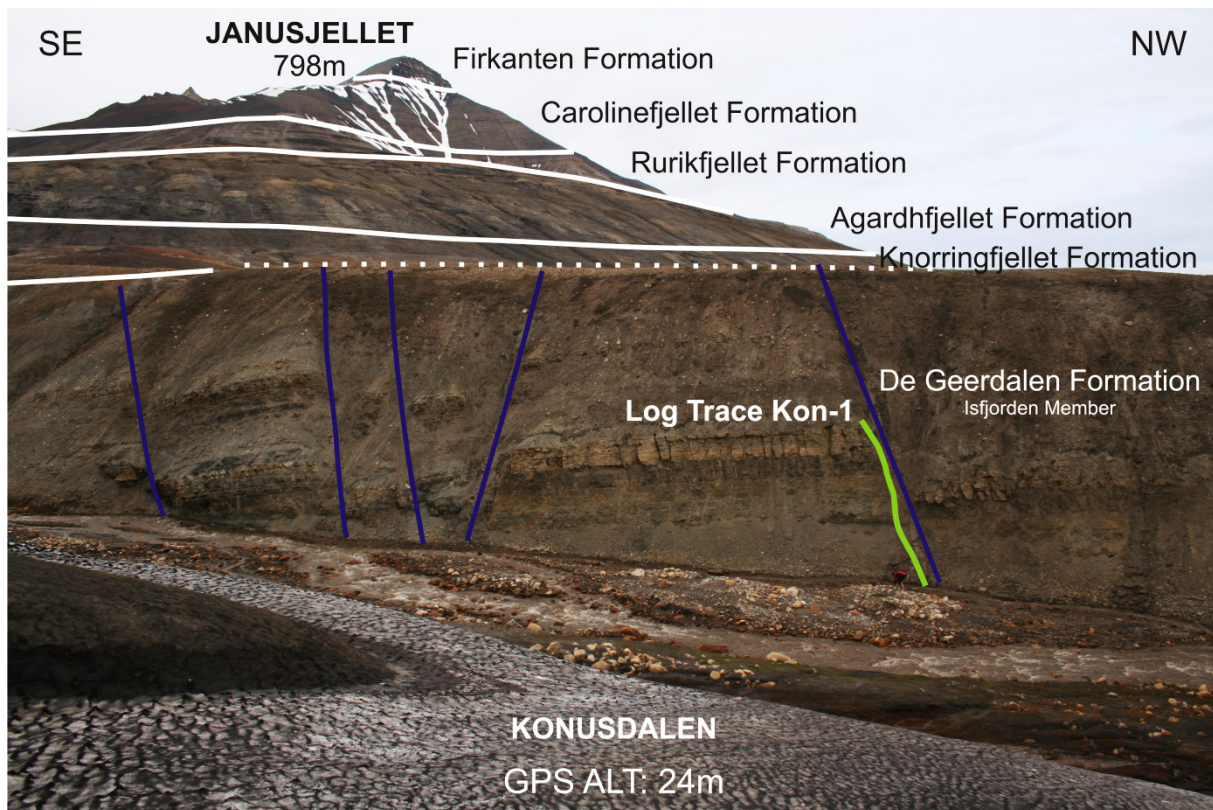
**Figure 13:** Annotated photograph showing the location of the Deltaneset Beach section and the log trace for Delta-1. Photo: Gareth S. Lord.

In this location one stratigraphical log 'DELTA-1' (Log trace shown in Figure 13) has been recorded with fracture scan-lines being taken at prominent intervals where, exposures allowed for good data collection. All data relating to this section has been entitled 'DELTA-1.#' the suffix representing the scan-line number from the base of the log vertically.

#### 4.1.1.2 Konusdalen

N78° 20' E15° 52'

Konusdalen (Figure 14) lies perpendicular to the southern coast of Sassenfjord and therefore presents the opportunity to obtain a 3D overview of fracture characteristics. The section comprises of the uppermost Isfjorden Member and can be extended up to the Slottet Bed at the base of the Knorringsfjellet Formation, pronounced here as a thin from 10 cm thick bed of phosphatic nodules and gravel.



**Figure 14:** Annotated photograph of the Triassic exposures seen within the valley of Konusdalen. Note the presence of extensional normal faulting. The log trace of Kon-1 is presented as is the overall stratigraphy throughout the area. Geologist for Scale. Photo: Gareth S. Lord.

The exposures in the valley also feature prominent, but relatively minor normal faults striking east west, shown in purple on Figure 14, with relatively steep dip angles and offsets of only a few metres. This section has also been logged for sedimentological and lithological characteristics and this log is presented as 'Kon-1', with fracture data taking the suffix 'Kon-1.#' (Log trace shown in Figure 14).

#### 4.1.2 Trehøgdene - Sassendalen

N78° 14' E17° 07'

Trehøgdene, aptly named due to its prominent 3 peaks, is a near 700 m high mountain, situated on the south eastern sides of the wide, postglacial valley, of Sassendalen (shown in figures 11 and 15). The mountain lies at a juncture between Eskerdalen and Sassendalen, some 33 km to the East of Longyearbyen and 30 km south east of Deltaneset. Stratigraphically speaking the mountain is host to; the gentle slope forming Vikinghøgda Formation, the prominent and steep black cliff forming paper shales of the Botneheia Formation, the shales of the Tschermakfjellet Formation and finally the lowermost sandstones and shales of the De Geerdalen Formation (Figure 15).



**Figure 15:** An annotated photo along the north western flank of Trehøgdene in Central Spitsbergen, highlighting the local stratigraphy and log traces of Tre-1 and Tre-2. Photo: Gareth S. Lord.

A thrust fault duplex which can be seen to have migrated in an east-north easterly direction and lay underneath Adventdalen, is expressed by the current (revised) geological map by Major et al. (1992) as outcropping along the easternmost exposure of Trehøgdene's north eastern flank. What is more, the floor thrust is also mapped as an assumed feature, along the south eastern flank of Sticky Keep (refer



to Figure 11), a neighbouring mountain to the north west of Trehøgdene. The thrust however is especially evident within the flanks of the mountain of Dalsnuten, to the south west of Trehøgdene, and is interpreted due to variations in thicknesses of strata within the Vikinghøgda Formation.

None of these thrusts however, have been observed or mapped at the localities visited by this thesis and no evidence for thrusting being present was evident in the field. Regardless of this factor, the potential presence of these local thrusts still remain a critical consideration, with regards to the analysis of fracture data given the proximity of these structures to the field locations.

Here two stratigraphical sections have been recorded TRH-1 and TRH-2. TRH-1 covers the extent of the De Geerdalen Formation from its base to the plateau where the section ends. Log TRH-2 is expressly related to lateral correlation of a prominent sandstone body, see Figure 13. All fracture data has been assigned the abbreviation TRH-1.# and TRH-2.# respectively.

### 4.1.3 Northern Agardhbukta – Storfjorden

N78° 02' E18° 41'

In the large embayment of Agardhbukta, a small exposure of Triassic rocks can be found along the northern coast (shown in figures 12 and 16) and is some of the easternmost Triassic exposures in Central Spitsbergen. The well exposed outcrop consists of the uppermost of the Isfjorden Member, of the De Geerdalen Formation and much alike the exposures in Konusdalen, is capped by the Slottet Bed, represented here as a sub metre thick carbonate bed. The stratigraphy is then overlain by Jurassic and Cretaceous strata of the Adventdalen Group, as shown on the geological map in Figure 12.



**Figure 16:** Overview photograph of the Agardhbukta beach section, showing the upper Isfjorden Member of the De Geerdalen Formation and the log trace for Agardh-1. Note the Slottet Bed lies just atop this cliff section. Geologists for scale. Photo: Gareth S. Lord.

Fracture data collection occurred here in a single day, during the summer of 2012. In addition a short log of the coastal cliff section has also been obtained; this log is presented as 'Agardh-1' (Trace shown on Figure 16), fracture data is termed Agardh-1.1.

## 4.2 Current Triassic Stratigraphy and Tectonics of Field Areas in Western Edgeøya

Edgeøya (See figures 1, 7 and 17) is situated in the east of the Svalbard archipelago and as the third largest island in Svalbard constitutes a landmass of some 5073 km<sup>2</sup> (Orheim and Hoel 2003). The island is comprised almost exclusively of Mesozoic exposures with only minor outcrops of the Permian being observed in the central region of Edgeøya (Mørk et al. 1982). Present on the island are the Permian cherty mudstones of the Kapp Starostin Formation, unconformably overlain by the Vikinghøgda Formation, Botneheia Formation, Tschermakfjellet and the De Geerdalen Formation (figures 17 and 18). The present Norwegian Polarinstitutt map of Edgeøya (Dallmann et al. 1994) also shows the presence of the Wilhemøya Subgroup in the southern parts, however this is debatable. It should also be of note, that the age of the De Geerdalen Formation on Edgeøya is older than that of Hopen, as deposits here were emplaced upon a palaeo-high thus and the top of the section is absent from Edgeøya.

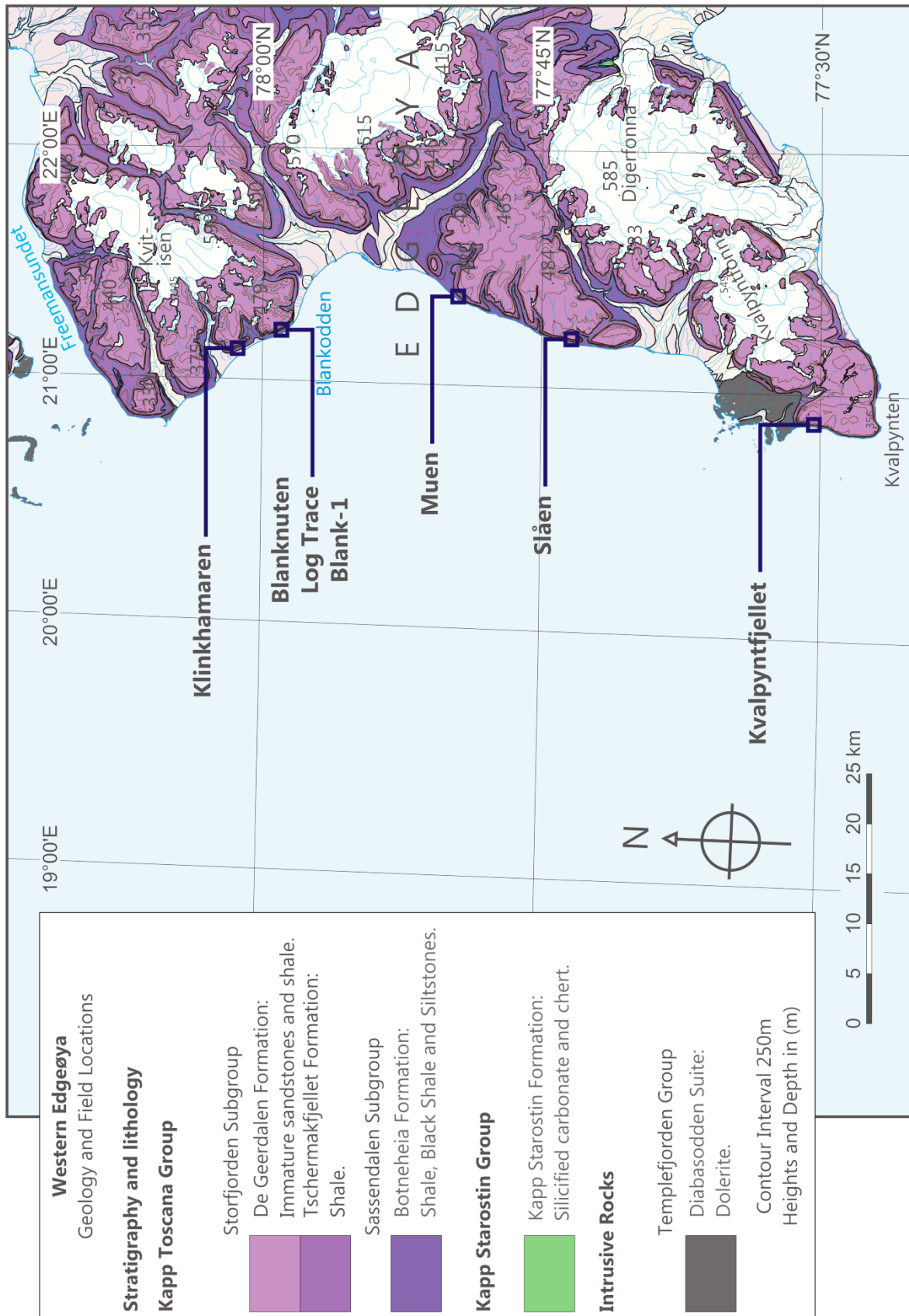
Recent evaluation of the De Geerdalen Formations sedimentology and lateral extent throughout Svalbard has been undertaken by Lock et al. (1974), Glørstad-Clark (2010), Hynne (2010) and Rød (2011). All of whom had a large focus on the Edgeøya region. The De Geerdalen Formation on Edgeøya can be seen to be representative of a prograding deltaic system with both fluvial and tidally influenced sediments of a pro-delta environment being present (Mørk et al. 1982; Hynne 2010; Rød 2011; Glørstad-Clark 2011). This is primarily based on the presence of upwards shallowing and coarsening trends, the presence of both tidally and fluvially influenced sedimentation along with the presence of delta top deposits and palaeosols. These features are specifically observed by Hynne (2010) and Rød (2011) and correspond well to the thin coals noted by Lock et al. (1974).

The mountain of Klinkhamaren in northern Edgeøya is a superbly exposed succession of the De Geerdalen Formation where large scale growth faulting of a delta front can be seen (Rød 2011). In addition to this, field teams from the University Centre in Svalbard have recently conducted new work in the area of Kvalpyntfjellet in south western Edgeøya, where Edwards (1976) observed distinct growth faults.

At present it can be seen that Edgeøya is relatively un-deformed in terms of recent tectonic structures when compared to western Svalbard. Consultation of the present geological map by Dallmann (in prep.) shows no major structural lineaments of any scale on the island. Whilst Cretaceous dolerite dykes and sills penetrate many mountains and form offshore shallows within Storfjorden, the only prominent structural features that have been observed in outcrop to date are those of syn-sedimentary growth faulting seen at various locations along the west coast. These are seen in their most spectacular fashion on steep coastal cliff exposures the mountain of Kvalpyntfjellet in south-western Edgeøya (see Edwards 1976; Osmundsen et al. 2013). Here shallow rooted normal faults detaching at the contact with the Botneheia Formation, can be seen to be overlain by later un-deformed Triassic strata.

The lack of overall regional structural observations however, may be due to the relatively limited exploration of the islands interior (Lock et al. 1978). In spite of this Lock et al. (1978), do relate a similarly north-south trending, but minor structure to those seen on the mountain of Teistberget, in eastern Spitsbergen. The 'Rindedalen Structure' as it is described; is a north-south trending, mono-clinal feature, seen on the southern side of the Freemansundet straight between Edgeøya and Barentsøya and is similar in nature to a further structural feature found nearer to the Lomfjorden Fault Zone at Teistberget. Despite this, the trace of the Rindedalen Structure's hinge point is reported to only be traceable for a mere 20 km (Lock et al. 1978). Both of these are suggested to be Cenozoic in age, by Lock et al. (1978) formed in relation to orogenesis in western Spitsbergen and/or movement along the Billefjorden Fault Zone.

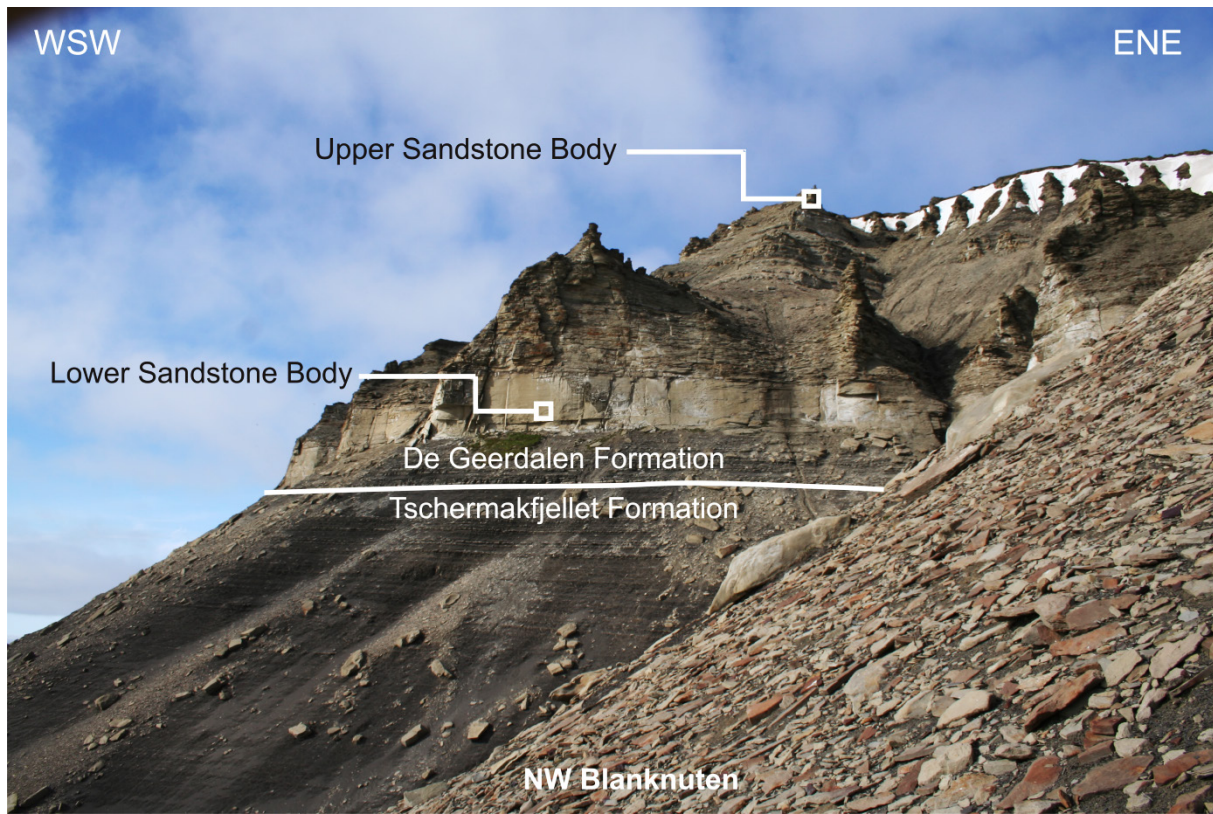
In further relation to regional tectonics, Edgeøya can be seen to form a dome structure (Lock et al. 1978), which rests on the Edgeøya platform (Bergsager 1986; Gabrielsen et al. 1990). This platform is at present informally named but is however defined at the top-Permian boundary (Grogan et al. 1999). It is possible that these domes and the platform itself that now forms Edgeøya may have been formed as a bulge, in relation to earlier tectonic episodes that pre-dated the West-Spitsbergen orogeny. Potentially as early as the onset of the late Triassic where the region was situated on a high, whilst neighbouring areas, notably Hopen were situated on a tectonic low, suggesting basin formation to the south (see Solvi 2013).



**Figure 17:** An overview geological map of the west coastline of Edgeøya and field locations visited. Map adapted after Dallmann (in prep.).

### 4.2.1 Blanknuten

N77° 59' E21° 14'



**Figure 18:** Overview photograph with annotations of the De Geerdalen Formation at Blanknuten. Note the presence of the lower and upper sandstone units. Photo: Gareth S. Lord.

The mountain of Blanknuten (Figure 17), situated on the north-west coast of Edgeøya, has been observed for its Triassic sedimentology, stratigraphy and structural geology, throughout numerous expeditions. The stratigraphy consist purely of the Triassic succession, with the Vikinghøgda, Botneheia, Tschermafjellet and De Geerdalen Formations as shown in Figure 18. For a primary sedimentological analysis readers are urged to consult the theses of Knarud (1980), Hynne (2009) and Rød (2010), which discuss the nature of sedimentology and sandstone architecture in detail. These discussions and interpretations will form the basis for the addition of structural data, by this thesis. A stratigraphical log of the mountain, drawn by Knarud (1980), will be used to constrain structural data to lithology as this section runs through the sandstone exposures observed for fracture analysis. This log is termed Blank-1 and fracture data is expressed as Blank-1.#.

The field time spent at this location could be considered somewhat minimal in comparison to other field areas. Therefore, fracture data collection focussed on two

key exposures of prominent sandstone bodies. The first; a lower, laterally discontinuous, medium grained sandstone body with poorly defined cross stratification, which can be seen to be near massive at its base (Seen in Figure 18). This unit fines upwards into prominently cross stratified sandstone and is capped by shales thin coal and palaeosol horizons. The second is a prominent sandstone exposure close to the mountain summit which features heavily defined, large scale cross stratification throughout its base, which becomes smaller in scale within prominent horizons at its top. The unit is also capped by thin coals and a palaeosol horizon.

#### **4.2.2 Klinkhamaren, Muen, Slåen & Kvalpyntfjellet**

The field areas of Klinkhamaren, Slåen and Muen (Located on the map in Figure 17) represent only a minor component of data taken in the Edgeøya region and presented in this thesis. This is a result of a limited working time allowed at each location, during industry organised excursions which had only a limited scope for fieldwork. However, fracture data collected at these locations is still highly relevant to this project in regional terms and is therefore included, but geology of these locations will be discussed only in brief.

The mountain of Klinkhamaren in north western Edgeøya can be seen to feature prominent growth faulting of a delta front succession, within the lower De Geerdalen Formation. The mountains stratigraphy is host to the main constituents of the Triassic succession with the Vikinghøgda, Botneheia, Tschermakfjellet and De Geerdalen formations all being present. Fracture data has been recorded along the first prominent sandstone horizon within the De Geerdalen Formation, a bed which forms a prominent expression of growth faulting, due to its gently inclined dip to the north-west and an overlying sandstone bed. This data is presented on log Klink-1, from Rød (2011) and fractures have been assigned the expression Klink-1.1 and 1.2.

Fracture data from the mountain of Muen, in mid-western Edgeøya is highly limited due to a very brief excursionary visit. However, the stepped plateau nature of the location allowed for the collection of fracture data in plan view through a short upwards coarsening section of the lower De Geerdalen Formation. This allowed for an excellent 2D constrain on fracture orientations in plain view, as well as providing an excellent opportunity to collect concise fracture distribution data.

The location of Slåen some 11.5 km to the south of Muen features a similar stratigraphy to other locations on Edgeøya; however the units of the Lower Triassic are much lower in altitude, with the Botneheia Formation forming the coastline at the foot of the mountain. Quite extensive fracture data collection has occurred at Slåen given a prolonged day of fieldwork during an Expedition in 2012. This data only covers one particular bed within the lower De Geerdalen Formation; however this is a relatively extensive dataset and allows for an augmentation of the regional fracture orientation dataset.

A minor volume of fracture data has also been collected on the north eastern flank of the mountain of Kvalpyntfjellet in south western Edgeøya. The data has been recorded within a sandstone bed of the De Geerdalen, in close proximity to a dolerite dyke, which cuts sub-vertically through the mountain. The De Geerdalen Formation at Kvalpyntfjellet is famed for the presence of prominent syn-sedimentary faults concluded by Edwards (1976) to be growth faulting of a prograding delta front. However this system suggests a southward progradation of sediments due to the orientation of faulting. This contradicts the general consensus on a north westwards direction of transportation (Osmundsen et al. 2013).



### 4.3 Current Triassic Stratigraphy and Tectonics of Field Areas on Central and Northern Hopen

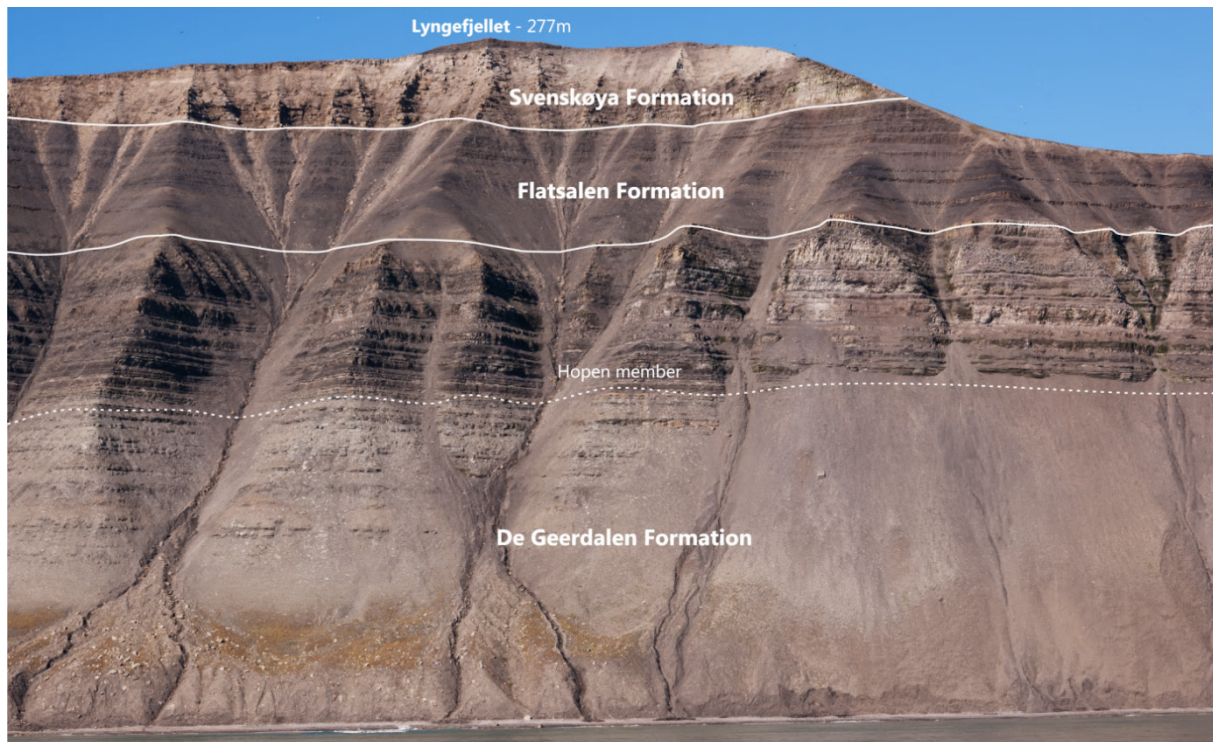


**Figure 19:** An aerial view over the northern and central areas of Hopen Island, South east Svalbard, showing the relatively thin and elongate topography. Photo from Norsk Meteorologisk institutt (2010).

The narrow and elongate island of Hopen, see figures 19 and 20, situated in the far south east of the Svalbard archipelago (refer to figures 1 and 9 for location), presents itself as a solitary bastion of upper Triassic strata, protruding to a height of some 370 m from the Barents Sea. At some 37 kilometres in length and only 2 kilometres in breadth at its widest point and its distal position from other Triassic exposures in Svalbard; the island therefore represents somewhat of a geological oddity to the region.

Hopen on a local scale can be seen to be in a relatively deformed state host to numerous faults and fold structures (Smith et al. 1975; Dallmann 2009; Klausen and Mørk Submitted; Solvi 2013), as seen on the geological map in Figure 21. Hopen rests on a structural high, termed the Hopen High (see Max and Ohta 1988; Doré 1995). This is a horst block system bound to the north-west and south east by large, normal fault systems (Max and Ohta 1988; Johansen et al. 1992; Doré 1995; Grogan et al. 1999) that oppose each other. Hopen may represent the uppermost and exposed segment of this system, albeit significantly eroded. However, Grogan et al. (1999) defined the island very simplistically, as a 'spur' at the south easternmost

segment of the Edgeøya platform, formed amongst a series of delineated terraces by a series of east north east – west south west trending faults.



**Figure 20:** An annotated overview picture of the Hopen Stratigraphy. Photo: Terje Hellem.

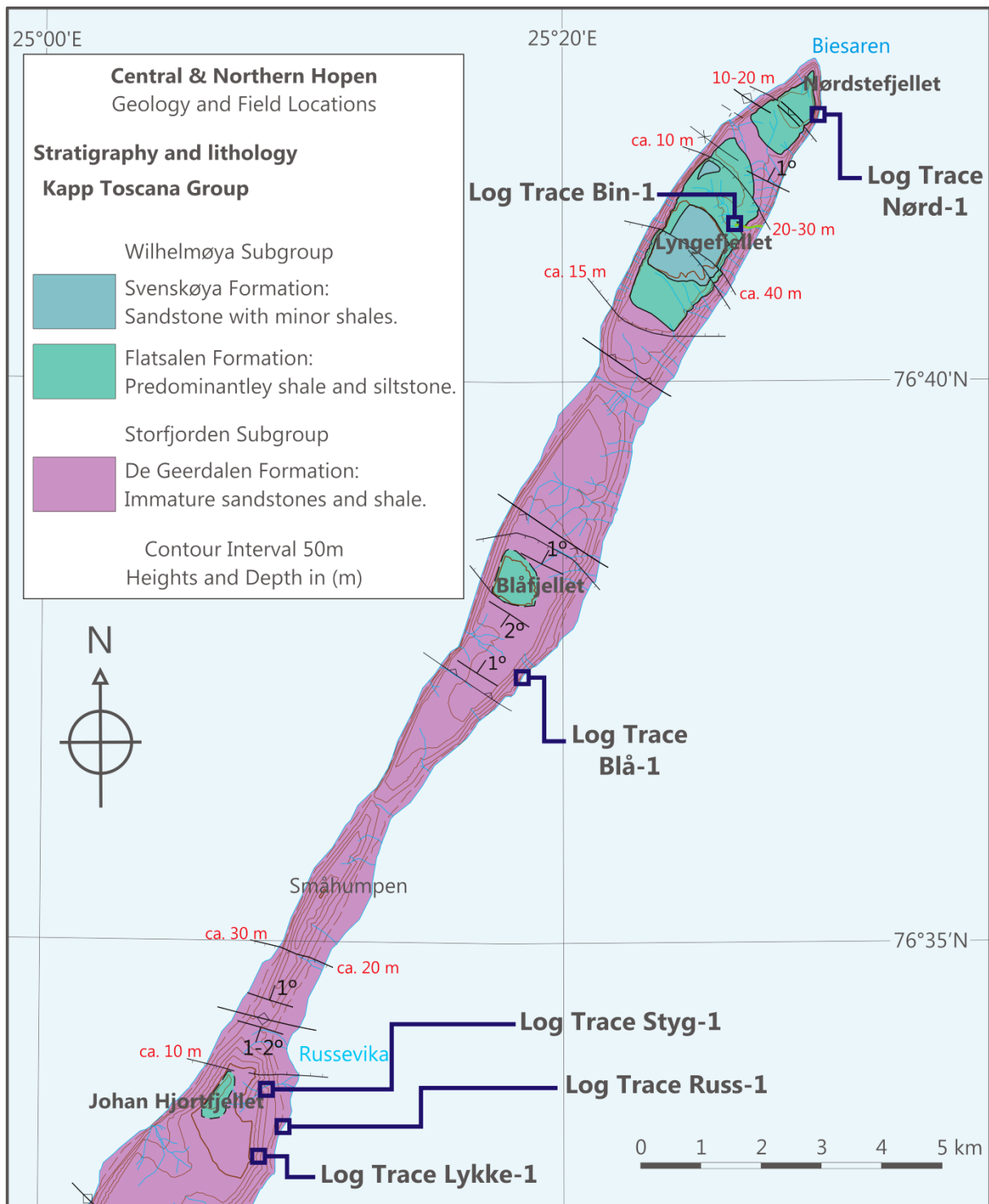
The general structure of the island is seen to be dissected by prominent north west - south east trending normal faults, with dips to both the south west and north east, along with gentle synclinal and monoclinical structures, as shown in Figure 21 (Smith et al. 1975; Klaussen and Mørk Submitted). In some cases faults have been observed to hold a minor component of rotational movement, due to the presence of contrasting fault throws being observed on opposite sides of the island and instances of syn-sedimentary deformation can also be seen (Osmundsen et al. 2013). These fault systems display a form consistent with that of minor graben and horst block structures of an extensional regime; however the orientations are relatively inconsistent with those of larger faults throughout the Northern Barents Sea region (see regional tectonic map, Figure 2).

The stratigraphy of Hopen (as shown in Figure 20), is host to the uppermost of the De Geerdalen Formation, which is subsequently overlain by the shale dominated Flatsalen Formation, with prominent grey sandstones of the Svenskøya Formation

being present only in the north of the island, all of which were deposited during the Late Triassic (Vigran et al. submitted).

The De Geerdalen Formation on Hopen represents an intermittent sequence of thick channel bodies and terrestrial deposits such as thin coals and palaeosols (Klausen and Mørk Submitted). The formation has undergone significant scrutiny throughout recent expeditions, many of which have been conducted in relation to this thesis. Current observations interpret the De Geerdalen Formation as representative of a proximal delta top Environment (Klausen and Mørk Submitted; Solvi 2013). A system home to large scale fluvial and fluvio-tidal channel bodies set amongst delta top and terrestrial deposits, in which several transgressive-regressive cycles can be observed.

The overlying dark shales of the upwards coarsening Flatsalen Formation represent a fully marine transition occurring throughout the late Triassic, with a prominent hard, carbonate rich bed at its base the 'Slottet Bed' (Mørk et al. 1999). This stratigraphically prominent and regionally extensive bed represents a condensed shelf deposit (Mørk et al. 1999) from the Early Norian (Korčinskaja 1980; Basov et al. 1993; Vigran et al. Submitted) and contains fossil specimens. The Flatsalen Formation is then overlain by the fluvially influenced, prominent, grey sandstones of the Svenskøya Formation.

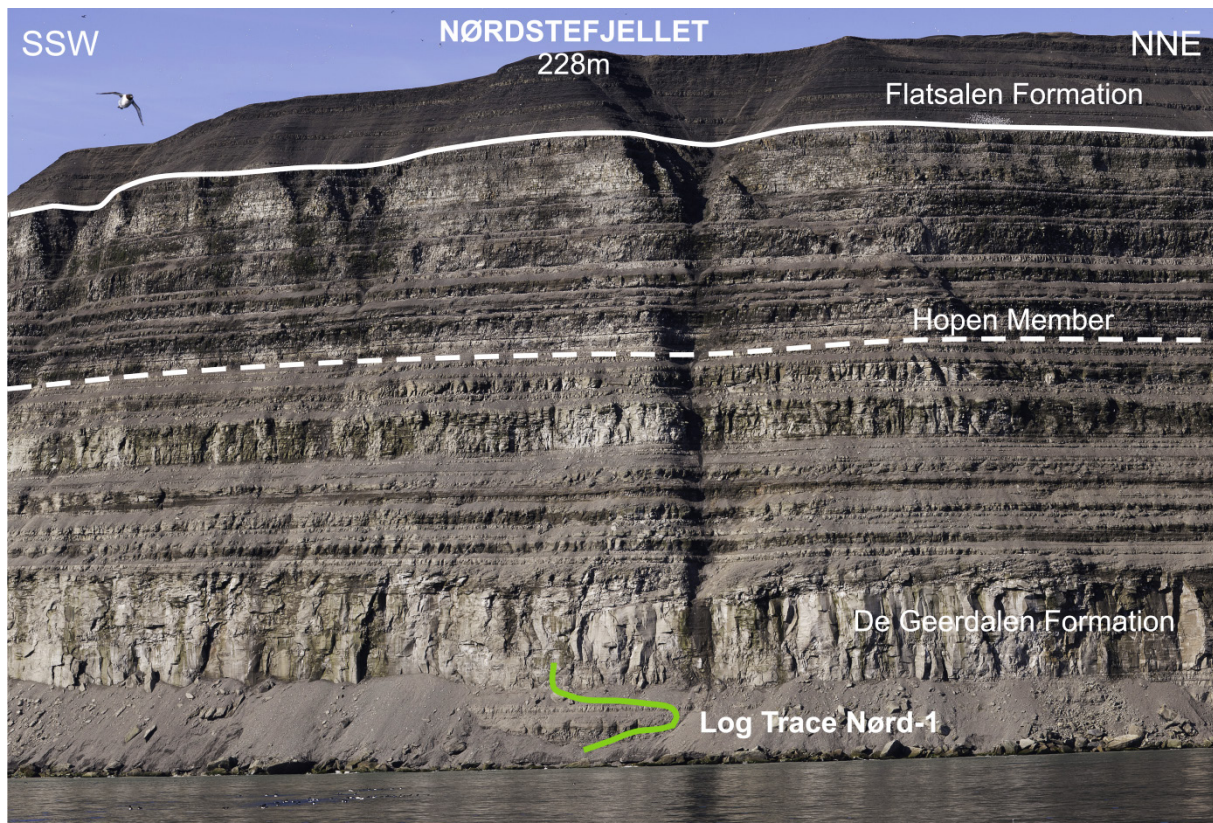


**Figure 21:** An overview geological map of Northern and Central Hopen showing the locations of field areas and log traces, Map adapted after Dallmann (2009).

### 4.3.1 Nørdstefjellet Channel Complex

N76° 42' E25° 29'

The prominent channel body, shown in Figure 22, seen in the north eastern cliffs of Hopen, at the base of the mountain of Nørdstefjellet was visited during the season of 2011. The section alike the following Blåfjellet channel, is home to an upwards coarsening strata capped by a thick sandstone channel body. The steep cliff sections have allowed for detailed sedimentological work to be undertaken alongside fracture observations, within the sandstone unit and its underlying constituents.



**Figure 22:** Overview photograph of the De Geerdalen and Flatsalen Formations at Nørdstefjellet. The lower sandstone body (c.36 m in thickness) forms a prominent fluvial channel complex on Hopen. The log trace of Nørd-1 is also shown. Photo: Terje Hellem.

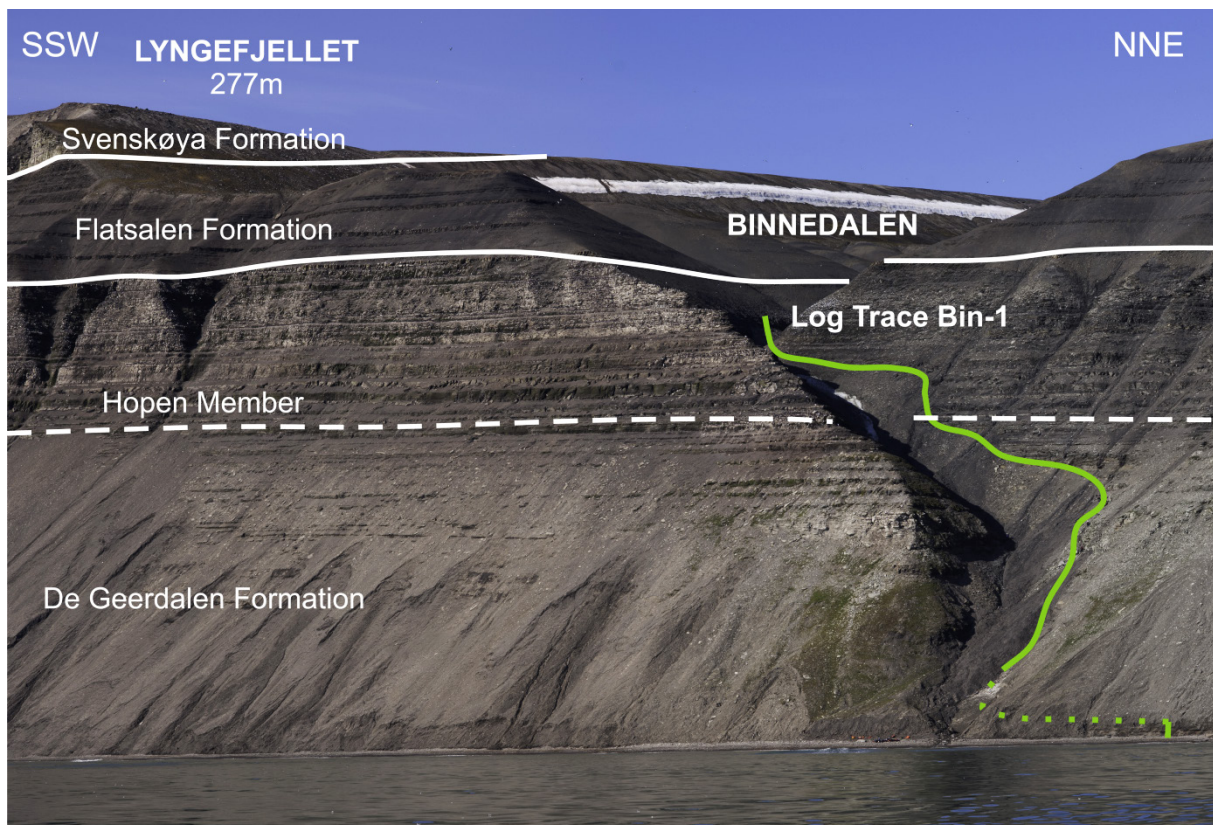
The south westernmost exposure of the sandstone is cut by a distinct normal fault, dipping to the south west, with an approximate throw of some 40 m (Dallman 2009). This fault has been observed at distance to be somewhat host to gentle syn-sedimentary tectonic deformation in the lower Flatsalen Formation, which caps the mountain of Nørdstefjellet. However in the lower coastal section, comprised of the De Geerdalen Formation, no evidence for syn-sedimentary deformation appears to be

present. The general dip of strata in this area of Hopen is placed at approximately  $1^\circ$  to the north east.

A stratigraphical log, Nørd-1 (Trace shown in Figure 22), has been recorded through the strata, from near sea level to a short height within the channel body. Naturally the vertical sandstone cliff limited the ability of data collection. However, the channel bodies thickness was measured at a distance with the aid of a laser range finder unit, housing a built in trigonometry function allowing for a digital estimate of the sandstone thickness. This was determined after multiple efforts to be in the region of some 36 m and this data has been incorporated into the log.

#### 4.3.2 Binnedalen

N76° 41' E25° 27'



**Figure 23:** An overview photograph of the Mountain of Lyngefjellet and Binnedalen in Northern Hopen. The log trace of Bin-1 is shown as is the entire Hopen Stratigraphy. Photo: Terje Hellem.

A long stratigraphical log through the De Geerdalen Formation was produced during the expedition of 2011, by workers; Gunn Mangerud, Morten Bergen and Audun Kjemperud. This 150 m section with the log trace shown in Figure 23, has been used

in order to constrain fracture data to lithology and stratigraphical level. In this thesis the log is denoted as Bin-1.

### 4.3.3 Blåfjellet Channel

N76° 37' E25° 18'

The Blåfjellet channel locality, shown in figures 21 and 24, has been visited numerous times throughout the various field seasons. Whilst the steep cliff sections present this locality as dangerous to work at, the steep cliff exposures of a stacked channel body allow for excellent sedimentological and structural observations. The strata in this area are relatively un-deformed with a gentle 1-2° dip to the north east being present. The lowermost cliff section is formed of a moderately upwards grading shale, erosively cut into by a thick sandstone body, representing a fluvial channel. The clean weathered exposures show clear evidence of tidally influenced sedimentation and clear loading structures are present.



**Figure 24:** An overview photograph of the locality at Blåfjellet. The log trace of Blå-1 is shown. Geologists for scale. Photo: Gareth S. Lord.

The channel body has been observed for sedimentology and fracture analysis with a line scan being recorded parallel to the cliff section. A stratigraphical log termed Blå-1 (Trace shown in Figure 24), obtained during the summer of 2011 during co-

work with Tore Klausen, will allow for constraint of fracture data to lithology and a detailed discussion of the channels sedimentology and structures can be found in Klausen and Mørk (Submitted.)

#### 4.3.4 Russevika Beach Section

N76° 33' E25° 9'

The Russevika beach section shown in figures 21 and 25, represents a small but excellent series of exposures within the lower parts of the De Geerdalen Formation at Hopen. The wave cut platform, consisting of a channel body that presently extends into the Barents Sea as a reef, not only allows for a plan view through the channel feature but also for detailed fracture measurements to be conducted. The clean and well exposed cliff section is host to a short upwards coarsening profile, host to a prominent coal bed and root horizons.



**Figure 25:** An overview photograph of the beach section to the south west of Russevika. Here clean, wave cut exposures allow for a detailed sedimentological analysis as well as fracture observations. Geologist for scale. Photo: Gareth S. Lord.

A short stratigraphic log; Russ-1, has also been recorded at this section (Trace shown in Figure 25) in partnership with Tore Klausen, allowing for fracture measurements recorded at this locality to be associated with their lithology. Further



fracture observations have been made on the wave cut platform extending out into the sea which becomes accessible at low tide. This reef forming platform can be seen from altitude to be remnant of a hard, erosion resistant sandstone body protruding into the Barents Sea.

#### 4.3.5 Johan Hjortfjellet – Styggdalen and Lykkedalen

N76° 33' E25° 8' and N76° 33' E25° 8' (Respectively)

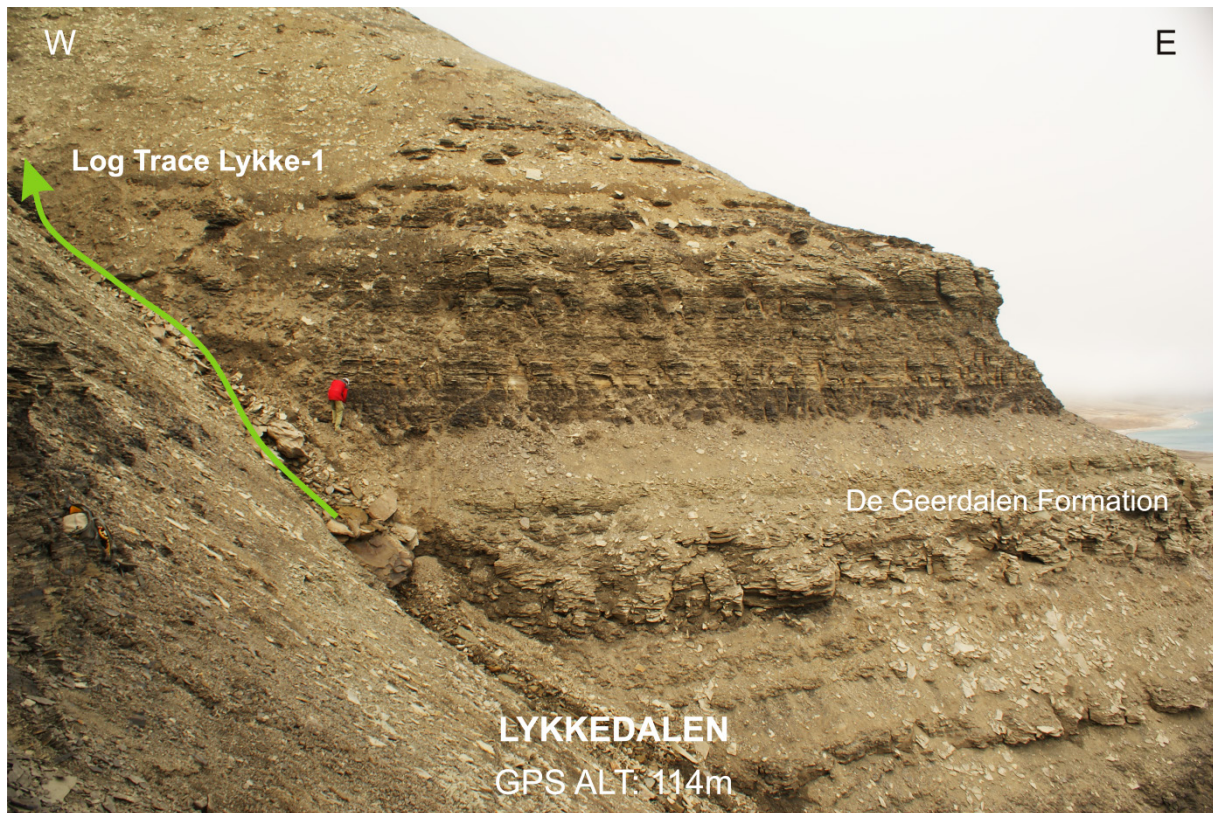
The local geology on the south eastern flank of the mountain of Johan Hjortfjellet is, alike Binnedalen, predominantly intermittent sandstones and shales, demarcated into the upper and lower channel zones and is capped by the Hopen member. The north easternmost corner of Johan Hjortfjellet is incised by a prominent valley, terminating in a steep, ice filled gorge, see Figure 26.



**Figure 26:** An overview of the location within the upper gorge of Styggdalen at Johan Hjortfjellet. Note the prominent trough cross bedding within the sandstone bed and nature of clean exposure lending well to fracture analysis. Geologist for Scale. Photo: Gareth S. Lord.

The valley named Styggdalen has been visited and a location defined within the upper gorge, where excellent exposures of trough cross bedded sandstone have been cleanly eroded. This gorge allowed for a relatively long scan-line of fracture data, through channel facies sandstone. On the south eastern slope of Johan

Hjortfjellet, a small quantity of fracture data has been collected alongside a stratigraphic log through the upper section of the De Geerdalen Formation, Figure 27.



**Figure 27:** An overview photograph of the De Geerdalen Formation on the south eastern slope of Johan Hjortfjellet, named Lykkedalen by the 2011 Hopen expedition. The log trace of Lykke-1 is shown. Geologist for Scale. Photo: Gareth S. Lord.

The sedimentological log in this instance has been produced by Tore Klausen and Morten Bergan, along a section within a small valley named Lykkedalen by the team in 2011. This section termed Lykke-1 (A small section of the log trace is shown in Figure 25) in this thesis will be used to constrain a small quantity of fracture data recorded in this area of the island. Midway through this section, a thick sandstone body has been measured and this is deemed to be correlatable with those seen within the upper gorge of Styggdalen.

## 5. Methodology

### 5.1 Sedimentological Logs

In order to tie lithological type, grain size and facies to fracture data, standard sedimentological logs have been recorded in the field. These focus primarily on; the measurement of beds/ packages of bed thicknesses, evaluation of grain size, a consideration for the mud:sand ratio within beds and any present sedimentological structures are recorded.

Logs have been drawn to scale in the field, typically 1:50 on standard graphical paper, but in some instances, for example in bad weather where field notebooks have been used, field logs have been drawn to a scale of 1:100 for ease of use. Upon return from field exploration all sedimentological logs have been graphically digitised with the aid of computer software and in this case CoreIDRAW x4 has been used. All logs are presented in Appendix 1, alongside a composite of fracture information from each location.

Logs that have been drawn in the field by other workers or are held within the Hopen Project Database have been accredited suitably where appropriate.

### 5.2 Fracture Orientation Data

Fracture orientation data has been collected in the field using a standard geological compass (Silva Type 15TDCL) with inbuilt clinometer. Orientations of planes deemed suitable have been recorded for their strike orientation and angle of dip. All measurements have been recorded in degrees and with the application of 'right hand rule' method of measurement. These fracture orientations will be displayed in the normal sense by way of stereographic projection (equal area – lower hemisphere), which allows for the graphical presentation of planar features in terms of both linear orientation and dip angles. Furthermore, rose-diagrams have been produced and these allow for the projection of strike orientations to be plotted against frequency of occurrence. These are shown as frequency weighted rose-diagrams, where individual fracture orientation data is presented as a percentage of the applied dataset.

### 5.3 Fracture Scan-Lines

The method of obtaining fracture data through the application of scan-lines, allows for a lateral transect along an outcrop to be observed for fracture characteristics. This method is therefore the most simplistic way to quantify the spacing and density of fractures with regards to horizontal distance. Each fracture has been measured with regards to its spacing along the scan-line and its relationship to other fractures.

For the purpose of this thesis, fracturing within exposures have been categorised into two prominent types. Those that can be seen to propagate through multiple lithologies/beds and those that do not, either being bed confined or terminating at a bed contact or mechanical layer (Gross et al. 1995), e.g. another fracture plane.

Each fracture has also had its planar orientation data recorded using the standard strike and dip measurement method. This data has then been extrapolated into stereo nets, rose plots and histograms in order to aid data analysis. Furthermore each scan-line has been visually recorded with photographs in order to allow for a visual representation of the scan-line to be displayed.

It should be noted that due to the intense nature of weathering and erosion that occurs in Svalbard, despite the lack of vegetation, laterally continuous exposures are often rare with much being scree covered therefore it is often the case that scan-lines are abruptly short. Furthermore scan-line orientation plays a key role in defining what fracture sets will be measured. For example, scan-lines parallel to one or more fracture sets will not feature any measurements, therefore these will only account for those fractures which are oblique or perpendicular to the orientation of measurement. Likewise scan-line orientations that are oblique to numerous fracture sets will not only show a greater variance in fracture orientation but also the densities.

### 5.4 Field Fracture Classification

In order to maintain control over the dataset, without over complication of fracture characteristics, a simple method of categorisation will be implemented, as fractures are measured along scan-lines. Whilst it would also be considered ideal to measure fracture aperture and trace length, the very nature of exposures in Svalbard renders this somewhat impossible and any data would be somewhat misleading. This is due to the often covered nature of exposures in which the entire fracture trace cannot be

seen and in instances where it can, it is often the case that outcrop architecture prevents access, in order to fully measure fracture traces. In order to account for this, fracture trace lengths will be defined as those that appear to be confined to individual layers and those that can be seen to penetrate multiple beds.

#### **5.4.1 Steep Fractures:**

The very nature of this thesis is to understand the nature of steep fracturing and jointing within the De Geerdalen Formation, thus when observing outcrops, only steep fracture measurements have been recorded. However, this presents somewhat of a grey area with regards to the definition of a steep fracture and therefore this will be defined here, for context use within this text.

Fractures observed in the field can be seen to come in many different forms thus in this thesis a steep fracture is defined as any with a dip surface greater than 60°. However it must be noted that fractures with a lower angle of dip, moderate fractures, have also been measured, most notably if these appear to intersect larger steep fractures.

##### **5.4.1.1 Through-going Fractures:**

Through-going fractures, shown in orange in Figure 28, are defined as those which can be observed to propagate through multiple layers of bedding and strata in a regular or irregular fashion of up to any trace length. Conjugate fractures that propagate through multiple layers but terminate against another fracture plane are also categorised as through-going.



**Figure 28:** A simplified overview photograph of a scan-line at within the Isfjorden Member at Deltaneset, the scan-line is recorded within an upwards coarsening package of shale and sandstone. Shown is the nature of through-going (Orange) and layer internal fracturing (Blue). Note how all fractures terminate along the contact with the finer grained bed of soft shale above the upwards coarsening package. Also note the nature of layer internal fracturing with regards to the shale to sand transition zone. Geologist for scale. Photo: Gareth S. Lord.

#### 5.4.1.2 Layer Internal Fractures:

Layer internal fractures, which are shown in turquoise in Figure 28, are defined quite simply as those that can be seen to be confined to a single lithological bed, where they either terminate against a primary fracture plane, without cutting other layers, or are seen to terminate at bed boundaries.

## 6. Results

Prior to any discussion of data, this following chapter will display the nature of fracture data both visually and graphically in order to allow for a concise discussion to be made. The field areas for regional analysis have been categorised as; Central Spitsbergen, Western Edgeøya and Central and Northern Hopen. Of these three areas; 16 field locations have been visited which has yielded 14 stratigraphical logs of which 6 are presented from project data and have been produced by other participants. The total numbers of fractures throughout Svalbard is tallied at 844 and these can be tied into a total of 58 fracture scan-lines; 21 within Central Spitsbergen, 23 on Western Edgeøya and 15 in Northern and Central Hopen.

### 6.1 Sedimentological Logs & Scan-line Data

At localities in Central Spitsbergen; 11 scan-lines have been recorded throughout the Beach Section at Deltanaset (Delta-1), with one scan-line within an upwards coarsening unit at Konusdalen (Kon-1). At the mountain of Trehøgdene; 8 have been recorded in total with 5 scan-lines with the section Tre-1 and 3 within the section of Tre-2. The Beach section at northern Agardhbukta has also been logged (Agardh-1), with one scan-line being recorded within a prominent, cliff forming, shale exposure of the Isfjorden Member.

Western Edgeøya has seen two scan-lines recorded in a gently dipping sandstone unit at Klinkhamaren and is presented on log, Klink-1. At the mountain of Blanknuten a series of 7 scan-lines have been recorded through various exposures in the lower section and are presented alongside log, Blank-1. At two scan-lines recorded on a plateau surface have been recorded and will be presented separately. Slåen, alike Klinkhamaren has been observed for fractures along a single sandstone unit and 9 scan-lines are displayed alongside log, Slå-1. Two scan-lines at Kvalpyntfjellet have been recorded in a sandstone bed with close proximity to a dolerite intrusion of Late Cretaceous age and are thus included as a minor component of the dataset.

In the north of the island of Hopen, one scan-line has been recorded through the channel complex at the base of Nørdstefjellet and is presented alongside log, Nørd-1. The section of Binnedalen (log Bin-1) has been extensively observed for fractures with 7 scan-lines being recorded from base to top of section; the lowermost includes fractures within close proximity to a normal fault. The channel complex at the base of

Blåfjellet has also been logged with one scan-line recorded through the sandstone body at this location. This is presented alongside log, Blå-1. In Central Hopen in the area around Johan Hjortfjellet a series of scan-lines has been recorded. Two have been recorded within the middle section of Styggdalen and these are presented on log, Styg-1. Three scan-lines have been recorded in the area of 'Lykkedalen' at the base, within and above a channel sandstone unit and are presented alongside log, Lykke-1. The beach section of Russevika has also been logged and one scan-line recorded through an upwards coarsening unit of mud and sand. Further fracture data has been observed on a wave cut platform determined to be a sandstone unit of a channel body.

These logs are displayed in Appendix 1.

## 6.2 Fracture Orientations

### 6.2.1 Regional Fracture Orientations

When observing the regional trends within the entire dataset, it can be seen that within the De Geerdalen Formation on Svalbard there is a prominent affinity of fracture orientations to align systematically, into two prominent sets. A third fracture set is also observed as being present in the region around Hopen with some relative dominance in the Hopen dataset, whilst it is observed to be found as a minor component at individual locations on Edgeøya. Smaller subsets, those confined to single field and are not found to be a regional fractures set are also seen to be present within the data. These are noticed due to their tendency to follow an alternative trend to the main fracture sets on non-regional, local scales as a direct result of the local geology. Only one notable fracture subset has been seen to be systematic enough between localities

The following fracture sets are defined purely on their prominence within the dataset with suggestions for their geological age/ timing of formation being discussed in the following discussion chapter.

The nature of these three regional fracture sets is shown in figures 29 and 30 and they are defined as follows:

**Fracture Set 1 (FS.1)** defines itself as a prominent, primarily NNW-SSE trending series of fractures that can be seen to be present on Central Spitsbergen, Western

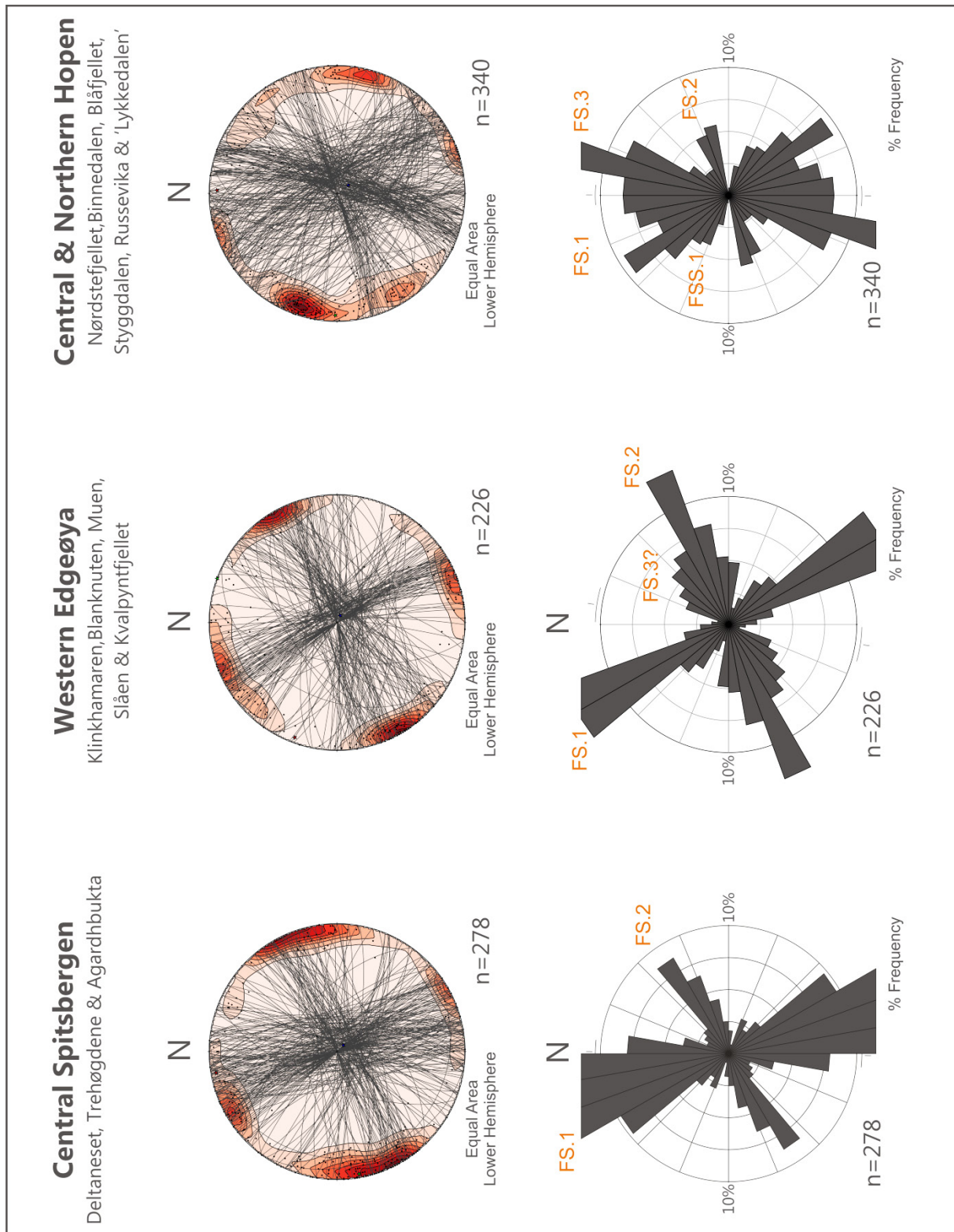


Edgeøya and Hopen. The set can be seen to have minor orientation fluctuations with a more prominent NW-SE trend being observed on Edgeøya and Hopen, whilst Central Spitsbergen features a wider array between NNE and N to SSE and S. FS.1 can be seen to be the most dominant fracture set within the dataset. FS.1 fractures are generally seen to be steeply dipping fractures, often with an irregular plane and a weathered surface. Fractures within FS.1 are generally observed to be Type I mode fractures featuring an open aperture or exposed fracture plane. There is seen to be a minor component of Type II fracturing within the general orientation of FS.1. These are defined within FS.1 where they are seen to be non-systematic and occur only on minor local scales. Systematic Type II fractures are defined within a separate subset.

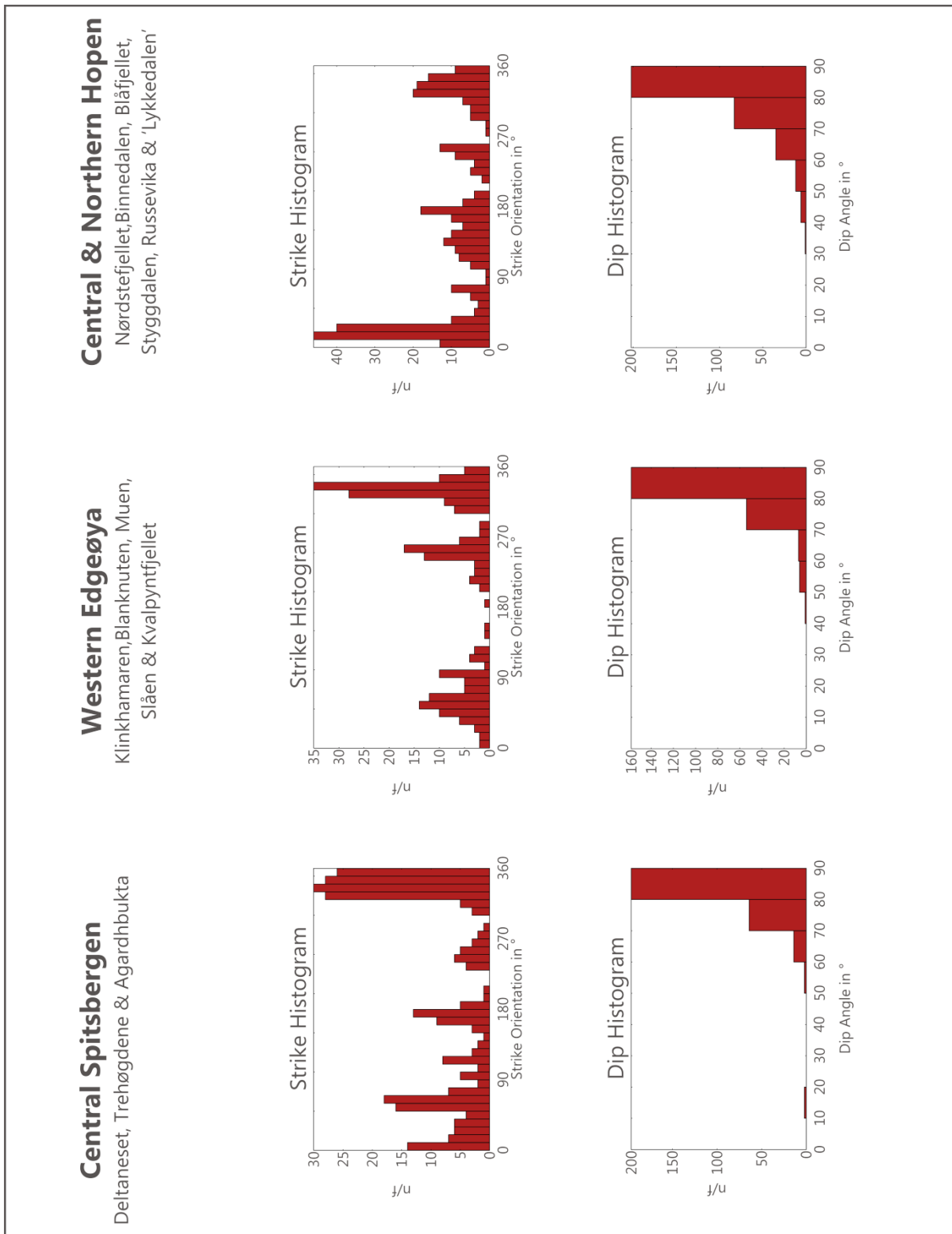
**Fracture Set 2 (FS.2)** can be seen as a prominent ENE-WSW oriented fracture set that can be observed throughout the region in Central Spitsbergen, Western Edgeøya and also in a minor component on Hopen. The set is seen to have little variation in orientation, being clearly constrained between a NE to E – SW to W spread. FS.2 fractures are generally seen to be vertical or sub vertical with few conjugate sets forming in parallel, suggesting a dominantly extensional jointing nature for fractures within this set. These fractures are often seen to be irregular in form with the general orientation of dip being recorded. Alike FS.1 fractures, the steeper fractures found within FS.2 are predominantly Type I fractures, but in instances where Type II fractures are observed in non-systematic form they are incorporated within the FS.1 set.

**Fracture Set 3 (FS.3)** is a fracture set primarily defined on the island of Hopen where they are seen to have a significant dominance within the dataset, but is also seen to be evident in a relatively minor component on Western Edgeøya. The set is oriented in a prominent NNE-SSW trend which is also notably similar to the orientation of Hopen itself. This set does not appear present with any definite prominence at any location on Central Spitsbergen, which cannot be explained in an alternative manner. This set can be considered significant with regards to regional structure due to its prominent orientation disunity with FS.1 and FS.2 and notable presence on Hopen. FS.3 fractures are seen to be Type I mode fractures with no evidence for Type II or III being observed in the field.

**Fracture Sub-Set 1 (FSS.1)** is a subset of systematic fractures found only on the island of Hopen. Whilst these are found to have a close affinity to the orientations of FS.1 fractures, those of FSS.1 distinguish themselves by their Type II mode of fracturing. These are nominally aligned to a more WNW-ESE to NW-SE orientation.



**Figure 29:** An overview of fracture orientations displayed on equal area lower hemisphere stereoplots and frequency by % rose diagrams. Note the identification of regional fracture sets on the rose diagrams.



**Figure 30:** An overview of fracture orientations displayed as strike histograms for each of the field areas, Dip histograms are incorporated to display the overall nature of fracture dip recorded in each dataset.

### 6.2.2 Local Fracture Trends

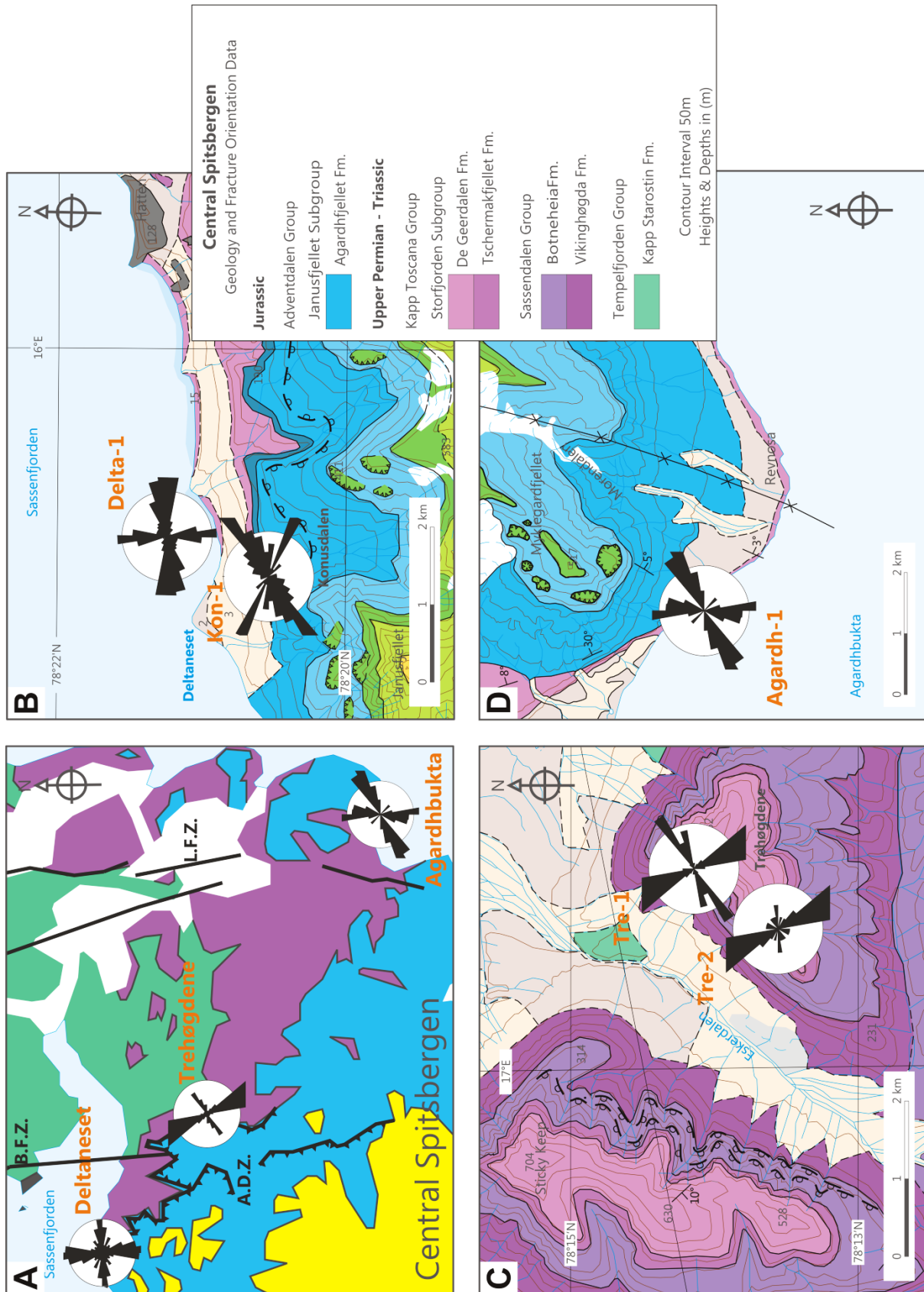
When observing fracture orientations and their respective sets on a local scale, numerous discordances between the observed orientations can be seen. Individual locations do not necessarily represent an area's affinity to any one fracture set; instead this is more a case of fracture density vs. outcrop orientation vs. number of scan-lines. These all play a considerable role in determining the ability to measure fractures within different sets in fair quantity. Anomalous fracture orientations that do not follow any of the three fracture set trends are also more noticeable when datasets are analysed on a local scale. Due to the large quantity of data recorded, results for fracture orientations at each location are displayed in Appendix 1. Thus referrals to these appendices will be made when presenting the results here in this text.

#### 6.2.2.1 Central Spitsbergen

When compiling the data for each individual location within Central Spitsbergen as shown in figures 29 and 31A, it can be seen that there is a minor distortion between the individual locations.

The area of Deltaneset (Figure 31B, Appendix 1.1.1) can be seen to be host to both FS.1 and FS.2 fractures which are clearly defined as being the only fracture sets present at this location. In contrast to this at Kon-1 (Figure 31 B, Appendix 1.1.2) only FS.2 fractures are present and there is evidence for the presence of a minor fracture set with a defined SSE-NNW strike orientation. These fractures are predominantly Type I in mode (see Figure 32). Type II shear fractures are also observed as a minor component within scan-lines along Delta-1 and Kon-1, where they appear as conjugate sets with moderate dip angles.

Likewise at Trehøgdene FS.1 and FS.2 are also seen to be present (Figure 31C), with a minor alteration of orientation of FS.1 being observed at both Tre-1 and 2, where the orientation is aligned more closely to the NNW-SSE directions. In addition FS.2 can be seen to have a more defined E-W strike at Tre-2, whilst it is recorded as being more ENE-WSW at Tre-1. This is evident in the rose diagrams of appendices 1.1.3a and 1.1.3b. FS.1 and FS.2 fractures at Trehøgdene are also characterised by their Type I mode of formation and open extensional nature, which can often be seen to feature a weathered fracture surfaces.



**Figure 31:** Overview maps of fracture orientations within the Central Spitsbergen region; A, shows an overview of regional trends. B, shows Deltanaset and Konusdalen. C, locations at Trehøgdene and D, the field location in Northern Agardhbukta.



**Figure 32:** Example of FS.2, Type I, irregular, steep fractures representing extensional jointing seen at Deltanaset, Central Spitsbergen. Photo is representative of scan-line Delta-1.6 taken through a thick package of laminated shale. Geologist for scale. Photo: Gareth S. Lord.



**Figure 33:** A field photograph showing the nature of vertical to sub-vertical, Type I fractures defined within FS.1 and observed at the beach section at Northern Agardhbukta. Note the tendency of fractures to terminate against beds composed of a finer grain size. Geologists for scale. Photo: Gareth S. Lord.

The locality visited at Northern Agardhbukta again has been observed to be host to FS.1 and FS.2 fractures (Figure 31 D and Appendix 1.1.4); however FS.1 can be seen to hold a slightly adjusted orientation with a slightly stronger N-S and NNE-SSW accordance as seen in appendices 1.1.4 FS.1 and FS.2 fractures seen here are both observed to be Type 1 mode fractures (also clearly shown in Figure 33). Triassic exposures at both locations form as part of the Isfjorden Member and clearly display an uncanny resemblance to those at Deltanaset, but with a significantly lower density.

#### 6.2.2.2 Western Edgeøya

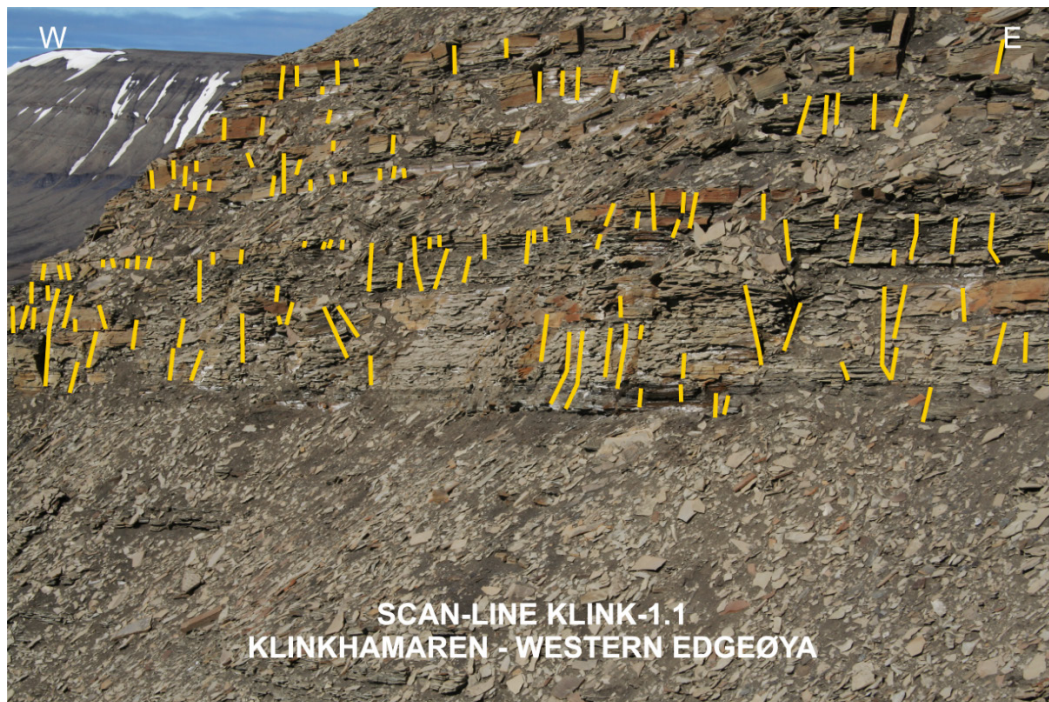
The field locations visited on Western Edgeøya (Figure 36, A and B) are also characterised by fracture orientations trending to the NNE-SSE and ENE-WSW. These have been defined within FS.1 and FS.2. In comparison to Central Spitsbergen the orientations are slightly more NW-SE for FS.1 and ENE-WSW for FS.2.

The northern field localities of Western Edgeøya; Klinkhamaren, Blanknuten (see figures 34, 35 and appendices 1.2.1 and 1.2.2) and Muen can be seen to host a prominent dataset of FS.1 fractures overall, in comparison to locations further south, where FS.1 is seen to be less noticeable at Slåen (Appendix 1.2.3) and absent from recordings made at Kvalpyntfjellet. There is a noticeable trend of fractures aligned to an E-W and ESE-WNW orientation seen at Kvalpyntfjellet and although considered to be misaligned FS.2 fractures, there may also be some evidence for a local subset in this area. The location of Muen was observed to have a clear pattern of Type I FS.1 and FS.2 fracture interactions that could be viewed on a flat plateau surface.

All of the areas visited on Edgeøya feature FS.2 fractures, with the most conformable orientations to fractures in Central Spitsbergen being found at the localities of Blanknuten (Figure 35) and Muen. The nature of FS.2 fracturing at Klinkhamaren, Slåen and Kvalpynten can be seen to hold a minor component of fractures offset in orientation with a stronger affinity to NE-SW strike at Klinkhamaren and Slåen. This may suggest evidence for a more local trend or presence of FS.3 fracture sets in these areas, which may be defined by a regional tectonic style in Eastern Svalbard. Alternatively these orientations could suggest the presence of a subset of systematic



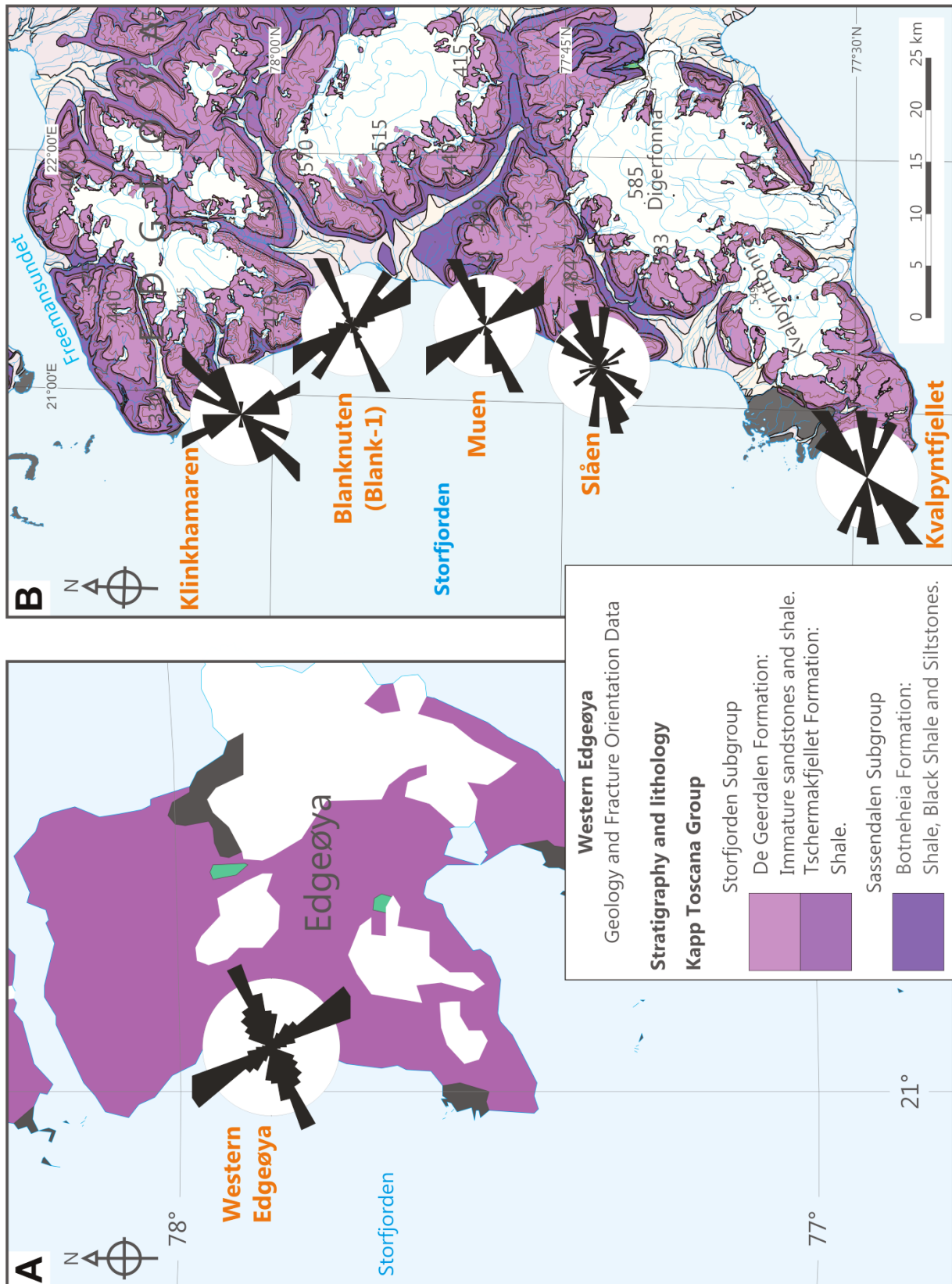
fractures, local to Edgeøya, which may be defined by the tectonic styles or geological features in these areas, rather than large-scale regional trends.



**Figure 34:** Field photograph displaying the open Type I nature of FS.1 fractures seen along scan-line klink-1.1 at Klinkhamaren, Edgeøya. Overall thickness of the sandstone package is c.10m. Photo: Gareth S. Lord.



**Figure 35:** Field photograph showing the nature of FS.2 fractures, observed in a thick sandstone body on Blanknuten, Edgeøya. Field notebook for scale. Photo: Gareth S. Lord.



**Figure 36:** Overview maps of fracture orientations within the Western Edgeøya region; A, regional trends. B Overview of fracture orientations at each field location.

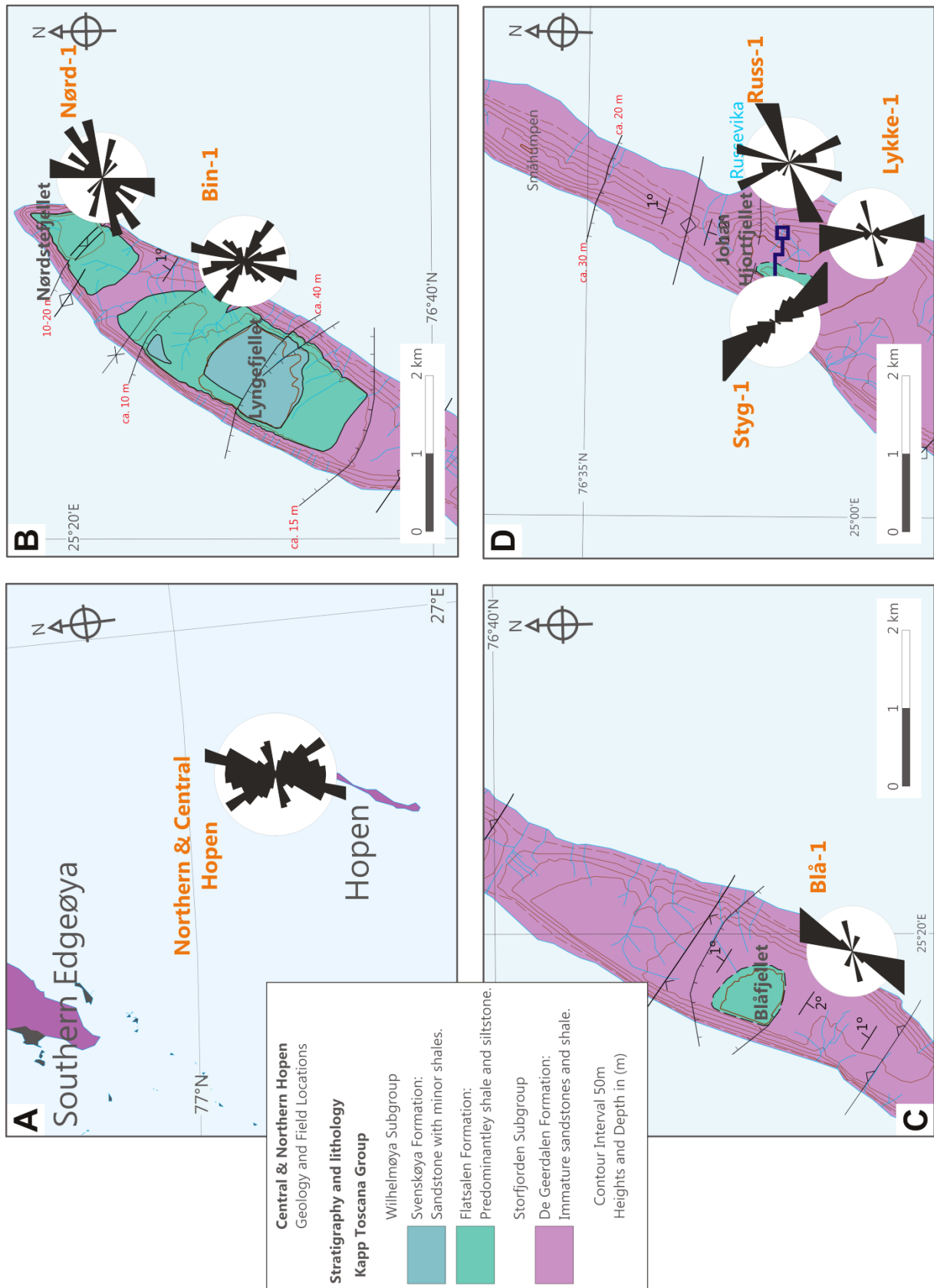
### 6.2.2.3 Central & Northern Hopen

The fracture patterns recorded on the island of Hopen are seen to be somewhat more chaotic than those recorded at other field areas, as shown in figures 29 and 38A. Steep fractures can be categorised into both FS.1 and FS.2 Type I fractures. In this region of Svalbard, a third fracture set FS.3 with Type I fracture mode is also seen to be present in a relatively high dominance within the dataset, far more so than those defined as FS.3 on Edgeøya. All of the visited locations on Hopen express a presence of FS.3 fractures. In addition to this, their prominence is noted as being mostly seen the thicker and more competent sandstone bodies present on Hopen.

At locations such as Nørdstefjellet, Blåfjellet, Johan Hjortfjellet and along a wave cut platform at Russevika, FS.3 fractures (Figure 38 B, C and D) are seen to form as large joints that can also be seen to act as exfoliation surfaces on the outcrop face as shown in Figure 37. Whilst these exposures are generally in parallel to the recorded scan-line, the staggered nature of exposure due to weathering of these thick sandstone bodies, allows for fracture orientation data to be recorded.



**Figure 37:** Field photograph showing the clear nature of sub-vertical, irregular, Type I fracturing seen in FS.3b fractures at Johan Hjortfjellet, Hopen. Geologist for Scale. Photo: Gareth S. Lord.



**Figure 38:** Overview maps of fracture orientations within the Hopen region; A displays regional trends, whilst B is local to Northern Hopen. C shows the area of Blåfjellet and D, Central Hopen.

At Styggdalen there is seen to be a component of conjugated fractures observed within a channel body. These fractures feature a moderate to steep dip and are seen to interact with other lower angle fractures and large through going Type I fractures of FS.1. They are observed as having a close spacing and often terminate against another fracture plane or bedding plane, forming triangular or rhombic blocks (Figure 39). Despite their strong FS.1 strike alignment these can be observed to differ from FS.1 fractures due to Type II fracture mode. This is in direct similarity to the fractures observed in the lower sections of Binnedalen (Bin-1.1) where fractures appear more Type II in mode but in a similar orientation to FS.1 fractures, these are also defined as FSS.1 fractures.



**Figure 39:** Detail field photograph showing the nature of Type II fracturing found in similar orientation to FS.1 fractures within a thick sandstone unit at Styggdalen, Johan Hjortfjellet. Note the interactions of the opposing fracture planes. Similar structures are observed at the base of Binnedalen in close proximity to a normal fault. These fractures are defined as a separate subset FSS.1. Photo card for scale (10cm). Photo: Gareth S. Lord.

### 6.3 Fracture Densities and Lithological Relationships

Alongside the orientation data, the spacing between individual fractures has been measured in order to allow for the density of fractures to be understood. Results presented in this chapter are derived from composite tables of fracture data presented in Appendix 3. Data will be presented and analysed on a regional scale, due to the limited collection of data at individual locations. The results will primarily focus on the regional variations in fracture spacing, average fractures per metre and the bed thickness of scan-lines.

In order to account for varying lithology, individual scan-lines have been assigned a lithological type based on the most dominant lithology observed along the scan-line. Each assignment of a lithological association to scan-lines is based on observations made in the field and those recorded in the sedimentological logs in Appendix 1.

These lithological associations are categorised as such:

- **Sandstone** dominated beds, homogeneously composed either entirely of sandstone or containing minor components of shale. Example shown in Figure 40. Sandstone dominated scan-line data is presented in Appendix 3.2
- **Sandstone and Shale** dominated beds, a primarily heterolithic bed of shale with inter-bedded sandstone, shales with a high overall percentage of sandstone or upwards coarsening beds which grade from shale into sand. Example shown in Figure 41. Shale and sandstone dominated scan-line data is presented in Appendix 3.3.
- **Shale** dominated beds, consisting primarily of homogeneous fine grained material with little or no sand seen within the exposure. Example shown in Figure 42. Shale dominated scan-line data is presented in Appendix 3.4.

Bed thicknesses have been measured in the field and are presented in the data tables of Appendix 3. Scan-line locations on sedimentological logs in Appendix 1 do not represent exact bed thicknesses due to variations in scale.



**Figure 40:** Example of a homogeneous sandstone dominated bed from Blanknuten Edgeøya. Notebook for Scale. Photo: Gareth S. Lord.



**Figure 41:** Example of a heterolithic sandstone and shale dominant bed, with a prominent upwards coarsening trend from shale to sandstone, from Deltanaset, Central Spitsbergen. Geologist for Scale. Photo: Gareth S. Lord.



**Figure 42:** Example of homogeneous shale dominated bed from Binnedalen, Hopen. Geologist for scale. Photo: Gareth S. Lord.

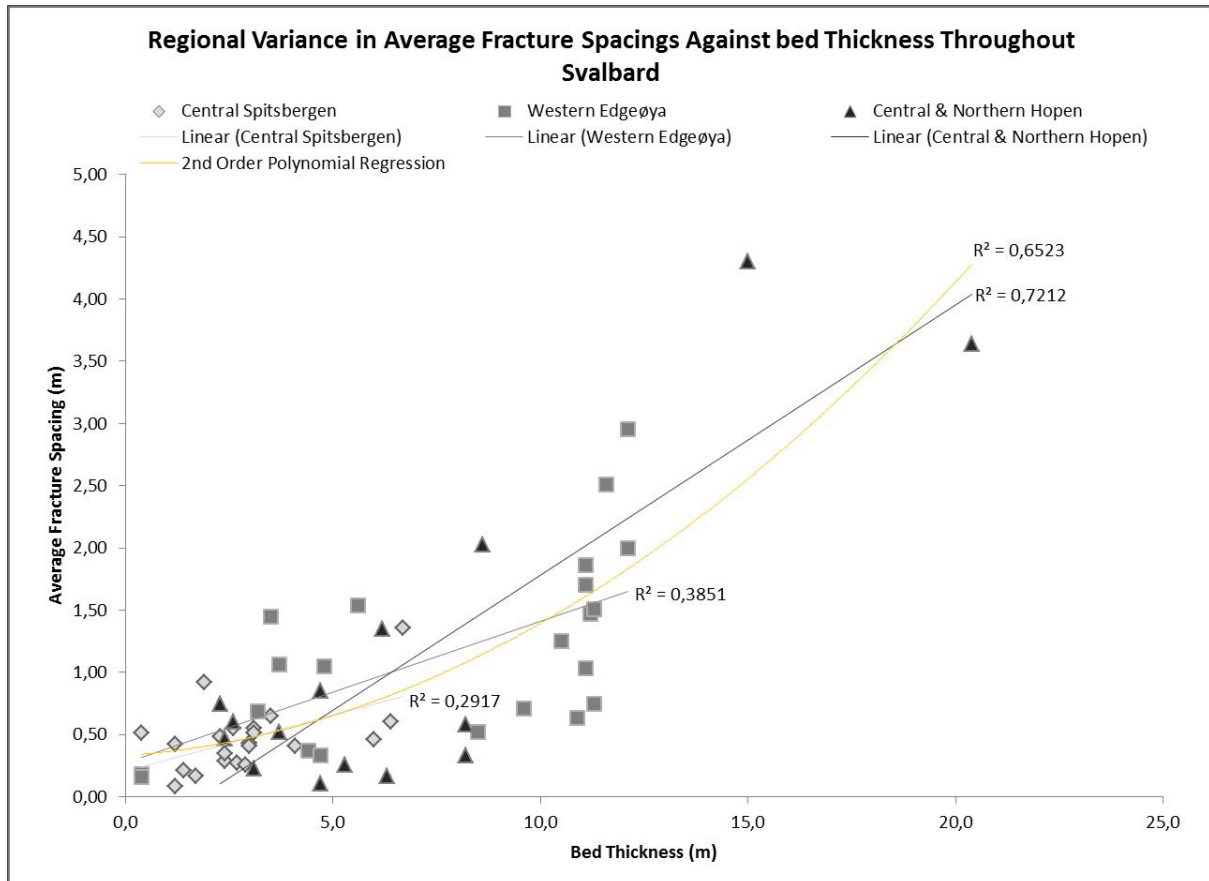
### 6.3.1 Regional Trends – Fracture density and bed thickness by area.

The graph of regional trends of average fracture spacing against bed thickness, (Figure 43), produced from data in Appendix 1.1, which includes all scan-lines measured in all lithologies, can be seen to show; a moderate, positive and partially linear correlation between the bed thickness and the average fracture spacing measured in the field. There is also a noticeable clustering of data from Central Spitsbergen which can be seen to occupy the lower left corner of the graph. Here it can be seen that in Central Spitsbergen bed thicknesses are relatively thinner than those seen on Western Edgeøya and have in general a lower average fracture spacing, but do not contrast significantly with data from Central and Northern Hopen which can be seen to occupy a relatively weak correlation, but does display a better dispersion of data along the trend line.

The  $R^2$  values displayed on Figure 43 show that there is an increasingly strong relationship between average fracture spacing and bed thickness from Central Spitsbergen to Western Edgeøya and further south to Central and Northern Hopen. The linear regression trend for Central Spitsbergen shows a relatively weak relationship to the data points, with a low  $R^2$  value ( $R^2=0,2917$ ), whilst data from Western Edgeøya has a slightly stronger relationship based on the  $R^2$  value of the data set ( $R^2=0,3851$ ). The linear regression applied to data from Central and



Northern Hopen shows a comparatively strong relationship to the data points with a higher  $R^2$  value ( $R^2=0,7212$ ). The second order polynomial trend line applied to the entire dataset shows a moderate strength value for the relationship between data points and the trend line itself with an  $R^2$  value of  $R^2=0,7212$ .

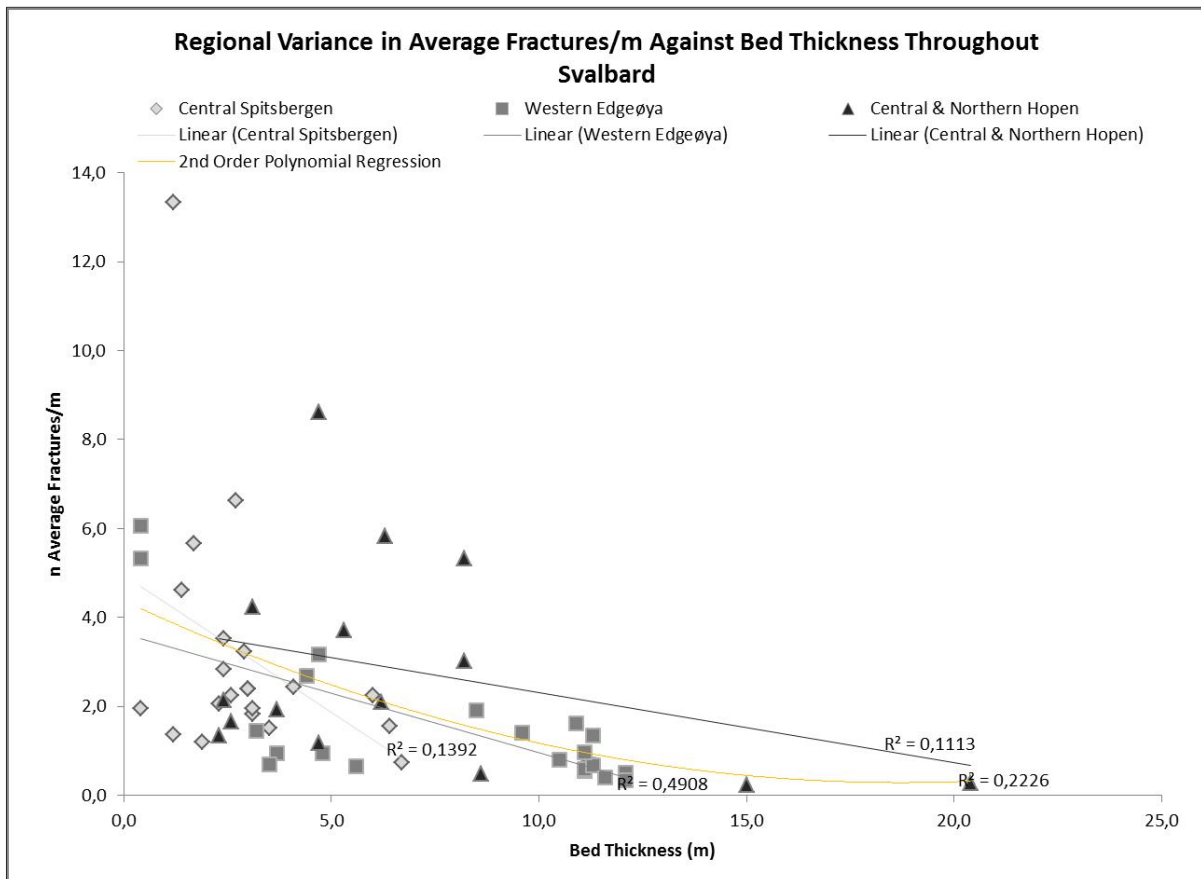


**Figure 43:** Regional variance graph displaying the correlation between average fracture spacing and bed thickness, grouped by field area. Linear regressions for each field area are displayed as are  $R^2$  values for each. Second order polynomial trend line has been applied and  $R^2$  value is shown.

In contrast to Figure 43, the graph in Figure 44 shows a distinctly negative trend with a somewhat moderate correlation when average fractures per metre are compared with bed thickness (not taking lithology into account). As with Figure 43, Central Spitsbergen and Edgeøya display the most noticeable clusters whilst data from Central and Northern Hopen is far more sporadic with a weaker correlation in general.

The  $R^2$  values displayed on Figure 44 show that there is a no noticeable relationship between these  $R^2$  values and average fractures per metre against bed thickness. As locations become more south eastern in Svalbard. The linear regression trend for Central Spitsbergen shows a relatively weak relationship to the data points, with a

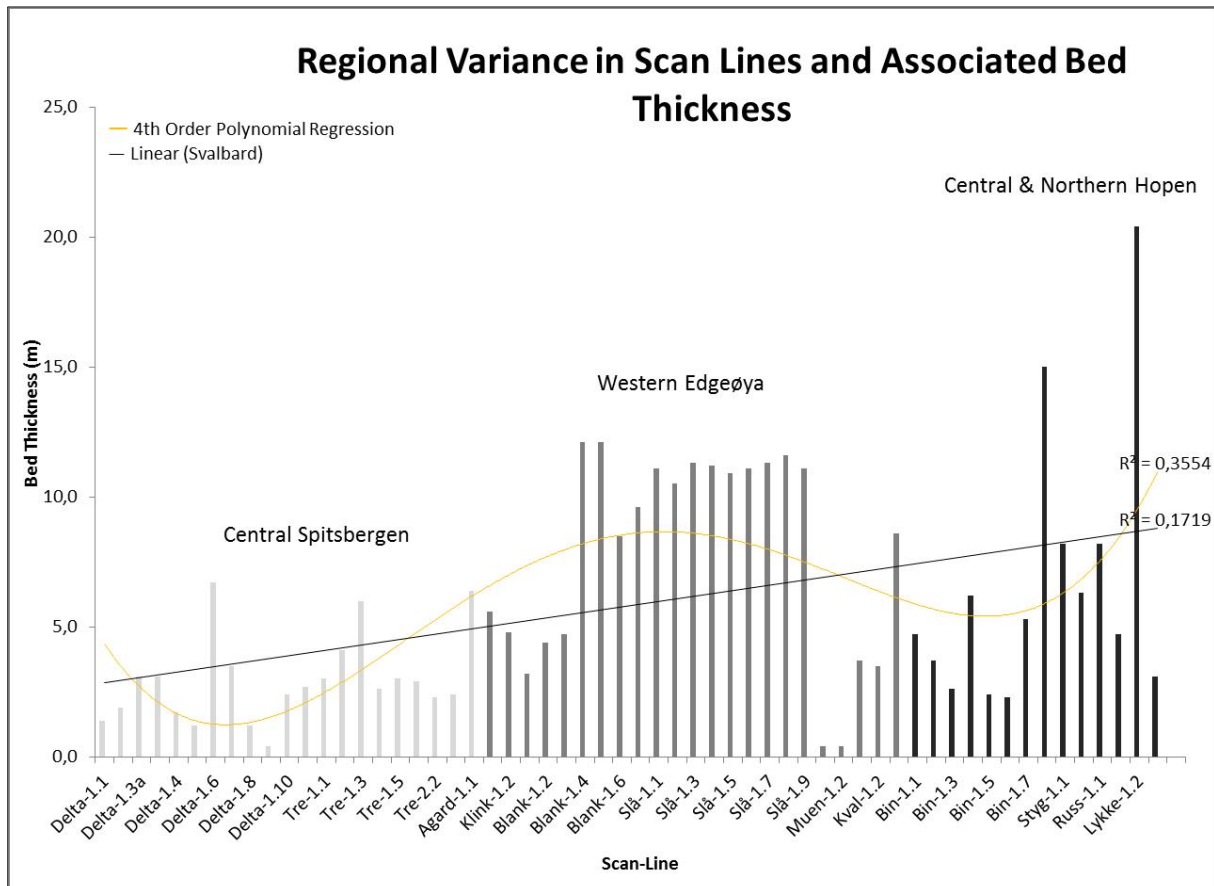
low  $R^2$  value ( $R^2=0,1392$ ), whilst data from Western Edgeøya has a slightly stronger relationship based on the  $R^2$  value of the data set ( $R^2=0,4908$ ), the strongest relationship shown. The linear regression applied to data from Central and Northern Hopen shows a weak relationship to the data points with a much lower  $R^2$  value ( $R^2=0,1113$ ). The second order polynomial trend line applied to the entire dataset shows a moderate strength value for the relationship between data points and the trend line itself with an  $R^2$  value of  $R^2=0,7212$ .



**Figure 44:** Regional variance graph displaying the correlation between average fractures per metre and bed thickness, grouped by field area. Linear regressions for each field area are displayed as are  $R^2$  values for each. Second order polynomial trend line has been applied and  $R^2$  value is shown.

Observing Figure 45, a bar chart plotting the entirety of the scan-line database against bed thickness, it can be seen that when segregated into scan-lines from each field area that there is a general increase in bed thickness from Central Spitsbergen to Edgeøya, with a more dispersed thickness of scan-line beds being measured on Central and Northern Hopen. Whilst this is an overgeneralisation of the nature of bed thicknesses within the De Geerdalen Formation, this must be considered when discussing the nature of fracturing by each regional area. This trend is lightly

highlighted by the linear regression line which shows a gentle increase in bed thicknesses throughout Svalbard towards the south east. The  $R^2$  value although positive does show a relatively weak correlation fit. The 4<sup>th</sup> order polynomial curve again suggests an increase and the applied  $R^2$  value shows a slightly stronger relationship of data values to this line.



**Figure 45:** Bar graph displaying the bed thickness for each measured scan-line throughout the De Geerdalen Formation, grouped by field area. Linear regression for the entire data set is displayed along with the associated  $R^2$  value. In addition a 4<sup>th</sup> order polynomial trend line has been applied and its associated  $R^2$  value is shown.

### 6.3.2 Regional Trends – Fracture density and bed thickness by lithological association.

Fracture density naturally varies not only as a result of bed thickness but also lithological type. Having defined scan-lines within one of three lithological associations, density data has been plotted against bed thickness for each lithological association. In addition to this, the bed thickness in relation to individual scan-lines and their location within Svalbard has also been plotted. This is in order to determine if there are any trends in the lithological type and the recorded bed thickness throughout the region, which may impart a discrepancy on the dataset.

#### 6.3.2.1 Sandstone dominant beds

In total 33 scan-lines have been categorised within the lithological association for sandstone. Within this group 13 are found to be from Central Spitsbergen, 15 from Western Edgeøya and a further 5 from Central and Northern Hopen. This supplies a relatively reasonable spread of data, throughout sandstones of the De Geerdalen Formation on Svalbard.

When comparing the average fracture spacing within these scan-lines against bed thickness, it can be seen from the graph in Figure 46 that there is a moderate, positive correlation between the average fracture spacing and the thickness of the bed they occur in. The regional dataset provides an  $R^2$  value of  $R^2=0,6299$ ) and is presented alongside a second order polynomial regression line. This curve shows that overall there is a good relationship between the trend line and data points, showing that in general average fracture spacing increases as bed thickness increases.

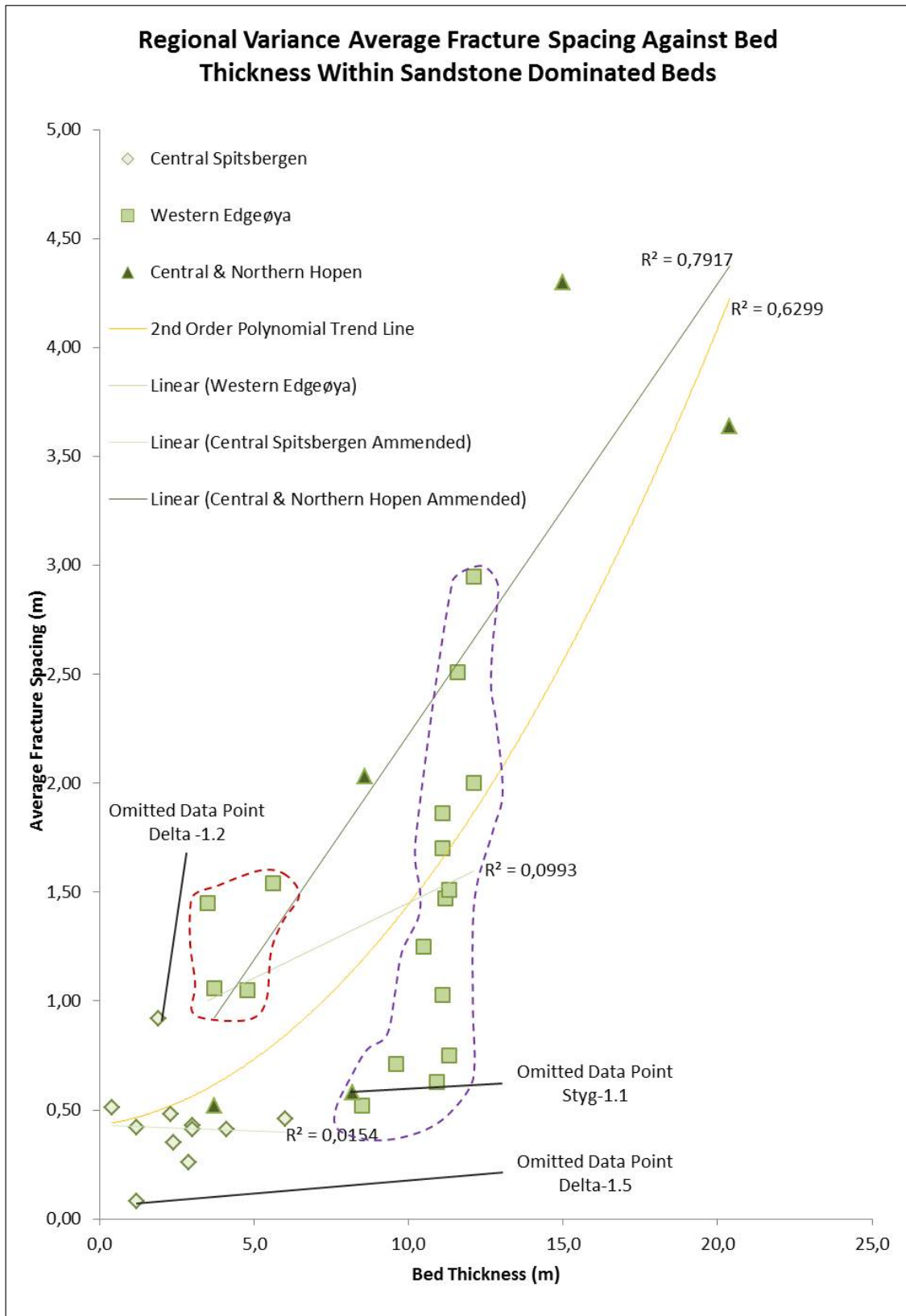
Upon closer scrutiny of Figure 46 there can also be seen to be present a general clustering of data points from Central Spitsbergen to the bottom left, where sandstone beds are found to be thinner. Whilst in general thicker sandstone beds are measured on Western Edgeøya. Data points for Central and Northern Hopen shows a weaker pattern of clustering with a greater linear dispersion, highlighting the greater variability of bed thicknesses measured on the island.

What is noticeable is that in Central Spitsbergen there is an apparent negative relationship between bed thickness and average fracture spacing in sandstones, suggesting within this region bed thickness does not impact the spacing of fractures

which according to the graph averages at approximately 0,43 m. The  $R^2$  value for the region of Central Spitsbergen can be seen to be  $R^2=0,0154$ , showing a very weak relationship between data points and the linear regression line. Data from scan-lines Delta-1.2 and 1.5 have been omitted from this analysis due to its anomalous results

The linear regression for Western Edgeøya shows a gentle positive increase in average fracture spacing as bed thickness increases, however when observing the nature of grouping, it can be seen that there is a strong positive relationship between bed thickness and average fracture spacing seen in scan-lines taken from Blanknuten and Slåen (highlighted in purple on figures 46 and 47). The left cluster of data points from Western Edgeøya are from either Klinkhamaren or Kvalpynten (highlighted in red on figures 46 and 47), the two locations on Edgeøya where clear syn-sedimentary growth faulting of a deltaic system is present. This may suggest implications for facies controls on fracture spacing. This clustering is reflected in the  $R^2$  value for the dataset from Western Edgeøya which at  $R^2=0,0993$ , a very weak relationship is seen.

In contrast to the Central Spitsbergen and Western Edgeøya datasets, the data from Central and Northern Hopen can be seen to have a positive more linear relationship and this is reflected in the stronger  $R^2$  relationship value, where  $R^2=0,7917$ . The scan-line Styg-1.1 has been omitted from this analysis due to its comparatively anomalous result, explainable due to the nature of geology at the scan-lines location (see discussion).



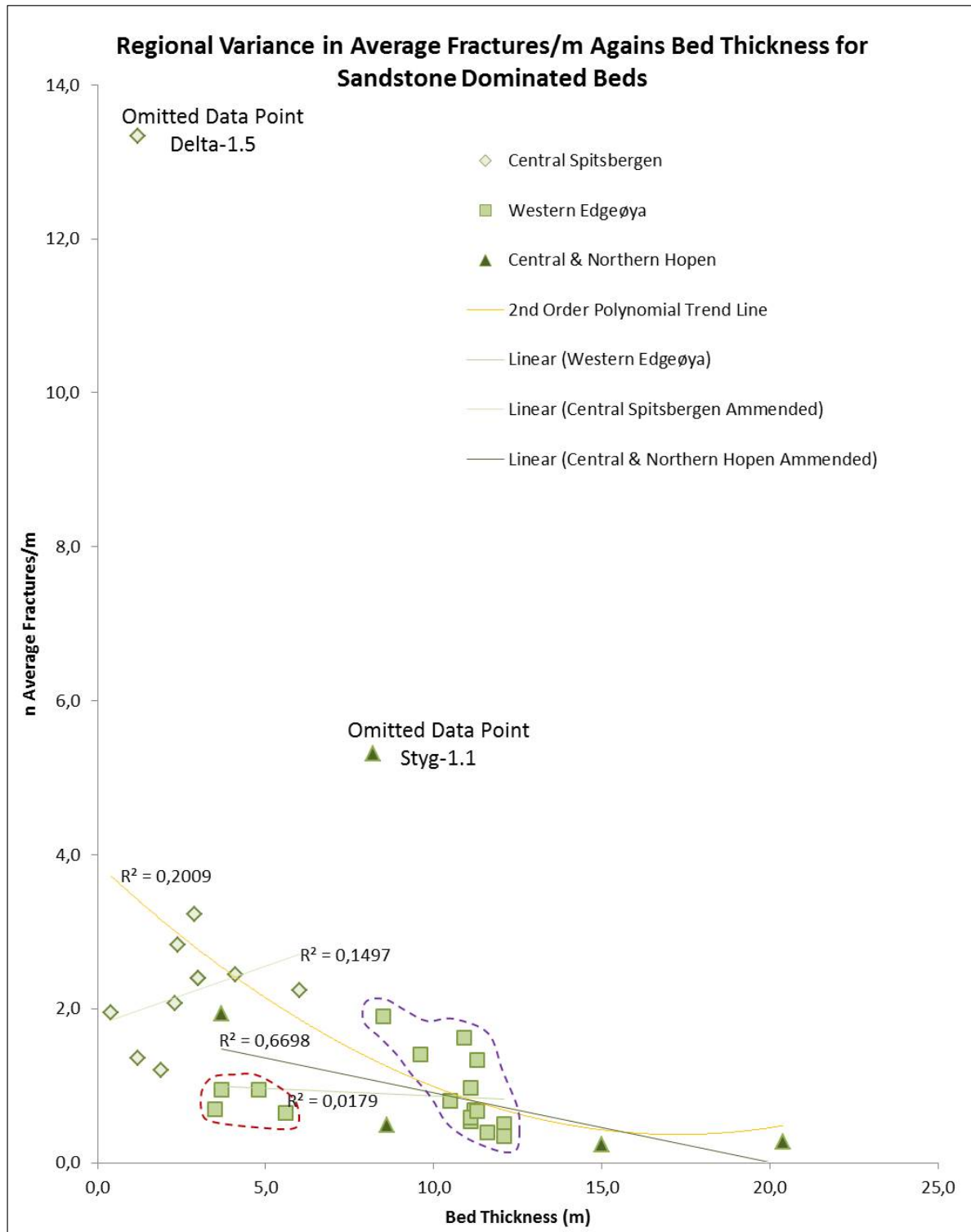
**Figure 46:** Regional variance graph showing the average fracture spacing in metres seen in sandstone dominated beds, plotted against bed thickness and grouped by field area with linear regression lines and  $R^2$  values applied. A second order polynomial trend line has been applied, with associated  $R^2$  value, to the entire dataset. Data point clustering from Western Edgeøya has been denoted, with those from Klinkhamaren and Kvalpyntfjellet being highlighted by the red dashed line and those points from Blanknuten and Slåen being highlighted by the purple dashed line.

The scatter graph in Figure 47 shows a relatively gentle, negative and moderate correlation trend, between the average number of fractures per metre in the sandstone scan-lines and bed thickness. Data from Western Edgeøya appears to conform to two small cluster sets, alike that in Figure 47, whilst Central Spitsbergen appears as a relatively loose single cluster with one notable outlier. The majority of data points from Central and Northern Hopen follow a very clear, partially linear, negative trend, with one prominent outlying data point from Central Spitsbergen.

Analysis of this regional dataset displayed in Figure 47, by field area, can be seen to yield interesting results. Data from Central Spitsbergen unusually displays a positive trend when a linear regression line is applied, with a weak  $R^2$  relationship ( $R^2=0,1497$ ). Data from scan-line Delta-1.5 has been omitted from this analysis due to its highly anomalous nature and the extreme effect this would have on the linear regression and  $R^2$  value.

Data points corresponding to field localities on Western Edgeøya shows a neither negative or positive direction, this suggests an influence on the dataset by location and the grouping of data points has been displayed on the graph. Those highlighted in red from Klinkhamaren and Kvalpyntfjellet suggest no influence on the average fractures per metre by bed thickness, whilst those from Blanknuten and Slåen, highlighted in purple, suggest a clear negative trend. These discrepancies have influenced the  $R^2$  value which shows a very weak relationship ( $R^2=0,0179$ ) between these data points and the linear regression line.

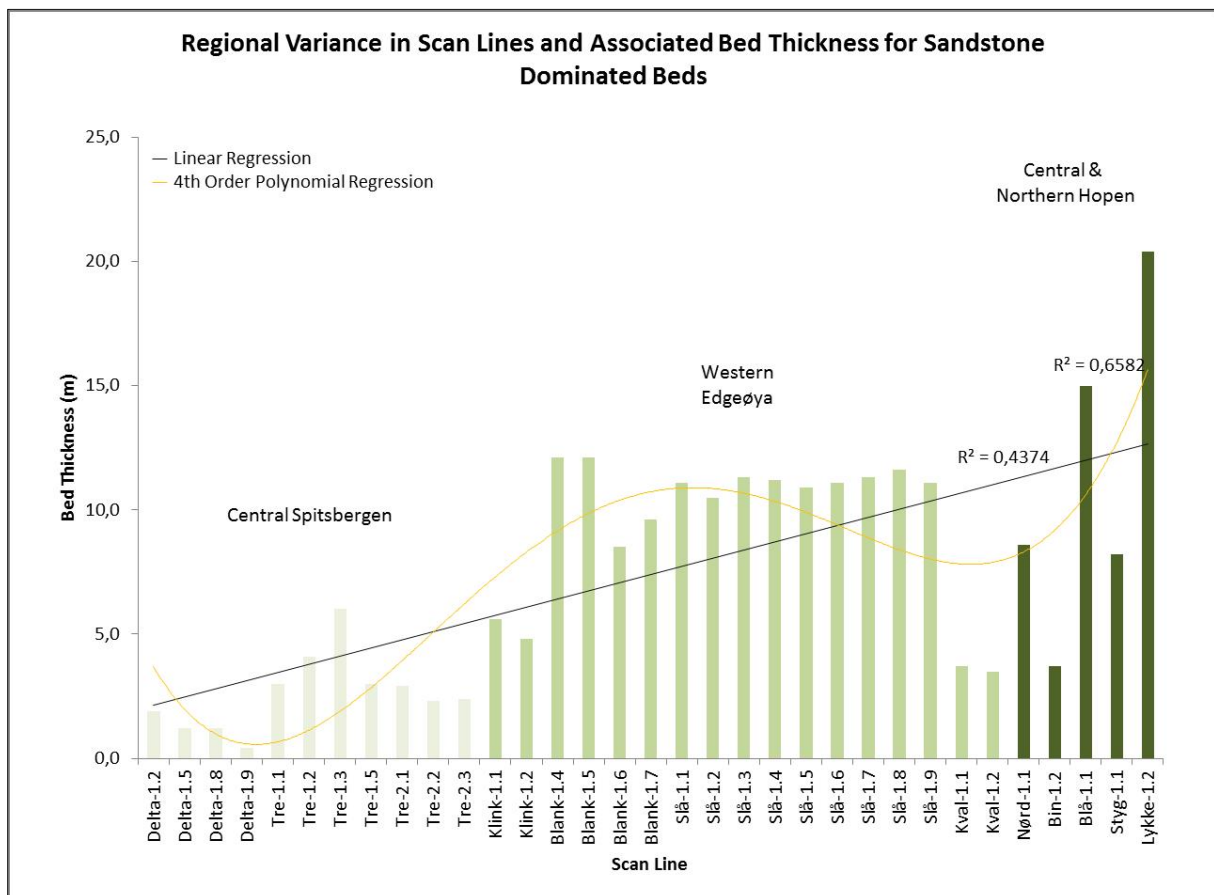
The Central and Northern Hopen dataset however displays a much stronger  $R^2$  relationship in comparison to the other field areas where  $R^2=6698$ . Data points can be seen to follow a gentle curved trend, with an outlying point (associated to scan-line Styg-1.1) being omitted, to avoid influencing the trend of the linear regression and  $R^2$  value, this omission is explainable by the nature of geology at the scan-lines location.



**Figure 47:** Regional variance graph showing the average fractures per metre seen in sandstone dominated beds, plotted against bed thickness and grouped by field area. Second order polynomial trend line has been applied to the entire dataset, whilst linear regression lines and  $R^2$  values are applied to data from individual field areas. Note the omission of anomalous outlying data from trend lines and  $R^2$  values. Data point clustering from Western Edgeøya has been denoted, with those from Klinkhamaren and Kvalpyntfjellet being highlighted by the red dashed line and those points from Blanknuten and Slåen being highlighted by the purple dashed line.



When taking into account variations in sandstone bed thickness by location, Figure 48 can be seen to show a relatively prominent disparity between the average bed thicknesses for scan-lines measured in Central Spitsbergen and Edgeøya. Whilst they are generally thicker in scan-lines recorded in Central and Northern Hopen. The average linear regression trend line does however, show a relatively positive correlation showing that for scan-lines categorised within the sandstone lithological association, there is a general increase in bed thickness from Central Spitsbergen to Western Edgeøya and further south to Central and Northern Hopen. This corresponds somewhat with the data shown in Figure 45, where no lithological distinction has been made. The polynomial regression curve applied to Figure 48 shows again a general increasing trend, yet still highlights the variability of bed thicknesses seen in field areas.



**Figure 48:** Bar graph displaying the relationship between bed thicknesses of each scan-line recorded within sandstone dominated beds, throughout Svalbard. Scan-lines are grouped into field areas. A linear regression for the entire data set is displayed along with the associated  $R^2$  value. In addition a 4<sup>th</sup> order polynomial trend line has been applied and its associated  $R^2$  value is shown.

The  $R^2$  values displayed on Figure 48 show that whilst there is an increasing trend of bed thicknesses to the east and south east in Svalbard, there is still an inherent variability. The  $R^2$  value for the linear regression of the regional sandstone bed thickness dataset ( $R^2=0,4374$ ) shows a moderate relationship, whilst the  $R^2$  value for the polynomial regression ( $R^2=0,6582$ ) shows a much stronger relationship.

#### 6.3.2.2 Sandstone & Shale Dominant Beds

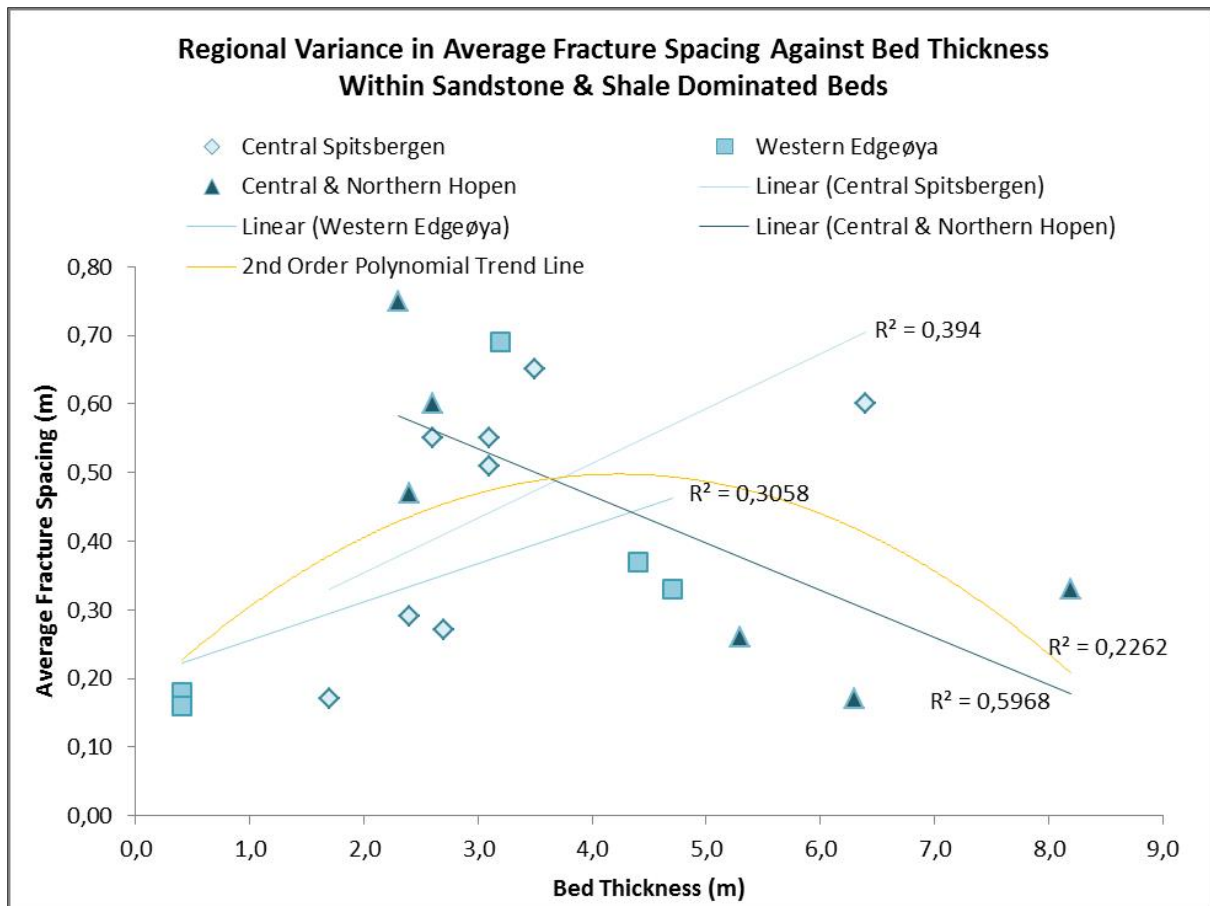
In total, 19 of the recorded scan-lines throughout Svalbard have been categorised as being homogeneously composed of sandstone and shale. Within this lithological association group, 8 scan-lines originate from Central Spitsbergen, 5 from Western Edgeøya and 6 from Central and Northern Hopen.

A comparison of the average fracture spacing for this lithological association and bed thickness, it can be seen from Figure 49 that there is generally a very vague dispersion of data points. No notable grouping of data sets from individual areas can be seen either. The polynomial trend line, suggests a curved trend in general, from positive to negative. The data points however do not reflect this due to their weak dispersion. This is reflected in the  $R^2$  value for the regional dataset along this polynomial curve. A low relationship value of  $R^2=0,2262$  is shown.

Analysis of the graph by field area can be seen to yield interesting results, which explain the nature of distribution displayed by the polynomial regression curve. Data from Central Spitsbergen and Western Edgeøya clearly show a positive linear regression, where average fracture spacing increases with increasing bed thickness. In stark contrast to this data from Central and Northern Hopen can be seen to display an overall negative, moderately linear regression, where fracture spacing can be seen to decrease with increasing bed thickness. This trend is accompanied by a moderate  $R^2$  relationship. The  $R^2$  values associated with linear regression lines for Central Spitsbergen and Western Edgeøya can be seen to show comparatively weak values ( $R^2=0,394$  and  $R^2=0,3058$  respectively) which reflect the dispersed nature of the data.

This vague and dispersed trend is also seen to be evident in Figure 50, a graph displaying the correlation between the average numbers of fractures per metre against bed thickness. Again alike Figure 49, there appears to be no specific grouping affinity for scan-lines by location, all showing a vague dispersion throughout

the plot. The polynomial trend line shows a curved correlation from negative to positive as bed thickness increases, which is poorly reflected in the distribution of data points, due to the sporadic distribution. The associated  $R^2$  value for this regression line further highlights this given the low value of  $R^2=0,2262$ .

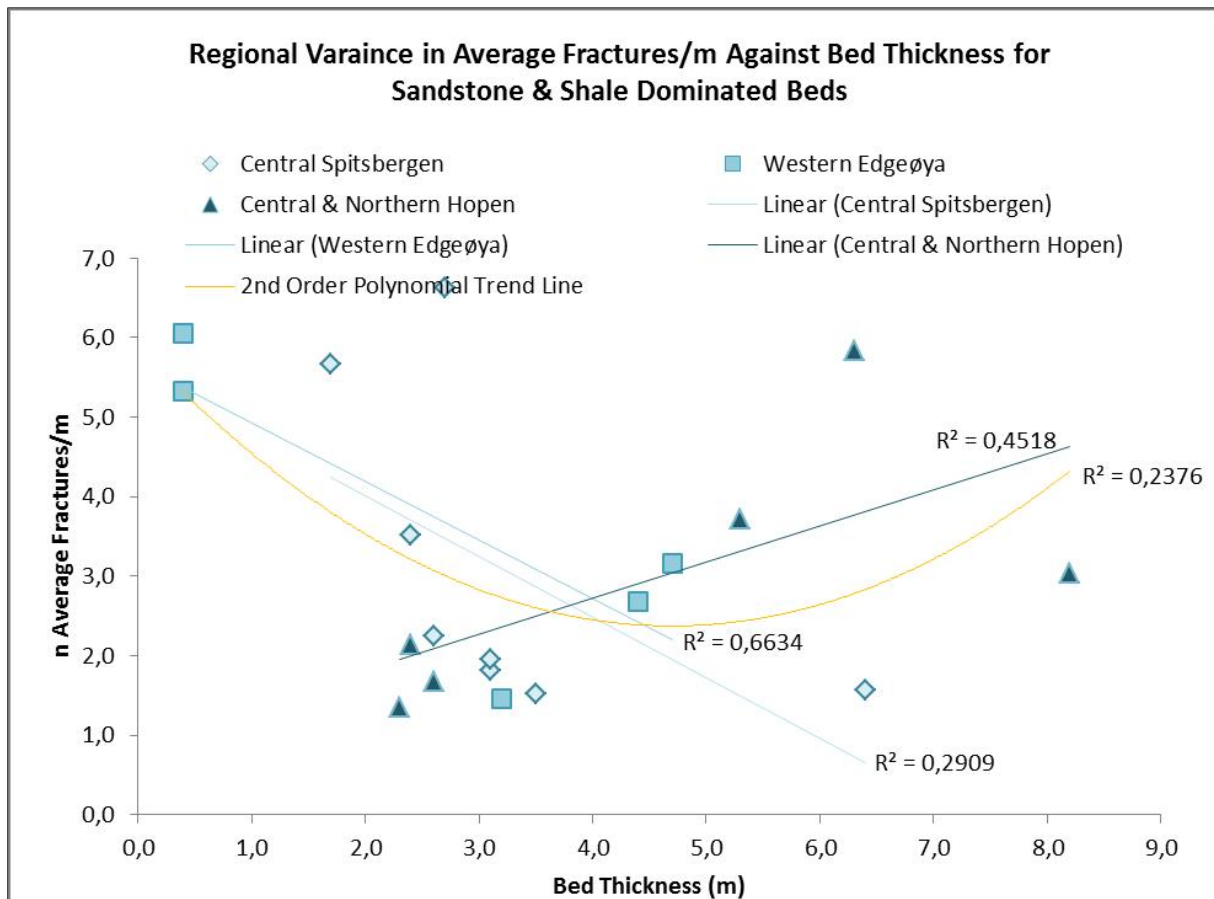


**Figure 49:** Scatter plot graph displaying the correlation between average fracture spacing in metres against bed thickness for scan-lines recorded in sandstone and shale dominated beds and grouped by field area. A second order polynomial trend line has been applied and its associated  $R^2$  value displayed. In addition, datasets based on field area have linear regression trend lines applied and their associated  $R^2$  values are also shown.

With the analysis of data points on Figure 50 by field area, again much alike Figure 49, there can be seen to be an interesting series of results. Data from both Central Spitsbergen and Western Edgeøya provide negative, linear regression relationships between average fracture spacing and bed thickness, whilst data from Central and Northern Hopen provides a positive linear regression, a stark contrast.  $R^2$  value for data from Central Spitsbergen can be seen to be relatively weak with a value of  $R^2=0,2909$ . Whilst data from Western Edgeøya suggests a more moderate relationship with a value of  $R^2=0,6634$ . The linear regression applied to data from

Central and Northern Hopen suggests a moderately weak relationship given the  $R^2$  value of  $R^2=0,4518$ .

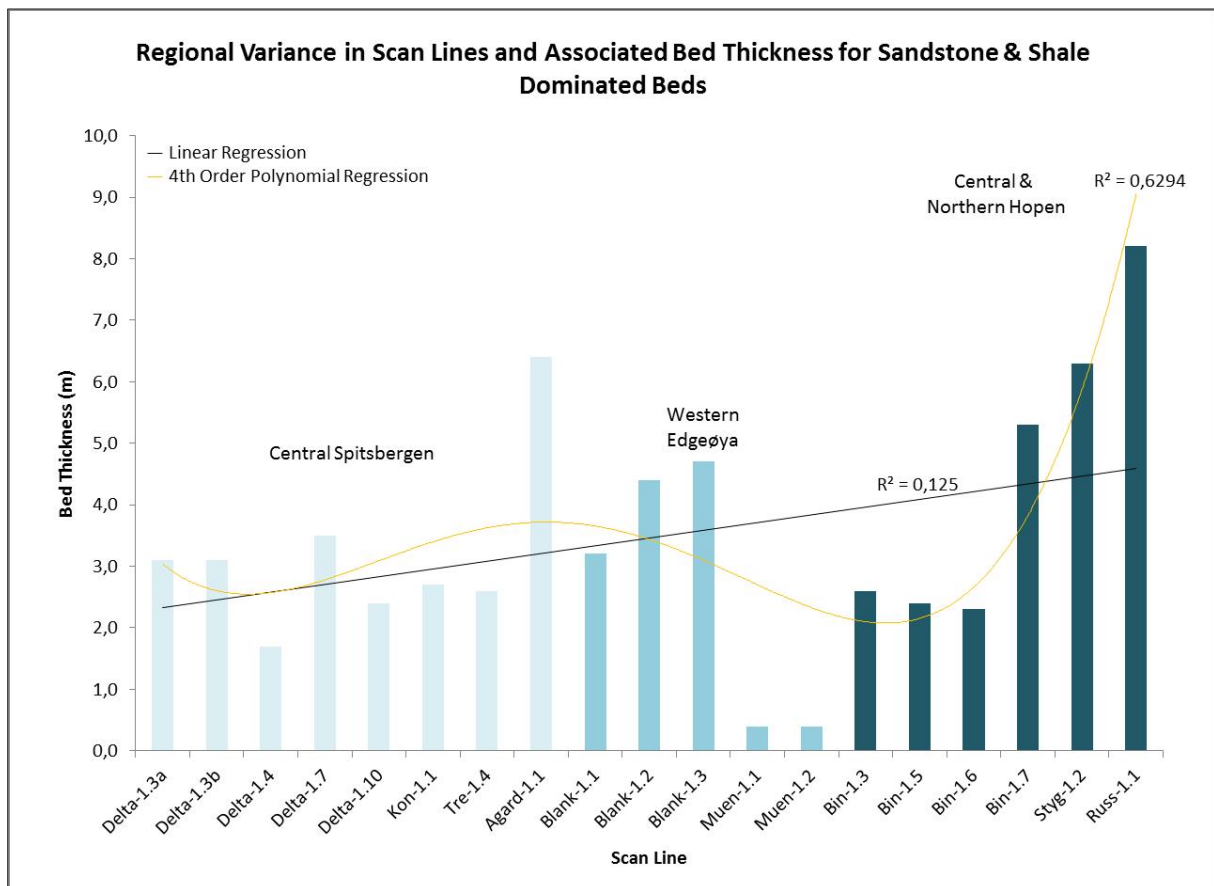
The nature of variation between the data from Central Spitsbergen and Western Edgeøya against that of Central and Northern Hopen provides the cause for the curved nature of the polynomial regression line and its low  $R^2$  value, when the regional dataset is analysed.



**Figure 50:** Scatter plot graph displaying the correlation between bed thickness and number of average fractures per metre, grouped by field area. A second order polynomial trend line has been applied and its associated  $R^2$  value displayed. In addition, datasets based on field area have linear regression trend lines applied and their associated  $R^2$  values are also shown.

Upon comparison of individual scan-lines and their bed thicknesses for this lithological association, it can be seen from Figure 51 that there is a relatively positive linear trend, showing an increase in bed thicknesses throughout Svalbard. Closer analysis shows that through Central Spitsbergen and Western Edgeøya bed thicknesses are relatively similar for this lithological type, whilst on Central and Northern Hopen they are seen to be more sporadic, with variable bed thicknesses.

Analysis of Figure 51, which shows the relationship between individual scan-lines and the observed bed thickness for those, categorised within the sandstone and shale lithological association allows for any regional variations in bed thickness to be observed. The application of a linear regression line shows a minor positive trend as areas become more eastern and south eastern, however this is accompanied by a low and weak  $R^2$  value of  $R^2=0,125$ . In addition a polynomial regression has been applied and this can be seen to display an undulose trend throughout the dataset and does not represent any significant increase in bed thickness of sandstone and shale dominant beds throughout the region. This polynomial regression is associated by a moderate  $R^2$  value of  $R^2=0,6294$ .



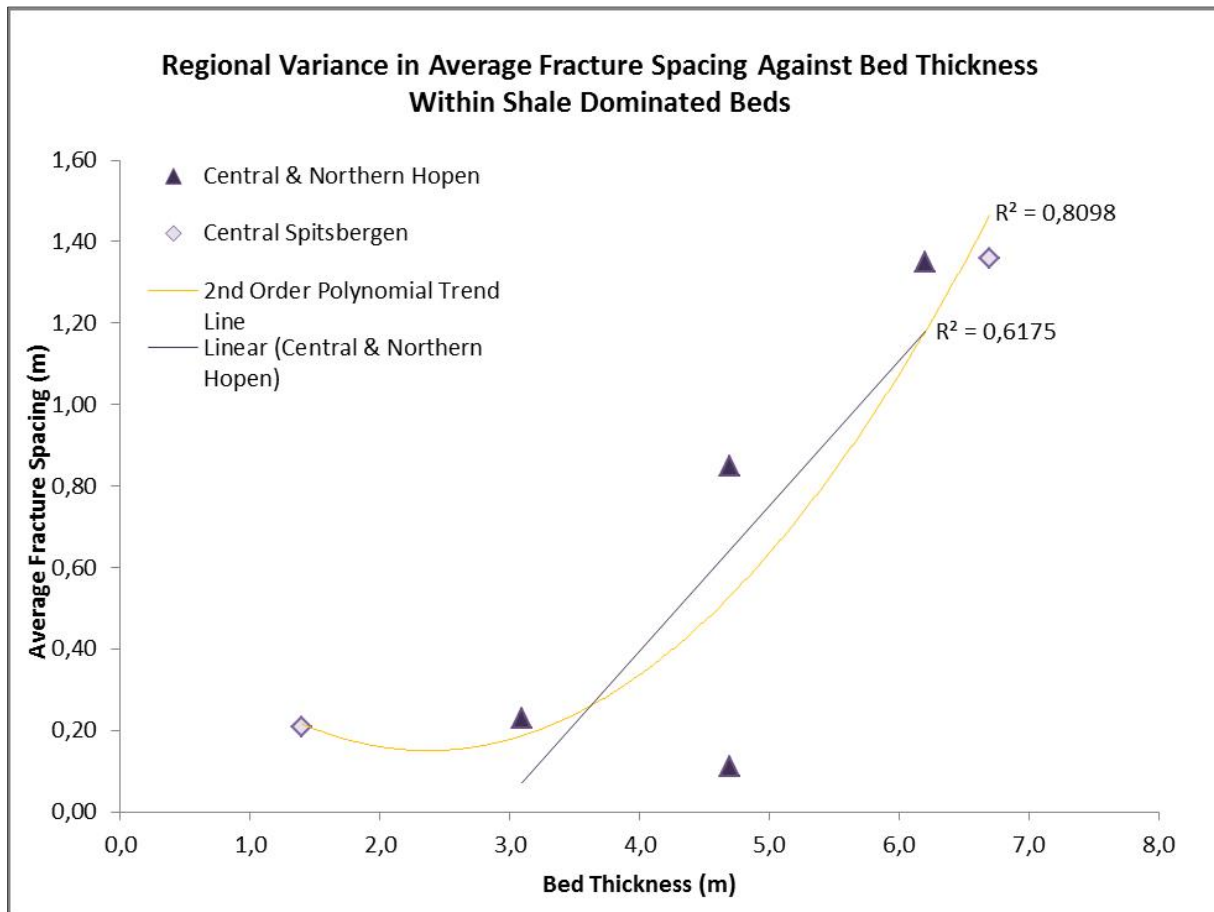
**Figure 51:** Bar graph displaying the relationship between bed thicknesses of each scan-line recorded within sandstone and shale dominated beds, grouped into field areas. A linear regression for the entire data set is displayed along with the associated  $R^2$  value. In addition a 4<sup>th</sup> order polynomial trend line has been applied and its associated  $R^2$  value is shown.

### 6.3.2.3 Shale Dominant Beds

To this lithological association, a total of 6 scan-lines have been assigned. Within this relatively small group, 2 originate from Central Spitsbergen and 4 originate from Central and Northern Hopen. No scan-lines were recorded from Western Edgeøya within this lithological association.

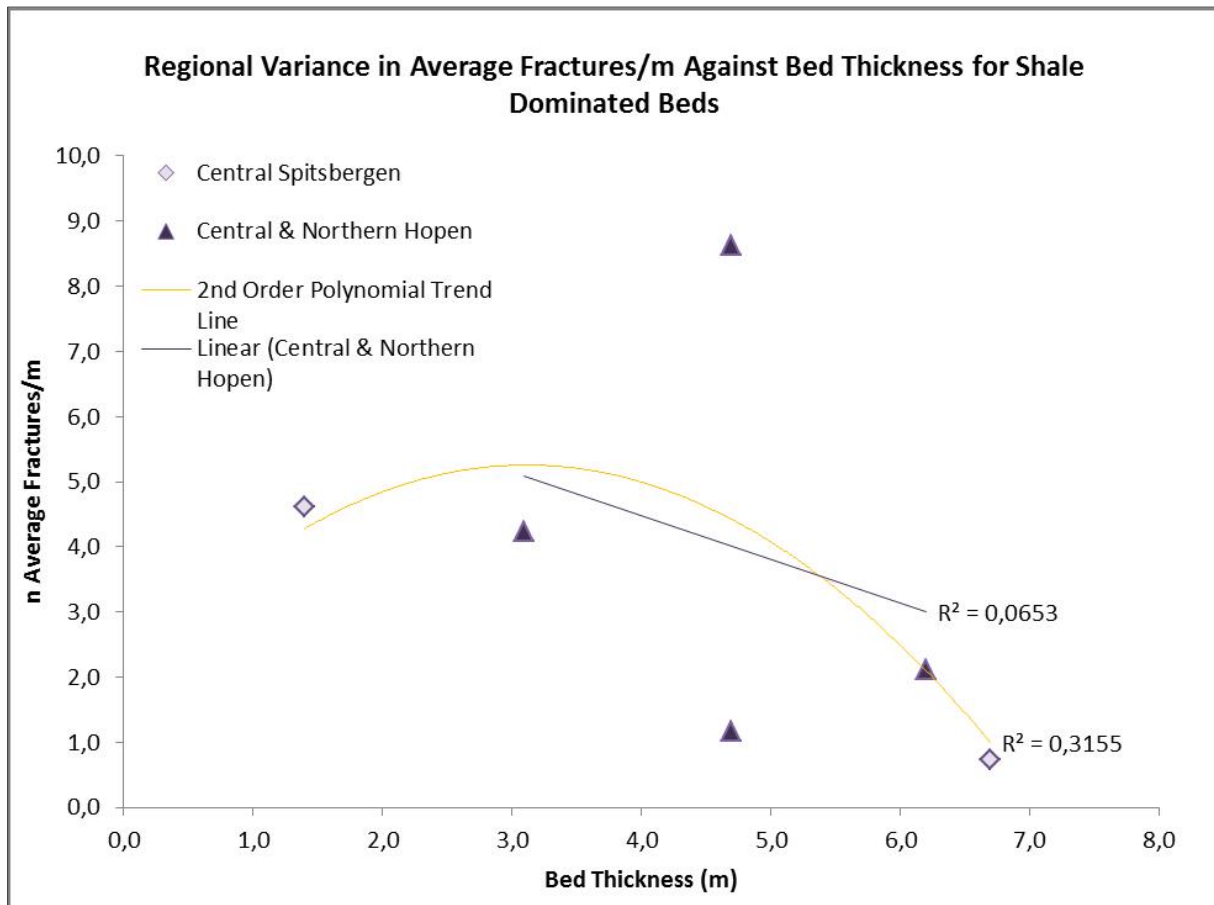
Application of scan-line data shows that when comparing the average fracture spacing within shales to the bed thickness, as shown in Figure 52, there is a noticeable positive, but weak correlation between the average fracture spacing and bed thickness. The second order polynomial trend line suggests a positive curved distribution of increasing fracture spacing with increasing bed thickness, for shale dominated beds and individual points display no particular grouping style by location. The  $R^2$  value displayed in association to the polynomial regression shows a moderately strong relationship between the line and data points, given its relatively high  $R^2$  value of  $R^2=0,8098$ .

A linear regression for scan-lines recorded in Central Spitsbergen has been omitted due to the relative lack of data (two data points), however a linear regression trend line has been applied to data from western Edgeøya. Within this dataset there can be seen to be a positive and near linear trend of data points and this is reflected in the  $R^2$  value applied in association to the linear trend line. Here it can be seen that there is a moderate but not strong relationship given the  $R^2$  value of  $R^2=0,6175$ . An outlying data point can be observed and this originates from scan-line Lykke-1.1, of which local geology at the outcrop does not explain the anomalous result (see discussion chapter). The local and regional data shows clear evidence for fracture spacing increasing with bed thickness in shale dominated beds.



**Figure 52:** Scatter plot graph displaying the correlation between average fracture spacing and bed thickness of measurements recorded in shale dominated beds, grouped by field area. A second order polynomial trend line has been applied. Note the absence of data from Edgeøya within this lithological dominance.

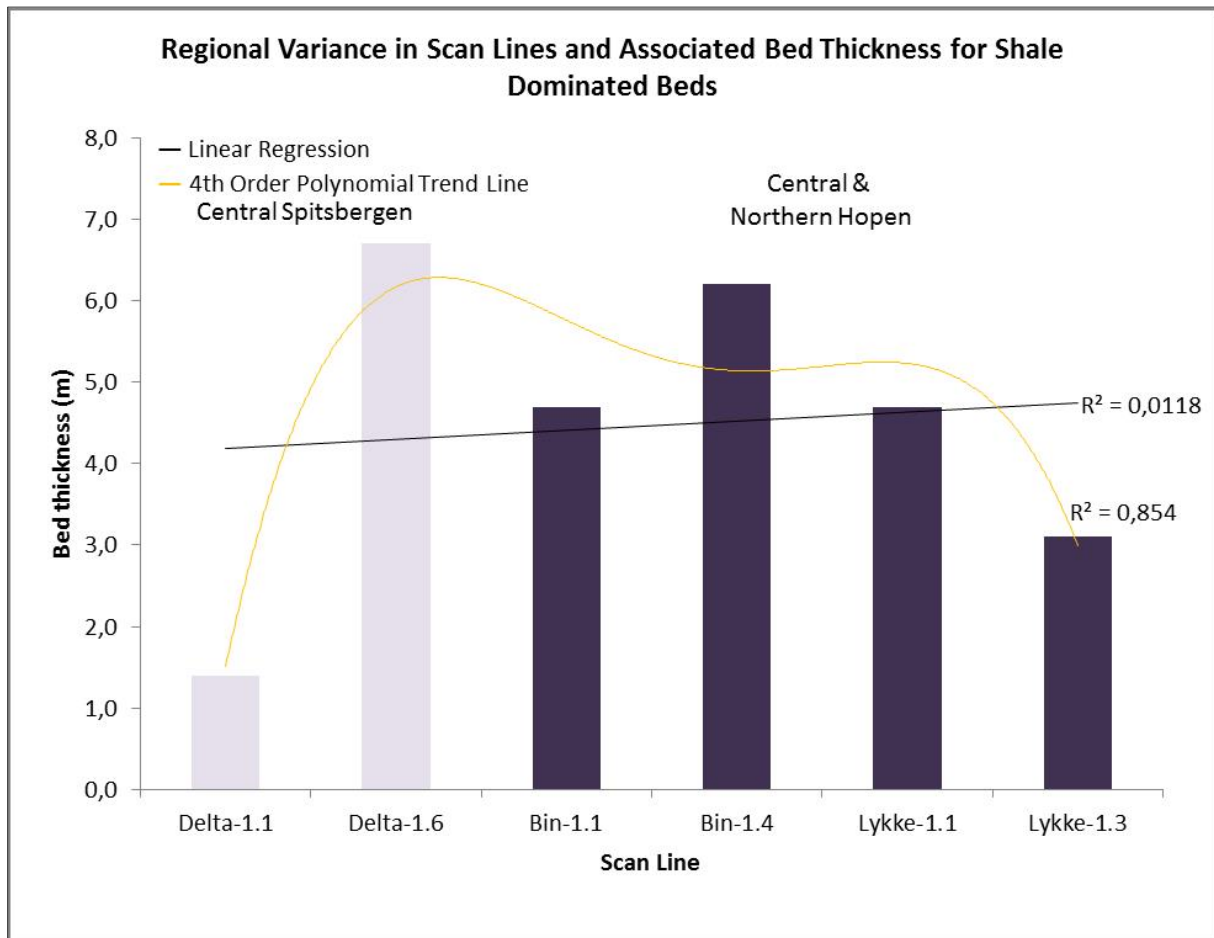
Analysis of average fractures per metre against bed thickness for scan-lines categorised within the shales lithological association, can be seen in Figure 53 to have a relatively very weak, negative correlation when viewed on a regional scale. The polynomial trend line applied suggests a curved distribution and the associated  $R^2$  value suggests a weak relationship between the regression line and data points, with a low  $R^2$  value of  $R^2=0,3115$ . However, when the outlying data point from Central and Northern Hopen (Lykke-1.1), located in the upper centre of the graph is disregarded, there can be seen to be a more modest linear correlation. This clearly shows a thickness in bed results in a decrease in average fractures per metre. No notable grouping of data points has been observed from this plot.



**Figure 53:** Scatter plot graph displaying the correlation between average fractures per metre and bed thickness for data collected within shale dominated beds and have been grouped by field area. A second order polynomial trend line has been applied. Note the absence of data from Edgeøya within this lithological dominance.

When constraining the bed thickness for individual scan-lines it can be seen from Figure 54, that there is a very weak, positive linear regression trend for scan-line bed thicknesses between Central Spitsbergen and Central and Northern Hopen. However the overall distribution is relatively uniform and essentially bias to data from Central and Northern Hopen, which is a larger dataset overall. No scan-lines on Western Edgeøya have been recorded within this lithological association, thus no inferences to regional variations in bed thickness within this group can be made.





**Figure 54:** Bar graph displaying the relationship between bed thicknesses of each scan-line recorded within shale dominated beds, grouped into field areas. A linear average regression has been applied. Note the absence of data from Edgeøya within this lithological dominance.

## 7. Discussion

### 7.1 Regional Fracture Orientations

Steep fracture orientations that have been measured throughout the De Geerdalen Formation on Svalbard are seen to occur in one of three prominent sets. These sets have been defined as FS.1, FS.2 and FS.3. Fractures within these sets are all predominantly Type I, steep, irregular fractures with dips of 70° or more. Lower angle fractures have also been measured along scan-lines however these fractures are seen to intersect or terminate against another discontinuity, or against a bedding surface. In some instances lower angled fractures of Type II mode are observed along scan-lines. Where these have been found to be in the same general strike orientation of one or more of the sets and have thus been included within a regional set. However their nature and mode of formation will be discussed separately.

The regions of Central Spitsbergen is heavily characterised by the presence of FS.1 and FS.2 fracture sets both forming at a near to normal angle with each other. In the areas of Deltanaset, Trehøgdene and Agardhbukta there is seen to be a consistent orientation of these sets with very little alteration of fracture strike within FS.1 and FS.2 being observed. Whilst FS.1 can be seen to be non-existent within Konusdalen, this does not reflect a change in structural style, as it purely represents the fact that the outcrop orientation is parallel to the orientation of the scan-line recorded at Kon-1. This has resulted in no fractures of FS.1 orientation being recorded at this location. Furthermore at Kon-1 there is seen to be a minor component of Type I fracturing to the WNW-ESE, which may be explained by the nature of normal faulting seen within Konusdalen. This corresponding nature between fracturing and faulting within Konusdalen has also been observed by Farrell (2011).

Throughout Central Spitsbergen there is a dominant structural trend of north-south aligned structural lineaments and tectonic features (shown in Figure 2). FS.1 fractures in Type I mode, are seen to form parallel to these regional lineaments. Their formation is thus primarily suggested to be related to a combination of Early-Cretaceous extension along the Billefjorden Fault Zone, see Figure 55 (Parker 1966; Harland et al. 1974; Haremo et al. 1990) and Late-Cretaceous uplift in northern Svalbard which has led to the formation of this NNW-SSE aligned fracturing.

However, fracturing does not follow the trend of regional lineaments exactly, which may suggest that local structural styles have influenced fracture orientation trends. Explanation for this subtle deviation may be derived from folding on a local scale, doleritic intrusions within the subsurface, or the by the partitioning of transpressional tectonics, during the Cenozoic (e.g. Fossen et al. 1994; Leever et al. 2011).

These fractures have then later been augmented by subsequent uplift of the entire Svalbard region, during the Late-Cretaceous and Cenozoic. In addition unloading of cover rocks may also have implications for fracture density and their extent throughout central Spitsbergen.

Within the region of Central Spitsbergen dolerite dykes and sills of Cretaceous age penetrate the Mesozoic succession at numerous locations. The formation of these sills will also have implications for fracture development and it is likely that these have assisted in the augmentation of the fracturing caused during Cretaceous tectonic episodes, e.g. Ogata et al. (2012).

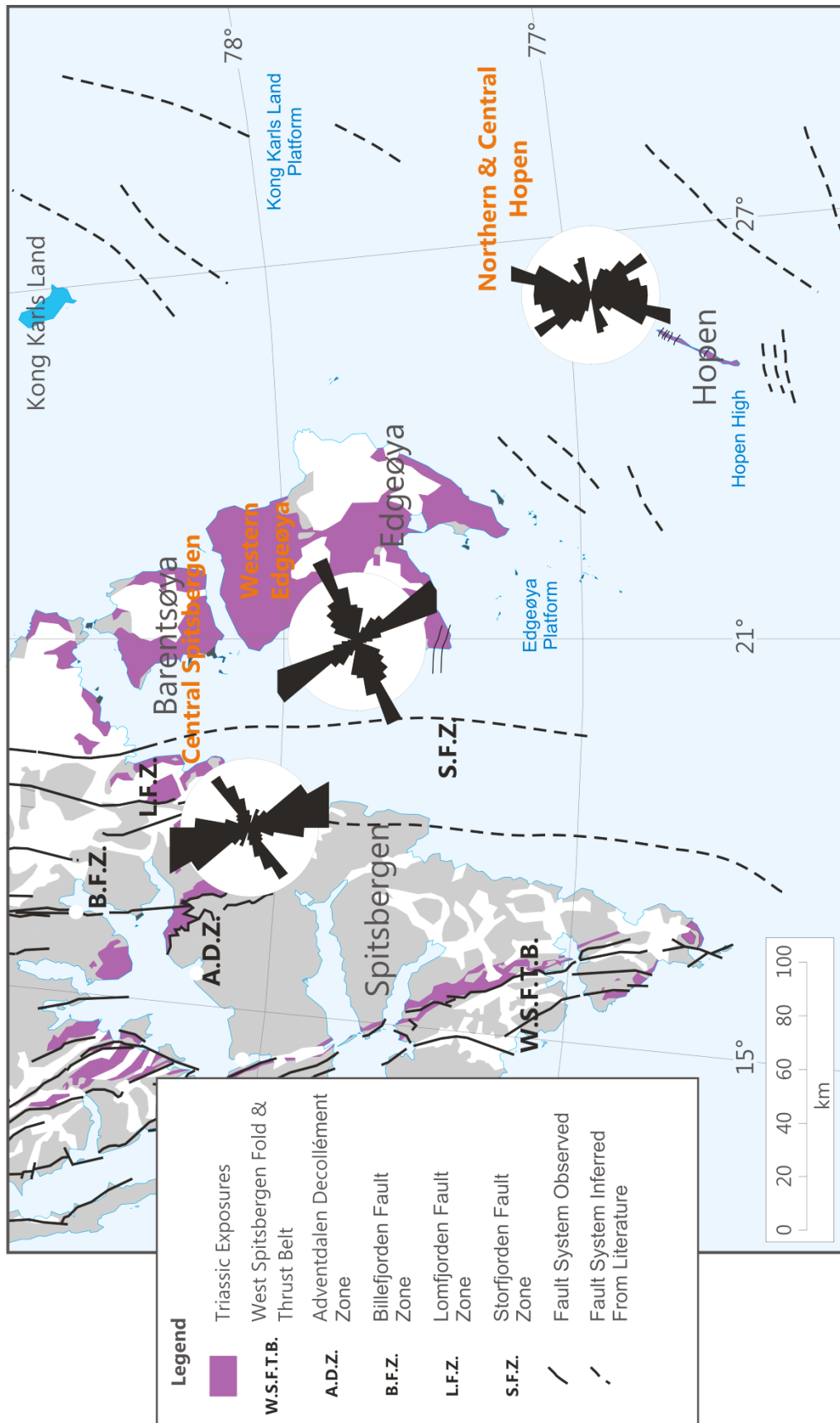
FS.2 fractures, due to their prominence throughout Central Spitsbergen and normal orientation to the maximum stress, formed as a result of compressional tectonics leading to the creation of the West Spitsbergen Fold and Thrust Belt (Figure 55), are most likely 'indenter' fractures (Engelder and Gaiser 1980; Ogata et al. 2012) formed normal to the regions compressive stress in response to thrusting in the Cenozoic. Jointing forming normal to regional compression has also been noted by Engelder and Peacock (2000), who show that joints normal to maximum regional compressive stress will not only form, but are seen to propagate more readily through multiple beds. Fracturing derived from Cenozoic compression is also noted in the works of Waerum (2011) and Ogata et al. (2012) from Central Spitsbergen, but suggests a much greater implication of Cenozoic tectonics throughout the region. Alike FS.1 fracturing in Central Spitsbergen, it is also important to consider the effects of intrusions, unloading and uplift allowing further extension of Type I fractures in this relative E-W orientation.

With regards to timing of fracture formation within Central Spitsbergen it can be considered that FS.2 fractures are the oldest in terms of formation age. This is based on the notion that these fractures are derived from Cenozoic tectonics, whilst the alignment of FS.1 fractures to longer lived tectonic structures suggest an earlier

formation. This earlier episode of fracture formation can most likely be related to the period of uplift and extension during the Late Cretaceous, which has then allowed for the enhanced of these fractures, by later Cenozoic tectonic episodes. In addition the presence of intrusive rocks within the Mesozoic succession may also provide an explanation for the origin of non-systematic fractures that do not relate to any particular fracture set.

On Edgeøya subtle local variations in the orientations of FS.1 and FS.2 fractures can be seen (Figure 55) however FS.2 is still relatively dominant throughout the region, with FS.1 being significantly less visible in the southern areas of Edgeøya, at Slåen and Klinkhamaren. FS.1 fractures are also seen to have a more prominent alignment to the strike orientation of the West Spitsbergen Fold and Thrust Belt as well as large-scale tectonic lineaments, such as the Billefjorden Fault Zone and Lomfjorden Fault Zone on Central Spitsbergen as well as the Storfjorden Fault Zone within Storfjorden (Figure 55). This suggests that despite the significant distance between these tectonic lineaments and field locations on Edgeøya, the mode of fracture formation for Type I FS.1 fractures is in similarity to those on Central Spitsbergen, which implies that FS.1 fractures seen on Edgeøya are at the earliest Late Cretaceous in Age, with Cenozoic tectonic episodes and crustal unloading further augmenting these existing fractures.

It is worthy of note that the FS.1 orientation on Edgeøya is also in similarity with the orientation of the Rindedalen structure reported by Lock et al. (1978). Whilst this structure may have had implications for these fractures (and likewise with FS.2 fractures), the lack of visibility of this structure on present geological maps and very brief discussion of the structure by Lock et al. (1978) leads to caution when relating the formation of fracture sets to this feature.



**Figure 55:** A regional structure map showing the major fault systems dissecting Svalbard. Regional fracture orientations have been overlain in order to show the correlation between these structures and tectonic features. Triassic Exposures are also shown. Refer to Figure 2 for fault references.

FS.2 fractures are also seen to have a subtle variation in orientations throughout Edgeøya, however their formation and near parallel alignment to the major West Spitsbergen Fold and Thrust Belt on Spitsbergen suggests that despite the relative distance, compressional tectonics during the Cenozoic. Edgeøya is also a platform structure in itself and thus the local structural style to Edgeøya may have implications for the presence of non-systematic fractures seen in the region, such as those seen at Kvalpyntfjellet where a prominent WNW-ESE alignment is present. These may be explained by the presence of the domal structure observed by Lock et al. (1978), or more likely these are formed due to the presence of severe dolerite intrusions of Cretaceous age at the locality.

A minor component of FS.3 oriented fractures have also been observed on Edgeøya, most notably at the locations of Klinkhamaren and Slåen where a series of fractures trending NE-SW are observed within the dataset. Given the relatively low potential for a local structural cause their formation can only be related to offshore extensional tectonics seen in the region of Kong Karls Land, to the east of Edgeøya (Doré 1995; Grogan et al. 1999). Here the structural style is predominantly extensional with a trend roughly NE-SW, which has resulted in basin formation to the east and south east of the Svalbard Archipelago during the Late-Palaeozoic (Doré 1995; Grogan et al. 1999; Faleide et al. 2008). Intrusive rocks may also present a potential cause for the presence of FS.3 fractures on Edgeøya; however these do not appear in any proximity to Slåen and are relatively distant from Klinkhamaren to have a significant effect. In contrast to this, in the area around Kvalpyntfjellet and Kvalpynten which is dominated by intrusive rocks, no FS.2 oriented fractures are evident. In addition to this the relatively minor component of FS.3 fractures within the Edgeøya dataset suggests that these can also not be related to any formation of the dome structures reported by Lock et al. (1978).

Hopen features a much more diverse structural geology than most other locations visited, with many obvious faults cutting perpendicularly through the island accompanied by numerous fold and monocline structures. Thus it must be considered that these structures will have a controlling factor on the nature of fracturing, seen on the island, especially at those locations that are in close proximity to faulting.

What can be considered significant is that Hopen appears to be host to both FS.1 and FS.2 fractures in very similar orientation to those of neighbouring Edgeøya and also Central Spitsbergen. This uncanny structural likeness of Type I fracture orientations on Hopen presents significant evidence for these fractures being derived in the same manner as their counterparts in Edgeøya and Spitsbergen. In that FS.1 fractures are controlled by Cretaceous extensional tectonics and FS.2 fractures are derived from Cenozoic tectonic events. With further fracturing and augmentation of existing fractures by uplift and unloading of the crust.

Whilst there is as strong correlation between fracture trends on Hopen and other regions of Svalbard, there is seen to be a component of fractures within the Hopen dataset, which instead can specifically be related to the structural style of the location at which they are found. This is most notable at Binnedalen where fractures observed along the beach section, within scan-line Bin-1.1, show as significant NW-SE trend which is parallel to the fault plane of a normal fault at the same location. Fractures are also noted to increase in density towards this plane, with same strike orientations being recorded as the fault plane itself (NE-SW).

Whilst having some similarity to the orientation of FS.1 fractures, this fault related fracture set distinguishes itself quite notably from those of FS.1 seen in Binnedalen due to the Type II nature of fracturing. Similarly within fracture data from Styggdalen, a component of Type II fracturing has been observed in a sandstone body (scan-line Styg-1.1) following the same orientation of FS.1 fractures but is distinguished from Type I FS.1 fractures due to their conjugate pattern in outcrop. The location of Styggdalen is also in close proximity to a normal fault and shear fractures in this area follow a similar but not same structural orientation.

The most striking fracture set that has been noticed in the region of Hopen belong to FS.3, which are also seen to have a significant alignment with the overall trend of the island itself. These purely Type I extensional mode fractures appear at numerous locations throughout the Central and Northern Hopen field area and suggest the presence of a significantly different structural trend throughout Hopen in comparison to the rest of Svalbard. These fractures are also seen to align very conformably to a series of extensional fault systems propagating throughout the Northern Barents Sea, in the region around Kong Karls Land, the seaway between Hopen and Edgeøya and

also offshore to the south east of Hopen itself (Doré 1995; Grogan et al. 1999; Faleide et al. 2008). Originally these faults formed during the Late-Palaeozoic (Grogan et al. 1999; Faleide et al. 2008) and underwent reactivation during the Mesozoic and Tertiary (Grogan et al. 1999). Unlike Edgeøya the island of Hopen rests on a structural high, a horst block bound to the north west and south east by faults. Thus it can be implied that this system of FS.3 extensional fractures bears significant relationship to the structural style which has led to the origin of the island itself.

Unlike Edgeøya and Central Spitsbergen, Hopen is also entirely unaffected by intrusive rocks, despite a significant proportion of southern Edgeøya and its offshore region being dominated by dolerite intrusions, no intrusive rocks are reported on the island or from either of the exploration wells drilled on the island. Thus intrusive rocks cannot be held accountable for any of the fracturing on the island. However recent uplift and un-roofing throughout the region is determined to have augmented

It can be considered significant that these FS.1 and FS.2 fractures are found at such widespread locations throughout the Triassic of Svalbard. Their presence suggests that both long lived and recent tectonic episodes have imparted a significant structural trend throughout the entirety of the Svalbard archipelago, which may have significant implications for structural styles throughout the Northern Barents Sea. Whilst FS.3 fractures are only found in significant abundance in some locations on Edgeøya and are a major fracture set on Hopen, their orientation resemblance to the strike of faulting to the east of Edgeøya and offshore zones around Kong Karls Land, suggests that these faults may have been a significant controlling factor in formation of these fractures. All of these fracture systems are suggested to have undergone significant modification by recent uplift of the Svalbard archipelago and also crustal unloading.

## **7.2 Fracture Density – Regional Variations and Lithological Controls**

Following graphical analysis of the entirety of scan-line data throughout Svalbard, there can be seen to be very good regional correlations between both the average number of fractures per metre against bed thickness and the average fracture spacing against bed thickness. Figures 43 and 44 can be seen to show a clear trend of fracture spacing, as bed thickness increases and moderately corroborated by the



$R^2$  value applied to the entire dataset. This does not however suggest that average fracture spacing increases regionally.

There is also a decrease in the average number of fractures per metre, as bed thickness increases. Within these plots there can also be seen to be a general clustering of scan-line data points by region. This suggests an indication that more eastern and southern field locations, i.e. those on Western Edgeøya and Central and Northern Hopen, have seen thicker beds being measured for fracture data. On a regional scale, overall the relationship between average fracture spacing and bed thickness is notable and confirmed by the relatively moderate  $R^2$  value. However, analysis shows a relatively low  $R^2$  value for the average fractures per metre when observed on a regional scale, suggesting a significant shortcoming for predictive models. This variation is interpreted as being linked, not only to lithological type but also the nature of tectonics at individual localities. For example anomalous results stemming from scan-lines recorded in close proximity to faulting, showing marked increases in average fractures and their spacing's, have impacted the trends seen in the dataset.

The nature of this increase in overall bed thicknesses measured throughout Svalbard has its origins in two separate variables. Most importantly the individual scan-line locations are entirely random with no specific bed thickness being observed, with no controls for selecting measured beds based on thickness being made, during data collection. Therefore the overall regional increase in bed thickness could simply be due to this lack of controlling criterion. Variability in bed thicknesses is reflected in the linear regression and  $R^2$  value applied in Figure 45, which although showing an increase, the relationship is still weak.

When considering the stratigraphical and sedimentological controls on bed thicknesses within the De Geerdalen Formation throughout Svalbard however, an important factor becomes evident. Scan-line locations in Central Spitsbergen are firstly within the uppermost of the De Geerdalen Formation in the Isfjorden Member at Deltanaset, and in the lowermost of the De Geerdalen Formation at Trehøgdene. Whilst on Western Edgeøya scan-line locations are within the lowermost of the formation, representing the lowest part of the succession, there is no indication for the quantity of the Mesozoic succession missing above Edgeøya. Scan-lines from

Central and Northern Hopen are stratigraphically within the uppermost of the formation, as the De Geerdalen Formation is overlain by the Flatsalen Formation on Hopen.

As the De Geerdalen Formation is a diachronous, time-transgressive unit formed in a prograding deltaic system, facies will change both laterally and vertically in response to time and position of depositional environment. The De Geerdalen Formation from field areas on Central Spitsbergen is characterised by its shallow marine depositional environment, with a more lagoonal environment being observed within the Isfjorden Member. Due to the facies within these systems, bed thicknesses of specific lithologies are generally relatively thin, in comparison to those at other locations.

The geology of the field areas visited on Western Edgeøya is dominated by delta front deposits and associated facies, where thick beds of clastic sediment have been able to accumulate. This is notable in the logs Blank-1 and Klink-1 where thick bed packages of sandstone are markedly different from those seen at locations in Central Spitsbergen. In Central and Northern Hopen the De Geerdalen Formation is stratigraphically younger than Edgeøya and is characterised by its predominantly fluvially derived sedimentology (Klausen and Mørk 2013). Here thick fluvial channel packages cut the island and these have been observed for fractures in numerous locations. The island also features marine derived sediments emplaced during an incursion that has later been overlain by a further series of fluvial channels. This highly complex heterolithic stratigraphy provides cause for the diversity of both bed thicknesses and lithological types seen on Hopen.

With regards to fracture densities and bed thickness for differing lithologies, it has long been appreciated that thicker beds will host less fractures and thinner beds will host more. In addition more competent lithologies will hold fewer fractures, whilst weaker, more brittle lithologies will hold more.

The most conclusive dataset can be found within the lithological association for sandstone dominated beds. Within this group a good regional spread has been attained and there is clear evidence for fracture spacing increasing and average fractures per metre decreasing as bed thickness increases. Regional variations can be seen to show a clear grouping of thinner beds of low thickness and low average fracture spacing's in Central Spitsbergen, whilst Western Edgeøya features a larger

group spread but in general thicker bedding with higher average fracture spacing. Central and Northern Hopen is relatively loosely grouped further attesting to the variable thickness of sandstone beds on the island, due to its complex and highly heterolithic stratigraphy.

On local scales within the sandstone lithological association, three noticeable anomalous data points are observed. Two of these points appear on both figures 46 and 47 whilst one is only evident on Figure 46. The anomalous points from Deltaneset (scan-lines Delta-1.2 and Delta-1.5), clearly show a deviation from the trends seen in figures 46 and 47. However there is no notable cause for this deviation that could be derived from the local tectonic style and no local faults are observed along the beach section.

Delta-1.5 represents a relatively thin bed, whilst Delta-1.2 is relatively thick in comparison. Such anomalously high average fractures per metre and anomalously low fracture spacing in comparison to others from Central Spitsbergen, can only be explained in one of two ways. Firstly by lithological controls that may have resulted in these bed becoming more brittle and susceptible to fracturing, or secondly, most likely and most simply is that as these are the only purely sandstone beds from the Deltaneset locality, sandstone specific beds are severely under sampled within the Isfjorden Member at Central Spitsbergen.

With regards to the anomalous result from Central and Northern Hopen, local geological styles can be used to infer the cause for this deviation from the regions trend. The data point relates to scan-line Styg-1.1 which can be seen to have been taken in close proximity to a large fault that dissects Johan Hjortfjellet in Central Hopen. The fracture orientations noted at this location are also in parallel to the strike of this fault and thus, it is suggested that this local tectonic style has impacted the density of fractures seen at this locality and the values represented in dataset from Central and Northern Hopen.

In addition to these anomalous points within the sandstone lithological association dataset, a distinct clustering of data points from Western Edgeøya has been observed and these can be related to the local geology. One cluster set can be seen to be related specifically to the localities of Klinkhamaren and Kvalpyntfjellet where growth faulting has occurred and dolerite intrusions are in close proximity,

within the De Geerdalen Formation. Whilst the other larger cluster originates from locations at Blanknuten and Slåen, displaying relative tectonic stability, with little or no evidence for faulting and no local dolerite intrusions have been seen. A variation at the locations of Klinkhamaren and Kvalpyntfjellet is also seen within the fracture orientation data, with anomalous NE-SW and SE-NW trends being observed. This suggests a notable tectonic or intrusive control upon fracture densities in this area. Anell et al. (2013) provides fault orientations from growth faults at Kvalpynten and the the anomalous fracture orientations recorded at Kvalpyntfjellet can be seen to follow this trend, whilst Rød (2010) shows a NW-SE trend for growth faulting at Klinkhamaren. In addition fractures are observed in the field to be open and no syn-sedimentary fractures have been recorded showing mud infill or diagenetic alteration by fluids. Thus it is most probable that the contrast in fracture densities seen at these locations is most likely related to dolerite intrusions, which appear in close proximity to both Klinkhamaren and Kvalpyntfjellet.

Beds that have been classified within either the sandstone and shale or shale dominated lithological association show very little alteration, with regards to any preferential direction of bed thickness changes throughout Svalbard. Whilst those categorised as sandstones and shales have a more extensive dataset, the minor linear regression trend and low  $R^2$  value, do not provide enough compelling evidence to support a regional change in variation of bed thickness by location.

A notable point seen in the results of scan-lines categorised as sandstone and shale is the unexpected regional variation seen in data from Central and Northern Hopen, which is in direct contradiction to data from Central Spitsbergen and Western Edgeøya. Here it can clearly be seen and supported with a moderate  $R^2$  value; that increasing bed thickness is in correlation with increasing average fractures per metre and decreasing average fracture spacing. No conclusive explanation for this unusual trend can be draw from an analysis of the local geology alone as the scan-lines originate from numerous locations throughout Central and Northern Hopen and are not characteristic of one individual place. Thus a modest and simple suggestion would be that there is a relative under sampling of fractures within this lithological association at Hopen, despite being the most sampled lithological association group. Resulting in a distortion of data where a grouping of data points may have been evident, with corresponding trends to other field locations, if a larger dataset been

obtained, within this lithological type. A more concise dataset for example may have yielded results like the prominent grouping seen within the sandstone lithological association dataset, from Western Edgeøya.

The relatively poor quantity of data assigned to the shales lithological association has caused a relatively disparate dataset, with a complete absence of data from Western Edgeøya. However despite the relatively limited data, it does provide compelling evidence for an increase in fracture spacing and a decrease in average fractures per metre, within this lithological association.

## 8. Conclusions

- A composite overview of the data has shown that throughout the localities observed for fracture orientation data, there is a prominent regional trend for steep fracturing within the De Geerdalen Formation on Svalbard.
- This trend shows two prominent fracture strike orientation sets FS.1 and FS.2, with the presence of a third set FS.3, which are all seen to align significantly with the present tectonic and structural style throughout Svalbard.
- FS.1 and FS.2, are observed to hold a strong NNW – SSE trend and an ENE – WSW trend respectively. These prominent regional fracture orientation sets are observed throughout central Spitsbergen, western Edgeøya and Hopen.
- FS.1 fractures throughout Svalbard are determined to have originated as a result of Cretaceous extension and tectonic activity along prominent structural lineaments that dissect Spitsbergen.
- FS.2 fractures are determined to have originated from compressional tectonics during the Cenozoic, where they have formed as indenter fractures, perpendicular to the maximum stress throughout the region.
- On the island of Hopen both of the regional fracture sets are observed, with the FS.1 (ENE-WSW) fracture set being less prominent on the island.
- A further fracture set is observed on the island of Hopen, with a notably inconsistent trend to the NNE-SSW. This has been defined as FS.3.
- FS.3 fractures on Hopen are determined to have originated as a result of extensional tectonics, to the east and south east of Svalbard, which have been associated with basin formation in the Northern Barents Sea. This is due to the shared strike of this extensional regime and the Type I nature of fracturing seen within this set on the island. These fractures also align to the general structural style controlling the Hopen High.
- The potential association of FS.3 fractures on Edgeøya may suggest a significant regional control by these NE-SW trending fault systems offshore of Eastern Svalbard. However the lack of any significant FS.3 fractures at other locations holds this statement as speculative.
- FS.1, FS.2 and FS.3 fractures all display dominance of Type I mode fractures with an open fracture form and most often an irregular trace. Therefore it has been determined that these fractures have undergone significant

augmentation during Cenozoic uplift and unloading. Where fracture propagation has occurred along these existing discontinuities.

- Intrusive rocks may also have an added effect upon fracturing and may well account for the presence of anomalous fracture orientations within the dataset.
- The effects of smaller scale and more local tectonics have also been recorded in the dataset. In both Hopen and Central Spitsbergen fault related fracturing has been seen to form a contrasting orientation of fractures in Konusdalen, whilst fault related fractures on Hopen display a Type II fracture mode. These Type II fractures have been defined as a separate subset on Hopen, termed FSS.1 and are seen to form perpendicular to the strike of normal faulting. However these orientations are seen to be somewhat concealed within the general orientation of FS.1 fractures and are defined as a subset based purely on their mode.
- Scan-line fracture data clearly shows fracture densities decrease with increasing bed thickness and decreases in bed grain size, where sandstones are seen to have the greater thickness and higher fracture spacings in comparison to beds composed of sandstone and shale or just shale. Shales are observed to have the highest overall density of fractures.
- Fracture densities can be seen to be variable throughout Svalbard, however a negative trend in average fractures per metre is observed as locations become more east and southeast within the De Geerdalen Formation on Svalbard.
- In some locations, notably; Binnedalen in Northern Hopen, Konusdalen in Central Spitsbergen and to an extent Styggdalen in Central Hopen, anomalously high fracture densities have been observed and these are concluded to be fault related fractures. Resulting from beds in close proximity to faults naturally feature higher densities of fractures.
- A positive increase in average fracture spacing has been observed within the regional dataset and good evidence for increasing fracture spacing's to the east and south east is seen.
- The increase in fracture spacing and decrease in average number of fractures, is highly dependent upon the bed thickness observed for each-scan-line and its regional position. Whilst a random collection factor for bed thicknesses has been accounted for, the stratigraphy and varying depositional environment of

the De Geerdalen Formation is considered to have the greater controlling factor.

- Thus as the dataset shows a general increase in bed thickness to the east and southeast of Svalbard it is concluded that fracture densities in general are seen to decrease within the dataset, in these directions.



---

## 9. References

- Andresen, A., Bergh, S., Hansen, H., Klovjan, O., Kristensen, S.E., Liffbjerg, F., Lund, T., Mair, B.F., Midboe, P. & Nøttvedt, A., 1988:** Geometry and structural development of the Billefjorden and Lomfjorden fault zones in the Isfjorden-Sabine Land area, Spitsbergen. Abstract 18, Nordiske Geologiske Vintermøde, Copenhagen, January 1988, pp. 33-34.
- Andresen, A., Haremo, P., Swensson, E. & Bergh, S.G., 1992:** Structural geology around the southern termination of the Lomfjorden fault complex, Agardhdalen, East-Spitsbergen. Norsk Geologisk Tidsskrift. Vol. 72, pp. 83–91.
- Andresen, A., Bergh, S.G., & Haremo, P., 1994:** Basin inversion and thin-skinned deformation associated with the Tertiary transpressional West Spitsbergen orogeny. Proceeding from International Conference on Arctic Margins, Anchorage, Alaska, 6 p.
- Anell, I., Braathen, A., Olausen, S. & Osmundsen, P.T., 2013:** Evidence of faulting contradicts quiescent northern Barents Shelf during the Triassic. First Break, Vol. 31, pp. 67-76.
- Ask, M., 2013:** Palynological dating of the upper part of the De Geerdalen Formation on central parts of Spitsbergen and Hopen. Master Thesis, University of Bergen, 79 pp.
- Bäckström, S.A. & Nagy J., 1985:** Depositional history and fauna of a Jurassic phosphorite conglomerate (the Brentskardhaugen Bed) in Spitsbergen. Norsk Polarinstitutt Skrifter Nr. 183, pp. 1-61.
- Basov, V.A., Pčelina T.M., Bro, E.G. and contributors, 1993:** Mesozoic sequences and zonal stratigraphy of the Barents shelf and adjacent islands. IKU Report, Arctic Correlation and Exploration Programme.
- Bergh, S.G. & Andresen, A., 1990:** Structural development of the Tertiary fold-and-thrust belt in East Oscar II Land, Spitsbergen. Polar Research 8, pp. 217-236.

- 
- Bergh**, S.G., Braathen, A. & Andresen, A., 1997: Interaction of basement-involved and thin-skinned tectonism in the Tertiary fold-and-thrust belt, central Spitsbergen, Svalbard. *American Association of Petroleum Geologist Bulletin*, Vol. 81, pp. 637–661.
- Bergh**, S.G., Maher, H.D. jr. & Braathen A., 2011: Late Devonian transpressional Hornsund High. *Journal of the Geological Society*, v.168, pp.441-456.
- Bergsager**, E., 1986: Future petroleum potential of the Barents Sea. In: Spencer, A.M., (Ed.): *Habitat of hydrocarbons on the Norwegian Continental Margin*. Norwegian Petroleum Society (Graham & Trottmann), pp. 319-338.
- Berndt**, C., Planke, S., Alvestad, E., Tsikalas, F. & Rasmussen, T., 2001: Seismic volcanostratigraphy of the Norwegian Margin: constraints on tectonomagmatic breakup processes. *Journal of the Geological Society, London*, Vol. 158, pp. 413 –426.
- Bjærke**, T. & Dypvik, H., 1977: Sedimentological and Palynological studies of Upper Triassic – Lower Jurassic sediments in Sassenfjorden, Spitsbergen. *Norsk Polarinstitutt Årbok 1976*, pp. 131-150.
- Birkenmajer**, K., 1972: Tertiary history and continental drift. *Acta Geologica Polonica*, Vol. 22, pp. 193-218.
- Braathen**, A., Bergh, S.G. & Maher, H., 1997: Thrust kinematics in the central part of the Tertiary transpressional fold-thrust belt in Spitsbergen. *NGU Bulletin*, Vol. 433, pp.32–33.
- Braathen**, A., Bergh S.G., & Maher, H.D., 1999: Application of a critical wedge taper model to the Tertiary transpressional fold-thrust belt on Spitsbergen, Svalbard. *Geological Society of America Bulletin* 1999, Vol. 111, Nr. 10, pp. 1468-1485.
- Braathen**, A., Balum, K., Christiansen, H.H., Dahl, T., Eiken, O., Elvebakk, H., Hansen, F., Hanssen, T.H., Jochmann, M., Johansen, T.A., Johnsen, H., Larsen, L., Lie, T., Mertes, J., Mørk, A., Mørk, M.B., Nemeč, W., Olaussen, S., Oye, V., Rod, K., Titlestad, G.O., Tveranger, J. & Vagle, K., 2012: The Longyearbyen CO<sub>2</sub> Lab of Svalbard, Norway—initial assessment of the

geological conditions for CO<sub>2</sub> sequestration. *Norwegian Journal of Geology*, Vol. 92, pp. 353–376.

**Bruhn**, R. & Steel, R., 2003: High resolution sequence stratigraphy of a clastic foredeep succession (Palaeocene, Spitsbergen): An example of peripheral-bulge-controlled depositional architecture. *Journal of Sedimentary Research*, Vol. 73, Nr. 5, pp. 745-755.

**Buchan**, S.H., Challinor, A., Harland, W.B., & Parker J.R., 1965: The Triassic Stratigraphy of Svalbard. *Norsk Polarinstitutt Skrifter* Nr. 135.

**Bælum**, K. & Braathen, A., 2012: Along-strike changes in fault array and rift basin geometry of the Carboniferous Billefjorden Trough, Svalbard, Norway. *Tectonophysics*, 456-457, pp.38-55.

**Chalmers**, J.A. & Laursen, K.H., 1995: Labrador Sea - the extent of continental and oceanic crust and the timing of the onset of seafloor spreading. *Marine and Petroleum Geology*, Vol. 12, pp. 205–217.

**Cocks**, L.R.M. & Torsvik, T.H., 2007: Siberia, the wandering northern terrane, and its changing geography through the Palaeozoic. *Earth-Science Reviews*, Vol. 82, pp. 29–74.

**Cox**, C.B. & Smith, D.G., 1973: A review of the Triassic vertebrate faunas of Svalbard. *Geological Magazine*, Vol. 110, pp. 405-418.

**Currie**, J.B.H., Patnode, W. & Trump, R.P., 1962: Development of folds in sedimentary strata. *Geological Society of America Bulletin*, v.73, pp.655-673.

**Dagys**, A.S., Weitschat, W., Konstantinov, A.G. & Sobolev, E.S., 1993: Evolution of the boreal marine biota and stratigraphy at the Middle/Upper Triassic boundary. *Mitteilungen aus dem Geologisch-Paläontologisches Institut der Universität Hamburg* 75, pp. 192–209.

**Dallmann**, W.K., Andreasen, A., Bergh, S.G., Maher, H.D. & Ohta, Y., 1993: Tertiary fold-and-Thrust belt of Spitsbergen. *Norsk Polarinstitutt Meddeleser*, Vol. 128, pp. 46.

- Dallmann, W.K., Ohta, Y., Elvevold, S. & Blomeier, D., (eds), 2002:** Bedrock map of Svalbard and Jan Mayen. Norsk Polar Institutt Temakart No.33.
- Dallmann, W.K., 2009:** Hopen Geological Map 1:100,000. Norwegian Polar Institute.
- Dallmann, W.K., (Ed.), (in prep):** Geoscience Atlas of Svalbard. Norsk Polarinstitutt, Tromsø.
- Doré, A.G., 1995:** Barents Sea Geology, Petroleum Resources and Economic Potential. Arctic, Vol. 48, Nr. 3, pp. 207-221.
- Dypvik, H., Nagy, J., Eikeland, T.A., Backer-Owe, K., Andresen, A., harem, P., Bjærke, T., Johansen, H. & Elverhøi, A., 1991:** The Janusfjellet Subgroup (Bathonian to Hauterivian) on Central Spitsbergen: A revised Lithostratigraphy. Polar Research 9, pp. 21-43.
- Edwards, M.B., 1976:** Growth faults in Upper Triassic deltaic sediments, Svalbard. The American Association of Petroleum Geologists Bulletin, Vol. 60, Nr. 3, pp. 341-355.
- Eiken, O., 1985:** Seismic mapping of the post-Caledonian strata in Svalbard. Polar Research 3, Norsk Skrifter, pp. 167-176.
- Eldholm, O., Faleide, J. I. & Myhre, A., 1987:** Continent-ocean transition at the western Barents Sea/Svalbard continental margin. Geology 15, pp. 1118-1122.
- Elvevold, S. (editor), Dallmann, W. & Blomeier, D., 2007:** Geology of Svalbard. Norwegian Polar Institute, Tromsø.
- Engelder, T., & Geiser, P., 1980:** On the use of regional joint sets as trajectories of palaeostress fields during development of the Appalachian Plateau, New York. Journal of Geophysical Research, Vol. 85 No. B11, pp. 6319-6341.
- Engelder, T., & Peacock, D.C.P., 2000:** Joint development normal to regional compression during flexural flow-folding: the Lilstock buttress anticline, Somerset, England. Journal of Structural Geology 23, pp. 259-277.

- Faleide**, J.I., Tsikalas, F., Breivik, A.J., Mjelde, R., Trizmann, O., Engen, Ø., Wilson, J. & Eldholm, O., 2008: Structure and evolution of the continental margin off Norway and the Barents Sea. *Episodes* 2008, Vol. 31, No. 1, pp. 51-61.
- Falcon**, N.L., 1928: Geology, Appendix III. In: Watkins, H.G., "The Cambridge Expedition to Edge Island." *Geographical Journal*, Vol.72, pp.134-139.
- Farrell**, L.R., 2011: Appraisal of the Longyearbyen CO<sub>2</sub> Project, a Fractured Reservoir. Master Thesis, University of Edinburgh, 108 pp.
- Flood**, B., Nagy, J. & Winsnes, T.S., 1971: The Triassic succession of Barentsøya, Edgeøya and Hopen (Svalbard). *Norsk Polarinstitutt Meddeler* Nr. 100.
- Fossen**, H., Tikoff, B. & Teyssier, C., 1994: Strain modelling of transpressional and transtensional deformation. *Norsk Geologisk Tidsskrift*, Vol. 74, pp. 134-145.
- Freund**, L.B., 1990: *Dynamic Fracture Mechanics*, Cambridge University Press, Cambridge.
- Gabrielsen**, R.H., Færseth, R.B., Jensen, L.N., Kalheim, J.E. & Riis, F., 1990: Structural elements of the Norwegian continental shelf Part 1: The Barents Sea Region. *NPD-Bulletin* No. 6, pp. 3-33.
- Glørstad-Clark**, E., Faleide, J.I., Lundschie, B.A. & Nystuen, J.P., 2010: Triassic seismic sequence stratigraphy and paleogeography of the western Barents Sea area. *Marine and Petroleum Geology*, Vol. 27, pp. 1448-1475.
- Glørstad-Clark**, E., 2011: Depositional dynamics in an epicontinental basin: De Geerdalen Formation on Edgeøya, Svalbard. In: Glørstad-Clark, E., (ed.): Basin analysis in the western Barents Sea area: The interplay between accommodation space and depositional systems. PhD thesis, University of Oslo, pp. 215-262.
- Grogan**, P., Østvedt-Ghazi, A-M., Larssen, G.B., Fotland, B., Nyberg, K., Dahlgren, S. & Eidvin, T., 1999: Structural elements and petroleum geology of the 1999: *Petroleum Geology of Northwest Europe: Proceedings of the 5th Conference*, London, 26-29 October 1997, Geological Society, Vol.1, pp. 247-259.

- Gross**, M.R. & Engelder, T., 1995: Fracture strain in adjacent units of the Monterey Formation: Scale effects and evidence for uniform boundary conditions. *Journal of Structural Geology*, Vol. 17, pp. 1303-1318.
- Gross**, M.R., Fischer, M.P., Engelder, T. & Greenfield, R.J., 1995: Factors controlling joint spacing in inter-bedded sedimentary rocks: Interpreting numerical models with field observations from the Monterey Formation, USA. In: Ameen, M.S., (ed) *Fractography: Fracture topography as a tool in fracture mechanics and stress analysis*. Geological Society of America Special Publication 92, pp.215-233.
- Hanks**, C.L., Lorenz, J., Lawrence, T. & Krumhardt, A.P., 1997: Lithologic and structural controls on natural fracture distribution and behaviour within the Lisburne Group, Northeastern Brooks Range and Northern Slope subsurface, Alaska. *American Association of Petroleum Geologists Bulletin*, Vol. 81, No.10, pp. 1700-1720.
- Haremo** P. & Andresen, A., 1992: Tertiary Décollement thrusting and inversion structures along Billefjord and Lomfjorden Fault Zones, East Central Spitsbergen. *Structural and Tectonic Modelling and Its Application to Petroleum Geology: Special Publication 1*, pp. 481-491.
- Harland**, W.B., 1969: Contribution of Spitsbergen to understanding of tectonic evolution of North Atlantic region. In: Kay, M. (eds): *North Atlantic: Geology and Continental Drift*, a symposium. *American Association of Petroleum Geologists Memoir 12*, pp. 817-851.
- Harland**, W. B., Cutbill, J. I., Friend. P. F., Gobbett. D. S., Holliday. D. W., Maton, P. I., Parker, J.K. & Wallis. R.H., 1974: *The Billefjorden Fault Zone, Spitsbergen*. Norsk Polar Institutt Skrifter Nr. 161.
- Harland**, W.B., 1979: A review of major faults in Svalbard. *Regional Tectonic Series (Cambridge Arctic Shelf Programme)*, No. 132, CASP 1979.
- Harland**, W.B., 1997: Chapter 3: Svalbard's geological frame. In: Harland, B. (ed.) *The Geology of Svalbard*. Geological Society, London, *Memoirs 17*, pp. 23–46.

- Helgeson**, D.E. & Aydin, A., 1991: Characteristics of joint propagation across layer interfaces in sedimentary rocks. *Journal of Structural Geology*, Vol. 13, pp. 897- 911.
- Hoel**, O. & Orheim, A., 2003: The Place Names of Svalbard. Norwegian Polar Institute Rapport Volume 122.
- Hynne**, I.B., 2010: Depositional environment on eastern Svalbard and central Spitsbergen during Carnian time (Late Triassic). Master Thesis, Norwegian University of Science and Technology, 144 pp.
- Høy**, T. & Lundschieen B.A., 2011: Triassic deltaic sequences in the northern Barents Sea. *Geological Society, London, Memoirs 2011*, Vol. 35, pp. 249-260.
- Johansen**, S.E., Ostistiy, B.K., Birkeland, Ø., Fedorovsky, Y.F., Martirosjan, V.N., Brunn Christensen, O., Cheredeev, S.I., Ignatenko, E.A. & Margulis, L.S., 1992: Hydrocarbon potential in the Barents Sea region: Play distribution and potential. *Arctic Geology and Petroleum Potential, NPF Special Publication, No.2*, Elsevier, Amsterdam, pp. 273-320.
- Johannessen**, E.P. & Steel, R.J., 1992: Mid Carboniferous extension and rift-infill sequences in the Billefjorden trough, Svalbard. *Norsk Geologisk Tidsskrift*, Vol. 72, pp. 35-48.
- Klausen**, T. & Mørk, A., Submitted: The Late Triassic Paralic Deposits of the De Geerdalen Formation on Hopen: Outcrop Analogue to the Subsurface Snadd Formation.
- Knarud**, R., 1980: En sedimentologisk og diagenetisk undersøkelse av Kapp Toscana Formasjonens sedimenter på Svalbard. Candidate Realfag Thesis, University of Oslo, 208 pp.
- Korčinskaja**, M.V., 1980: Rannenorijskja fauna archipelago Sval'bard. (Early Norianfauna of the archipelago of Svalbard). In: Semevskij, D.V., (ed): *Geologija osadočnogo čechla archipelago Sval'bard* (Geology of the sedimentary platform cover of the archipelago of Svalbard). NIIGA, Leningrad.

- Korčinskaja**, M.V., 1982: Ob'jasnitel'naja zapiska k stratigrafičeskoj scheme mezozoja (trias) Sval'barda (Explanatory note to the stratigraphic scheme of Mesozoic (Triassic) Svalbard). PGO "Sevmorgeologija", Leningrad, pp. 40-99.
- Kulander**, B.R., Barton, C.C. & Dean, S.L. 1979: The application of fractography to core and outcrop fracture investigations. U.S. Dept. of Energy, METC/SP-79/3; National Technical Information Service, U.S. Dept. of Commerce, Springfield, VA 22161.
- Krajewski**, K.P., Karcz, P., Wozny, E. & Mørk A., 2007: Type section of the Bravaisberget Formation (Middle Triassic) at Bravaisberget, western Nathorst Land, Spitsbergen, Svalbard. Polish Polar Research 28, 79–122.
- Krajewski**, K.P., 2008: The Botneheia Formation (Middle Triassic) in Edgeøya and Barentsøya Svalbard: Lithostratigraphy facies, phosphogenesis, paleoenvironment. Polish Polar Research, Vol. 29, No. 4, pp. 317-362.
- Lamar**, D.L., Reed, W.E. & Douglass, D.N., 1986: Billefjorden fault zone, Spitsbergen: Is it part of a major Late Devonian transform? Geological Society of America Bulletin, September, 1986, Vol. 97, No. 9, pp. 1083-1088.
- Laubach**, S.E., Olson, J.E. & Gross, M.R., 2009: Mechanical and Fracture Stratigraphy, AAPG Bulletin, v.93, pp.1413-1426.
- Leever**, K.A., Gabrielsen, R., Faleide, J.I. & Braathen, A. 2011: A transpressional origin for the West-Spitsbergen fold-and-thrust belt: Insight from analogue modelling. Tectonics, Vol. 30, pp. 1-24.
- Lock**, B.E., Pickton, C.A.G., Smith, D.G., Batten, D.J. & Harland, W.B., 1978: The Geology of Edgeøya and Barentsøya, Svalbard. Norsk Polarinstitutt Skrifter Nr. 168.
- Lord**, G.S., 2012: Characterisation of steep, natural fracture patterns and their relationships within the Triassic De Geerdalen Formation of Central Spitsbergen. Project Thesis, Norwegian University of Science and Technology, 74 pp.



- Lowell**, J.D., 1972: Spitsbergen Tertiary Orogenic Belt and the Spitsbergen Fracture Zone. Geological Society of America Bulletin, October 1972, Vol. 83, Nr. 10, pp. 3091-3102.
- Lyberis** N. & Manby, G., 1993: The West Spitsbergen Fold Belt: The result of Late Cretaceous-Palaeocene Greenland Svalbard convergence? Geological Journal, Vol. 28, Issue 2, pp. 125-136.
- Maher**, H.D., Braathen, A., Bergh, S.G., Dallmann, W.K. & Harland W.B., 1995: Tertiary or Cretaceous age for Spitsbergen's fold-thrust belt on the Barents Shelf. Tectonics, Vol. 14, pp. 1321-1326.
- Major**, H. & Nagy, J., 1972: Geology of the Adventdalen map area. Norsk Polarinstitutt Skrifter Nr. 138.
- Major**, H., Nagy, J., Haremo, P., Dallman, W.K., Andresen, A. & Salvigsen O., 1992: Adventdalen (Revised after Major & Nagy, 1964) Geological Map Svalbard 1:100 000, Sheet CG9, Preliminary Edition, Norwegian Polar Institute.
- Manby**, G.M., Lyberis, N., Chorowicz, J. & Thiedig, F., 1994: Post-Caledonian tectonics along the Billefjorden fault zone, Svalbard and implications for the Arctic region. Geological Society of America Bulletin, February 1994, Vol. 106, Nr. 2, pp. 201-216.
- Manum**, S.B. & Throndsen, T., 1986: Age of Tertiary formations on Spitsbergen. Polar Research 4, Norsk Polarinstitutt Skrifter, pp. 103-131.
- Max**, M.D. & Ohta, Y., 1988: Did major fractures in continental crust control orientation of the Knipovich Ridge – Lena Trough segment of the plate margin? Polar Research 6, pp. 85-93.
- Miller**, E.L., Soloviev, A.V., Prokopiev, A.V., Toro, J., Harris, D., Kuzmichev, A.B. & Gehrels, G.E., 2012: Triassic river systems and the paleo-Pacific margin of northwestern Pangea. Gondwana Research.
- Myhre**, A.M., Eldholm, O. & Sundvor, E., 1982: The margin between Senja and the Spitsbergen Fracture Zones: Implications from plate tectonics. Tectonophysics 89, pp. 33-50.

- 
- Myhre**, A.M. & Eldholm, O., 1988: The western Svalbard Margin (74°-80°N). *Marine and Petroleum Geology*, Vol. 5, pp. 134-156.
- Müller**, R.D. & Spielhagen, R.F., 1990: Evolution of the Central Tertiary Basin of Spitsbergen: towards a synthesis of sediment and plate tectonic history. *Palaeogeography, Palaeoclimatology, Palaeoecology*, vol.80, pp. 153-172.
- Mørk** A. & Bjørøy, M., 1984: Mesozoic source rocks on Svalbard. *Petroleum Geology of the North European Margin*. Norwegian Petroleum Society (Graham & Trotman, 1984), pp. 371-382.
- Mørk**, A., Knarud, R. & Worsley, D., 1982: Depositional and Diagenetic Environments of The Triassic and Lower Jurassic Succession of Svalbard. *Arctic Geology and Geophysics, Memoir 8*.
- Mørk**, A., Embry, A.F. & Weitschat, W., 1989: Triassic transgressive-regressive cycles in the Sverdrup Basin, Svalbard and the Barents Sea. In: Collinson, J.D. (ed.), *Correlation in Hydrocarbon Exploration*. Norwegian Petroleum Society, Graham & Trotman, London, 1989, pp. 113-130.
- Mørk**, A., Dallmann, W.k., Dypvik, H., Johannessen, E.P., Larssen, G.B., Nagy, J., Nøttvedt, A., Olaussen, S., Pčelina, T.M. & Worsley, D., 1999: Mesozoic Lithostratigraphy. In: Dallmann, W.K., (Ed.) 1999: *Lithostratigraphic Lexicon of Svalbard, Upper Palaeozoic to Quaternary Bedrock – Review and recommendations for nomenclature use*. Norwegian Polar Institute, Tromsø. 1999.
- Mørk**, A. & Smelror, M., 2001: Correlation and Non-Correlation of High Order Circum-Arctic Mesozoic Sequences. *Polarforschung* 69, pp. 65-72. Erschienen, 2001.
- Nelson**, R.A., 1985: *Geological Analysis of Naturally Fractured Reservoirs*. Gulf Publishing Company, Houston – Texas.
- Norsk Meteorologisk Institutt**, 2010: Hopen, [ONLINE], Available at: [http://met.no/Klima/Klimastatistikk/Varet\\_i\\_Norge/2010/September\\_2010/filestore/M-HOPEN\\_6959\\_met.jpg?size=500x1000](http://met.no/Klima/Klimastatistikk/Varet_i_Norge/2010/September_2010/filestore/M-HOPEN_6959_met.jpg?size=500x1000). [Accessed: 13/05/2013].

- Nøttvedt**, A., & Rasmussen, E., 1988: Tertiary deformation in central-west Spitsbergen, as interpreted from marine reflection seismic data. Abstract 18, Nordiske Geologiske Vintermøde, Copenhagen, January 1988, pp. 320-321.
- Ogata**, K., Senger, K., Braathen, A., Tveranger, J., & Olausen, S., 2012: The importance of natural fractures in a tight reservoir for potential CO<sub>2</sub> storage: the case study of the upper Triassic to middle Jurassic Kapp Toscana Group (Spitsbergen, Svalbard). *Journal of the Geological Society, London* Vol. 347, pp. 374-395.
- Olausen**, S., Braathen, A., Hansen, T.H., Johansen, T.A., Mørk, A., Mørk, M.B., Oye, V., Riis, F., Tveranger, J., Sand, G. and the project team, 2011: Results from characterisation and testing of a low-pressured unconventional reservoir, the Triassic De Geerdalen Formation in well DH4 Longyearbyen CO<sub>2</sub> lab, Adventdalen, Svalbard Vinterkonferansen, Stavanger, 11-13 January. Abstract and Proceeding of the Geological Society of Norway, pp. 73-74.
- Olson**, J.E. & Pollard, D.D., 1989: Inferring palaeostresses from natural fracture patterns: A new method. *Geology*, Vol. 17, pp. 345-348.
- Orvin**, A. K. 1940: Outline of the geological history of Spitsbergen. *Skrifter om Svalbard og Ishavet*, Vol. 78, pp. 1-57.
- Osmundsen**, P.T., Braathen, A., Sande, Rød, R. & Hynne, I., 2013: Styles of normal faulting and fault controlled deposition in the Triassic of Hopen and Edgeøya, Svalbard. *Norwegian Petroleum Directorate Bulletin*, In press.
- Parker**, J.R., 1966: Folding, faulting and dolerite intrusions in the Mesozoic rocks of the fault zone of Central Spitsbergen. *Norsk Polarinstitutts Årbok 1964*, pp. 47-55.
- Parker**, J.R., 1967: The Jurassic and Cretaceous sequence in Spitsbergen. *Geological Magazine*, Vol. 104, pp. 487-505.
- Pčelina**, T.M., 1965: Mezozojskie otloženija rajona Van-Kjlenf'orda Zapadnyj Špicbergen (Mesozoic deposits around Van Keulenfjorden, Western Spitsbergen). In: *Materialy po geologii Špicbergena*. Leningrad, 1965.

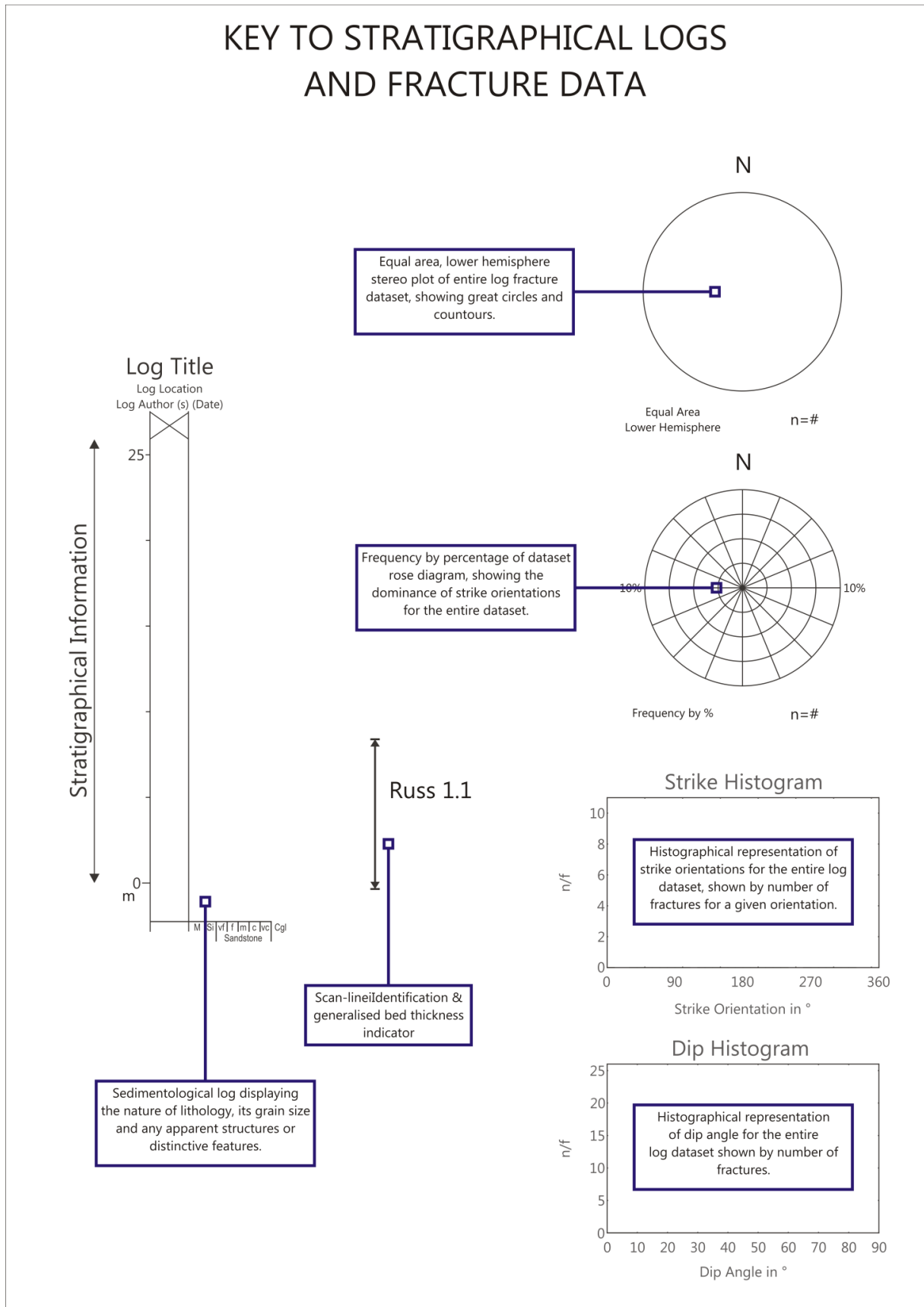
- Pčelina**, T.M., 1972: Concerning the age of sedimentary strata on Hopen. In: Sokolov, V.N. & Vasilevskaya, N.D., (eds): Mesozoic deposits in Svalbard. Leningrad, pp. 75-81.
- Pčelina**, T.M., 1983: Novye dannye po stratigrafii mezozoja archipelago Špicbergena, (New Material on the Geology of the Spitsbergen Archipelago). In: Geologija Špicbergena (The Geology of Spitsbergen). PGO "Sevmorgeologija", Leningrad, pp. 121-141.
- Pollard**, D.D., Segall, P. & Delaney, P.T., 1982: Formation and interpretation of dilatant echelon cracks. Geological Society of America Bulletin, Vol. 93, pp. 1291-1303.
- Ramsey**, J.M. & Chester, F.M., 2004: Hybrid fracture and the transition from extension fracture to shear fracture. Nature, Vol. 428, pp. 63-66.
- Riis**, F., Lundschieen, B.A., Høy, T., Mørk, A. & Mørk, M-B.E., 2008: Evolution of the Triassic shelf in the northern Barents Sea region. Polar Research 27, pp. 318-338.
- Ringset**, N. & Andresen, A., 1988: The Gipshuken fault system - Evidence of Tertiary thrusting along the Billefjorden Fault Zone. Norsk Polarinstitutt. Rapport. Vol. 46, pp. 67-70.
- Rød**, R.S., 2011: Spatial occurrences of selected sandstone bodies in the De Geerdalen Formation, Svalbard, and their relation to depositional facies. Master Thesis, Norwegian University of Science and Technology, 122 pp.
- Senger**, K., Ogata, K., Braathen, A., Olaussen S. & Tveranger J., 2011: Modeling Natural Fractures Using Borehole and Outcrop Data. SES - EAGE Sustainable Earth Sciences Conference & Exhibition - Technologies for the Sustainable Use of the Deep Subsurface - November 2011, Valencia, Spain.
- Smith**, D.G., 1974: Late Triassic pollen and spores from the Kapp Toscana Formation, Hopen, Svalbard; a preliminary account. Review of Palaeobotany and Palynology. Vol. 17, pp. 175-178.

- Smith, D.G.**, 1975: The stratigraphy of Wilhelmøya and Hellwaldfjellet, Svalbard. *Geological Magazine* 112, pp. 481-491.
- Smith, D.G.**, Harland, W.B. & Hughes, N.F., 1975: Geology of Hopen, Svalbard. *Geological Magazine*, Vol. 112, Nr. 1, pp. 1-23.
- Solvi, K.H.**, 2013: Visualize and interpret the geometry, heterogeneity and lateral continuation of channel bodies in the De Geerdalen Formation at Hopen, Master Thesis, Norwegian University of Science and Technology, 122 pp.
- Steel, R.J. & Worsley, D.**, 1984: Svalbard's post-Caledonian strata – an analysis of sedimentational patterns and paleogeographic evolution. In: Spencer, A.M., Johnsen, S.O., Mørk, A., Nysæter, E., Songstad, P. & Spinnangr, Å., (Eds.), *Petroleum Geology of the North European Margin*. Norwegian Petroleum Society, Graham & Trotman, pp. 109-135.
- Sundvor, E. & Eldholm, O.**, 1976: Marine Geophysical survey on the continental margin from Bear Island to Hornsund, Spitsbergen. Universitetet i Bergen Seismology, Observations Scientific Report, Vol. 3, 28 pp.
- Sysselmannen**, 2008: Geology, [ONLINE], Available at: <http://oldweb.sysselmannen.no/hovedEnkel.aspx?m=45298>, [Accessed: 06/05/2013].
- Torsvik, T.H. & Cocks, L.R.M.**, 2004: Earth geography from 400 to 250 million years: a palaeomagnetic, faunal and facies review. *Journal of the Geological Society*, London, Vol.161, pp.555–572.
- Torsvik, T.H.**, Van der Voo, R., Preeden, U., Mac Niocaill, C., Steinburger, B., Doubrovine, P.V., van Hinsbergen, D.J.J., Domeier, M., Gaina, C., Tohver, E., Meert, J.G., McCausland, P.J.A. & Cocks, L.R.M., 2012: Phanerozoic polar wander, palaeogeography and dynamics. *Earth Sciences Review*, Vol. 114, pp. 325-368.
- Tozer, E.T.**, & Parker, J.R., 1968: Notes on the Triassic biostratigraphy of Svalbard. *Geological Magazine* 105, pp. 526-542.

- Twiss, R.J. & Moores, E.M., 2007:** Structural Geology - Second Edition. W.H. Freeman, California.
- Underwood, C.A., Cooke, M.L., Simo, J.A. & Muldoon, M.A., 2002:** Stratigraphic controls on vertical fracture patterns in Silurian dolomite, Northeastern Wisconsin. AAPG Bulletin, v.17, pp.121-142.
- UNIS CO<sub>2</sub> Lab, 2012:** UNIS - The University Centre in Svalbard, Home - CO<sub>2</sub> - CCS - Unis CO<sub>2</sub> Lab - UNIS - The University Centre in Svalbard. [ONLINE] Available at: <http://co2-ccs.unis.no/>. [Accessed: 08/5/2012].
- Vigran, J.O., Mangerud, G., Mørk, A., Worsley, D. and Hochuli, P.A., Submitted:** Palynology and geology of the Triassic succession of Svalbard and the Barents Sea. Geological Survey of Norway, Special Paper.
- Waerum, G.O., 2011:** Bruddmønstre i øvre Triaslagrekken ved Vindodden på Svalbard: Opptreden, geometri og dannelsesmekanismer samt betydning for CO<sub>2</sub> lagring. Master Thesis (Norwegian), University of Tromsø, 101 pp.
- Weitschat, W. & Lehmann, U., 1983:** Stratigraphy and ammonoids from the Middle Triassic Botneheia Formation (Daonella Shales) of Spitsbergen. *Mittelungen, Geologisch-Paläontologisches institute der Universität Hamburg* 48, pp. 27-54.
- Våagnes, E., 1997:** Uplift at thermo-mechanically coupled ocean-continent transforms: Modelled at the Senja Fracture Zone, south-western Barents Sea. *Geo-Mar. Letters*. 17, pp. 100–109.
- Willis, B., 1984:** Mechanics of Appalachian structure. U.S. Geological Survey, 13th Annual Report, pp. 211-281.
- Worsley, D., 1973:** The wilhemøya Formation – a new lithostratigraphic unit from the Mesozoic of Eastern Svalbard. *Norsk Polarinstitutt Årbok* 1971, pp. 7-16.
- Worsley, D., 2008:** The post Caledonian development of Svalbard and the western Barents Sea. *Polar Research* 27, pp. 298-317.










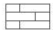

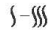































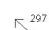



## **10. Appendix 1 –Stratigraphical Logs and Composite Fracture Orientation Data**

# KEY TO STRATIGRAPHICAL LOGS AND FRACTURE DATA



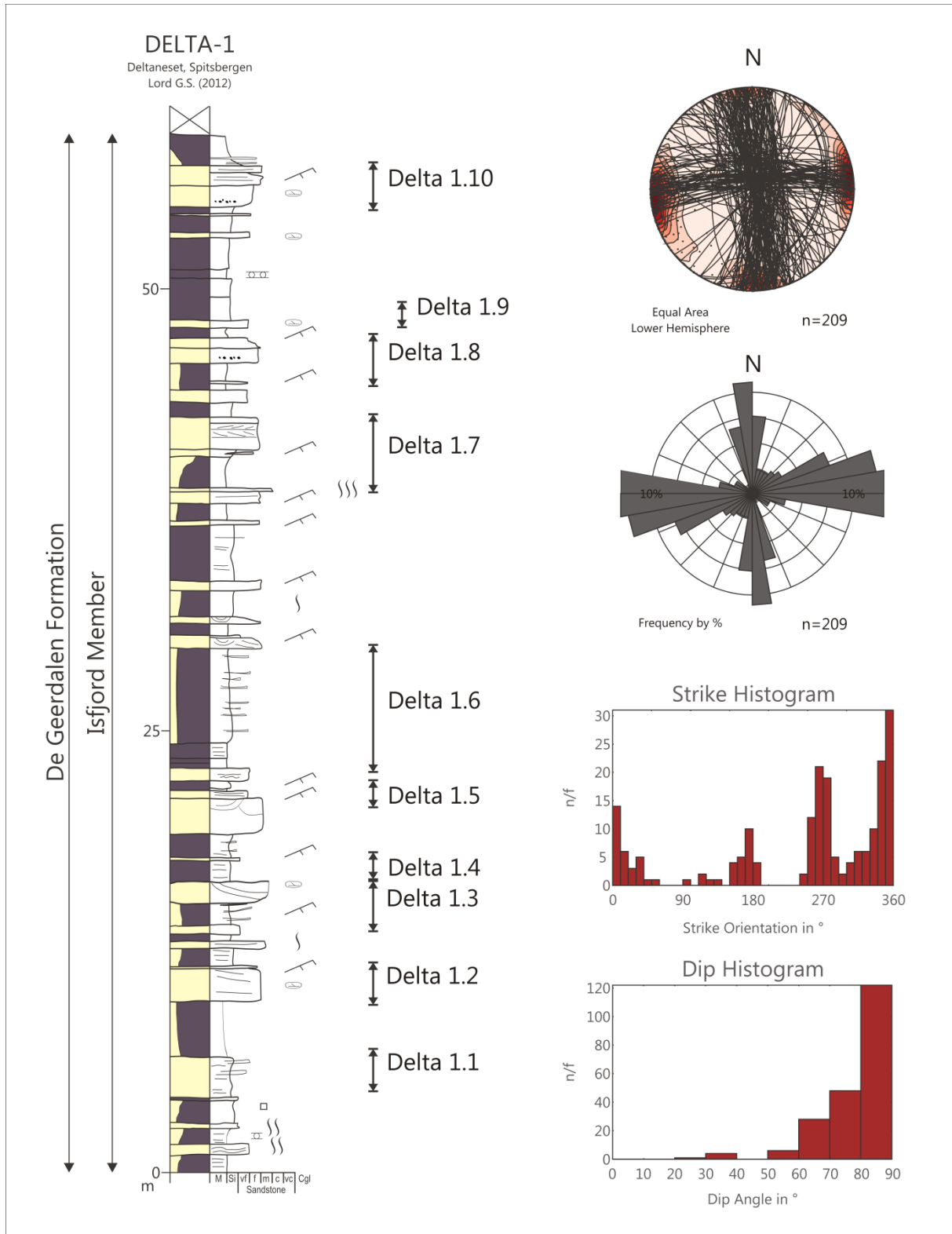


## Legend

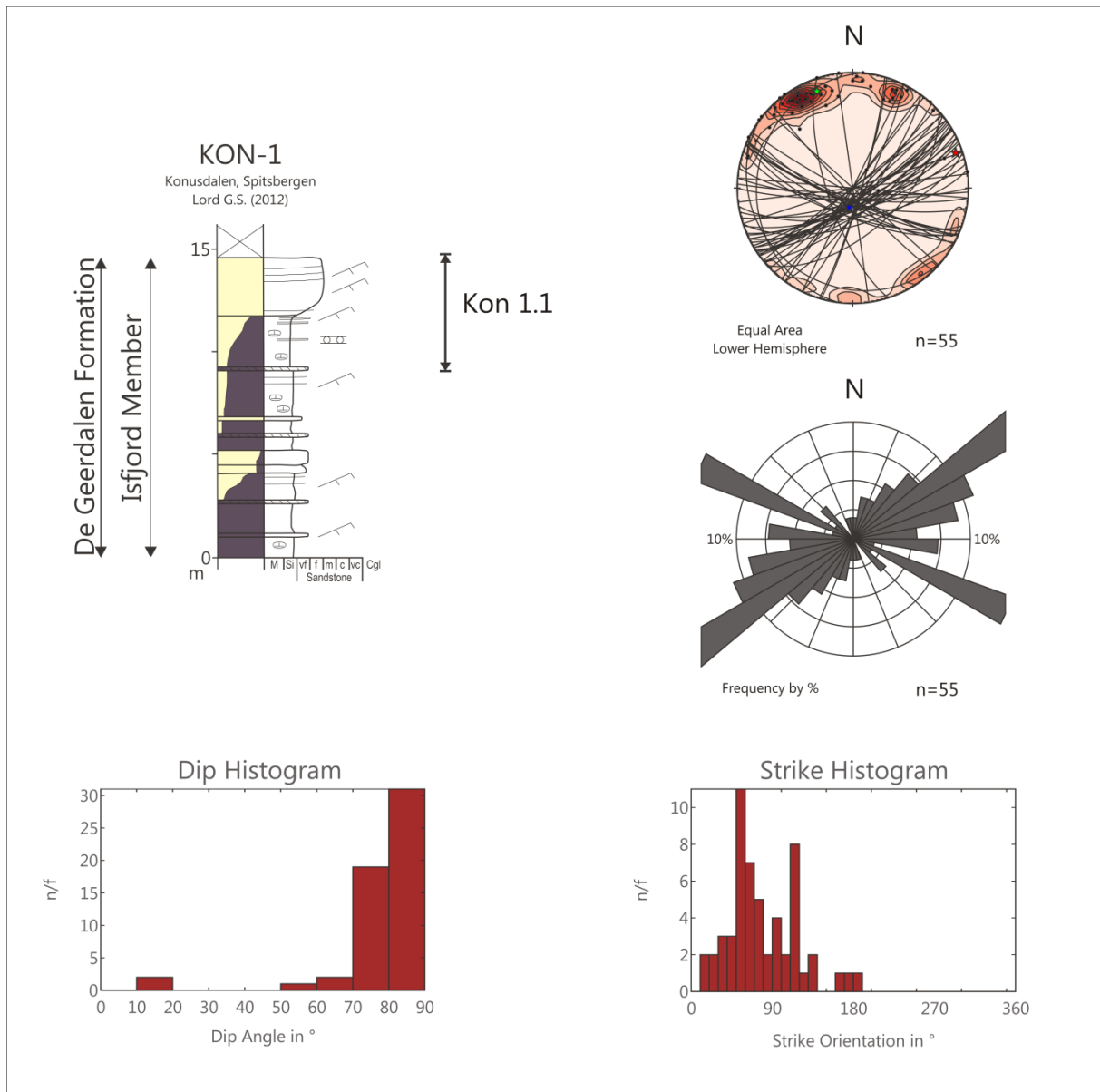
	Sandstone		Large scale hummocky bedding		Cone in cone
	Claystone / mudstone		Small scale hummocky cross bedding		Wood / Plant fragments
	Covered / partly covered		Large scale trough cross-stratification		Roots
	Limestone		Large scale tangential cross-stratification		Increasing bioturbation
	Coal		Large scale angular cross-stratification		Skolithos
	Coal-shale		Mud drapes		Rhizocorallium
	Current ripples (3D)		Mud flakes		Diplocraterion
	Current ripples (2D)		Erosional surface		Palaeophycus (+ unidentified tunnels)
	Wave ripples		Desiccation cracks		Bivalves
	Unspecified ripple lamination		Loading (major)		Coquina
	Herringbone lamination		Loading (minor)		Unidentified fossil fragment
	Planar lamination		Soft sediment deformation		Nodule
	Low angle cross-bedding		Convolute lamination		Calcite cementation
	Lenticular lamination		Bidirectional paleocurrent measurement		Siderite cementation
	Climbing ripples		directional paleocurrent measurement		Pyrite
	Lenticular and ripple lamination				Unspecified cementation

## Appendix 1.1 – Central Spitsbergen

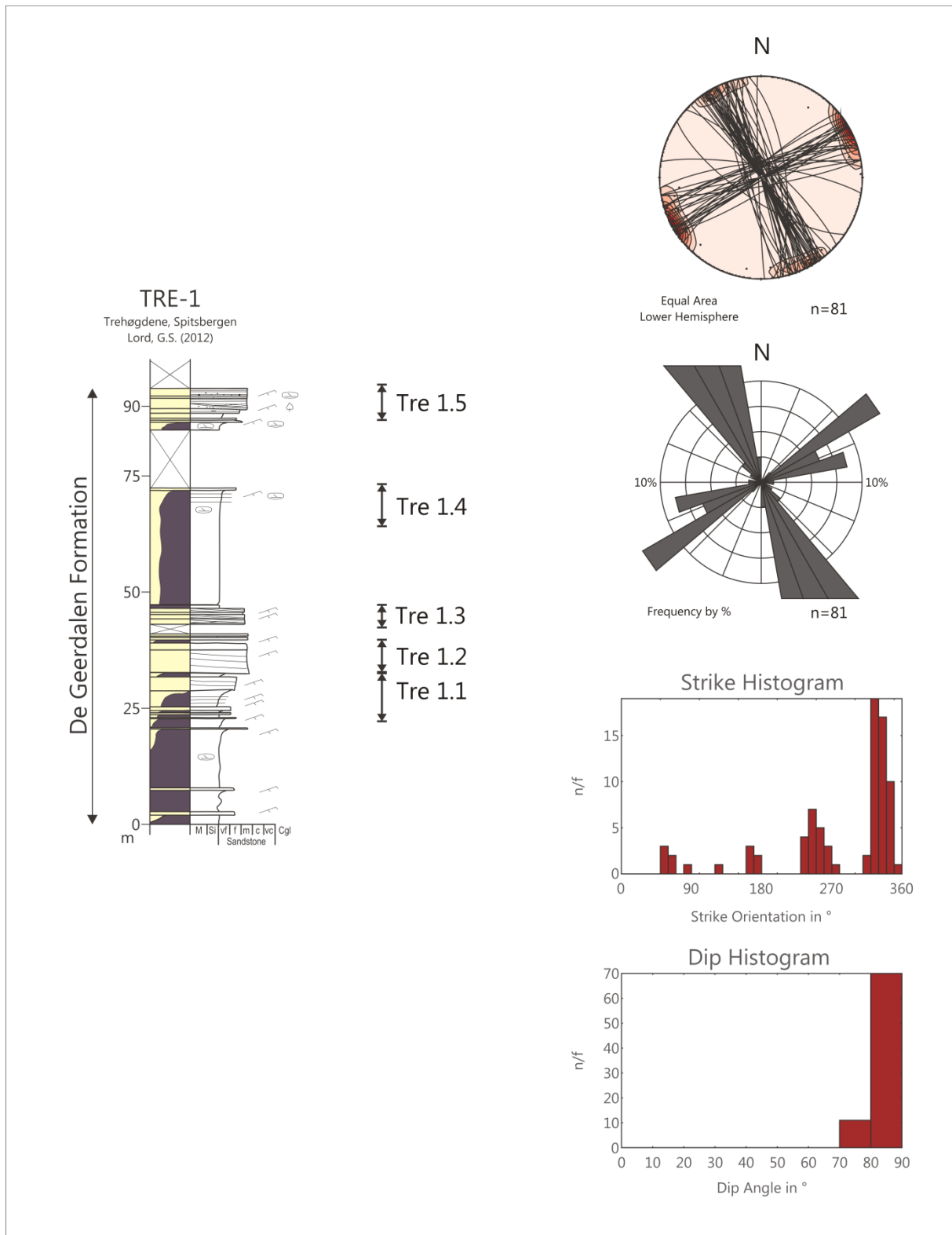
### Appendix 1.1.1 – Deltaneset



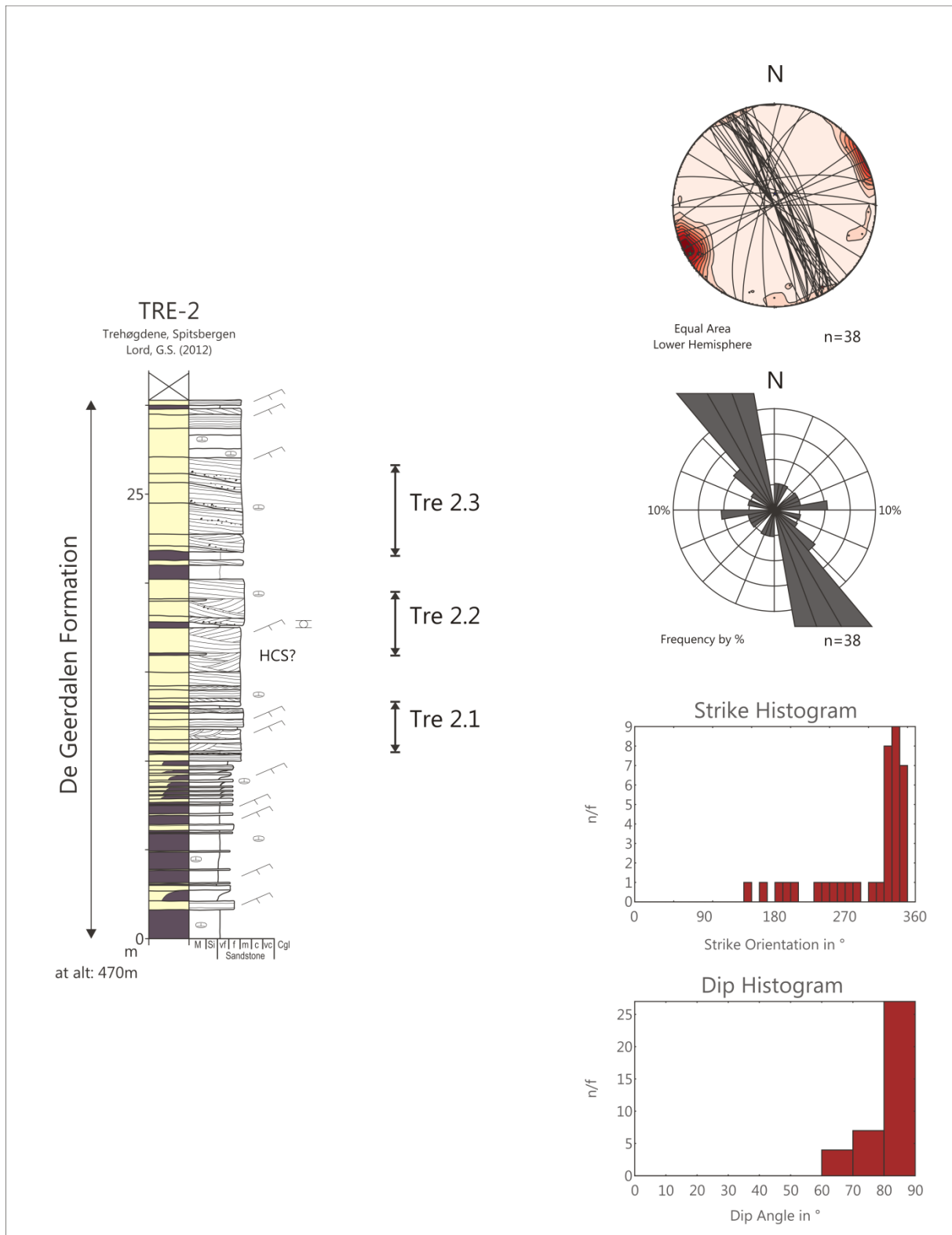
Appendix 1.1.2 – Konusdalen



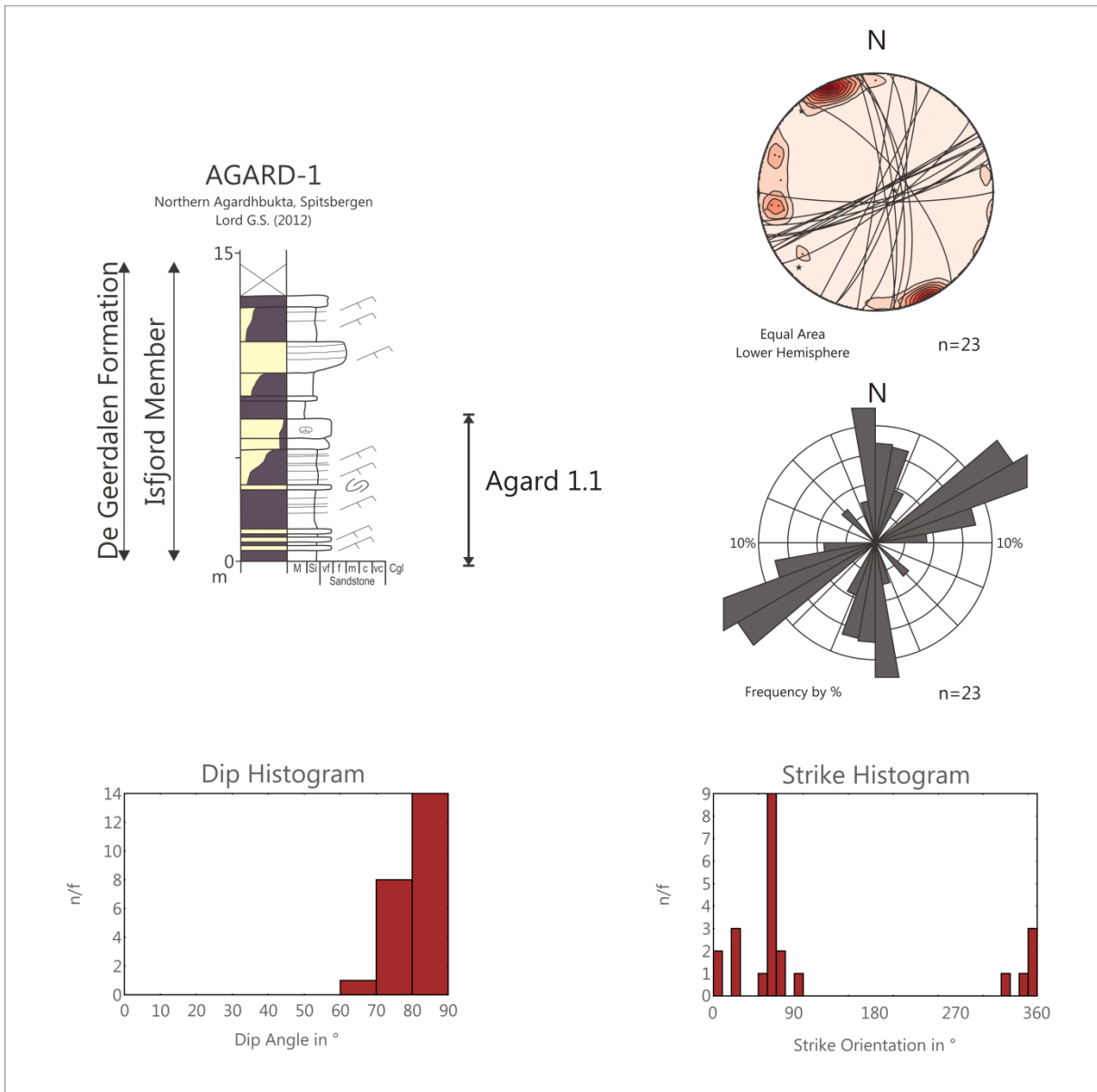
Appendix 1.1.3a – Trehøgdene (Tre-1)



Appendix 1.1.3b – Trehøgdene (Tre-2)

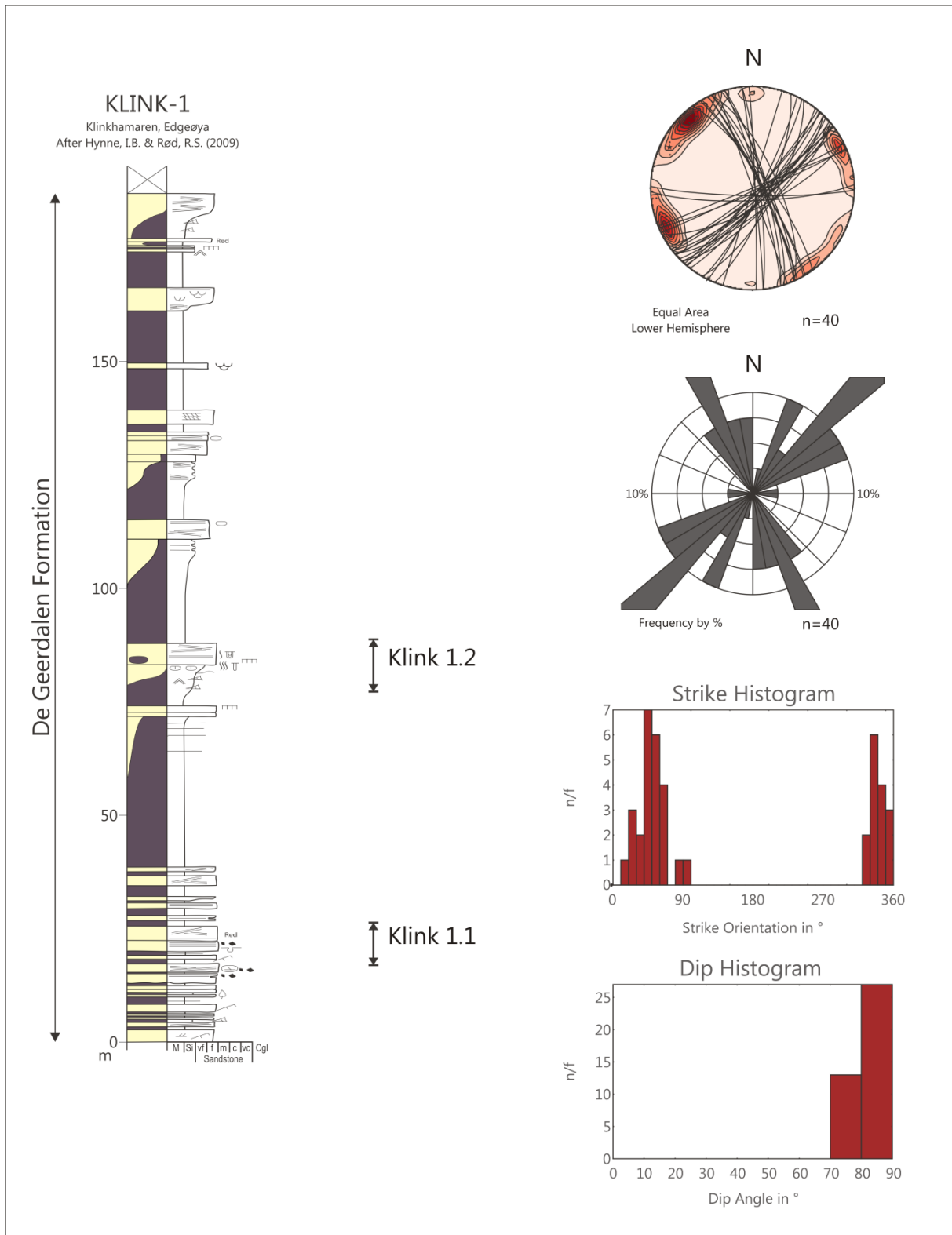


Appendix 1.1.4 – Agardhbukta

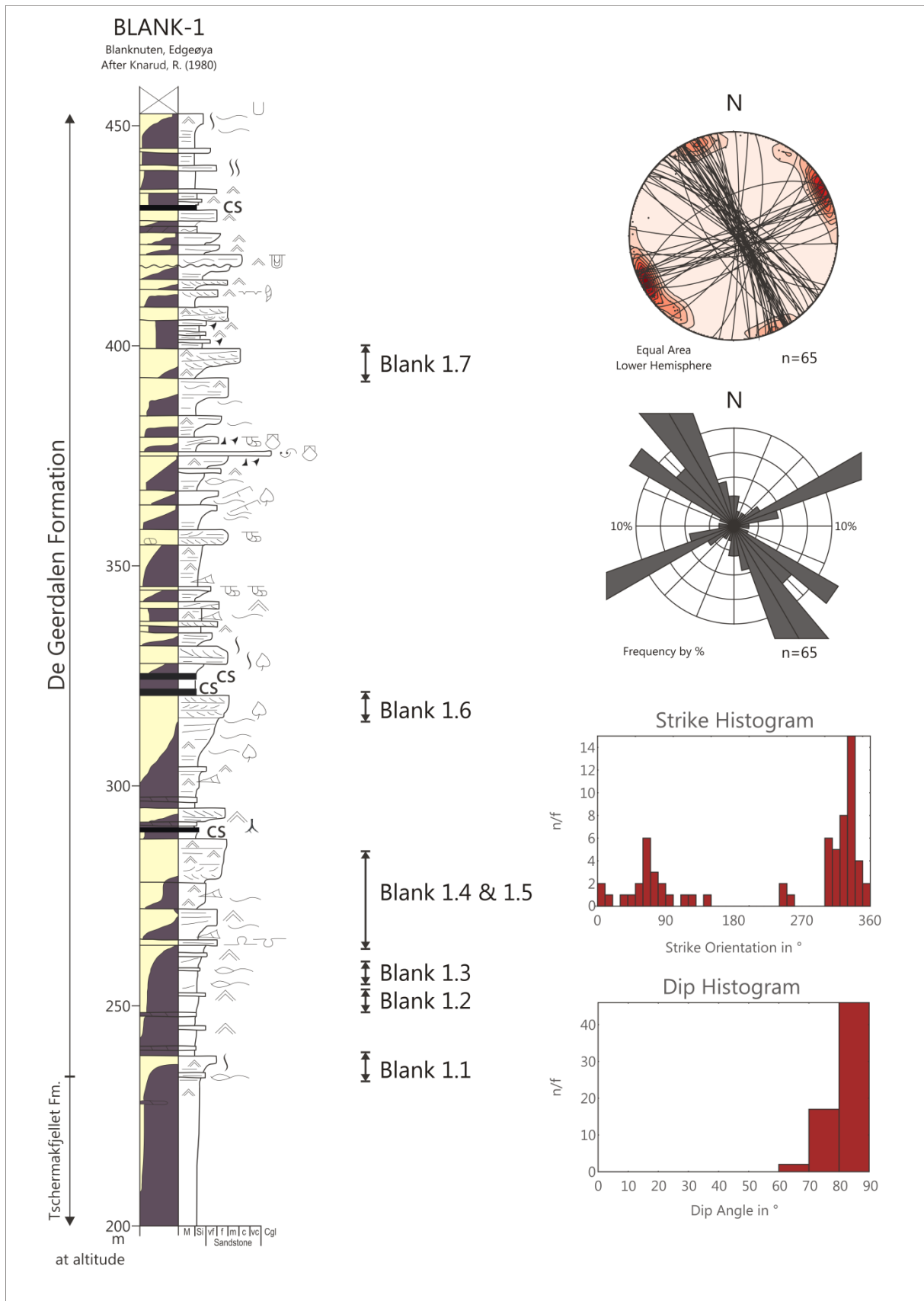


## Appendix 1.2 – Western Edgeøya

### Appendix 1.2 .1 – Klinkhamaren

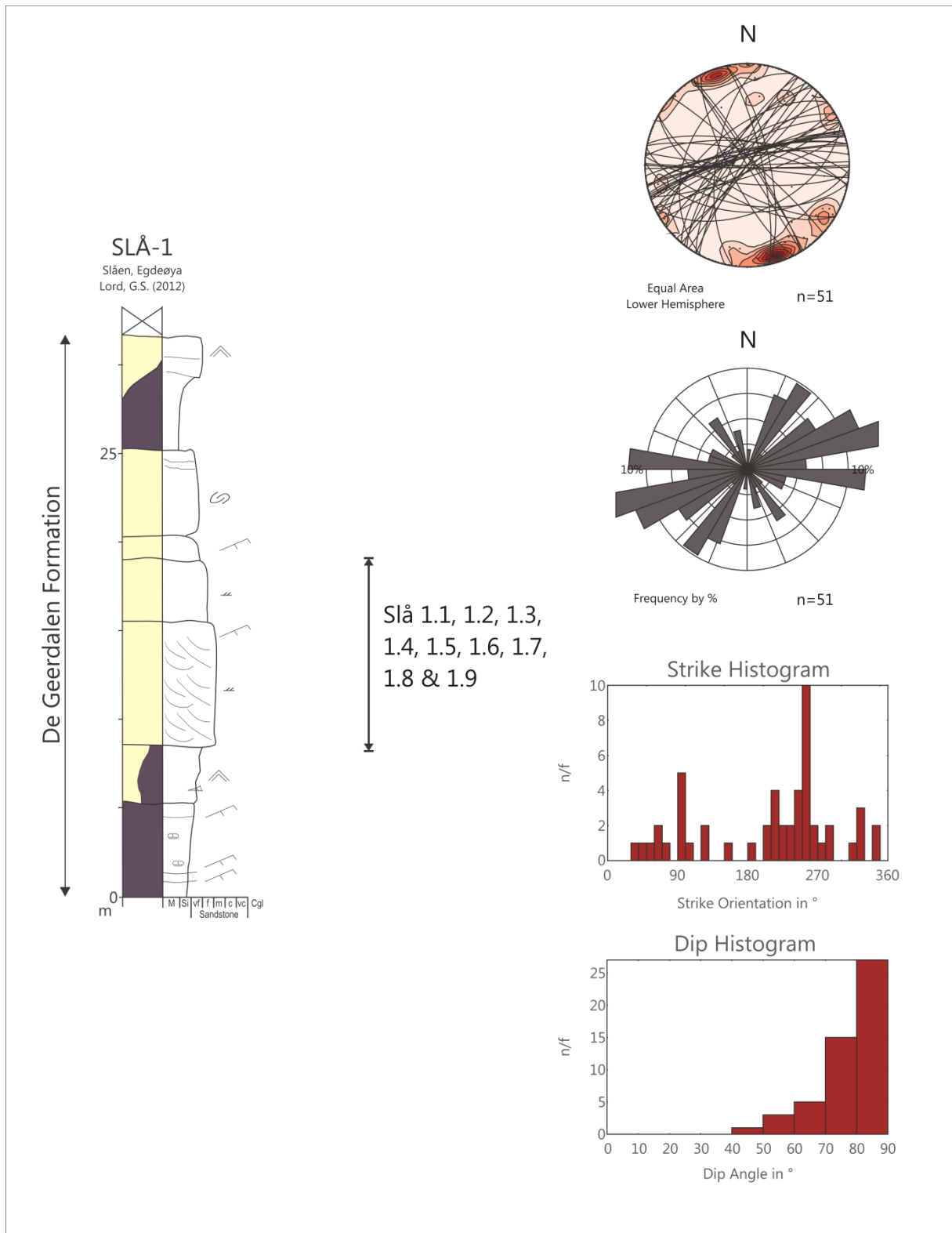


Appendix 1.2 .2 – Blanknuten



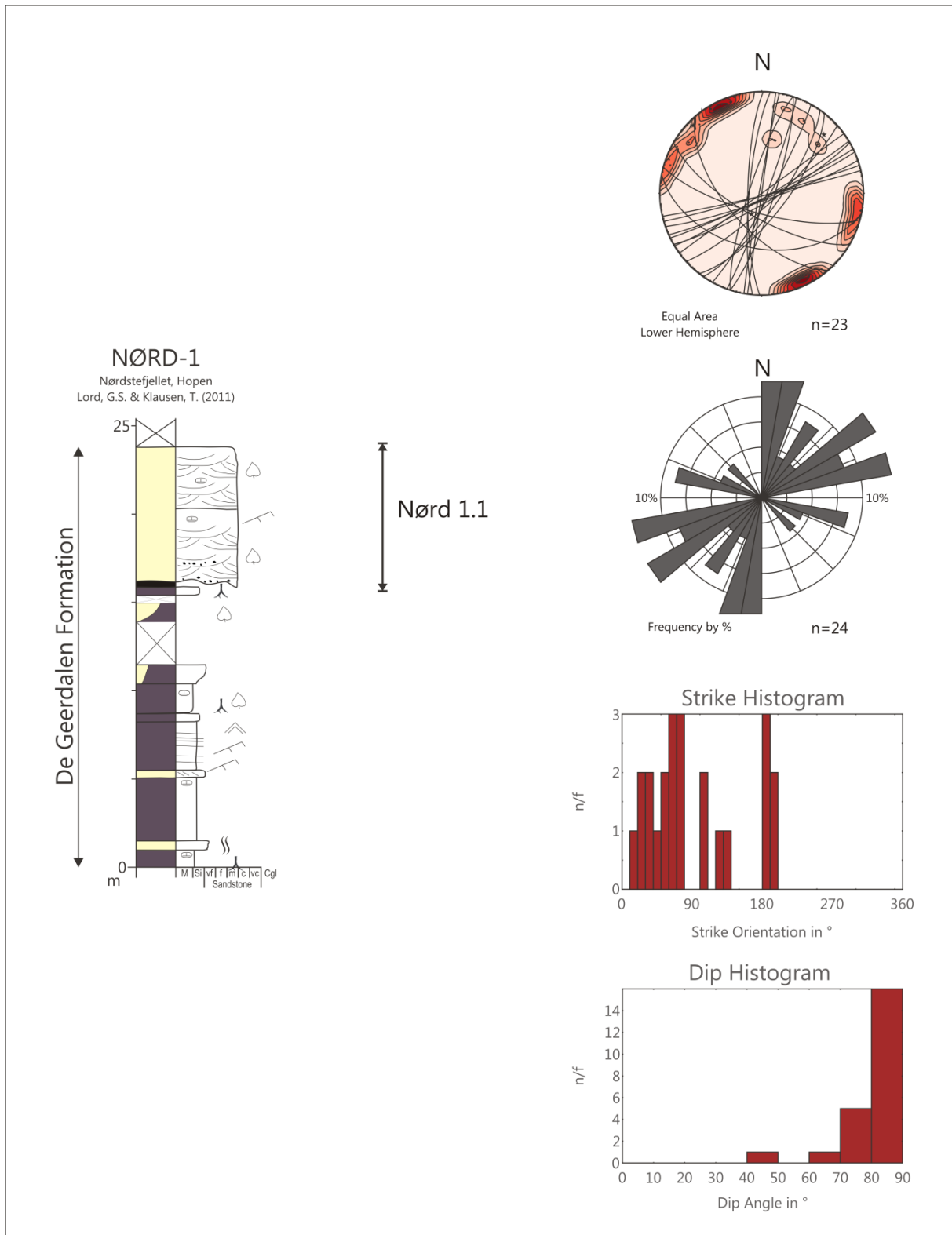


Appendix 1.2 .3 – Slåen

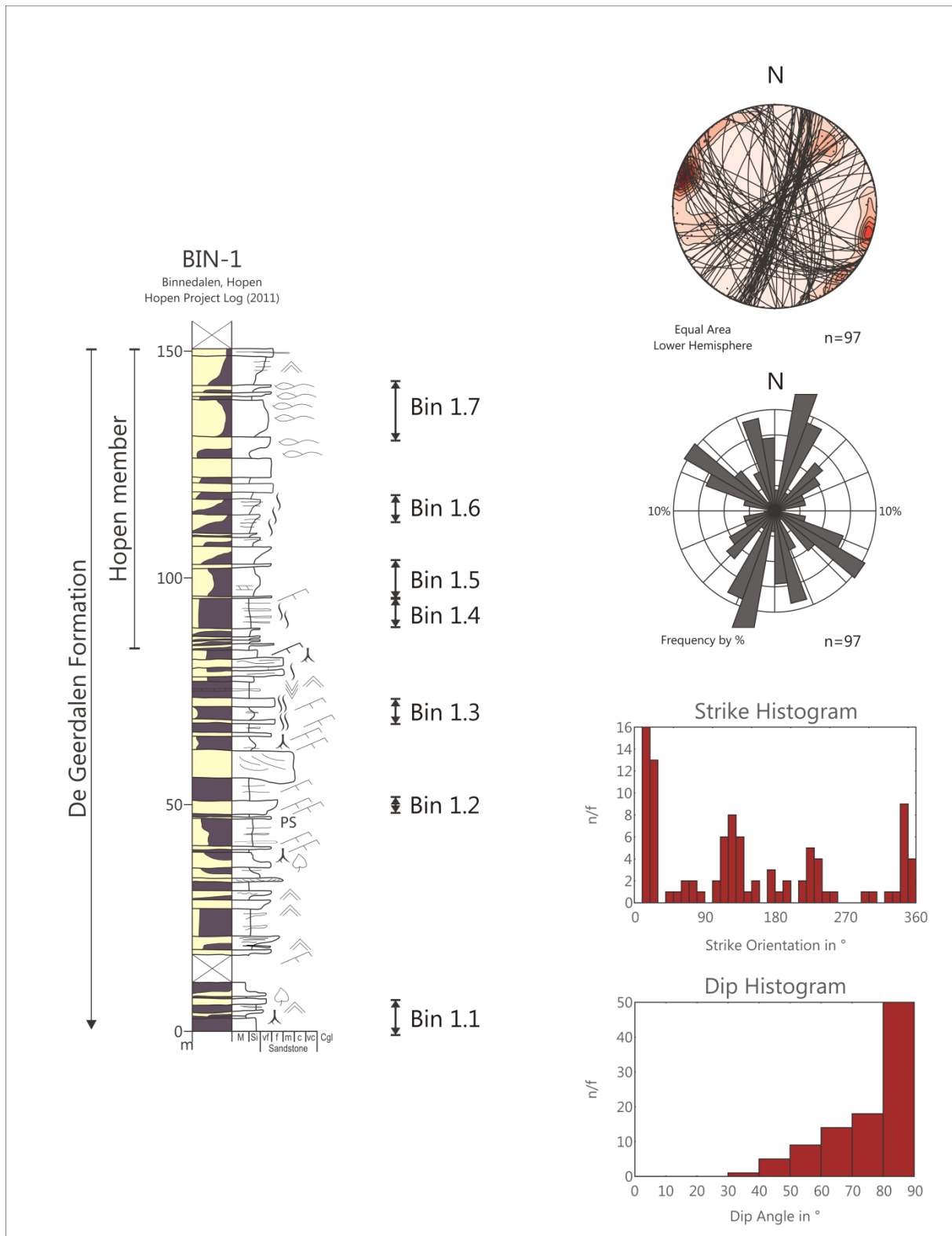


## Appendix 1.3 – Central & Northern Hopen

### Appendix 1.3.1 – Nørdstefjellet

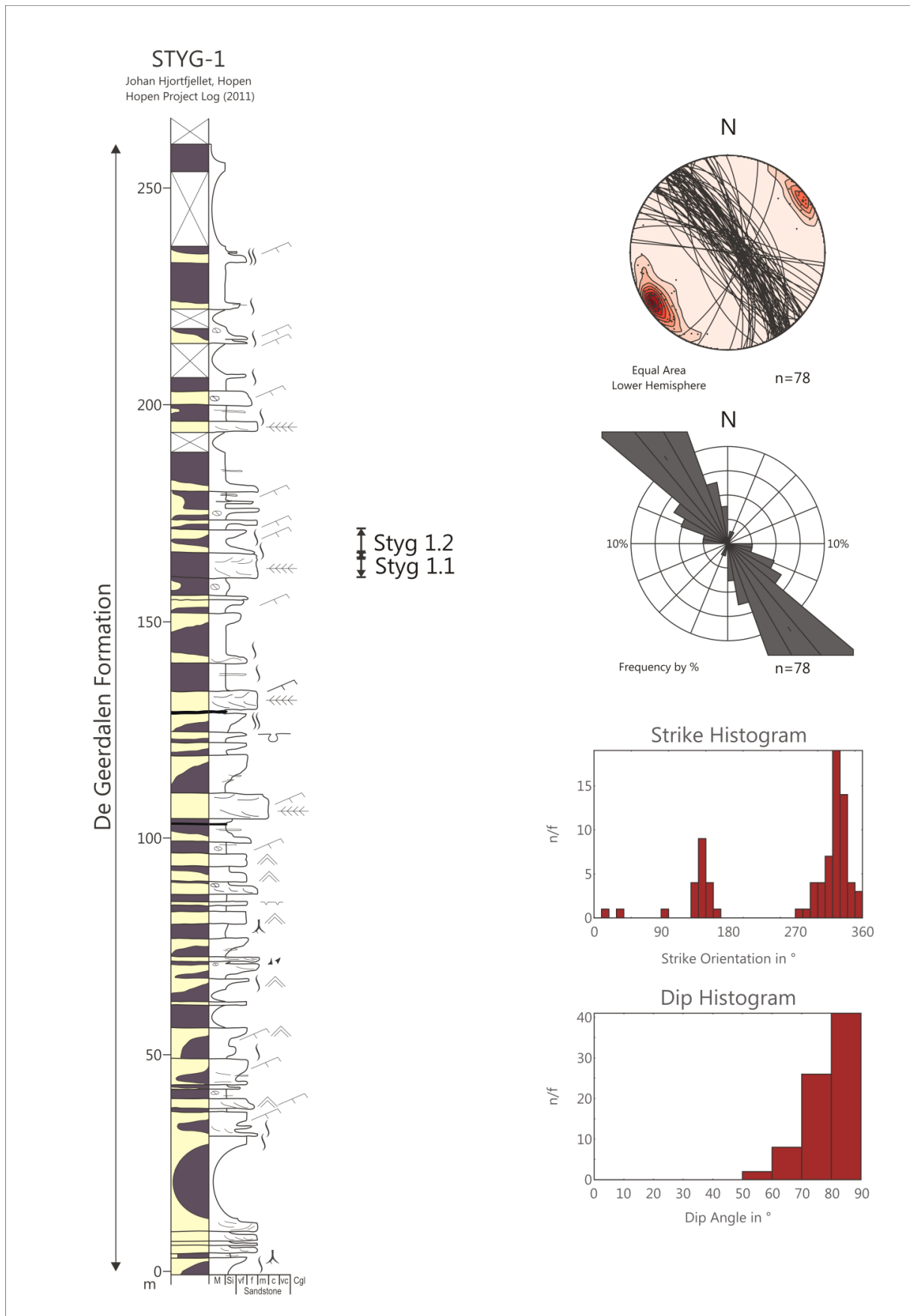


Appendix 1.3.2 – Binnedalen

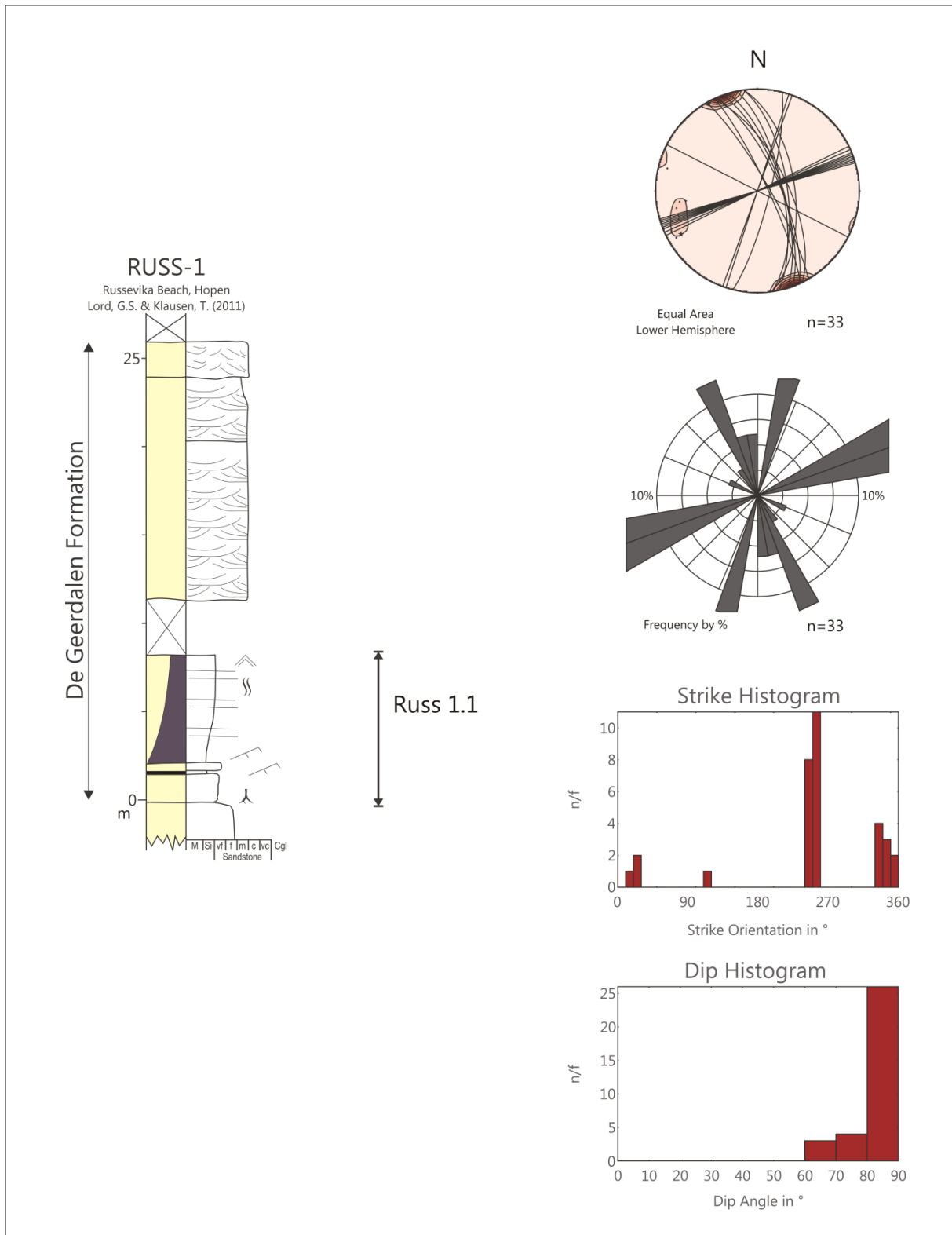




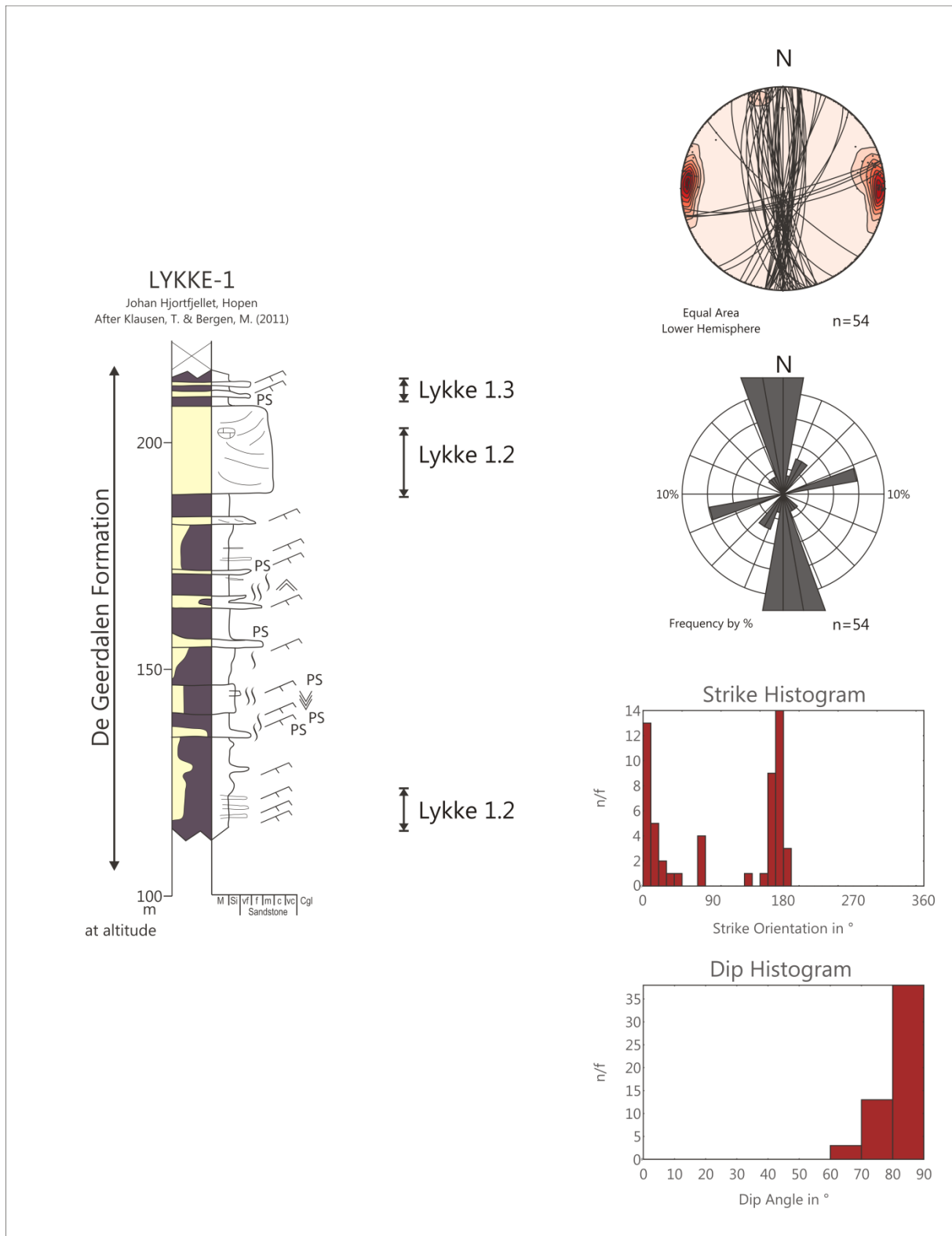
Appendix 1.3.4 – Styggdalen



Appendix 1.3.5 – Russevika



Appendix 1.3.6 – Lykkedalen



## 11. Appendix 2 – Fracture Data



## Appendix 2.1 – Central Spitsbergen Fracture Data

### Appendix 2.1.1 – Deltanaset

<b>Location</b>	<b>Deltanaset Beach</b>			
<b>Scan-line</b>	<b>DELTA-1.1</b>			
<b>Start Co-Ordinates</b>	<b>N78° 21' 00.5" E015° 54' 33.0"</b>			
<b>End Co-Ordinates</b>	<b>N78° 21' 00.4" E015° 54' 32.9"</b>			
<b>Measurement on Tape (cm)</b>	<b>Space (cm)</b>	<b>S/D</b>	<b>Through Going</b>	<b>Terminates at Fracture Plane</b>
0	0	275/75/SW	Yes	No
15	15	270/78/N	Yes	No
31	16	275/90	No	No
47	16	294/80/SW	Yes	Yes
97	50	270/78/N	Yes	No
145	48	326/77/NE	Yes	Yes
147	2	252/88/N	Yes	No
167	20	270/80/N	No	No
195	28	257/72/NW	Yes	No
<b>195</b>	<b>195</b>			

<b>Location</b>	<b>Deltanaset Beach</b>			
<b>Scan-line</b>	<b>DELTA-1.2</b>			
<b>Start Co-Ordinates</b>	<b>N78° 20' 59.6" E015° 54' 26.4"</b>			
<b>End Co-Ordinates</b>	<b>N78° 20' 59.5" E015° 54' 24.7"</b>			
<b>Measurement on Tape (cm)</b>	<b>Space (cm)</b>	<b>S/D</b>	<b>Through Going</b>	<b>Terminates at Fracture Plane</b>
0	0	269/90	Yes	Yes
40	40	237/90	Yes	No
62	22	279/90	No	No

119	57	275/82/N	Yes	No
619	500	005/72/W	No	No
637	18	351/83/W	No	No
651	14	355/74/W	No	No
644	13	009/69/W	No	No
681	17	006/87/W	No	Yes
961	280	021/84/NW	Yes	No
1046	85	359/84/W	Yes	No
1426	380	001/83/W	No	No
1456	30	269/90	Yes	No
1491	35	111/60/NE	Yes	No
1566	75	268/79/N	Yes	Yes
1593	27	256/85/NW	Yes	No
1605	12	266/75/N	No	No
1610	5	272/65/N	Yes	No
1625	15	292/68/NE	No	No
1663	38	009/76/E	Yes	No
<b>1663</b>	<b>1663</b>			

<b>Location</b>	<b>Deltanaset</b>			
<b>Scan-line</b>	<b>Beach</b>			
	<b>DELTA-1.3a</b>			
<b>Start Co-Ordinates</b>	<b>N78° 20'</b>			
	<b>58.8" E015°</b>			
	<b>54' 17.9"</b>			
<b>End Co-Ordinates</b>	<b>N78° 20'</b>			
	<b>58.8" E015°</b>			
	<b>54' 17.7"</b>			
<b>Measurement on Tape (cm)</b>	<b>Space (cm)</b>	<b>S/D</b>	<b>Through Going</b>	<b>Terminates at Fracture Plane</b>
0	0	136/68/NE	Yes	No
48	48	258/90	Yes	No
73	25	242/59/NE	Yes	No
136	63	315/88/SW	Yes	Yes
161	25	355/66/E	Yes	Yes
231	70	337/68/NE	Yes	No
401	170	276/81/N	Yes	No
441	40	348/82/E	Yes	No
<b>441</b>	<b>441</b>			

<b>Location</b>	<b>Deltanaset Beach</b>			
<b>Scan-line</b>	<b>DELTA-1.3b</b>			
<b>Start Co-Ordinates</b>	<b>N78° 20' 58.5" E015° 54' 14.6"</b>			
<b>End Co-Ordinates</b>	<b>N78° 20' 58.5" E015° 54' 13.5"</b>			
<b>Measurement on Tape (cm)</b>	<b>Space (cm)</b>	<b>S/D</b>	<b>Through Going</b>	<b>Terminates at Fracture Plane</b>
0	0	253/63/E	No	No
33	33	373/82/E	No	Yes
111	78	345/67/E	Yes	No
179	68	354/62/W	No	Yes
236	57	329/90	Yes	No
251	15	270/88/N	No	Yes
401	150	348/88/W	Yes	No
421	20	249/90	Yes	No
433	12	275/50/N	No	Yes
465	32	274/66/N	Yes	Yes
470	5	341/71/NE	Yes	Yes
528	58	354/71E	No	No
625	97	332/68/NE	No	No
639	14	351/72/E	Yes	Yes
773	134	340/88/W	No	No
<b>773</b>	<b>773</b>			

<b>Location</b>	<b>Deltanaset Beach</b>			
<b>Scan-line</b>	<b>DELTA-1.4</b>			
<b>Start Co-Ordinates</b>	<b>N78° 20' 58.4" E015° 54' 11.2"</b>			
<b>End Co-Ordinates</b>	<b>N78° 20' 58.2" E015° 54' 10.4"</b>			
<b>Measurement on Tape (cm)</b>	<b>Space (cm)</b>	<b>S/D</b>	<b>Through Going</b>	<b>Terminates at Fracture Plane</b>
0	0	277/69/N	Yes	No
11	11	282/79/N	Yes	Yes
38	27	300/84/N	Yes	Yes
82	44	367/86/N	Yes	No
103	21	258/80/N	Yes	No
118	15	283/66/N	No	No
131	13	257/65/N	No	No
161	30	266/82/N	Yes	No
189	28	257/63/N	Yes	No
196	7	262/90	No	No
206	10	257/72/N	Yes	No
226	20	360/82/W	No	No
236	10	272/61/N	Yes	No
248	12	267/69/N	Yes	No
266	18	274/81/N	No	No
277	11	265/71/N	No	No
287	10	269/90	No	No
294	7	275/90	No	No
304	10	273/90	No	No
335	31	264/80/N	Yes	No
351	16	263/82/N	No	No
372	21	276/64/N	Yes	No
412	40	256/86/N	Yes	No
431	19	257/83/N	Yes	No
457	26	276/77/N	Yes	No
474	17	269/89/N	No	No
489	15	266/84/N	Yes	No
496	7	272/78/N	Yes	No
506	10	283/72/N	Yes	Yes
596	30	268/78/S	No	Yes
<b>536</b>	<b>536</b>			

<b>Location</b>	<b>Deltanaset Beach</b>			
<b>Scan-line</b>	<b>DELTA-1.5</b>			
<b>Start Co-Ordinates</b>	<b>N78° 20' 57.7" E015° 54' 03.2"</b>			
<b>End Co-Ordinates</b>	<b>N78° 20' 57.7" E015° 54' 03.9"</b>			
<b>Measurement on Tape (cm)</b>	<b>Space (cm)</b>	<b>S/D</b>	<b>Through Going</b>	<b>Terminates at Fracture Plane</b>
0	0	266/87/N	Yes	No
3	3	260/82/N	No	Yes
23	20	260/89/N	No	Yes
33	10	271/82/N	Yes	No
41	8	269/84/N	No	No
54	13	267/78/N	Yes	Yes
58	4	268/82/N	No	No
66	8	262/87/N	Yes	No
<b>66</b>	<b>66</b>			

<b>Location</b>	<b>Deltanaset Beach</b>			
<b>Scan-line</b>	<b>DELTA-1.6</b>			
<b>Start Co-Ordinates</b>	<b>N78° 20' 55.9" E015° 53' 35.2"</b>			
<b>End Co-Ordinates</b>	<b>N78° 20' 55.7" E015° 53' 32.4"</b>			
<b>Measurement on Tape (cm)</b>	<b>Space (cm)</b>	<b>S/D</b>	<b>Through Going</b>	<b>Terminates at Fracture Plane</b>
0	0	316/52/NE	Yes	No
174	174	338/82/SW	No	No
238	64	347/90	No	No
388	150	341/90	Yes	No
443	55	339/76/SW	Yes	No
500	57	336/79/SW	No	Yes
698	198	323/74/SW	No	No

978	280	350/68/E	Yes	No
1080	102	332/90	Yes	No
1095	15	310/69/NE	No	No
1290	195	309/89/SW	Yes	No
1444	154	321/83/SW	Yes	No
1704	260	330/78/NE	Yes	No
1767	63	341/90	No	Yes
2047	280	340/86/NE	Yes	No
<b>2047</b>	<b>2047</b>			

<b>Location</b>	<b>Deltanaset Beach</b>			
<b>Scan-line</b>	<b>DELTA-1.7</b>			
<b>Start Co-Ordinates</b>	<b>N78° 20' 55.3" E015° 53' 19.2"</b>			
<b>End Co-Ordinates</b>	<b>N78° 20' 55.1" E015° 53' 15.7"</b>			
<b>Measurement on Tape (cm)</b>	<b>Space (cm)</b>	<b>S/D</b>	<b>Through Going</b>	<b>Terminates at Fracture Plane</b>
0	0	295/82/NE	No	No
83	83	340/89/NE	No	No
142	59	005/58/E	Yes	Yes
182	40	341/85/SW	Yes	No
209	27	005/90	Yes	No
358	149	337/88/SW	Yes	No
408	50	355/82/W	Yes	Yes
447	39	346/67/E	Yes	Yes
529	82	345/90	Yes	No
564	35	346/82/SW	No	No
627	63	341/90	Yes	No
658	31	331/90	Yes	No
750	92	367/87/W	Yes	Yes
781	31	004/82/NW	Yes	No
798	17	004/85/NW	No	No
830	32	050/85/NW	No	Yes
869	39	002/75/E	Yes	Yes
1029	160	351/89/W	Yes	No
1057	28	019/78/NW	No	No
1137	80	009/82/W	Yes	No
1245	108	318/68/NE	Yes	No

1312	67	009/77/W	Yes	No
1427	115	352/86/W	Yes	No
1529	102	354/82/E	Yes	Yes
1600	71	337/85/NE	No	No
1657	57	347/89/W	No	No
1717	60	331/75/SW	No	No
1747	30	339/75/SW	No	No
1862	115	012/90	Yes	Yes
1912	50	306/58/NE	No	Yes
1997	85	307/84/NE	Yes	No
2105	108	359/85/W	Yes	No
2162	57	306/80/SW	Yes	No
2228	66	346/85/SW	Yes	Yes
2304	76	355/88/NE	Yes	Yes
2370	66	357/89/W	No	Yes
<b>2370</b>	<b>2370</b>			

<b>Location</b>	<b>Deltanaset Beach</b>			
<b>Scan-line</b>	<b>DELTA-1.8</b>			
<b>Start Co-Ordinates</b>	<b>N78° 20' 54.8" E015° 53' 14.8"</b>			
<b>End Co-Ordinates</b>	<b>N78° 20' 54.9" E015° 53' 11.6"</b>			
<b>Measurement on Tape (cm)</b>	<b>Space (cm)</b>	<b>S/D</b>	<b>Through Going</b>	<b>Terminates at Fracture Plane</b>
0	0	347/80/E	Yes	No
45	45	356/68/E	Yes	No
92	47	350/82/E	Yes	No
166	74	359/85/W	Yes	Yes
252	86	350/90	Yes	Yes
326	74	345/89/SW	Yes	Yes
346	20	356/82/W	Yes	No
367	21	006/76/E	No	No
435	68	353/77/E	No	No
487	52	318/82/NE	Yes	Yes
717	230	347/77/NE	Yes	Yes
837	120	354/78/W	No	No
887	50	022/86/NW	Yes	No
941	54	357/88/W	Yes	No

996	55	358/81/W	Yes	Yes
1054	58	351/90	No	No
1140	86	007/68/E	Yes	No
1206	66	333/66/E	Yes	Yes
1303	97	004/90	No	No
1359	56	341/80/NE	Yes	No
1583	224	007/75/E	No	No
1606	23	000/88/W	Yes	Yes
1680	74	005/78/W	Yes	Yes
1772	92	357/68/E	Yes	No
1839	67	351/76/E	Yes	Yes
1919	80	357/82/W	Yes	Yes
2007	88	357/90	Yes	No
2042	35	011/90	Yes	No
2142	100	345/90	Yes	No
<b>2142</b>	<b>2142</b>			

<b>Location</b>	<b>Deltaneset Beach</b>			
<b>Scan-line</b>	<b>DELTA-1.9</b>			
<b>Start Co-Ordinates</b>	<b>N78° 20' 54.8" E015° 53' 09.9"</b>			
<b>End Co-Ordinates</b>	<b>N78° 20' 54.7" E015° 53' 08.7"</b>			
<b>Measurement on Tape (cm)</b>	<b>Space (cm)</b>	<b>S/D</b>	<b>Through Going</b>	<b>Terminates at Fracture Plane</b>
0	0	005/85/W	Yes	No
82	82	355/90	Yes	No
162	80	009/90	Yes	Yes
212	50	353/70/E	Yes	No
240	28	004/72/E	No	No
294	54	355/88/W	Yes	No
324	30	335/72/SE	No	No
349	25	352/90	No	No
509	160	331/86/NE	Yes	No
537	28	352/78/W	Yes	No
587	50	351/82/E	Yes	No
635	48	352/65/E	Yes	No
725	90	009/86/W	Yes	No
750	25	000/72/E	Yes	No



784	34	346/90	Yes	No
828	44	348/90	Yes	No
<b>828</b>	<b>828</b>			

<b>Location</b>	<b>Deltanaset Beach</b>			
<b>Scan-line</b>	<b>DELTA-1.10</b>			
<b>Start Co-Ordinates</b>	<b>N78° 20' 54.4" E015° 53' 02.2"</b>			
<b>End Co-Ordinates</b>	<b>N78° 20' 54.4" E015° 53' 01.2"</b>			
<b>Measurement on Tape (cm)</b>	<b>Space (cm)</b>	<b>S/D</b>	<b>Through Going</b>	<b>Terminates at Fracture Plane</b>
0	0	339/74/SW	Yes	Yes
10	10	337/90	No	Yes
72	62	359/84/W	Yes	Yes
92	20	038/90	Yes	Yes
120	28	031/78/SE	Yes	No
132	12	019/84/NW	Yes	Yes
164	32	007/82/E	Yes	No
188	24	031/85/NW	Yes	No
217	29	045/88/NW	Yes	No
299	82	348/86/W	No	Yes
311	12	002/69/E	Yes	Yes
319	8	009/82/E	No	No
377	58	019/90/NW	Yes	No
<b>377</b>	<b>377</b>			

## Appendix 2.1.2 – Konusdalen

<b>Location</b>		<b>Konusdalen</b>		
<b>Scan-line</b>		<b>Kon-1.1</b>		
<b>Start Co-Ordinates</b>		<b>N78° 20'</b>		
<b>End Co-Ordinates</b>		<b>40.2" E015°</b>		
<b>Altitude (a.s.l)</b>		<b>51' 54.9"</b>		
<b>Measurement on Tape</b>		<b>N78° 20'</b>		
<b>Space</b>		<b>41.3" E015°</b>		
<b>S/D</b>		<b>51' 54.9"</b>		
<b>Through Going</b>		<b>18m</b>		
<b>Terminates at Fracture Plane</b>				
0		100 78	No	No
15		095 90	No	No
20		127 16	No	No
24		081 69	No	No
30		090 82	No	No
70		071 74	No	No
80		186 18	No	No
91		072 64	No	No
130		062 76	No	No
148		059 78	No	No
156		109 70	No	No
157		054 90	No	No
165		083 90	No	No
170		046 86	No	No
171		072 90	No	No
183		054 82	No	No
190		092 86	No	No
191		172 90	No	No
195		075 80	No	No
205		056 81	No	No
220		059 82	Yes	No
232		026 82	No	Yes
240		114 82	No	No
249		064 72	No	No
252		112 80	No	Yes
263		058 72	No	No
270		057 77	No	No
258		067 76	No	No
287		112 81	No	No

298		016 84	No	No
300		017 84	Yes	No
470		136 86	No	Yes
503		060 84	No	No
522		119 86	No	No
544		050 84	No	No
570		064 80	No	No
584		036 90	No	No
590		095 82	No	No
610		036 78	No	No
627		078 75	No	No
640		026 90	Yes	No
650		114 74	No	No
670		055 81	No	Yes
680		132 90	No	No
686		066 78	No	No
716		051 90	No	No
743		113 70	Yes	Yes
745		051 72	Yes	No
765		048 58	Yes	No
770		038 90	No	No
780		062 76	Yes	No
790		114 79	Yes	No
803		043 82	No	No
818		162 72	No	No
830		118 78	No	No
<b>830</b>				

## Appendix 2.1.3 – Trehøgdene 1

<b>Location Scan-line</b>		<b>Trehøgdene TRE-1.1</b>		
<b>Start Co- Ordinates</b>		<b>N78° 13' 47.0" E017° 04' 19.1"</b>		
<b>End Co- Ordinates</b>		<b>N78° 13' 46.6" E017° 04' 18.2"</b>		
<b>Altitude (a.s.l)</b>		<b>492m</b>		
<b>Measurement on Tape (cm)</b>	<b>Space (cm)</b>	<b>S/D</b>	<b>Through Going</b>	<b>Terminates at Fracture Plane</b>
0	0	240/83/SE	Yes	No
83	83	248/78/SE	Yes	No
177	94	253/82/SE	Yes	No
225	48	260/84/SE	Yes	Yes
230	5		No	Yes
238	8		No	Yes
247	9	234/81/SE	Yes	Yes
285	38	260/83/NW	Yes	No
372	87	253/80/SE	Yes	Yes
391	19		No	Yes
410	19	260/90	Yes	Yes
470	60		Yes	No
535	65	238/80/NW	Yes	Yes
618	83		Yes	Yes
638	20		No	Yes
662	24		No	No
672	10		No	No
712	40	238/84/SE	Yes	No
780	68	251/78/SE	Yes	Yes
872	92	248/90	Yes	Yes
909	37		No	No
956	47	254/90	Yes	No
996	40	348/76/SW	Yes	Yes
1003	7	342/87/SW	No	Yes
1059	56	240/88/NW	Yes	No
1095	36	245/82/SE	No	No
1108	13	243/90	Yes	Yes
1168	60	279/80/S	No	No
1246	78	264/78/S	Yes	No

1282	36	235/90	Yes	No
1307	25	250/90	No	Yes
1320	13	240/90	No	Yes
1388	68	237/88/NW	Yes	No
<b>1388</b>	<b>1388</b>			

<b>Location Scan-line</b>	<b>Trehøgdene TRE-1.2</b>			
<b>Start Co- Ordinates</b>	<b>N78° 13' 46.9" E017° 04' 19.9"</b>			
<b>End Co- Ordinates</b>	<b>N78° 13' 46.8" E017° 04' 18.6"</b>			
<b>Altitude (a.s.l)</b>	<b>503m</b>			
<b>Measurement on Tape (cm)</b>	<b>Space (cm)</b>	<b>S/D</b>	<b>Through Going</b>	<b>Terminates at Fracture Plane</b>
0	0	250/82/SE	Yes	No
69	69	239/88/NW	Yes	No
98	29		No	No
175	77	240/88/NW	Yes	No
262	87	240/90	Yes	No
297	35	325/83/SW	No	Yes
329	32	312/78/SW	Yes	Yes
357	28	326/80/SW	No	No
394	37	327/82/SW	No	No
411	17	334/86/SW	Yes	No
<b>411</b>	<b>411</b>			

<b>Location Scan-line</b>		<b>Trehøgdene TRE-1.3</b>		
<b>Start Co-Ordinates</b>		<b>N78° 13' 46.2" E017° 04' 23.1"</b>		
<b>End Co-Ordinates</b>		<b>n/a</b>		
<b>Altitude (a.s.l)</b>		<b>509m</b>		
<b>Measurement on Tape (cm)</b>	<b>Space (cm)</b>	<b>S/D</b>	<b>Through Going</b>	<b>Terminates at Fracture Plane</b>
0	0	358/88/NE	Yes	No
65	65	347/76/NE	Yes	Yes
113	48	323/90	No	Yes
137	24		No	Yes
147	10	328/77/SW	No	Yes
163	16		No	No
176	13		No	No
204	28		No	No
298	94	339/90	No	Yes
398	100	339/90	Yes	Yes
461	63	353/70/W	No	No
516	55	341/77/E	Yes	Yes
589	73	347/90	No	No
<b>589</b>	<b>589</b>			

<b>Location Scan-line</b>	<b>Trehøgdene TRE-1.4</b>			
<b>Start Co-Ordinates</b>	<b>N78° 13' 42.4" E017° 04' 15.6"</b>			
<b>End Co-Ordinates</b>	<b>N78° 13' 42.3" E017° 04' 14.1"</b>			
<b>Altitude (a.s.l)</b>	<b>535m</b>			
<b>Measurement on Tape (cm)</b>	<b>Space (cm)</b>	<b>S/D</b>	<b>Through Going</b>	<b>Terminates at Fracture Plane</b>
0	0	321/90	Yes	No
125	125	323/90	Yes	No
187	62	331/90	Yes	No
240	53	344/90	Yes	No
286	46	323/90	No	No
352	66	326/90	Yes	No
412	60	327/90	Yes	No
502	90	331/90	Yes	No
551	49	323/90	No	No
651	100	328/90	Yes	No
707	56	321/90	Yes	No
830	123	339/90	No	No
892	62	331/90	Yes	No
952	60	334/90	Yes	No
1003	51	326/90	Yes	No
1038	35	332/90	No	No
1070	32	335/90	Yes	No
<b>1070</b>	<b>1070</b>			

<b>Location Scan-line</b>	<b>Trehøgdene TRE-1.5</b>			
<b>Start Co-Ordinates</b>	<b>N78° 13' 43.9" E017° 04' 30.5"</b>			
<b>End Co-Ordinates</b>	<b>N78° 13' 43.9" E017° 04' 29.7"</b>			
<b>Altitude (a.s.l)</b>	<b>562m</b>			
<b>Measurement on Tape (cm)</b>	<b>Space (cm)</b>	<b>S/D</b>	<b>Through Going</b>	<b>Terminates at Fracture Plane</b>
0	0	331/90	Yes	Yes
55	55	324/80/SW	No	Yes
105	50	339/76/SW	No	No
155	50	339/87/SW	Yes	No
205	50	333/90	Yes	No
256	51	349/82/W	Yes	No
289	33	347/78/NE	No	No
329	40	350/82/E	No	No
393	64	337/84/SW	No	No
457	64	304/72/NE	No	No
485	28	326/87/SW	Yes	No
523	38	340/82/SW	Yes	No
576	53	332/90	No	Yes
602	26	329/90	No	No
625	23	329/90	No	No
654	29	329/90	No	No
713	59	329/88/SW	Yes	No
<b>713</b>	<b>713</b>			



## Appendix 2.1.4 – Trehøgdene 2

<b>Location Scan-line</b>	<b>Trehøgdene TRE-2.1</b>			
<b>Start Co- Ordinates</b>	<b>N78° 13' 42.4" E017° 03' 51.8"</b>			
<b>End Co- Ordinates</b>	<b>N78° 13' 42.4" E017° 03' 51.4"</b>			
<b>Altitude (a.s.l)</b>	<b>483m</b>			
<b>Measurement on Tape (cm)</b>	<b>Space (cm)</b>	<b>S/D</b>	<b>Through Going</b>	<b>Terminates at Fracture Plane</b>
0	0	321/80/NE	No	No
30	30	327/78/SW	No	No
66	36	332/90	Yes	No
90	32	328/76/SW	Yes	No
120	22	344/82/NE	No	No
144	24	342/90	Yes	No
174	30	314/78/SE	Yes	No
203	29	301/90	No	No
235	30	335/68/SW	No	No
271	36	341/80/SW	Yes	No
311	40	341/90	Yes	No
<b>311</b>	<b>311</b>			

<b>Location Scan-line</b>	<b>Trehøgdene TRE-2.2</b>			
<b>Start Co-Ordinates</b>	<b>N78° 13' 42.2" E017° 03' 52.6"</b>			
<b>End Co-Ordinates</b>	<b>N78° 13' 42.2" E017° 03' 52.1"</b>			
<b>Altitude (a.s.l)</b>	<b>484m</b>			
<b>Measurement on Tape (cm)</b>	<b>Space (cm)</b>	<b>S/D</b>	<b>Through Going</b>	<b>Terminates at Fracture Plane</b>
0	0	335/80/SW	Yes	Yes
189	189	184/82W	No	No
254	65	327/90	Yes	No
285	31	202/68/SE	No	Yes
307	22	198/80/NW	Yes	Yes
352	45	194/90	Yes	Yes
357	5	244/88/NW	Yes	No
364	7	235/90	Yes	No
431	67	320/78/SW	No	No
492	61	320/90	Yes	Yes
521	29	322/90	No	No
542	21	321/90	No	No
634	92	314/64/SW	Yes	Yes
<b>634</b>	<b>634</b>			

<b>Location Scan-line</b>	<b>Trehøgdene TRE-2.3</b>			
<b>Start Co- Ordinates</b>	<b>N78° 13' 41.8" E017° 03' 53.7"</b>			
<b>End Co- Ordinates</b>	<b>N78° 13' 41.7" E017° 03' 53.9"</b>			
<b>Altitude (a.s.l)</b>	<b>499m</b>			
<b>Measurement on Tape (cm)</b>	<b>Space (cm)</b>	<b>S/D</b>	<b>Through Going</b>	<b>Terminates at Fracture Plane</b>
0	0	326/74/SW	Yes	No
26	26	335/84/SW	Yes	No
64	38	335/90	No	No
81	17	331/90	No	Yes
109	28	340/90	No	Yes
130	21	347/86/SW	Yes	No
167	37	332/70/SW	Yes	No
187	20	259/69/SE	Yes	No
242	55	270/80/S	Yes	No
257	15	269/90	No	No
261	4	286/78/SW	Yes	No
401	140	314/87/SW	Yes	No
436	35	332/80/SW	Yes	No
469	33	334/90	Yes	Yes
535	66	324/90	Yes	No
<b>535</b>	<b>535</b>			

## Appendix 2.1.5 – Agardhbukta

<b>Location</b>	<b>Agardhbukta</b>			
<b>Scan-line</b>	<b>Agard - 1.1</b>			
<b>Start Co-Ordinates</b>	<b>N78° 02' 52.2" E018° 40' 33.1"</b>			
<b>End Co-Ordinates</b>	<b>N78° 02' 50.4" E017° 04' 33.8"</b>			
<b>Altitude (a.s.l)</b>	<b>2m</b>			
<b>Measurement on Tape</b>	<b>Space</b>	<b>S/D</b>	<b>Through going</b>	<b>Terminates at Fracture Plane</b>
0	0	320 70	No	No Data
60	60	351 84	Yes	No Data
95	35	353 78	No	No Data
265	170	352 72	Yes	No Data
295	30	349 68	Yes	No Data
445	150	053 78	Yes	No Data
565	120	007 70	Yes	No Data
705	140	009 90	Yes	No Data
770	65	020 76	Yes	No Data
810	40	076 84	Yes	No Data
820	10	074 80	Yes	No Data
865	45	068 78	Yes	No Data
1035	170	060 90	Yes	No Data
1082	47	066 90	Yes	No Data
1112	30	067 90	Yes	No Data
1114	2	062 90	Yes	No Data
1117	3	066 90	Yes	No Data
1153	36	090 83	Yes	No Data
1211	58	069 78	Yes	No Data
1286	75	020 80	Yes	No Data
<b>1286</b>	<b>1286</b>			

## Appendix 2.2 – Western Edgeøya Fracture Data

### Appendix 2.2.1 – Klinkhamaren

Location Scan-line	Klinkhamaren Klink 1.1			
Start Co-Ordinates	N78° 01' 02.1" E021° 08' 33.0"			
End Co-Ordinates	N78° 01' 01.8" E021° 08' 39.6"			
Altitude (a.s.l)	211m			
Measurement on Tape (cm)	Space (cm)	S/D	Through Going	Terminates at Fracture Plane
0	0	336 78	No	No
16	16	330 82	No	Yes
66	50	038 80	Yes	Yes
106	40	088 80	No	Yes
126	20	091 84	No	No
226	100	029 82	Yes	No
286	60	044 72	No	Yes
296	10	022 76	No	Yes
366	70	354 88	No	No
486	120	334 84	No	No
686	200	358 88	Yes	No
866	180	354 84	Yes	Yes
1326	460	342 78	Yes	No
1766	440	344 80	Yes	No
2016	250	324 78	No	No
2081	65	049 81	No	Yes
2151	70	329 82	Yes	Yes
2206	55	050 72	Yes	No
2316	110	050 78	Yes	No
2351	35	067 86	No	Yes
2411	60	344 84	Yes	Yes
2591	180	336 70	Yes	No
2831	240	340 90	Yes	No
3151	320	042 86	No	Yes
3183	32	334 83	No	No
3583	400	055 82	Yes	No
3638	55	044 78	Yes	No

3858	220	040 86	Yes	No
3988	130	041 80	Yes	No
4123	135	052 84	Yes	Yes
4433	310	017 90	Yes	No
4693	260	030 72	No	No
4733	40	026 84	Yes	No
5248	515	336 82	Yes	No
<b>5248</b>	<b>5248</b>			

<b>Location</b>	<b>Klinkhamaren</b>			
<b>Scan-line</b>	<b>Klink 1.2</b>			
<b>Start Co-Ordinates</b>	<b>N78° 00' 59.6"</b>			
	<b>E021° 08'</b>			
	<b>45.2"</b>			
<b>End Co-Ordinates</b>	<b>n/a</b>			
<b>Altitude (a.s.l)</b>				
<b>Measurement on Tape (cm)</b>	<b>Space (cm)</b>	<b>S/D</b>	<b>Through going</b>	<b>Terminates at Fracture Plane</b>
0	0	046 78	Yes	No
220	220	052 78	Yes	No
326	106	053 86	Yes	Yes
334	8	064 88	Yes	No
472	138	068 90	Yes	Yes
632	160	063 74	Yes	Yes
<b>632</b>	<b>632</b>			

## Appendix 2.2.2 – Blanknuten

<b>Location Scan-line</b>		<b>Blanknuten Blank-1.1</b>		
<b>Start Co-Ordinates</b>		<b>N77° 58' 30.5"</b>		
<b>End Co-Ordinates</b>		<b>E021° 13' 43.5"</b>		
<b>Altitude (a.s.l)</b>		<b>N/A</b>		
<b>Altitude (a.s.l)</b>		<b>231m</b>		
<b>Measurement on Tape</b>	<b>Space</b>	<b>S/D</b>	<b>Through Going</b>	<b>Terminates at Fracture Plane</b>
0	0	346 84	Yes	No
7	7	330 78	No	No
87	80	310 78	No	No
193	106	336 82	No	No
221	28	339 84	Yes	No
300	79	001 86	No	Yes
319	19	335 84	Yes	No
575	256	351 86	No	No
662	87	331 83	No	No
696	34	339 76	No	No
<b>696</b>	<b>696</b>			

<b>Location Scan-line</b>		<b>Blanknuten Blank-1.2</b>		
<b>Start Co-Ordinates</b>		<b>N77° 58' 45.0"</b>		
<b>End Co-Ordinates</b>		<b>E021° 13' 46.8"</b>		
<b>Altitude (a.s.l)</b>		<b>N77° 58' 44.8"</b>		
<b>Altitude (a.s.l)</b>		<b>E021° 15' 47.3"</b>		
<b>Altitude (a.s.l)</b>		<b>241m</b>		
<b>Measurement on Tape</b>	<b>Space</b>	<b>S/D</b>	<b>Through Going</b>	<b>Terminates at Fracture Plane</b>
0	0	059 84	No	No
64	64	038 78	Yes	Yes
94	30	094 86	Yes	Yes
139	45	047 70	No	Yes
209	70	068 90	Yes	No

218	9	062 88	No	No
258	40	066 78	Yes	No
318	60	054 90	Yes	No
353	35	068 90	Yes	No
360	7	070 90	No	No
410	50	067 82	No	Yes
<b>410</b>	<b>410</b>			

<b>Location</b>	<b>Blanknuten</b>			
<b>Scan-line</b>	<b>Blank-1.3</b>			
<b>Start Co-Ordinates</b>	<b>N77° 58' 42.7"</b>			
<b>End Co-Ordinates</b>	<b>E021° 13' 55.7"</b>			
<b>Altitude (a.s.l)</b>	<b>247m</b>			
<b>Measurement on Tape</b>	<b>Space</b>	<b>S/D</b>	<b>Through Going</b>	<b>Terminates at Fracture Plane</b>
0	0	071 79	No	No
40	40	062 66	Yes	Yes
122	82	085 74	Yes	No
143	21	080 82	No	No
163	20	070 78	Yes	No
198	35	148 72	No	No
<b>198</b>	<b>198</b>			



<b>Location Scan-line</b>	<b>Blanknuten Blank-1.4</b>			
<b>Start Co-Ordinates</b>	<b>N77° 58' 40.3" E021° 14' 00.9"</b>			
<b>End Co-Ordinates</b>	<b>N/A</b>			
<b>Altitude (a.s.l)</b>	<b>247m</b>			
<b>Measurement on Tape</b>	<b>Space</b>	<b>S/D</b>	<b>Through Going</b>	<b>Terminates at Fracture Plane</b>
0	0	118 82	Yes	No
400	400	121 75	Yes	No
<b>400</b>	<b>400</b>			

<b>Location Scan-line</b>	<b>Blanknuten Blank-1.5</b>			
<b>Start Co-Ordinates</b>	<b>N77° 58' 38.2" E021° 14' 12.9"</b>			
<b>End Co-Ordinates</b>	<b>N77° 58' 37.9" E021° 14' 20.4"</b>			
<b>Altitude (a.s.l)</b>	<b>248m</b>			
<b>Measurement on Tape</b>	<b>Space</b>	<b>S/D</b>	<b>Through Going</b>	<b>Terminates at Fracture Plane</b>
0	0	321 78	No	Yes
80	80	305 72	Yes	Yes
110	30	012 72	No	Yes
170	60	307 78	No	No
279	109	320 88	Yes	Yes
327	48	318 86	Yes	Yes
677	350	308 80	Yes	No
1377	700	317 82	Yes	No
2577	1200	351 90	Yes	Yes
3377	800	306 88	Yes	No
3827	450	314 76	No	No
3870	43	008 87	No	Yes
3945	75	338 82	Yes	Yes
3978	33	342 82	Yes	No

4378	400	331 88	Yes	No
4728	350	326 84	Yes	Yes
<b>4728</b>	<b>4728</b>			

<b>Location Scan-line</b>	<b>Blanknuten Blank-1.6</b>			
<b>Start Co- Ordinates</b>	<b>N77° 58' 31.1" E021° 14' 57.6"</b>			
<b>End Co- Ordinates</b>	<b>N/A</b>			
<b>Altitude (a.s.l)</b>	<b>282m</b>			
<b>Measurement on Tape</b>	<b>Space</b>	<b>S/D</b>	<b>Through Going</b>	<b>Terminates at Fracture Plane</b>
0	0	347 82	Yes	No
9	9	331 85	Yes	No
109	100	336 81	Yes	No
179	70	330 88	Yes	No
200	21	331 90	Yes	No
225	25	330 83	Yes	No
393	168	327 86	Yes	No
435	42	247 84	Yes	No
492	57	329 90	Yes	No
535	43	326 90	Yes	No
608	73	328 89	Yes	No
635	27	329 90	Yes	No
<b>635</b>	<b>635</b>			

<b>Location Scan-line</b>	<b>Blanknuten Blank-1.7</b>			
<b>Start Co- Ordinates</b>	<b>N77° 58' 34.4"</b>			
<b>End Co- Ordinates</b>	<b>E021° 15' 04.6"</b>			
<b>Altitude (a.s.l)</b>	<b>364m</b>			
<b>Measurement on Tape</b>	<b>Space</b>	<b>S/D</b>	<b>Through Going</b>	<b>Terminates at Fracture Plane</b>
0	0	331 76	No	No
150	150	318 90	Yes	No
190	40	305 90	Yes	No
236	46	302 84	Yes	No
278	42	339 88	No	No
418	140	242 60	Yes	Yes
448	30	340 82	No	No
573	125	257 87	Yes	No
<b>573</b>	<b>573</b>			

## Appendix 2.2.3 – Slåen

<b>Location Scan-line</b>	<b>Slåen Slå-1.1</b>			
<b>Start Co- Ordinates</b>	<b>N77° 42' 51.2"</b>			
<b>End Co- Ordinates</b>	<b>E021° 12' 12.4"</b>			
<b>Altitude (a.s.l)</b>	<b>N77° 42' 51.6"</b>			
	<b>E021° 12' 12.3"</b>			
	<b>258m</b>			
<b>Measurement on Tape</b>	<b>Space</b>	<b>S/D</b>	<b>Through Going</b>	<b>Terminates at Fracture Plane</b>
0	0	240 70	Yes	Yes
150	150	281 78	Yes	Yes
270	120	208 80	Yes	No
478	208	258 77	Yes	Yes
778	300	254 80	Yes	No
1118	340	268 90	Yes	Yes
<b>1118</b>	<b>1118</b>			

<b>Location Scan-line</b>	<b>Slåen Slå-1.2</b>			
<b>Start Co- Ordinates</b>	<b>N77° 42' 54.0"</b>			
<b>End Co- Ordinates</b>	<b>E021° 12' 11.7"</b>			
<b>Altitude (a.s.l)</b>	<b>N77° 42' 54.3"</b>			
	<b>E021° 12' 11.8"</b>			
	<b>257m</b>			
<b>Measurement on Tape</b>	<b>Space</b>	<b>S/D</b>	<b>Through Going</b>	<b>Terminates at Fracture Plane</b>
0	0	072 81	No	Yes
60	60	097 88	No	Yes
230	170	282 71	No	Yes
500	270	058 86	Yes	Yes
<b>500</b>	<b>500</b>			

<b>Location Scan-line</b>	<b>Slåen Slå-1.3</b>			
<b>Start Co-Ordinates</b>	<b>N77° 42' 55.3" E021° 12' 11.6"</b>			
<b>End Co-Ordinates</b>	<b>N77° 42' 55.5" E021° 12' 11.4"</b>			
<b>Altitude (a.s.l)</b>	<b>247m</b>			
<b>Measurement on Tape</b>	<b>Space</b>	<b>S/D</b>	<b>Through Going</b>	<b>Terminates at Fracture Plane</b>
0	0	066 52	Yes	Yes
160	160	220 69	No	Yes
205	45	232 60	Yes	Yes
280	75	258 78	Yes	No
320	40	232 79	Yes	No
450	130	218 79	Yes	No
<b>450</b>	<b>450</b>			

<b>Location Scan-line</b>	<b>Slåen Slå-1.4</b>			
<b>Start Co-Ordinates</b>	<b>N77° 42' 56.4" E021° 12' 13.0"</b>			
<b>End Co-Ordinates</b>	<b>N77° 42' 56.4" E021° 12' 13.4"</b>			
<b>Altitude (a.s.l)</b>	<b>250m</b>			
<b>Measurement on Tape</b>	<b>Space</b>	<b>S/D</b>	<b>Through Going</b>	<b>Terminates at Fracture Plane</b>
0	0	348 78	Yes	Yes
130	130	188 65	No	Yes
205	75	210 74	Yes	Yes
415	210	210 86	Yes	Yes
735	320	216 72	Yes	Yes
<b>735</b>	<b>735</b>			

<b>Location Scan-line</b>	<b>Slåen Slå-1.5</b>			
<b>Start Co- Ordinates</b>	<b>N77° 42' 56.8" E021° 12' 12.8"</b>			
<b>End Co- Ordinates</b>	<b>N77° 42' 57.0" E021° 12' 11.4"</b>			
<b>Altitude (a.s.l)</b>	<b>254m</b>			
<b>Measurement on Tape</b>	<b>Space</b>	<b>S/D</b>	<b>Through Going</b>	<b>Terminates at Fracture Plane</b>
0	0	090 88	No	Yes
60	60	206 40	Yes	No
115	55	253 82	Yes	Yes
181	66	251 82	No	No
291	110	250 83	Yes	
379	88	252 82	Yes	
<b>379</b>	<b>379</b>			

<b>Location Scan-line</b>	<b>Slåen Slå-1.6</b>			
<b>Start Co- Ordinates</b>	<b>N77° 42' 57.4" E021° 12' 12.0"</b>			
<b>End Co- Ordinates</b>	<b>N77° 42' 57.3" E021° 12' 12.3"</b>			
<b>Altitude (a.s.l)</b>	<b>246m</b>			
<b>Measurement on Tape</b>	<b>Space</b>	<b>S/D</b>	<b>Through Going</b>	<b>Terminates at Fracture Plane</b>
0	0	312 85	Yes	No
280	280	328 90	Yes	No
470	190	327 86	Yes	Yes
680	210	348 72	Yes	Yes
<b>680</b>	<b>680</b>			

<b>Location Scan-line</b>	<b>Slåen Slå-1.7</b>			
<b>Start Co-Ordinates</b>	<b>N77° 42' 58.8" E021° 12' 11.4"</b>			
<b>End Co-Ordinates</b>	<b>N77° 42' 59.9" E021° 12' 12.5"</b>			
<b>Altitude (a.s.l)</b>	<b>246m</b>			
<b>Measurement on Tape</b>	<b>Space</b>	<b>S/D</b>	<b>Through Going</b>	<b>Terminates at Fracture Plane</b>
0	0	264 81	Yes	No
70	70	259 84	Yes	No
155	85	275 71	Yes	No
605	450	258 84	Yes	Yes
<b>605</b>	<b>605</b>			

<b>Location Scan-line</b>	<b>Slåen Slå-1.8</b>			
<b>Start Co-Ordinates</b>	<b>N77° 43' 03.0" E021° 12' 14.7"</b>			
<b>End Co-Ordinates</b>	<b>N77° 43' 03.2" E021° 12' 15.6"</b>			
<b>Altitude (a.s.l)</b>	<b>259m</b>			
<b>Measurement on Tape</b>	<b>Space</b>	<b>S/D</b>	<b>Through Going</b>	<b>Terminates at Fracture Plane</b>
0	0	244 73	Yes	Yes
35	35	245 83	No	Yes
405	370	251 80	Yes	Yes
865	460	242 90	Yes	No
1375	510	220 90	No	Yes
1510	135	328 84	Yes	Yes
<b>1510</b>	<b>1510</b>			

<b>Location Scan-line</b>	<b>Slåen Slå-1.9</b>			
<b>Start Co- Ordinates</b>	<b>N77° 42' 56.0" E021° 13' 03.9"</b>			
<b>End Co- Ordinates</b>	<b>N77° 42' 56.3" E021° 13' 04.4"</b>			
<b>Altitude (a.s.l)</b>	<b>259m</b>			
<b>Measurement on Tape</b>	<b>Space</b>	<b>S/D</b>	<b>Through Going</b>	<b>Terminates at Fracture Plane</b>
0	0	044 87	No	Yes
20	20	035 90	No	No
190	170	153 76	No	Yes
208	18	092 52	Yes	Yes
343	135	091 88	Yes	No
438	95	065 85	Yes	No
573	135	120 62	Yes	Yes
873	300	100 58	No	Yes
923	50	120 69	Yes	No
1033	110	095 75	Yes	No
<b>1033</b>	<b>1033</b>			



## Appendix 2.2.4 – Muen

<b>Location</b>		<b>Muen</b>		
<b>Scan-line</b>		<b>Muen-1.1</b>		
<b>Start Co-Ordinates</b>		<b>N77° 49' 00.2"</b>		
<b>End Co-Ordinates</b>		<b>E021° 21' 35.7"</b>		
<b>Altitude (a.s.l)</b>		<b>203m</b>		
<b>Measurement on Tape</b>	<b>Space</b>	<b>S/D</b>	<b>Through Going</b>	<b>Terminates at Fracture Plane</b>
0	0	334 90	Yes	No Data
36	36	335 90	Yes	No Data
44	8	331 90	Yes	No Data
73	29	334 90	Yes	No Data
96	23	306 90	Yes	No Data
123	27	327 90	Yes	No Data
148	25	318 90	Yes	No Data
163	15	316 90	Yes	No Data
186	23	321 90	Yes	No Data
215	29	327 90	Yes	No Data
232	17	332 90	Yes	No Data
258	26	328 90	Yes	No Data
282	24	338 90	Yes	No Data
301	19	311 90	Yes	No Data
317	16	320 90	Yes	No Data
329	12	320 90	Yes	No Data
343	14	338 90	Yes	No Data
363	20	332 90	Yes	No Data
392	29	330 90	Yes	No Data
418	26	334 90	Yes	No Data
428	10	327 90	Yes	No Data
443	15	326 90	Yes	No Data
450	7	321 90	Yes	No Data
480	30	328 90	Yes	No Data
490	10	338 90	Yes	No Data
517	27	326 90	Yes	No Data
536	19	325 90	Yes	No Data
551	15	331 90	Yes	No Data
571	20	325 90	Yes	No Data
598	27	322 90	Yes	No Data

608	10	336 90	Yes	No Data
616	8	328 90	Yes	No Data
626	10	336 90	Yes	No Data
<b>626</b>	<b>626</b>			

<b>Location Scan-line</b>	<b>Muen Muen-1.2</b>			
<b>Start Co-Ordinates</b>	<b>N77° 49' 00.3"</b>			
<b>End Co-Ordinates</b>	<b>E021° 21' 36.3"</b>			
<b>Altitude (a.s.l)</b>	<b>203m</b>			
<b>Measurement on Tape</b>	<b>Space</b>	<b>S/D</b>	<b>Through Going</b>	<b>Terminates at Fracture Plane</b>
0	0	248 90	Yes	No
55	55	244 90	Yes	No
67	12	259 90	Yes	No
84	17	263 90	Yes	No
111	27	241 90	Yes	No
129	18	249 90	Yes	No
142	13	251 90	Yes	No
146	4	261 90	Yes	No
186	40	234 90	Yes	No
206	20	250 90	Yes	No
216	10	249 90	Yes	No
224	8	256 90	Yes	No
239	15	244 90	Yes	No
259	20	262 90	Yes	No
276	17	264 90	Yes	No
291	15	246 90	Yes	No
307	16	255 90	Yes	No
314	7	258 90	Yes	No
318	4	273 90	Yes	No
339	21	221 90	Yes	No
<b>339</b>	<b>339</b>			

### Appendix 2.2.5 – Kvalpyntfjellet

<b>Location</b>	<b>Kvalpyntfjellet</b>			
<b>Scan-line</b>	<b>Kval-1.1</b>			
<b>Start Co-Ordinates</b>	<b>N77° 30' 42.9"</b>			
<b>End Co-Ordinates</b>	<b>E020° 52' 50.0"</b>			
<b>Altitude (a.s.l)</b>	<b>n/a</b>			
<b>Measurement on Tape</b>	<b>Space</b>	<b>S/D</b>	<b>Through Going</b>	<b>Terminates at Fracture Plane</b>
0	0	050 72	No Data	No Data
65	65	054 79	No Data	No Data
137	72	110 75	No Data	No Data
247	110	112 80	No Data	No Data
487	240	084 58	No Data	No Data
582	95	042 74	No Data	No Data
792	210	111 82	No Data	No Data
877	85	035 80	No Data	No Data
997	120	081 72	No Data	No Data
1062	65	095 75	No Data	No Data
<b>1062</b>	<b>1062</b>			

<b>Location Scan-line</b>	<b>Kvalpyntfjellet Kval-1.2</b>			
<b>Start Co- Ordinates</b>	<b>N77° 30' 41.1" E020° 52' 50.1"</b>			
<b>End Co- Ordinates</b>	<b>N77° 30' 40.9" E020° 52' 50.2"</b>			
<b>Altitude (a.s.l)</b>	<b>122m</b>			
<b>Measurement on Tape</b>	<b>Space</b>	<b>S/D</b>	<b>Through Going</b>	<b>Terminates at Fracture Plane</b>
0	0	090 74	Yes	No
70	70	092 76	No	No
280	210	070 84	Yes	Yes
680	400	057 58	No	No
785	105	056 80	Yes	No
925	140	036 72	Yes	No
1015	90	051 56	No	Yes
<b>1015</b>	<b>1015</b>			

## Appendix 2.3 – Central & Northern Hopen Fracture Data

### Appendix 2.3.1 – Nørdstefjellet

<b>Location Scan-line</b>		<b>Nørdstefjellet Nørd 1.1</b>		
<b>Start Co-Ordinates</b>	<b>N76° 42' 31.07" E025° 29' 56.63"</b>			
<b>End Co-Ordinates</b>	<b>N76° 42' 29" E025° 29' 54"</b>			
<b>Altitude (a.s.l)</b>	<b>35m</b>			
<b>Measurement on Tape (cm)</b>	<b>Space (cm)</b>	<b>S/D</b>	<b>Through Going</b>	<b>Terminates at Fracture Plane</b>
0	0	038 71	No	No Data
55	55	060 82	Yes	No Data
185	130	048 80	No	No Data
367	182	029 84	Yes	No Data
597	230	074 88	Yes	No Data
867	270	054 90	Yes	No Data
887	20	077 88	Yes	No Data
1067	180	059 86	Yes	No Data
1100	33	066 85	Yes	No Data
1500	400	071 84	Yes	No Data
2000	500	101 45	Yes	No Data
2030	30	105 74	Yes	No Data
2063	33	020 86	Yes	No Data
2283	220	064 86	Yes	No Data
2733	450	018 80	Yes	No Data
3021	288	188 90	Yes	No Data
3197	176	198 80	Yes	No Data
3287	90	120 71	Yes	No Data
3527	240	139 62	Yes	No Data
3827	300	035 76	Yes	No Data
4117	290	185 80	Yes	No Data
4557	440	181 79	Yes	No Data
4677	120	190 88	Yes	No Data
<b>4677</b>	<b>4677</b>			

## Appendix 2.3.2 – Binnedalen

<b>Location Scan-line</b>	<b>Binnedalen Bin-1.1</b>			
<b>Start Co- Ordinates</b>	<b>N76° 41' 28.2" E025° 27' 43.5"</b>			
<b>End Co- Ordinates</b>	<b>N76° 41' 27.8" E025° 27' 44.3"</b>			
<b>Altitude (a.s.l)</b>	<b>4m</b>			
<b>Measurement on Tape</b>	<b>Space</b>	<b>S/D</b>	<b>Through Going</b>	<b>Terminates at Fracture Plane</b>
0	0	180 42	Yes	No Data
23	23	356 85	No	No Data
143	120	122 47	Yes	No Data
258	115	121 48	Yes	No Data
282	24	054 62	Yes	No Data
312	30	062 48	Yes	No Data
382	70	137 68	No	No Data
445	63	109 80	No	No Data
646	201	130 70	Yes	No Data
746	100	139 67	Yes	No Data
841	95	132 65	No	No Data
1011	170	296 90	Yes	No Data
1216	205	154 59	Yes	No Data
1351	135	119 41	No	No Data
1391	40	121 52	Yes	No Data
1401	10	124 53	Yes	No Data
1412	11	118 60	Yes	No Data
1541	129	107 58	Yes	No Data
<b>1541</b>	<b>1541</b>			

<b>Location Scan-line</b>	<b>Binnedalen Bin-1.2</b>			
<b>Start Co-Ordinates</b>	<b>N76° 41' 24.0" E025° 27' 26.4"</b>			
<b>End Co-Ordinates</b>	<b>N76° 41' 24.0" E025° 27' 26.5"</b>			
<b>Altitude (a.s.l)</b>	<b>47m</b>			
<b>Measurement on Tape</b>	<b>Space</b>	<b>S/D</b>	<b>Through Going</b>	<b>Terminates at Fracture Plane</b>
0	0	226 84	No	Yes
80	80	219 85	No	Yes
140	60	217 89	No	No
290	150	018 69	Yes	No
383	93	222 85	No	Yes
408	25	238 88	Yes	No
468	60	235 88	Yes	No
542	74	224 89	Yes	No
548	6	225 84	Yes	No
552	4	237 84	Yes	No
579	27	047 82	No	No
626	47	235 89	No	No
<b>626</b>	<b>626</b>			

<b>Location Scan-line</b>	<b>Binnedalen Bin-1.3</b>			
<b>Start Co-Ordinates</b>	<b>N76° 41' 25.0" E025° 27' 27.1"</b>			
<b>End Co-Ordinates</b>	<b>N76° 41' 25.2" E025° 27' 20.7"</b>			
<b>Altitude (a.s.l)</b>	<b>62m</b>			
<b>Measurement on Tape</b>	<b>Space</b>	<b>S/D</b>	<b>Through Going</b>	<b>Terminates at Fracture Plane</b>
0	0	343 64	Yes	No
56	56	331 65	No	No
262	206	346 54	No	Yes
314	52	347 63	No	No

378	64	329 56	No	No
418	40	019 90	No	Yes
434	16	193 81	No	Yes
508	74	193 54	No	Yes
548	40	347 56	Yes	No
<b>548</b>	<b>548</b>			

<b>Location Scan-line</b>	<b>Binnedalen Bin-1.4</b>			
<b>Start Co- Ordinates</b>	N76° 41' 24.2" E025° 27' 11.3"			
<b>End Co- Ordinates</b>	N76° 41' 24.0" E025° 27' 10.2"			
<b>Altitude (a.s.l)</b>	87m			
<b>Measurement on Tape</b>	<b>Space</b>	<b>S/D</b>	<b>Through Going</b>	<b>Terminates at Fracture Plane</b>
0	0	341 75	No	No
150	150	300 82	No	No
347	197	155 88	No	No
540	193	349 50	No	No
<b>193</b>	<b>193</b>			

<b>Location Scan-line</b>	<b>Binnedalen Bin-1.5</b>			
<b>Start Co- Ordinates</b>	N76° 41' 23.0" E025° 27' 03.6"			
<b>End Co- Ordinates</b>	N76° 41' 22.9" E025° 27' 03.3"			
<b>Altitude (a.s.l)</b>	92			
<b>Measurement on Tape</b>	<b>Space</b>	<b>S/D</b>	<b>Through Going</b>	<b>Terminates at Fracture Plane</b>
0	0	074 76	Yes	No
40	40	340 80	No	No
65	25	064 81	No	No
115	50	174 70	Yes	Yes



195	80	243 88	Yes	Yes
285	90	343 68	Yes	No
<b>285</b>	<b>285</b>			

<b>Location</b>	<b>Binnedalen</b>			
<b>Scan-line</b>	<b>Bin-1.6</b>			
<b>Start Co-Ordinates</b>	N76° 41' 23.3" E025° 26' 53.9"			
<b>End Co-Ordinates</b>	N76° 41' 23.3' E025° 26' 54.8"			
<b>Altitude (a.s.l)</b>	118			
<b>Measurement on Tape</b>	<b>Space</b>	<b>S/D</b>	<b>Through Going</b>	<b>Terminates at Fracture Plane</b>
0	0	227 79	No	No
40	40	359 89	Yes	Yes
80	40	075 84	No	Yes
130	50	081 80	No	No
290	160	356 73	No	No
390	100	349 81	No	Yes
445	55	251 80	No	Yes
465	20	350 87	Yes	Yes
675	210	179 79	Yes	No
<b>675</b>	<b>675</b>			

<b>Location Scan-line</b>		<b>Binnedalen Bin-1.7</b>		
<b>Start Co-Ordinates</b>		<b>N76° 41' 21.7" E025° 27' 00.9"</b>		
<b>End Co-Ordinates</b>		<b>N/A</b>		
<b>Altitude (a.s.l)</b>		<b>127m</b>		
<b>Measurement on Tape</b>	<b>Space</b>	<b>S/D</b>	<b>Through Going</b>	<b>Terminates at Fracture Plane</b>
0	0	028 88	No	No Data
22	22	018 87	Yes	No Data
52	30	020 80	No	No Data
77	25	010 85	No	No Data
101	24	177 81	Yes	No Data
123	22	024 80	No	No Data
140	17	028 79	Yes	No Data
176	36	015 78	No	No Data
230	54	020 90	Yes	No Data
252	22	016 86	No	No Data
276	24	020 76	Yes	No Data
305	29	024 80	Yes	No Data
337	32	115 71	No	No Data
347	10	021 80	No	No Data
362	15	020 78	Yes	No Data
379	17	022 80	No	No Data
404	25	017 85	No	No Data
437	33	017 68	No	No Data
489	52	010 84	Yes	No Data
521	32	012 90	No	No Data
542	21	021 82	Yes	No Data
570	28	012 76	No	No Data
603	33	016 84	Yes	No Data
645	42	015 84	Yes	No Data
662	17	016 84	yes	No Data
706	44	023 88	No	No Data
741	35	018 76	Yes	No Data
763	22	012 86	No	No Data
781	18	010 82	Yes	No Data
<b>781</b>	<b>781</b>			

## Appendix 2.3.3 – Blåfjellet

<b>Location</b>	<b>Blåfjellet</b>			
<b>Scan-line</b>	<b>Blå-1.1</b>			
<b>Start Co-Ordinates</b>	<b>N76° 37'</b>			
	<b>26.8" E025°</b>			
	<b>18' 27.5"</b>			
<b>End Co-Ordinates</b>	<b>N76° 37'</b>			
	<b>23.1" E025°</b>			
	<b>18' 15.1"</b>			
<b>Altitude (a.s.l)</b>	<b>12m</b>			
<b>Measurement on Tape (cm)</b>	<b>Space (cm)</b>	<b>S/D</b>	<b>Through Going</b>	<b>Terminates at Fracture Plane</b>
0	0	037 56	No	n/a
320	320	032 73	Yes	n/a
850	530	034 72	No	n/a
1300	450	026 64	Yes	n/a
1420	120	032 82	Yes	n/a
1980	560	017 76	Yes	n/a
2570	590	045 88	Yes	n/a
3050	480	254 88	Yes	n/a
3400	350	078 90	Yes	n/a
3925	525	019 75	Yes	n/a
4175	250	026 80	Yes	n/a
4935	760	038 69	Yes	n/a
5715	780	039 69	Yes	n/a
6275	560	106 68	Yes	n/a
6395	120	020 81	Yes	n/a
6845	450	020 78	Yes	n/a
7165	320	021 88	Yes	n/a
7725	560	116 74	Yes	n/a
8205	480	018 88	Yes	n/a
8475	270	028 65	Yes	n/a
9235	760	024 83	Yes	n/a
9703	468	021 72	Yes	n/a
9892	189	016 71	Yes	n/a
<b>9892</b>	<b>9892</b>			

## Appendix 2.3.4 – Styggdalen

<b>Location</b>		<b>Styggdalen</b>		
<b>Scan-line</b>		<b>Styg-1.1</b>		
<b>Start Co-Ordinates</b>		N76° 33' 43.4" E025° 08' 15.6"		
<b>End Co-Ordinates</b>		N76° 33' 43.8" E025° 08' 19.3"		
<b>Altitude (a.s.l)</b>		c.84m		
<b>Measurement on Tape (cm)</b>	<b>Space (cm)</b>	<b>S/D</b>	<b>Through Going</b>	<b>Terminates at Fracture Plane</b>
	0	324 60	No	No Data
	23	141 83	No	No Data
	32	312 85	No	No Data
	16	300 88	No	No Data
	29	326 81	No	No Data
	60	320 74	No	No Data
	8	349 78	No	No Data
	23	323 80	No	No Data
	58	335 78	No	No Data
	48	312 81	No	No Data
	5	133 65	No	No Data
	2	313 76	No	No Data
	36	147 79	No	No Data
	54	320 79	No	No Data
	54	332 80	No	No Data
	56	312 68	No	No Data
	91	310 80	No	No Data
	8	309 77	No	No Data
	29	324 97	No	No Data
	4	140 85	No	No Data
	26	132 88	No	No Data
	46	331 78	No	No Data
	55	337 62	No	No Data
	60	330 81	No	No Data
	60	144 86	No	No Data
	56	132 89	No	No Data
	32	150 88	No	No Data
	13	146 86	No	No Data
	17	134 80	No	No Data
	28	158 80	No	No Data
	23	320 82	No	No Data

---

	27	150 76	No	No Data
	36	331 81	No	No Data
	16	030 75	No	No Data
	45	316 68	No	No Data
	4	158 80	No	No Data
	15	332 50	No	No Data
	53	326 74	No	No Data
	10	328 85	No	No Data
	32	018 80	No	No Data
	56	284 75	No	No Data
	68	305 85	No	No Data
	10	320 82	Yes	No Data
	937	295 90	No	No Data
	23	290 78	No	No Data
	1	332 78	No	No Data
	8	142 70	Yes	No Data
	55	098 90	Yes	No Data
	200	298 84	Yes	No Data
	280	294 80	Yes	No Data
	<b>945</b>			

<b>Location Scan-line</b>	<b>Styggdalen Styg-1.2</b>			
<b>Start Co-Ordinates</b>	<b>N76° 33' 43.3" E025° 08' 15.4"</b>			
<b>End Co-Ordinates</b>	<b>N76° 33' 42.8" E025° 08' 15.0"</b>			
<b>Altitude (a.s.l)</b>	<b>c.84m</b>			
<b>Measurement on Tape (cm)</b>	<b>Space (cm)</b>	<b>S/D</b>	<b>Through Going</b>	<b>Terminates at Fracture Plane</b>
0	0	146 90	No	Yes
11	11	140 89	No	Yes
26	15	330 76	No	Yes
36	10	148 84	No	Yes
50	14	330 78	No	Yes
69	19	321 81	No	Yes
106	37	330 78	No	Yes
146	40	321 85	No	Yes
163	17	352 82	No	Yes
166	3	346 78	No	Yes
178	12	276 89	No	Yes
194	16	359 77	No	Yes
200	6	347 80	No	Yes
223	23	328 69	No	Yes
235	12	334 70	No	Yes
240	5	351 71	No	Yes
242	2	346 74	No	Yes
255	13	329 84	No	Yes
269	14	323 75	No	Yes
285	16	335 83	No	Yes
299	14	325 81	No	Yes
328	29	327 86	No	Yes
339	11	330 75	No	Yes
376	37	161 64	No	Yes
405	29	309 80	No	Yes
449	44	324 57	No	Yes
476	27	323 69	No	Yes
480	4	310 75	No	Yes
<b>480</b>	<b>480</b>			

### Appendix 2.3.5 - Russevika

<b>Location</b>	<b>Russevika</b>			
<b>Scan-line</b>	<b>Russ-1.1</b>			
<b>Start Co-Ordinates</b>	N76° 33' 22.0" E025° 08' 58.53"			
<b>End Co-Ordinates</b>	N76° 33' 20.0" E025° 08' 59.6"			
<b>Altitude (a.s.l)</b>	<b>2m</b>			
<b>Measurement on Tape (cm)</b>	<b>Space (cm)</b>	<b>S/D</b>	<b>Through Going</b>	<b>Terminates at Fracture Plane</b>
0	0	336 72	Yes	No
6	6	374 80	Yes	No
66	60	334 66	Yes	Yes
131	65	343 70	Yes	No
136	5	348 70	Yes	Yes
149	13	335 82	No	No
189	40	330 81	Yes	No
190	1	352 66	No	Yes
230	40	340 71	Yes	No
330	100	352 60	Yes	Yes
<b>330</b>	<b>330</b>			

## Appendix 2.3.6 - Lykkedalen

<b>Location</b>	<b>Lykkedalen</b>			
<b>Scan-line</b>	<b>Lykke-1.1</b>			
<b>Start Co-Ordinates</b>	N76° 33' 10.8" E025° 08' 14.5"			
<b>End Co-Ordinates</b>	N76° 33' 10.6" E025° 08' 15.4"			
<b>Altitude (a.s.l)</b>	115m			
<b>Measurement on Tape</b>	<b>Space</b>	<b>S/D</b>	<b>Through Going</b>	<b>Terminates at Fracture Plane</b>
0	0	008/80 E	No	No Data
10	10	179/84 E	No	No Data
16	6	171/84 E	No	No Data
25	9	022/85 E	No	No Data
27	2	010/88 E	No	No Data
37	10	010/86 E	No	No Data
53	16	074/81 E	Yes	No Data
71	18	179/86 E	No	No Data
88	17	178/82 E	No	No Data
108	20	181/86 E	Yes	No Data
116	8	008/84 E	No	No Data
137	21	005/84 E	No	No Data
142	5	172/86 E	No	No Data
149	7	025/88 E	No	No Data
157	8	008/84 E	No	No Data
163	6	003/82 E	No	No Data
168	5	009/83 E	No	No Data
183	15	010/80 W	No	No Data
199	16	001/82 W	No	No Data
218	19	161/90	No	No Data
234	16	163/76 E	No	No Data
250	16	010/90	Yes	No Data
280	30	008/82 E	Yes	No Data
286	6	160/83 E	No	No Data
296	10	178/84 E	No	No Data
<b>296</b>	<b>296</b>			



<b>Location Scan-line</b>	<b>Lykkedalen Lykke-1.2</b>			
<b>Start Co-Ordinates</b>	<b>N76° 33' 12.2" E025° 07' 58.9"</b>			
<b>End Co-Ordinates</b>	<b>N/a</b>			
<b>Altitude (a.s.l)</b>	<b>190m</b>			
<b>Measurement on Tape</b>	<b>Space</b>	<b>S/D</b>	<b>Through Going</b>	<b>Terminates at Fracture Plane</b>
0	0	040/74	Yes	No Data
650	650	079/76	Yes	No Data
1120	470	174/80	Yes	No Data
1456	336	132/83	Yes	No Data
<b>1456</b>	<b>1456</b>			No Data

<b>Location Scan-line</b>	<b>Lykkedalen Lykke-1.3</b>			
<b>Start Co-Ordinates</b>	<b>N76° 33' 12.7" E025° 07' 57.7"</b>			
<b>End Co-Ordinates</b>	<b>N76° 33' 12.9" E025° 07' 58.0"</b>			
<b>Altitude (a.s.l)</b>	<b>213m</b>			
<b>Measurement on Tape</b>	<b>Space</b>	<b>S/D</b>	<b>Through Going</b>	<b>Terminates at Fracture Plane</b>
0	0	177/88 E	No	No Data
16	16	001/85 E	No	No Data
24	8	168/64 E	No	No Data
62	38	180/62 E	No	No Data
76	14	166/60 E	No	No Data
94	18	172/72 E	No	No Data
99	5	167/82 E	yes	No Data
129	30	008/76 E	No	No Data
144	15	036/70 SW	Yes	No Data
189	45	004/82 E	No	No Data
229	40	074/86 E	No	No Data
244	15	174/88 E	No	No Data
250	6	019/82 E	No	No Data

---

252	2	170/86 E	No	No Data
297	45	161/71 W	No	No Data
337	40	150/71 NE	No	No Data
357	20	176/74 E	No	No Data
367	10	001/72 E	No	No Data
467	100	075/79 E	Yes	No Data
482	15	180/90	No	No Data
502	20	166/90	Yes	No Data
514	12	176/90	No	No Data
544	30	174/72 E	No	No Data
559	15	008/74 E	Yes	No Data
594	35	164/80 E	No	No Data
<b>594</b>	<b>594</b>			

# 12. Appendix 3 – Composite Scan-Line Data Tables

## Appendix 3.1 – Regional Scan-Line Data

Area	Location	Scan Line	Orientation (°)	Length (m)	Bed Thickness (m)	Number of Fractures	Average Fracture Spacing (m)	Through Going Fractures	Layer Confined Fractures	Average Fractures /m	Through Going Fractures /m	Layer Confined Fractures /m	Lithological Association	
Central Spitsbergen	Deltaneset	Delta-1.1	52	2.0	1.4	9	0.21	7	2	4.6	3.6	0.5	Shale	
		Delta-1.2	100	16.6	1.9	20	0.92	11	9	1.2	0.7	1.0	Sandstone	
		Delta-1.3a	98	4.4	3.1	8	0.55	8	0	1.8	1.8	0.0	Sandstone & Shale	
		Delta-1.3b	102	7.7	3.1	15	0.51	7	8	1.9	0.9	1.0	Sandstone & Shale	
		Delta-1.4	130	5.3	1.7	30	0.17	18	12	5.7	3.4	2.3	Sandstone & Shale	
		Delta-1.5	98	0.6	1.2	8	0.08	4	4	13.3	6.7	6.7	Sandstone	
		Delta-1.6	94	20.4	6.7	15	1.36	9	6	0.7	0.4	0.3	Shale	
		Delta-1.7	80	23.7	3.5	36	0.65	24	12	1.5	1.0	0.5	Sandstone & Shale	
		Delta-1.8	91	21.4	1.2	29	0.42	23	6	1.1	1.1	0.3	Sandstone	
		Delta-1.9	85	8.2	0.4	16	0.51	13	3	2.0	1.6	0.4	Sandstone	
		Delta-1.10	108	3.7	2.4	13	0.29	3	3	3.5	2.7	0.8	Sandstone & Shale	
		Konusdalen	Kon-1.1	7	8.3	2.7	55	0.27	8	47	6.6	1.0	5.7	Sandstone & Shale
		Trehøgdenene	Tre-1.1	165	13.8	3	33	0.43	21	12	2.4	1.5	0.9	Sandstone
			Tre-1.2	60	4.1	4.1	10	0.41	6	4	2.4	1.5	1.0	Sandstone
			Tre-1.3	72	5.8	6	13	0.46	4	9	2.2	0.7	1.6	Sandstone
			Tre-1.4	58	10.7	2.6	24	0.55	20	4	2.2	1.9	0.4	Sandstone & Shale
Tre-1.5	57		7.1	3	17	0.41	7	10	2.4	1.0	1.4	Sandstone		
Tre-2.1	67		3.1	2.9	10	0.26	5	5	3.2	1.6	1.6	Sandstone		
Tre-2.2	100		6.3	2.3	13	0.48	8	5	2.1	1.3	0.8	Sandstone		
Tre-2.3	85		5.3	2.4	15	0.35	11	4	2.8	2.1	0.8	Sandstone		
Agardhbukta	Agard-1.1		135	12.8	6.4	20	0.60	18	2	1.6	1.4	0.2	Sandstone & Shale	
Klinkhamaren	Klink-1.1		120	52.4	5.6	34	1.54	20	14	0.6	0.4	0.3	Sandstone	
	Klink-1.2		155	6.3	4.8	6	1.05	6	0	1.0	1.0	0.0	Sandstone	
	Blank-1.1		170	6.9	3.2	10	0.89	3	7	1.4	0.4	1.0	Sandstone & Shale	
	Blank-1.2	166	4.1	4.4	11	0.37	6	5	2.7	1.5	1.2	Sandstone & Shale		
Blanknuten	Blank-1.3	175	1.9	4.7	6	0.33	3	3	3.2	1.6	1.6	Sandstone & Shale		
	Blank-1.4	120	4.0	12.1	2	2.00	2	0	0.5	0.5	0.0	Sandstone		
	Blank-1.5	65	47.2	12.1	16	2.95	11	5	0.3	0.2	0.1	Sandstone		
	Blank-1.6	80	6.3	8.5	12	0.52	12	0	1.9	1.9	0.0	Sandstone		
	Blank-1.7	74	5.7	9.6	8	0.71	5	3	1.4	0.9	0.5	Sandstone		
Western Edgeeya	Slå-1.1	177	11.1	11.1	6	1.86	6	0	0.5	0.5	0.0	Sandstone		
	Slå-1.2	172	5.0	10.5	4	1.25	1	3	0.8	0.2	0.6	Sandstone		
	Slå-1.3	130	4.5	11.3	6	0.75	5	1	1.3	1.1	0.2	Sandstone		
	Slå-1.4	140	7.3	11.2	5	1.47	4	1	0.7	0.5	0.1	Sandstone		
	Slå-1.5	120	3.7	10.9	6	0.63	4	2	1.6	1.1	0.5	Sandstone		
	Slå-1.6	155	6.8	11.1	4	1.70	4	0	0.6	0.6	0.0	Sandstone		
	Slå-1.7	165	6.0	11.3	4	1.51	4	0	0.7	0.7	0.0	Sandstone		
	Slå-1.8	162	15.1	11.6	6	2.51	4	2	0.4	0.3	0.1	Sandstone		
	Slå-1.9	174	10.3	11.1	10	1.03	6	4	1.0	0.6	0.4	Sandstone		
Muen	Muen-1.1	57	6.2	0.4	33	0.18	33	0	5.3	5.3	0.0	Sandstone & Shale		
	Muen-1.2	158	3.3	0.4	20	0.16	20	0	6.1	6.1	0.0	Sandstone & Shale		
	Kval-1.1	10	10.6	3.7	10	1.06	No Data	No Data	0.9	No Data	No Data	Sandstone		
Kvalbyntfjellet	Kval-1.2	7	10.1	3.5	7	1.45	4	3	0.7	0.4	0.3	Sandstone		
	Nerd-1.1	2	46.7	8.6	23	2.03	21	2	0.5	0.4	0.0	Sandstone		
	Nerd-1.1	26	15.4	4.7	18	0.85	13	5	1.2	0.8	0.3	Shale		
	Bin-1.2	94	6.2	3.7	12	0.52	6	5	1.9	1.0	0.8	Sandstone		
Binndalen	Bin-1.3	110	5.4	2.6	9	0.6	2	7	1.7	0.4	1.3	Sandstone & Shale		
	Bin-1.4	94	1.9	6.2	4	1.35	0	4	2.1	0.0	2.1	Shale		
	Bin-1.5	82	2.8	2.4	6	0.47	4	2	2.1	1.4	0.7	Sandstone & Shale		
	Bin-1.6	104	6.7	2.3	9	0.75	3	6	1.3	0.4	0.9	Sandstone & Shale		
	Bin-1.7	120	7.8	5.3	29	0.26	13	16	3.7	1.7	2.1	Sandstone & Shale		
	Blåfjellet	Blå-1.1	88	98.9	15.0	23	4.3	21	2	0.2	0.2	0.0	Sandstone	
Styggedalen	Syg-1.1	52	9.4	8.2	50	0.58	5	45	5.3	0.5	4.8	Sandstone		
	Syg-1.2	47	4.8	6.3	28	0.17	0	28	5.8	0.0	5.8	Sandstone & Shale		
Russevika	Russ-1.1	48	3.3	8.2	10	0.33	8	2	3.0	2.4	0.6	Sandstone & Shale		
	Lykke-1.1	140	2.9	4.7	25	0.11	4	25	8.6	1.4	8.6	Shale		
Lykkedalen	Lykke-1.2	83	14.5	20.4	4	3.64	4	0	0.3	0.3	0.0	Sandstone		
	Lykke-1.3	138	5.9	3.1	25	0.23	5	20	4.2	0.8	3.4	Shale		
Central & Northern Hopen														

## Appendix 3.2 – Regional Scan-Line Data: Sandstone Beds

Area	Location	Scan Line	Orientation (°)	Length (m)	Bed Thickness (m)	Number of Fractures	Average Fracture Spacing	Through Going Fractures	Layer Confined Fractures	Average Fractures /m	Through Going Fractures /m	Layer Confined Fractures /m	Lithological Association	
Central Spitsbergen	Deltaneset	Delta-1.2	100	16.6	1.9	20	0.92	11	9	1.2	0.7	0.5	Sandstone	
		Delta-1.5	98	0.6	1.2	8	0.08	4	4	13.3	6.7	6.7	Sandstone	
		Delta-1.8	91	21.4	1.2	29	0.42	23	6	1.4	1.1	0.3	Sandstone	
	Trehøgden	Delta-1.9	85	8.2	0.4	16	0.51	13	3	2.0	1.6	0.4	Sandstone	
			Tre-1.1	165	13.8	3	33	0.43	21	12	2.4	1.5	0.9	Sandstone
		Tre-1.2	60	4.1	4.1	10	0.41	6	4	2.4	1.5	1.0	Sandstone	
		Tre-1.3	72	5.8	6	13	0.46	4	9	2.2	0.7	1.6	Sandstone	
		Tre-1.5	57	7.1	3	17	0.41	7	10	2.4	1.0	1.4	Sandstone	
		Tre-2.1	67	3.1	2.9	10	0.26	5	5	3.2	1.6	1.6	Sandstone	
		Tre-2.2	100	6.3	2.3	13	0.48	8	5	2.1	1.3	0.8	Sandstone	
Western Edgeøya	Klinkhamaren	Tre-2.3	85	5.3	2.4	15	0.35	11	4	2.8	2.1	0.8	Sandstone	
		Klink-1.1	120	52.4	5.6	34	1.54	20	14	0.6	0.4	0.3	Sandstone	
		Klink-1.2	155	6.3	4.8	6	1.05	6	0	1.0	1.0	0.0	Sandstone	
	Blanknuten	Blank-1.4	120	4.0	12.1	2	2.00	2	0	0.5	0.5	0.0	Sandstone	
		Blank-1.5	65	47.2	12.1	16	2.95	11	5	0.3	0.2	0.1	Sandstone	
		Blank-1.6	80	6.3	8.5	12	0.52	12	0	1.9	1.9	0.0	Sandstone	
		Blank-1.7	74	5.7	9.6	8	0.71	5	3	1.4	0.9	0.5	Sandstone	
	Slåten	Slå-1.1	177	11.1	11.1	6	1.86	6	0	0.5	0.5	0.0	Sandstone	
		Slå-1.2	172	5.0	10.5	4	1.25	1	3	0.8	0.2	0.6	Sandstone	
		Slå-1.3	130	4.5	11.3	6	0.75	5	1	1.3	1.1	0.2	Sandstone	
Slå-1.4		140	7.3	11.2	5	1.47	4	1	0.7	0.5	0.1	Sandstone		
Slå-1.5		120	3.7	10.9	6	0.63	4	2	1.6	1.1	0.5	Sandstone		
Slå-1.6		155	6.8	11.1	4	1.70	4	0	0.6	0.6	0.0	Sandstone		
Slå-1.7		165	6.0	11.3	4	1.51	4	0	0.7	0.7	0.0	Sandstone		
Central & Northern Hopen	Kvalpynfjellet	Slå-1.8	162	15.1	11.6	6	2.51	4	2	0.4	0.3	0.1	Sandstone	
		Slå-1.9	174	10.3	11.1	10	1.03	6	4	1.0	0.6	0.4	Sandstone	
		Kval-1.1	10	10.6	3.7	10	1.06	No Data	No Data	No Data	No Data	No Data	Sandstone	
	Nørdstefjellet	Kval-1.2	7	10.1	3.5	7	1.45	4	3	0.7	0.4	0.3	Sandstone	
		Nørd-1.1	2	46.7	8.6	23	2.03	21	2	0.5	0.4	0.0	Sandstone	
		Bin-1.2	94	6.2	3.7	12	0.52	6	5	1.9	1.0	0.8	Sandstone	
		Blåfjellet	88	98.9	15.0	23	4.3	21	2	0.2	0.2	0.0	Sandstone	
		Styggdalen	Styg-1.1	52	9.4	8.2	50	0.58	5	45	5.3	0.5	4.8	Sandstone
		Lykkedalen	Lykke-1.2	83	14.5	20.4	4	3.64	4	0	0.3	0.3	0.0	Sandstone

## Appendix 3.3 – Regional Scan-Line Data: Sandstone &amp; Shale Beds

Area	Location	Scan Line	Orientation (°)	Length (m)	Bed Thickness (m)	Number of Fractures	Average Fracture Spacing (m)	Through Going Fractures	Layer Confined Fractures	Average Fractures /m	Through Going Fractures /m	Layer Confined Fractures /m	Lithological Association
Central Spitsbergen	Deltaneset	Delta-1.3a	98	4.4	3.1	8	0.55	8	0	1.8	1.8	0.0	Sandstone & Shale
		Delta-1.3b	102	7.7	3.1	15	0.51	7	8	1.9	0.9	1.0	Sandstone & Shale
		Delta-1.4	130	5.3	1.7	30	0.17	18	12	5.7	3.4	2.3	Sandstone & Shale
		Delta-1.7	80	23.7	3.5	36	0.65	24	12	1.5	1.0	0.5	Sandstone & Shale
	Konusdalen	Delta-1.10	108	3.7	2.4	13	0.29	10	3	3.5	2.7	0.8	Sandstone & Shale
		Kon-1.1	7	8.3	2.7	55	0.27	8	47	6.6	1.0	5.7	Sandstone & Shale
		Trehøgdene	58	10.7	2.6	24	0.55	20	4	2.2	1.9	0.4	Sandstone & Shale
Western Edgeøya	Agardfbukta	Tre-1.4	135	12.8	6.4	20	0.60	18	2	1.6	1.4	0.2	Sandstone & Shale
		Agard-1.1	170	6.9	3.2	10	0.69	3	7	1.4	0.4	1.0	Sandstone & Shale
	Blanknuten	Blank-1.1	166	4.1	4.4	11	0.37	6	5	2.7	1.5	1.2	Sandstone & Shale
		Blank-1.2	175	1.9	4.7	6	0.33	3	3	3.2	1.6	1.6	Sandstone & Shale
		Blank-1.3	175	1.9	4.7	6	0.33	3	3	3.2	1.6	1.6	Sandstone & Shale
Central & Northern Hopen	Muen	Muen-1.1	57	6.2	0.4	33	0.18	33	0	5.3	5.3	0.0	Sandstone & Shale
		Muen-1.2	158	3.3	0.4	20	0.16	20	0	6.1	6.1	0.0	Sandstone & Shale
	Binnedalen	Bin-1.3	110	5.4	2.6	9	0.6	2	7	1.7	0.4	1.3	Sandstone & Shale
		Bin-1.5	82	2.8	2.4	6	0.47	4	2	2.1	1.4	0.7	Sandstone & Shale
		Bin-1.6	104	6.7	2.3	9	0.75	3	6	1.3	0.4	0.9	Sandstone & Shale
	Styggdalen	Bin-1.7	120	7.8	5.3	29	0.26	13	16	3.7	1.7	2.1	Sandstone & Shale
		Styg-1.2	47	4.8	6.3	28	0.17	0	28	5.8	0.0	5.8	Sandstone & Shale
Russevika	Russ-1.1	48	3.3	8.2	10	0.33	8	2	3.0	2.4	0.6	Sandstone & Shale	

## Appendix 3.4 – Regional Scan-line-Data: Shale Beds

Area	Location	Scan Line	Orientation (°)	Length (m)	Bed Thickness (m)	Number of Fractures	Average Fracture Spacing (m)	Through Going Fractures	Layer Confined Fractures	Average Fractures /m	Through Going Fractures /m	Layer Confined Fractures /m	Lithological Association
Central Spitsbergen	Deitaneset	Della-1.1	52	2.0	1.4	9	0.21	7	2	4.6	3.6	1.0	Shale
		Della-1.6	94	20.4	6.7	15	1.36	9	6	0.7	0.4	0.3	Shale
Central & Northern Hopen	Binnedalen	Bin-1.1	26	15.4	4.7	18	0.85	13	5	1.2	0.8	0.3	Shale
		Bin-1.4	94	1.9	6.2	4	1.35	0	4	2.1	0.0	2.1	Shale
	Lykkedalen	Lykke-1.1	140	2.9	4.7	25	0.11	4	25	8.6	1.4	8.6	Shale
Lykke-1.3		138	5.9	3.1	25	0.23	5	20	4.2	0.8	3.4	Shale	